

University of Strathclyde
Department of Immunology

**Effect of phosphorylcholine-based small
molecule analogues of the immunomodulatory
nematode product ES-62 on mast cell function**

Moninder Saggarr

**A thesis presented in fulfillment of the requirements for the
degree of Doctor of Philosophy 2010**

This thesis is the result of the author's original research. It has been composed by the author and has not been previously submitted for examination which has led to the award of a degree.

The copyright of this thesis belongs to the author under the terms of the United Kingdom Copyright Acts as qualified by University of Strathclyde Regulation 3.50. Due to acknowledgement must always be made of the use of any material contained in, or derived from, this thesis.

Signed:

Date:

Acknowledgements

I would like to thank my supervisor, Prof. William Harnett, for his supervision, guidance and patience during my research and in the writing of this thesis.

I would also like to extend my gratitude to Prof. Maggie Harnett for showing me the LSC techniques and Dr. A. Melendez for help in my work.

Amongst others, I would like to offer my thanks to Dr. Theresa Thalhamer, Dr. Abed Khalaf, and Dr. Peter Pushparaj for their timely help. I would also like to add a note of thanks to Lamyaa and Justyna for their help.

Finally I would like to thank my friends, Brenda and Caroline and family members including my husband, Pankaj, my in-laws and my parents for their never ending support and blessings in this endeavour.

Abstract

ES-62, a phosphorylcholine (PC)-containing glycoprotein derived from the filarial nematode *Acanthocheilonema viteae* has a plethora of immunomodulatory properties. By virtue of its PC moieties ES-62 has been shown to be anti-inflammatory in nature having the ability to reduce arthritis and asthma in animal models. With respect to this project, it was also shown that ES-62 prevented degranulation of human mast cells by forming a complex with TLR-4 and subsequently sequestering PKC- α away from the high affinity receptor for IgE, Fc ϵ RI. In this work, PKC- α was found to be critical for mast cell degranulation and its degradation provided a mechanism for the ES-62-mediated disruption of key PLD-SPHK-dependent pathways of calcium, PKC and NF- κ B activation. These data raised the possibility that ES-62 could be employed as an anti-allergy drug however is a large molecule and hence immunogenic molecule and PC attachment is nematode-specific. Therefore, 65 small molecule analogues were developed based on PC and tested for their ability to mimic some of the effects of ES-62. On testing these molecules on bone marrow derived mast cells, it was discovered that the mast cells pre-incubated with SMA-63 and SMA-64 when sensitised and cross-linked with the antigen, showed inhibition of peak intracellular calcium mobilization dependent on SPHK. Furthermore, these molecules prevented degranulation in RBL-2H3 cells which is a rat mast cell line. In addition, these molecules reduced levels of IL-6 and TNF- α produced by BMDC activated by cross-linking bound IgE or ionomycin/PMA. Finally, immunofluorescent staining showed that SMAs 63 and 64 and in addition 39, induced the global degradation of PKC- α from both the cytoplasm and the plasma membrane. It can be assumed from these data, that these SMAs particularly 63 and 64 could be taken further to be developed for novel treatment of asthma and other allergic diseases.

CONTENTS	Page
Title page	i
Copyright	ii
Acknowledgements	iii
Abstract	iv
Contents	v
List of Abbreviations	xi
List of Figures	xviii
List of Images	xxv
List of Tables	xxvii

CHAPTER I: INTRODUCTION

1.1 Introduction	1
1.2 Pathogenesis	2
1.2.1 Inflammation	3
(i) Mast cells	3
(ii) Eosinophils	4
(iii) Macrophages and lymphocytes	4
(iv) Th-17	5
(v) Role of IgE	5
1.2.2 Remodelling	9
(i) The Epithelium	9
(ii) Epithelial basement membrane	9
(iii) Smooth Muscle	10
(iv) Nerves	10
1.3 Clinical Features	14
1.4 Management	14

1.8.2.1 ES-62 and its influence on various antibody subclasses	49
1.8.2.2 Effects of ES-62 on B cells and B cell signaling	50
1.8.2.3 Effects of ES-62 on T cell signaling	52
1.8.2.4 Effects of ES-62 on APC (macrophages and dendritic cells)	53
1.8.3 ES-62 and Mast cells	56
1.9 Aims	64

CHAPTER II: MATERIALS AND METHODS

2.1 Reagents	66
2.2 Preparation of Bone marrow derived mast cells	67
(i) Animals	67
(ii) Mast cell culture medium	67
(iii) Culturing of Mast cells	67
(iv) Staining of BMMC	68
2.3 Preparation of PC-conjugated to BSA	69
2.4 Fluorescence activated cell sorting analysis (FACS)	69
2.5 Determination of β -hexosaminidase release in BMMC	70
2.6 Determining the effects of SMAs on cytosolic calcium ion concentration in BMMC	71
(i) Materials	71
(ii) Method	71
2.7 Culturing RBL-2H3 cells	72
(i) Preparation of RBL-2H3 cell line	72
(ii) RBL-2H3 cell culture medium	72
(iii) Maintenance of cell line	73

2.8 FACS analysis for determination of TLR4 receptor on RBL-2H3 cells	73
(i) Harvesting spleen cells	73
(ii) Procedure for FACS	74
2.9 Degranulation of RBL-2H3 cells	74
(i) Materials	74
(ii) Procedure	74
2.10 Effects of SMAs on degranulation of RBL-2H3 cells after 4 hr incubation	75
2.11 Cytokine analysis of BMNC after stimulation with SMAs by	75
Enzyme-Linked Immuno-Sorbent Assay, (ELISAs)	
(i) Materials and methods	76
(ii) Procedure	77
2.12 Preparation of slides for signaling studies	78
(i) Protocol for plating of cells for immunofluorescent staining	78
and preparation of BMNC for staining	
(ii) Materials and methods	78
(iii) Procedure	78
2.13 Analysis of Laser Scanning Cytometry data using WinCYTE software	79
(i) LSC Data collection	79
(ii) Data Analysis	80
2.14 Statistics	80

CHAPTER III: RESULTS

3.1 Small Molecule Analogues	81
3.1.2 List of Small Molecule Analogue formulae	88
3.2 Selection of Assays for Measuring Mast Cell Degranulation	94

3.2.1 Degranulation assay using β -hexosaminidase	94
3.2.2 Degranulation assay employing BMMC	95
3.3 Calcium Mobilisation studies	103
3.4 Degranulation Assay using the RBL-2H3 cell line	120
3.4.1 Degranulation assay with stimulation in the presence of small molecular analogues based on PC	121
3.5 Cytokine Analysis of BMMC after incubation with SMAs	131
3.5.1 Spontaneous IL-6 release	133
3.5.2 IL-6 release after cross-linking of bound IgE	133
3.5.3 IL-6 release with ionomycin/PMA	134
3.5.4 Spontaneous TNF- α release	134
3.5.5 TNF- α release after cross-linking of IgE	135
3.5.6 TNF- α release with ionomycin/PMA	135
3.6 Determination of the effects of SMAs on Protein Kinase C- α , Phospholipase-D and Sphingosine Kinase in BMMC	156
3.6.1 Laser scanning cytometry	156
3.6.2 The effects of SMAs on PKC- α signaling	159
3.6.3 The effects of SMAs on PLD1 signaling	184
3.6.4 The effects of SMAs on SPHK1 signaling	204
 CHAPTER IV: DISCUSSION	
4.1 Introduction	224
4.2 The Hygiene hypothesis and helminths as a link to immunomodulation	224
4.2.1 Studies showing experimental use of worm therapy	225
4.2.2 Helminth molecules with anti-allergy activity	227

4.2.2.1 PAS-1	227
4.2.2.2 Cystatin (Av-17)	228
4.2.2.3 DiAg	231
4.2.2.4 sm-CKBP	234
4.2.2.5 ES-62	235
4.3 Reasons for disparity in mouse BMMC degranulation as compared to human mast cells	239
4.3.1 Effects of SMAs on calcium mobilisation in BMMC	240
4.3.2 Effects of SMAs on degranulation of RBL-2H3 cells	241
4.3.3 Effects of SMAs on levels of IL-6 and TNF- α in BMMC	242
4.3.4 Effects of SMAs on the expression of PKC- α , PLD1 and SPHK1	242
4.4 Categorising of SMAs into inhibitory and stimulatory molecules	244
4.4.1 Therapeutic implications of the use of SMAs as immuno-modulatory drugs	245
4.4.2 Future prospects	248
References	256

LIST OF ABBREVIATIONS

µg	micro gram
µl	micro litre
µM	micro molar
°C	degree centigrade
AAMφ	alternatively activated macrophages
Ab	antibody
AD	atopic dermatitis
Ag	antigen
APAS	allergenic protein of <i>A.suum</i>
APC	antigen presenting cells
Av-17	<i>A.viteae</i> derived cystatin
BAL	broncho alveolar lavage fluid
BCR	B-cell receptor
bm-DC	bone marrow derived dendritic cells
BMMC	bone marrow derived mast cells
BR	blocking reagent
BSA	bovine serum albumin
CaCl ₂	calcium chloride
CCR	C-C chemokine receptor
CD	cluster of differentiation
CDAI	Crohn's disease activity index
CT	cholera toxin
CTLA-4	cytotoxic T lymphocyte antigen-4

CXCL	CXC chemokine ligand
Cys-LTs	cysteinyl leukotrienes
DAG	diacylglycerol
DAPI	4'6'-diamidino-2-phenylindole
DC	dendritic cells
dH ₂ O	distilled water
DiAg	<i>Dirofilaria immitis</i> derived antigen
DMAE	dimethylethanolamine
dMM	deoxymannojirimycin
DNBS	dinitrobenzene sulphonic acid
DNP	dinitrophenol
DSS	dextran sulphate sodium
EAE	experimental autoimmune encephalitis
ECP	eosinophil cationic protein
EDTA	ethylenediaminetetraacetic acid
EGF	epidermal growth factor
EIA	exercise induced asthma
ELISA	enzyme-linked immunosorbent assay
EPO	eosinophil peroxidase
ES	excretory/secretory
ET	endothelin
FcεRI	Fc receptor for IgE
FITC	fluorescein isothiocyanate
Foxp3	forkhead box P3
FSC	forward scatter

Fura-2AM	Fura-2 acetoxymethyl
g	gravity
GDP	guanine diphosphate
GTP	guanine triphosphate
GEO	generalised onchocerciasis
GITR	glucocorticoid induced TNF receptor family related gene
GM-CSF	granulocyte-macrophage colony stimulating factor
gms	grams
H ₂ O ₂	hydrogen peroxide
H ₂ SO ₄	sulphuric acid
HCL	hydrochloric acid
HEL	hen egg lysosyme
hr/s	hour/s
HRP	horseradish peroxidase
HSA	human serum albumin
IBD	inflammatory bowel disease
IFN- γ	interferon gamma
i.g.	intra gastric
IgE	immunoglobulin E
IGF	insulin like growth factor
IL	interleukin
INF	infected
iNOS	inducible nitric oxide synthase
IP3	inositol 1, 4, 5-triphosphate

ITAM	immunoreceptor tyrosine based activation motif
IU	international units
JNK	c-Jun N-terminal kinase
KCl	potassium chloride
KO	knockout
LPS	lipopolysaccharide
LSC	laser scanning cytometry
LTB4	leukotriene B4
LTC4	leukotriene C4
M	molar
mAb	monoclonal antibody
MAPK	mitogen activated protein kinase
MBP	major basic protein
MCP	monocyte chemotactic protein
MEM	minimum essential medium
Mf	microfilariae
MFI	mean fluorescence intensity
mg	milligrams
MgCl ₂	magnesium chloride
MHC	major histocompatibility complex
min	minute/s
MIP	macrophage inflammatory protein
ml	milliliter
mM	millimolar
MyD88	myeloid differentiation primary response gene 88

N	normal
NaCl	sodium chloride
NaHCO ₃	sodium bicarbonate
NaOH	sodium hydroxide
NeM ϕ	nematode-elicited macrophages
NF- κ B	nuclear factor kappa-light-chain
ng	nano grams
NGF	nerve growth factor
NK cells	natural killer cells
nm	nano metre
nM	nano molar
NOD	non-obese diabetic
NO	nitric oxide
NSAIDs	non-steroidal anti-inflammatory drugs
OVA	ovalbumin
OvAg	antigen of <i>O.vovulus</i>
OxPAPC	oxidised 1-palmitoyl-2-arachidonoyl- <i>sn</i> -glycerol-3-phosphocholine
PAF	platelet activating factor
PAS	protein of <i>A.suum</i>
PBMC	peripheral blood mononuclear cells
PC	phosphorylcholine
PCA	passive cutaneous inflammation
PEC	peritoneal cells
PE	phycoerythrin

pg	pico grams
PGD2	prostaglandin D2
PGDF	platelet derived growth factor
PI	patent infected
P-I	phosphatidyl inositol
PIP2	phosphatidylinositol -4, 5 biphosphate
PKC	protein kinase C
PLC	phospholipase C
PLD	phospholipase D
PLP	proteolipid protein
PMA	phorbol myristate acetate
PMT	photomultiplier tubes
PN	peanut
PS	phosphatidylserine
PtdCho	phosphatidylcholine
RANTES	regulated on activation normal T expressed and secreted
RBL	rat basophil cell line
RPMI	Roswell park memorial institute medium
SAv	streptavidin
SCF	stem cell factor
SCID	severe combined immunodeficiency disease
SDS-PAGE	sodium dodecyl sulphate polyacrylamide gel electrophoresis
SHP	Src homology region 2 domain-containing phosphatase

SMA	small molecule analogues
sm-CKPB	<i>S.mansoni</i> derived chemokine binding protein
SPHK	sphingosine kinase
SSC	side scatter
T1D	Type 1 diabetes
TCR	T-cell receptor
tg	transgenic
TGF- β	transforming growth factor beta
TIR	Toll/Interleukin-1 receptor
TLR	toll like receptor
TMB	tetramethylbenzidine
TNF- α	tumour necrosis factor- α
Treg	T regulatory cells
v/v	volume/volume
v/w	volume/weight
VEGF	vascular endothelial growth factor
w/w	weight/ weight
ZAP-70	zeta chain associated protein kinase

LIST OF FIGURES

Figure 1.1	2
Flow chart representing pathogenesis in Asthma	
Figure 1.2	8
Role of IgE in the activation of mast cells	
Figure 1.3	13
Tissue remodeling in Asthma	
Figure 1.4	48
Structure of Phosphorylcholine-glycan of ES-62	
Figure 1.5	63
Mechanism of action of ES-62	
Figure 3.1.1	83
Sulphonamide attachment to the benzyl group (a) <i>via</i> the sulphur atom, (b) <i>via</i> the nitrogen atom.	
Figure 3.1.2	84
Basic structure of Choline	
Figure 3.1.3	84
Structure of Analogue of Choline	
Figure 3.1.4	84
Basic Structure of SMAs	
Figure 3.1.5	85
Structures of the various substituents of methyl groups in choline	

Figure 3.2.1 a, b and c	98
Flow cytometric analysis for co-expression of CD117 and FcεRI receptors on the cultured BMMC	
Figure 3.2.3	102
Histogram showing inadequate degranulation in bone marrow derived mast cells.	
Figure 3.3.1	108
Line graph depicting a decrease in Ca ²⁺ concentration in the presence of ES-62 compared to control cells.	
Figure 3.3.2 a, b and c	115
Line graph depicting an increase in Ca ²⁺ concentration in the presence of SMAs as compared to control cells.	
Figure 3.3.3 a, b and c	117
Line graph depicting a decrease in Ca ²⁺ ion concentration in the presence of SMAs as compared to control cells	
Figure 3.3.4 a, b and c	119
Line graph showing no change in Ca ²⁺ ion concentration in the presence of SMAs compared to control cells.	
Figure 3.4.1 a and b	124
Area graph showing the presence of TLR4 on RBL-2H3 cells by FACS analysis.	
Figure 3.4.2	126
Histogram showing degranulation in RBL-2H3 mast cell line as assessed by release of β-hexosaminidase.	

Figure 3.4.3 a, b and c	128
Histograms of three different experiments showing the effects of SMAs 63, 64, 65 and ES-62 on degranulation in RBL-2H3 cell line.	
Figure 3.4.4	130
Comparison of the mean degranulation values normalised with respect to the BSA control.	
Figure 3.5.1	137
Histograms showing the effects of ES-62 and SMAs on spontaneous IL-6 release.	
Figure 3.5.2 a, b and c	139
Histograms showing the effects of SMAs on IL-6 release when activated with antigen.	
Figure 3.5.3 a, b and c	141
Histograms showing the effects of SMAs on IL-6 release when activated with ionomycin/PMA.	
Figure 3.5.4	147
Histograms showing the effects of SMAs on spontaneous TNF- α release.	
Figure 3.5.5 a and b	149
Histograms showing the effects of SMAs on TNF- α release when activated with antigen.	
Figure 3.5.6 a, b and c	151
Histograms showing the effects of SMAs on TNF- α release when activated with ionomycin/PMA.	
Figure 3.6.1	167
Diagrammatic representation of the various contours used for the analysis in laser scanning cytometry.	

Figure 3.6.1.3 a-e	173
Dot plots and histograms representing gating used for the quantitative analysis of immunofluorescence staining with mouse anti-PKC- α of BMMC exposed to SMAs for sensitised and sensitised/cross-linked samples.	
Figure 3.6.1.4 a and b	175
Histograms representing the % of BMMC expressing detectable levels of PKC- α relative to the isotype control.	
Figure 3.6.1.5 a and b	177
Histogram representing the quantitative analysis of immunofluorescence staining associated with mouse anti-PKC- α binding to BMMC for sensitised and sensitised/cross-linked samples after calculation of Mean Total Fluorescence integral (Wincyte software) following gating of specific staining relative to the isotype control.	
Figure 3.6.1.6 a and b	179
Histogram representing the quantitative analysis of immunofluorescence staining associated with mouse anti-PKC- α binding to BMMC for sensitised and sensitised/cross-linked samples after calculation of Peripheral Fluorescence integral (Wincyte software) following gating of specific staining relative to the isotype control.	
Figure 3.6.1.7 a and b	181
Histogram representing the non cytoplasmic fluorescence obtained by subtracting the peripheral fluorescence values from the total fluorescence within the cell between the sensitised and sensitised/cross-linked samples associated with binding of mouse anti-PKC- α of BMMC	
Figure 3.6.1.8 a and b	183
Histogram representing the Max pixel fluorescence between the sensitised and sensitised/cross-linked samples associated with binding of mouse anti-PKC- α of BMMC	

Figure 3.6.2.3 a-e	193
Dot plots and histograms representing the gating used for the quantitative analysis of immunofluorescence staining with polyclonal rabbit anti-PLD1 of BMMC exposed to SMAs for sensitised and cross-linked samples.	
Figure 3.6.2.4 a and b	195
Histograms representing the % of BMMC expressing detectable levels of PLD1 relative to the isotype control.	
Figure 3.6.2.5 a and b	197
Histogram representing the quantitative analysis of immunofluorescence staining associated with polyclonal rabbit anti-PLD1 binding to BMMC for sensitised and sensitised/cross-linked samples after calculation of Mean Total Fluorescence integral (Wincyte software) following gating of specific staining relative to the isotype control.	
Figure 3.6.2.6 a and b	199
Histogram representing the quantitative analysis of immunofluorescence staining associated with polyclonal rabbit anti-PLD1 binding to BMMC for sensitised and sensitised/cross-linked samples after calculation of Peripheral Fluorescence integral (Wincyte software) following gating of specific staining relative to the isotype control.	
Figure 3.6.2.7 a and b	201
Histogram representing the non cytoplasmic fluorescence obtained by subtracting the peripheral fluorescence values from the total fluorescence within the cell between the sensitised and sensitised/cross-linked samples associated with binding of polyclonal rabbit anti-PLD1 of BMMC.	
Figure 3.6.2.8 a and b	203
Histogram representing the Max pixel fluorescence between the sensitised and sensitised/cross-linked samples associated with binding of mouse polyclonal rabbit anti-PLD1 of BMMC.	

Figure 3.6.3.3 a-e	213
Dot plots and histograms representing the gating used for the quantitative analysis of immunofluorescence staining with polyclonal rabbit anti-SPHK1 of BMMC exposed to SMAs for sensitised and cross-linked samples.	
Figure 3.6.3.4 a and b	215
Histograms representing the % of BMMC expressing detectable levels of SPHK1 relative to the isotype control.	
Figure 3.6.3.5 a and b	217
Histogram representing the quantitative analysis of immunofluorescence staining associated with polyclonal rabbit anti-SPHK1 binding to BMMC for sensitised and sensitised/cross-linked samples after calculation of Mean Total Fluorescence integral (Wincyte software) following gating of specific staining relative to the isotype control.	
Figure 3.6.3.6 a and b	219
Histogram representing the quantitative analysis of immunofluorescence staining associated with polyclonal rabbit anti-SPHK1 binding to BMMC for sensitised and sensitised/cross-linked samples after calculation of Peripheral Fluorescence integral (Wincyte software) following gating of specific staining relative to the isotype control.	
Figure 3.6.3.7 a and b	221
Histogram representing the non cytoplasmic fluorescence obtained by subtracting the peripheral fluorescence values from the total Fluorescence within the cell between the sensitised and sensitised/cross-linked samples associated with binding of polyclonal rabbit anti-SPHK1 of BMMC	
Figure 3.6.3.8 a and b	223
Histogram representing the Max pixel fluorescence staining between the sensitised and sensitised/cross-linked samples associated with binding of polyclonal rabbit anti- SPHK1 of BMMC.	

Figure 4.1

255

Figure suggesting mechanism of action of SMAs as compared with ES-62.

LIST OF IMAGES

Figure 3.2.2	100
Picture of Toluidine blue staining of BMMC showing metachromatic granules indicating the majority of the cells to be mast cells.	
Figure 3.6.1.1 a-j	169
Representative images (40x magnification) of BMMC incubated with mouse anti-PKC- α and anti-mouse IgG2a showing nucleus (blue) and primary antibody (green) in the samples sensitised with DNP-IgE.	
Figure 3.6.1.2 a-j	171
Representative images (40x magnification) of BMMC incubated with mouse anti-PKC- α and anti-mouse IgG2a showing nucleus (blue) and primary antibody (green) in the samples sensitised with DNP-IgE and cross-linked with DNP-HSA.	
Figure 3.6.2.1 a-j	189
Representative images (40x magnification) of BMMC incubated with polyclonal anti-PLD1 and anti-rabbit IgG showing nucleus (blue) and primary antibody (green) in the samples sensitised with DNP-IgE.	
Figure 3.6.2.2 a-j	191
Representative images (40x magnification) of BMMC incubated with polyclonal anti-PLD1 and anti-rabbit IgG showing nucleus (blue) and primary antibody (green) in the samples sensitised with DNP-IgE and cross-linked with DNP-HSA.	
Figure 3.6.3.1 a-j	209
Representative images (40x magnification) of BMMC incubated with polyclonal anti-SPHK1 and anti-rabbit IgG showing nucleus (blue) and primary antibody (green) in the samples sensitised with DNP-IgE.	

Figure 3.6.3.2 a-j

211

Representative images (40x magnification) of BMMC incubated with polyclonal anti- SPHK1 and anti-rabbit IgG showing nucleus (blue) and primary antibody (green) in the samples sensitised with DNP-IgE and cross-linked with DNP-HSA.

LIST OF TABLES

Table 1.1	22
Studies in support of the hygiene hypothesis	
Table 1.2	28
Table showing animal models of asthma	
Table 3.3.1	110
Table depicting the effects of the SMAs on the peak intracellular calcium mobilisation that is mediated by the activation of SPHK	
Table 3.3.2	113
List of SMAs selected for further analysis, depending upon their ability to increase or decrease the initial peak of Ca ²⁺ mobilisation based on SPHK activation	
Table 3.5.1	143
Table showing the results (in percentage) of three different experiments depicting the effects of SMAs on the release of IL-6 in the presence of the antigen	
Table 3.5.2	145
Table representing the results (in percentage) of three different experiments depicting the effects of SMAs on the release of IL-6 in the presence of Ionomycin/PMA	
Table 3.5.3	153
Table showing the results (in percentage) of three different experiments depicting the effects of SMAs on the release of TNF- α in the presence of the antigen	

Table 3.5.4	155
Table showing the results (in percentage) of three different experiments depicting the effects of SMAs on the release of TNF- α in the presence of Ionomycin/PMA	
Table 4.0	238
Table representing the mechanisms of action and effects of various immuno-modulators excreted-secreted by helminths	
Table 4.1	250
Table summarising the effects of SMAs	
Table 4.2 a and b	252
Table representing the final structure of molecules based on their a) inhibitory or b) stimulatory character	

CHAPTER I

INTRODUCTION

1.1 Introduction

Asthma is a chronic inflammatory disorder of the airways. The histo-pathological features consist of denudation of the airway epithelium, collagen deposition beneath the basement membrane, airway oedema, mast cell activation and inflammatory cell infiltration with neutrophils, eosinophils and lymphocytes (especially T- lymphocytes [1]). Hypertrophy of the bronchial smooth muscles and hypertrophy of the mucous glands with plugging of the small airways with thick mucous can occur. This airway inflammation underlies the disease chronicity and contributes to airway hyper-responsiveness, airflow limitation and respiratory symptoms (including recurrent episodes of wheezing, breathlessness, chest tightness, and cough) [1].

Genetic pre-disposition to asthma is also recognised [2, 3]. The strongest identifiable predisposing factor to asthma is atopy. Exposure of sensitive individuals to inhaled allergens increases airway inflammation, airway hyper-responsiveness and allergy symptoms. Symptoms may develop immediately (immediate asthmatic response) or 4-6 hours after allergen exposure (late asthmatic response). Common aeroallergens are associated with house dust mites (often found in pillows, mattresses, upholstered furniture, carpets and drapes), cockroaches, cats and seasonal pollens. Substantially reducing exposure to allergen reduces pathological findings and clinical symptoms [2, 3].

Non-specific precipitants of asthma include exercise, upper respiratory tract infections, rhinitis, sinusitis, post-nasal drip, aspiration, gastro-oesophageal reflux, changes in weather and stress. Exposure to environmental tobacco smoke increases asthma symptoms and need for medications and reduces lung function. Occupational asthma is triggered by the various agents at the work place and may occur weeks to years after the initial exposure and sensitisation [4]. Women may experience

catamenial asthma at predictable times during their menstrual cycles. Non-steroidal anti-inflammatory drugs (NSAIDs) particularly aspirin have a major role in development and precipitation of attacks [5]. Drugs such as propranolol (used as a beta blocker in cardiac conditions and in hypertensive patients), lead to bronchoconstriction and airflow limitation in asthmatic patients.

1.2 Pathogenesis

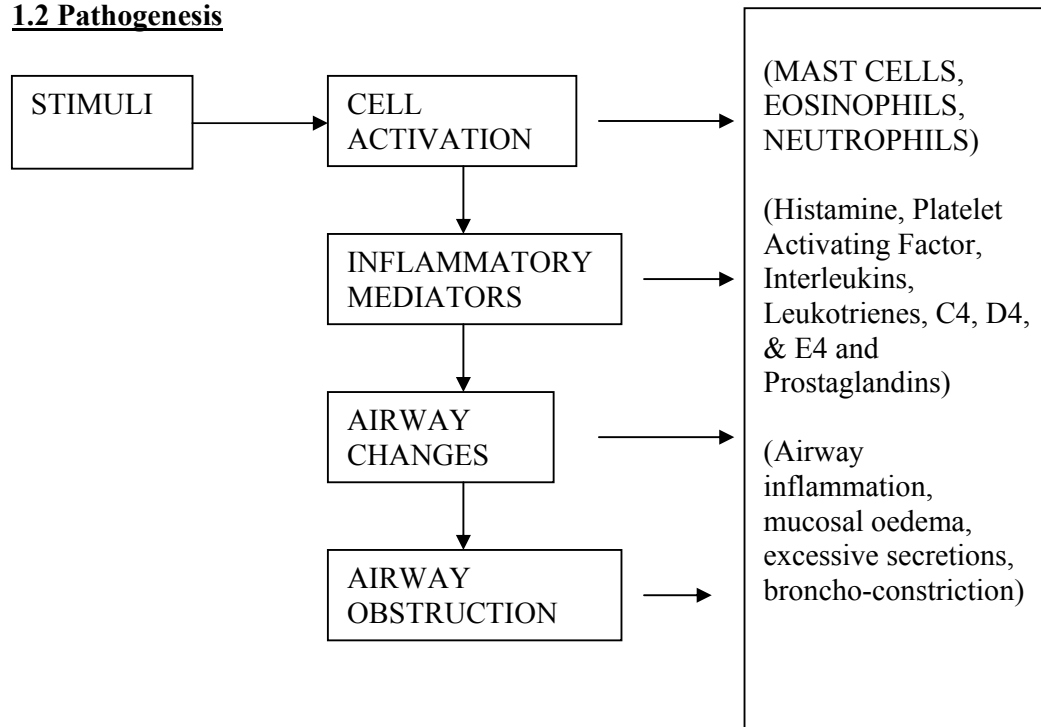


Fig 1.1 Pathogenesis in asthma

Pathogenesis (Fig. 1.1) involves a number of cells, mediators, neuronal cells (a source of neurotrophins which regulate the growth, differentiation and maintenance of neurons) [6] and vascular leakage that can be activated by several different mechanisms, of which exposure to allergens is the most important. The varying

clinical severity and chronicity of asthma is dependent on interplay between a special type of airway inflammation and airway remodelling.

1.2.1 Inflammation

Several key cells are involved in the inflammatory response that characterises asthma.

- (i) Mast cells are increased in both epithelial and surface secretions (sputum) of asthmatics and can generate powerful mediators that act on smooth muscles and small blood vessels. These include preformed mediators when the membrane of mast cells' cytoplasmic granules fuses with the plasma membrane in a process called degranulation. The released mediators include biogenic amines (histamine and little or no serotonin in humans, but both histamine and serotonin in mice and rats), serglycin proteoglycans (such as heparin and chondroitin sulphate), serine proteases (such as tryptases, chymases and carboxypeptidases), and various other enzymes and cytokines and growth factors that can be associated with granules (such as tumour necrosis factor- α (TNF- α) and vascular endothelial growth factor A (VEGFA)). Mast cells activated by the aggregation of the high-affinity receptor for the Fc region of immunoglobulin E (IgE) (Fc ϵ RI) also release lipid-derived mediators. They metabolise arachidonic acid through cyclooxygenase and lipoxygenase pathways, resulting in the release of prostaglandins (particularly prostaglandin D₂ (PGD₂), leukotriene B₄ (LTB₄) and cysteinyl leukotrienes (cys-LTs, particularly LTC₄)). Some activated mast cells can also release platelet-activating factor (PAF). Mast cells are critical trigger cells during episodes of asthma [7-12].

- (ii) Eosinophils are found in large numbers in the bronchial wall and secretions of asthmatics. They are attracted to the airways by eosinophilopoietic cytokines IL-3, IL-5, granulocyte-macrophage colony stimulating factor (GM-CSF) as well as chemokines which attach on type 3 C-C chemokine receptors (CCR-3) (i.e. eotaxin, regulated on activation normal T expressed and secreted (RANTES), monocyte chemotactic proteins -1, 2, 3 & 4 (MCP-1, MCP-2, MCP-3, and MCP-4)). These mediators also prime eosinophils for enhanced mediator secretion. When activated, they release leukotriene C4 (LTC4) and basic proteins such as major basic protein (MBP), eosinophil cationic protein (ECP) and peroxidase (EPO) that are toxic to epithelial cells [7-9].
- (iii) Macrophages and lymphocytes - these cells are abundant in the mucous membranes of the airways and alveoli. Macrophages play a role in the initial uptake and presentation of allergens to lymphocytes. They can release prostaglandins; thromboxane, LTC4, LTB4 and PAF. T-helper lymphocytes (CD4) show evidence of activation in release of their cytokines that play a part in migration and activation of mast cells (IL-3, IL-4, and IL-9) and eosinophils (IL-3, IL-5 and GM-CSF). In addition, production of IL-4 leads to maintenance of an allergic (Th2) T cell phenotype, favouring switching of antibody production by B-lymphocytes to IgE. In asthma, there occurs a selective up-regulation of Th2 type cells with reduced evidence of a Th1 immune response (cells producing IFN- γ and IL-2). This polarisation is mediated by dendritic cells and involves antigen presentation, co-stimulation and exposure to polarising cytokines (IL-4 and IL-5, IL-13) [8-13].

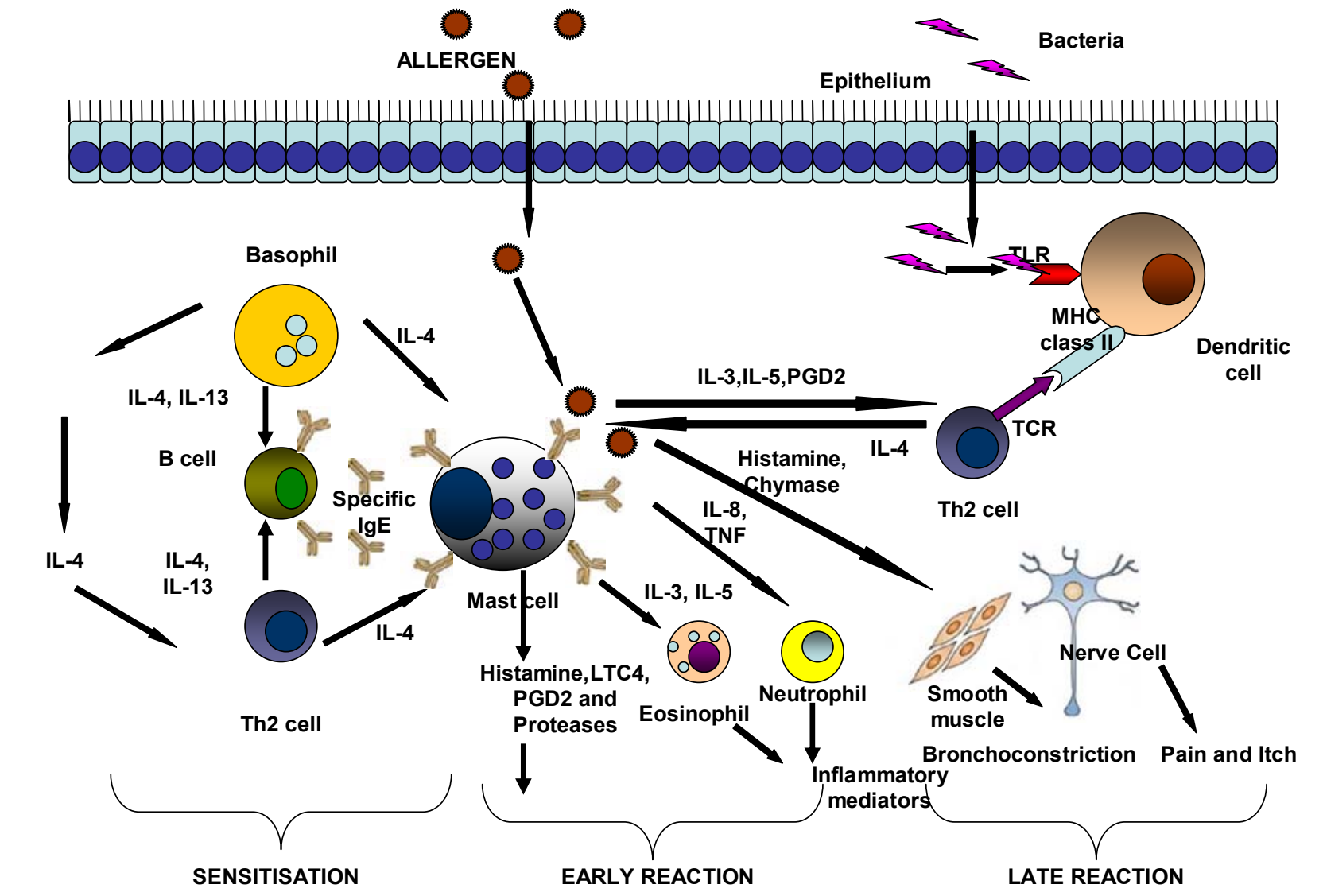
- (iv) Th-17- It has been proposed that following antigenic stimulation, CD4⁺ T cells differentiate into various subsets to enable different effector functions namely Th1, Th2, Treg and the recently discovered Th-17. These IL-17 producing cells have been implicated in tissue inflammation and autoimmunity [14-16]. Th-17 cells are characterised by the production of IL-17A and IL-17 F and to a lesser extent IL-6 and TNF- α . IL-6 has been shown to be a remodelling associated cytokine while TNF- α is a powerful pro-inflammatory cytokine [17-20]. However, in lieu of the above reports, some findings suggest a more regulatory role for Th-17 cells. One of the chains of thought suggests that the IL-17-IL-22 axis aids alleviation of asthma in its resolution phase. As shown in a study in mouse models of asthma, IL-17 assisted in the initiation of allergic asthma. However, during the effector phase, neutralisation of IL-17 augmented the allergic response in sensitised mice. On the other hand, exogenous IL-17 reduced pulmonary recruitment, bronchial hyperactivity and chemokine production [21]. In another study, it was shown that neutralisation of IL-22 in the lungs of mice during an allergic response, further augmented eosinophil recruitment. Similarly, pre-incubation with IL-17A abolished DC-driven eosinophil recruitment, thus indicating that both Th-17 cytokines attenuated allergic responses [22].
- (v) Role of IgE in the activation of mast cells - Immunoglobulin IgE occupies a key role in the pathogenesis of allergy. IgE is produced by B-lymphocytes that directly interact with allergen but their production is also dependent on co-stimulation and cytokines produced by activated T cells. Allergen-specific IgE antibodies are produced within a few weeks after

exposure to the particular antigen and are released into the bloodstream. These IgE antibodies may attach to receptors on inflammatory cells such as mast cells. When an allergic individual re-encounters the allergen, cross-linking of IgE bound on the mast cells results in the release of chemical mediators such as histamine, prostaglandins and leukotrienes. These chemical mediators can cause inflammatory responses in the body. Such inflammatory responses have been linked to signs and symptoms of asthma [23, 24] (Fig.1.2 depicts the role of IgE in the activation of mast cells [26]).

One of the earlier classifications has divided asthma into ‘intrinsic’ asthmatics who tend to have a later onset of the disease, no obvious allergic triggers and a low level of IgE in the blood stream; and ‘extrinsic’ asthmatics who tend to have the onset of the disease at an earlier age, more obvious allergic triggers and elevated levels of IgE [25]. This classification is being reconsidered, because biopsies of airways from both allergic and non-allergic airways show evidence of high affinity receptors for IgE as well as evidence of the presence of IL-5, IL-9 and IL-13, the cytokines associated with Th2 lymphocytes. While studies have shown that increasing levels of IgE within the blood stream are associated with increased risk of asthma and other atopic disorders, many patients with elevated levels of IgE do not have asthma. It is also important to note that in patients with asthma, the serum IgE level does not appear to be a predictor of severe airflow obstruction, in contrast to the correlation between circulating eosinophil numbers and obstructive physiology.

Fig.1.2

Role of IgE in the activation of mast cells showing sensitisation phase where antigen specific IgE is synthesised by B cells (with the assistance from T cells and basophils) under the influence of IL-4 and IL-13; early reaction showing the release of mast cell mediators such as histamine, LTC₄ and PGD₂ that affect the mucosa, blood vessels and sensory nerves and late phase consisting of release of other mediators such as IL-3, IL-5, IL-8, TNF, that effect the nerve cells, smooth muscles, endothelial cells and epithelium. There is activation of other antigen presenting cells (dendritic cells) due to the loss of barrier function. (Adapted from Ref. 26)



1.2.2 Remodelling

The characteristic feature of asthma is an alteration of structure and function of formed elements of the airway. These structural changes interact with inflammatory cells and mediators to cause characteristic features of the disease. Deposition of the matrix proteins, swelling and other cellular infiltrates cause an expansion of the sub-mucosa beneath the epithelium so that for a given degree of smooth muscle shortening, there is excess airway narrowing. Swelling outside the smooth muscle layer (in the adventitial layer) spreads the retractile forces exerted by the surrounding alveoli over the greater surface area so that the airways close more easily. These factors as well as the alteration of the smooth muscle contractility cause the hyper-responsiveness, characteristic of asthma. Several factors contribute to these changes [6]. Fig 1.3 represents diagrammatic representation of tissue remodelling in asthma [26].

i) *The epithelium*: In asthma, there is desquamation of the epithelium into the lumen of the bronchi leading to damage to the conducting airways [27]. The epithelium also undergoes metaplasia with resultant increase in the number and activity of the mucous-secreting goblet cells. The epithelium is the major source of mediators, cytokines and growth factors that serve to enhance inflammation and promote tissue remodelling. Damage and activation of the epithelium makes it more vulnerable to infection by common respiratory viruses, e.g. rhinovirus, corona virus, and to the effects of air pollutants [28, 29].

(ii) *Epithelial basement membrane*: A pathognomic feature of asthma is the deposition of repair collagens (type I, III and IV) on the lamina reticularis beneath the basement membrane in the lungs. This, along with the deposition of other matrix proteins such as laminin, tenascin and fibronectin causes the appearance of a

thickened basement membrane. This collagen reflects activation of an underlying sheath of fibroblasts that transform into contractile myofibroblasts. Aberrant signaling between the epithelium and underlying myofibroblasts is thought to be the principal cause of airway wall remodelling, since the cells are prolific producers of a range of tissue growth factors such as epidermal growth factor (EGF), transforming growth factor β (TGF- β), connective tissue-derived growth factor, platelet-derived growth factor (PDGF), endothelin (ET), insulin like growth factors (IGF), nerve growth factors and VEGF. Increased deposition of collagen, proteoglycans and matrix proteins creates a micro-environment conducive to the on-going inflammation since these complex molecules possess important cell-signaling functions which prolong inflammatory cell survival and prime them for mediator secretion [7, 30, 31].

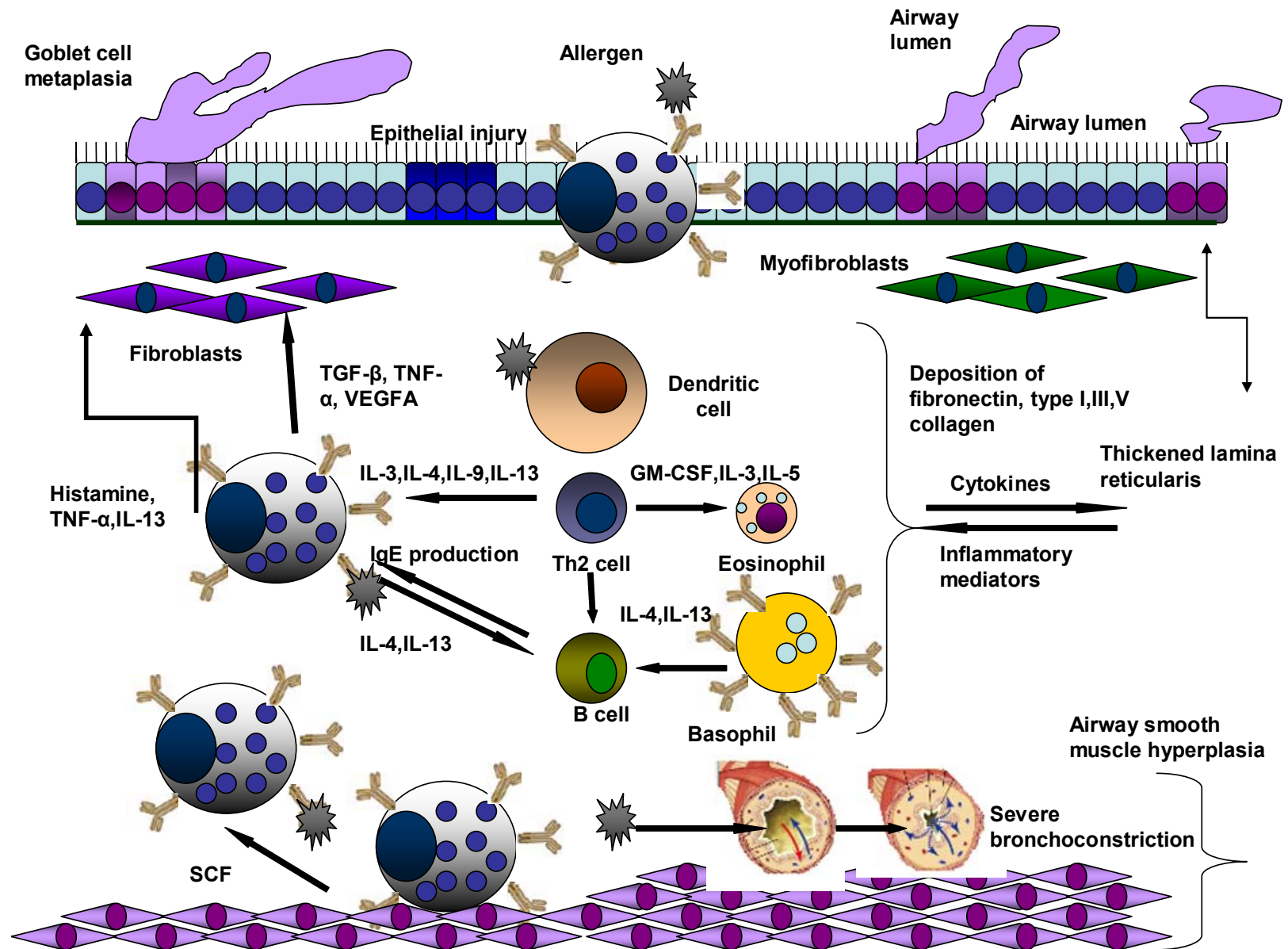
(iii) *Smooth muscles*: A prominent feature of asthma is the hyperplasia of the helical band of airway smooth muscles. In addition to increasing in amount, the smooth muscle alters in function to contract more easily and stays contracted because of the changes in actin-myosin cross-link cycling. These changes allow the asthmatic airways to contract too much and too easily at the least provocation [32].

(iv) *Nerves*: Central and peripheral neural reflexes, both contribute to the irritability of asthmatic airways [33]. It has been shown that neuropeptides released from sensory nerve endings are potential mediators of airway inflammation in asthma and lung injury. Evidence of an increase in the neurotrophins such as nerve growth factor (NGF) was found in the serum of patients with asthma and allergy [34]. It was also demonstrated that in genetically modified animal models, overexpression of neurotrophins in peripheral body tissues resulted in sensory hyperinnervation. Transgenic mice with constitutive NGF overexpression exhibited an increased

number of neuropeptide-containing sensory as well as sympathetic nerve fibers in the airways[6].

Fig 1.3

Diagrammatic representation of tissue remodelling in asthma showing the effects of eosinophils, basophils, neutrophils, antigen presenting cells, T cells, B cells and mast cells in the tissues in the case of chronic asthma. There are structural changes initiated by the cells from innate and adaptive immune system and epithelial cells, fibroblasts, myofibroblasts and airway smooth muscle cells, blood vessels, lymphatic vessels and nerves. These changes lead to thickening of the airway walls, deposition of extracellular matrix proteins and hyperplasia of goblet cells and increased mucous production leading to constriction of the bronchioles and airway narrowing. (Adapted from Ref. 26)



1.3 Clinical features: Asthma is characterised by episodic wheezing, difficulty in breathing, chest tightness, and cough. The frequency of occurrences of the asthma symptoms is highly variable. Some patients may have only chronic dry cough and others a productive cough. Some patients have infrequent, brief attacks of asthma and others may suffer with near continuous symptoms. Asthma symptoms may occur spontaneously or may be precipitated by many different triggers. Asthma symptoms are frequently worse at night; circadian variations in the bronchomotor tone and bronchial reactivity reach their nadir between 3am and 4am, increasing the symptoms of broncho-constriction. Some physical findings increase the probability of asthma. Nasal mucosal swelling, increased nasal secretions and nasal polyps are often seen in patients with allergic asthma. Eczema, atopic dermatitis, or other manifestations of allergic skin disorders may also be present. Hunched shoulders and use of accessory muscles of respiration suggests laboured breathing. Chest examination may be normal between exacerbations in patients with mild asthma. Wheezing during normal breathing or a prolonged forced expiratory phase correlates well with the presence of airflow obstruction whereas wheezing during forced expiration does not. During severe asthmatic exacerbations, airflow may be too limited to produce wheezing and the only diagnostic clue during auscultation may be globally reduced breath sounds with prolonged expiration [35, 36].

1.4 Management:

1.4.1 Control of extrinsic factors

(i) Measures must be taken to avoid all the causative agents particularly in childhood. This emphasises the importance of rapid identification of extrinsic causes of asthma and their removal wherever possible (for example, occupational agents, and family

pets). This is because of the fact that once extrinsic asthma is initiated, it may become self-perpetuating. (ii) Cessation of smoking should be encouraged in asthmatic patients.

1.4.2 Drug treatment [37, 38, 39]

1.4.2a Anti-inflammatory drugs

(i) *Inhaled Corticosteroids*, also called glucocorticoids or steroids, are powerful anti-inflammatory drugs. Steroids do not relax the airways and have little effect on symptoms. Instead, they reduce inflammation and prevent permanent injury in the lungs. They can also help prevent asthma attacks from occurring. Many studies have shown that the use of inhaled corticosteroids in patients with moderate-to-severe asthma significantly reduces the rate of re-hospitalizations and deaths from asthma. Inhalation of corticosteroids makes it possible to provide effective local anti-inflammatory activity in the lungs with minimal systemic effects. Inhaled corticosteroids are recommended as the primary therapy for any asthmatic condition more serious than occasional episodes of mild asthma. Low-doses of inhaled steroids may even be safe and effective for some people with mild asthma, particularly those who find themselves using beta2-agonists daily or when treatment with bronchodilators alone is not effective. Examples of inhaled corticosteroids include fluticasone, budesonide, triamcinolone, and flunisolide. In general, these newer steroids are more powerful than the older generation of inhaled steroids (beclomethasone and dexamethasone). These steroids are sometimes combined with a long-acting beta2-agonist in a single inhaler. Traditionally, patients have been advised to take corticosteroids on a daily basis. However, intermittent corticosteroid therapy may be appropriate for some patients with mild persistent asthma. Optimal timing of the dose is important and may vary depending on the medication. Most of

the newer inhaled steroids and even some older ones are now available as a single daily dose. Inhaled steroids are generally considered safe and effective and only rarely cause any of the more serious side effects such as osteoporosis, hypertension and diabetes reported with prolonged use of systemic steroids [40, 41].

1.4.2b Bronchodilators

(i) *Cromolyn* sodium is both an anti-inflammatory drug and has anti-histamine properties that blocks asthma triggers such as allergens, cold, or exercise. Nedocromil is similar to cromolyn. It is often used in children with allergic asthma. In addition, it has been an important drug of choice for exercise-induced asthma (EIA) in all age groups and including pregnant women. Both cromolyn and nedocromil appear to be useful for patients with aspirin-induced asthma. These drugs do not effectively treat asthma once an attack is underway. They also have very little long-term benefits on lung function compared to inhaled corticosteroids [40-42].

(ii) *Beta2-Agonists* a) *Short acting beta-2 agonists* act on the β_2 adrenergic receptor, thereby causing smooth muscle relaxation resulting in dilation of bronchial passages. All beta2 agonists are available in an inhaler form (either metered-dose inhalers, which aerosolize the drug, or dry powder which can be inhaled). Salbutamol also comes in a solution form for nebulisation, which is more commonly used than inhalers in emergency rooms. Salbutamol and terbutaline are also available in oral forms. b) *Long acting beta-2 agonists* are used in combination with inhaled corticosteroids for treating patients with moderate-to-severe asthma. These drugs include salmeterol and formoterol. Long-acting beta2-agonists are used for preventing an asthma attack (not for treating attack symptoms). The effects of one dose of a long-acting beta2-agonist last for about 12 hours, so they are particularly effective during the night. These drugs may also be used for prevention of EIA and to

protect against aspirin-induced asthma. The use of long-acting beta2-agonists is recommended only if other medicines (such as steroids) have not helped in controlling asthma. A short-acting bronchodilator is used to treat sudden wheezing [42].

(iii) Phosphodiesterase inhibitors such as *Theophylline* relax the muscles around the bronchioles and also stimulate breathing. They have anti-inflammatory qualities, enhance mucociliary clearance and strengthen diaphragmatic contractility. Chronic smokers metabolize theophylline much more quickly and require higher doses of the drug than non-smokers; prolonged-release versions are helpful for such people. Too much caffeine can increase the concentration of this drug and the amount of time it stays in the body. Theophylline also interacts with many other drugs that are taken for other common medical conditions, including asthma [42].

1.4.2c Leukotriene-Antagonists also called anti-leukotrienes or leukotriene modifiers are oral medications that block leukotrienes. Leukotrienes can cause inflammation and spasms in the airways of people with asthma. As with other anti-inflammatory drugs, leukotrienes-antagonists are used for prevention and not for treating acute asthma attacks. Leukotriene-antagonists include zafirlukast, montelukast, zileuton, and pranlukast. These drugs are proving to be effective for long-term prevention of asthma, including EIA and aspirin (or NSAID)-induced asthma.

1.4.2d Immuno-sensitisation for specific allergens may be considered in selected asthma patients who have exacerbations of asthma symptoms when exposed to allergens to which they are sensitive to, but who do not respond to environmental control measures or other forms of conventional therapy [40-42].

1.4.2e Omalizumab is a recombinant antibody that binds to IgE without activating mast cells. It is approved for patients aged 12 and older, who have moderate to severe persistent asthma related to allergies. Omalizumab is administered by injection every 2 - 4 weeks. It is used only to treat patients whose symptoms are not controlled by inhaled corticosteroids. Omalizumab prevents the IgE from triggering the inflammatory events that lead to asthmatic attacks. Studies have shown excellent benefits of the drug, including a reduced need for corticosteroids, fewer hospitalizations, and significant symptomatic improvements [43].

1.5 Side effects of asthma medications

(i) Corticosteroids- The most common side effects are throat irritation, hoarseness, and dry mouth. These effects can be minimized or prevented by using a spacer device and rinsing the mouth after each treatment. Rashes, wheezing, facial swelling (oedema), fungal infections (thrush) in the mouth and throat, and bruising are also possible but not common with inhalators. There is higher risk of developing cataracts in patients over the age of 40 with steroid therapy. Some studies report a higher risk for bone loss in patients who take inhaled steroids regularly, a side effect which is known to occur with oral steroids. A number of bone-preserving medications are now available that might safely offset this effect such as calcium supplements and Bisphosphonates. There is some concern that the more potent drugs, particularly fluticasone, suppress the adrenal system (which secretes natural steroids) to a greater degree than other steroid inhalants. This is a serious side effect of oral steroids [40].

(ii) Beta 2 agonists a) Short acting beta-2 agonists- Side effects such as insomnia, anxiety, and tremors occur in some patients. b) Long-acting beta2-agonists- can worsen asthma by increasing symptom severity. These drugs may also increase the

risk for asthma-related deaths. Experts are still trying to determine when long-acting beta₂-agonists should be added to an asthma treatment plan. Warnings for salmeterol and formoterol products emphasise that these medicines can increase the risk of severe asthma episodes. If these episodes occur, they can be fatal. Long-acting beta₂-agonists require up to 20 minutes to achieve effectiveness, and there is a danger of overdose if a patient is not aware of this delay and takes additional doses to achieve faster relief [41].

(iii) Side effects of Cromolyn include nasal congestion, coughing, sneezing, wheezing, nausea, nosebleeds, and dry throat. Nedocromil has an unpleasant taste, and some people have complained of nausea, headache, and spasms in the airways, but no serious side effects have been reported.

(iv) Leukotriene-antagonists- Gastrointestinal distress is the most common side effect of leukotriene-antagonists. Churg-Strauss syndrome has been reported in a few people taking zafirlukast or montelukast. Churg-Strauss syndrome is very rare, but it causes blood vessel inflammation in the lungs and can be life threatening. Other concerns are indications of liver injury in patients taking zileuton and zafirlukast when taken at higher than standard doses. No adverse effects on the liver have been reported to date with montelukast.

(v) Theophylline- If it is not taken exactly as prescribed, an overdose can easily occur. Toxicity can cause nausea, vomiting, headache, insomnia, and, in rare cases, disturbances in heart rhythm and convulsions [42].

(vi) Omalizumab -1 in 1,000 patients who take omalizumab develops anaphylaxis (a life-threatening allergic reaction). Some patients can develop anaphylaxis after any dose of Omalizumab. The patients can even develop an anaphylactoid as well as serum sickness type reaction after the first dose because although it is a more than

90% humanised monoclonal antibody, some of other biological agents used in its manufacturing can cause a reaction. Anaphylaxis may occur up to 24 hours after the dose is given. Anaphylaxis symptoms include difficulty in breathing, chest tightness, dizziness, fainting, itching, hives, and swelling of the mouth and throat [41, 42, 44]

1.6 Hygiene hypothesis

The ‘Hygiene hypothesis’ proposes that the increase in allergic and autoimmune diseases like asthma, dermatitis, inflammatory bowel disease (IBD), multiple sclerosis and diabetes in the West has been due to the decrease in the incidence of infections such as those due to helminths during childhood. Strachan was the first to propose a link between hygiene and allergic diseases in the West [45]. He reported an inverse relationship between family size and the development of allergic disorders. This can be attributed to better lifestyle, improved sanitation and a clean sterile environment due to which the “normal” development of the immune system has been compromised. Thus, there is no priming of the immune system in childhood by various bacterial, viral and helminthic infections. This hypothesis is tested by the following studies, which suggest that stimulation of the immune system by helminthic infections protects against aberrant immune responses, which cause autoimmune diseases and allergic disorders. It was reported by van de Biggelaar that treatment of children chronically infected with *A. lumbricoides* and *T. trichiura*, resulted in an increase in allergic skin sensitivity [46] while an active infection with geohelminths (*A. lumbricoides* or *Ancylostoma duodenale*) was protective against development of allergen skin test reactivity [47]. A study conducted by Rodrigues *et al* noted that children with heavy infections with *T. trichiura* in early childhood had a significantly low prevalence of allergen skin reactivity later in childhood even in the

absence of *T. trichiura* infection at the time of skin testing later in childhood [48]. In an investigation of young children in Ethiopia, between the ages of 1-4 years, it was observed that infection with *Ascaris* and hookworm offered protection against wheeze [49]. Furthermore, infection with *Schistosoma mansoni* resulted in reduction in the severity of asthma in a rural group endemic for the infection [50]. Table 1.1 shows relevant studies in support of the hygiene hypothesis.

Study	Observation	Reference
Strachan 1989	An inverse relationship between family size and the development of allergic disorders.	45
van den Biggelaar 1997	Anthelmintic treatment of chronically infected (<i>Ascaris lumbricoides</i> and <i>Trichuris trichiura</i>) children resulted in an increase in allergic skin sensitivity.	46
Cooper 2003	Active infection with geohelminths (<i>Ascaris lumbricoides</i> or <i>Ancylostoma duodenale</i>) was protective against allergen skin test reactivity.	47
Rodrigues 2008	Children with heavy infections with <i>Trichuris trichiura</i> in early childhood had a significantly low prevalence of allergen skin reactivity later in childhood even in the absence of <i>T. trichiura</i> infection at the time of skin testing later in childhood.	48
Dagoye 2003	Infection with <i>Ascaris</i> and hookworm offered protection to young Ethiopian children against wheeze.	49
Medeiros 2003	Reduction in severity of asthma in rural group endemic for <i>S. mansoni</i> infection.	50

Table 1.1 Studies in support of hygiene hypothesis.

1.6.1 Animal models of asthma

The hypothesis regarding protection of the host from inflammatory and auto-immune diseases by helminths was tested in various murine models.

BALB/cByJ mice were infected with the nematode parasite *S. stercoralis* prior to ovalbumin (OVA) immunization and intratracheal challenge. Broncho-alveolar lavage fluid (BAL) was collected and cellular and humoral immune responses were measured. It was hypothesized that the presence of a Type 2 response to parasite antigens would hinder the development of Type 2 responses to the allergen. Intracellular cytokine staining revealed increased IL-4 and IL-5 producing cells in the BAL from mice infected with *S. stercoralis* before OVA sensitization. Increased IL-5 protein levels and decreased IFN- γ protein levels were also observed in the BAL. The findings of this study, however, clearly demonstrated that infection with *S. stercoralis* prior to exposure to OVA resulted in decreased eotaxin levels, static eosinophil infiltration and a virtual absence of OVA-specific IgE in the lungs. These results suggested that a pre-existing helminth infection might potentiate a systemic Type 2-type response yet simultaneously suppress, in the lungs, allergen-specific IgE responses and eotaxin levels in response to subsequent exposure to allergens [51].

Kitagaki *et al* demonstrated that intestinal helminths (*Heligmosomoides polygyrus*) protected against atopic responses in murine models of asthma [52] by suppressing the airway eosinophilic inflammation in mice sensitised with OVA. Bronchial hyper-reactivity and *in vitro* allergen-recall Th2 responses were also suppressed and in an IL-10 dependent manner. In the worm-infected mice, both total and OVA-specific IgE levels were enhanced and this corresponded with the suppression of both total IgG2a and OVA specific IgG2a. It was observed that Con A-induced splenocyte IL-5 release was significantly and similarly increased in each

of helminth-infected, OVA-challenged and helminth-infected/OVA challenged mice. This finding suggested a non-specific systemic Th2 bias induced by both the parasites and the atopic inflammation. In addition, OVA-induced IL-5 release was suppressed both in the helminth-infected group and helminths-infected/OVA challenged group which demonstrated a Th2-skewed response following helminthic infection. [52]

In another study, by Bashir *et al* [53], a mouse model was tested for protection offered by *H. polygyrus* infection against food allergy. It was noticed that the anaphylactic symptoms, on administration of intragastric (i.g.) peanut (PN) Ag in the presence of the Th2-inducing mucosal adjuvant cholera toxin (CT), were greatly reduced in the helminth-infected mice. It was also observed that the failure to induce a PN Ag specific allergic response was directly related to the inability of the mice to generate PN-specific IL-13. The down-regulation of Ag-specific IgE observed was also correlated to a reduction in the generation of Ag-specific T cells secreting IL-13. Treatment of infected mice with neutralising Abs to IL-10 abrogated infection-mediated protection against allergic symptoms. In this report, it was concluded that chronic helminth infection could block the induction of allergen-specific IgE by influencing the behaviour of the Ag-specific T-cells that were required for this response. The reduction in allergen-specific IgE correlated with the abrogation of anaphylactic symptoms. It was speculated by the authors that, in their model, the effects of parasite-induced immuno-regulation (mediated, at least in part, via IL-10) occurred at the level of allergen presentation by APC, presumably dendritic cells.

In a further study, mice were infected intra-peritoneally with third stage larvae of a mouse- adapted strain of *Nippostrongylus brasiliensis* by Wohlleben *et al* [54]. The larvae and the adult worms induced strong Th2 responses, first in the lung and then in the gut, which were responsible for the elimination of the parasites. It was

reported that infection with *N. brasiliensis* reduced the production of eotaxin in the airways and inhibited the development of allergen-induced airway eosinophilia with the effect being dependent on the time point of infection. This effect was not observed in mice deficient of IL-10. This result suggested that infection with *N. brasiliensis* induces the production of IL-10, which then leads to the suppression of allergen-induced airway eosinophilia and reduction in the production of eotaxin.

In 2005, it was shown by Itami *et al* that different protein components from *A. suum* had opposite effects on a murine model of experimental asthma [55]. The allergenic protein of *A.suum* (APAS-3) was able to induce allergic asthma, demonstrated by eosinophilic inflammatory infiltrate in airways and lungs, the production of anaphylactic antibodies, the induction of IL-4, IL-5, eotaxin and RANTES and the presence of pulmonary hyper-responsiveness. The immunomodulatory protein of *A.suum* (PAS-1) suppressed this response elicited by APAS-3. It was also reported that PAS-1 had a potent anti-inflammatory activity because of its ability to stimulate IL-10 and TGF- β production in macrophages, thus leading to the inhibition of pro-inflammatory cytokine production [56]. In addition, PAS-1 suppressed IgE and anaphylactic IgG1 antibody production induced by APAS-3. The suppressive effect of PAS-1 on eosinophil influx into airway and lung tissue was also confirmed by the inhibition of EPO activity detected in these sites. The suppression of eosinophilic inflammation by PAS-1 was thought to be due to the reduction in IL-5 and eotaxin production, both of which are potent chemo-attractants for eosinophils [57, 58, and 59]. Furthermore, RANTES, another eosinophil chemo-attractant [60, 61], was also decreased by PAS-1 in the asthma model, indicating that the eosinophil migration might have been diminished because of this suppressive effect too. Further studies involving the PAS-1 component of *A.suum* revealed that its

immunomodulatory effect was mediated through IL-10 and IFN- γ . This was evident from the fact that IFN- $\gamma^{-/-}$ and IL-10 $^{-/-}$ mice immunised with OVA+PAS-1 developed allergic inflammation similar to OVA-immunised mice. In contrast, it was noticed that IL-12 $^{-/-}$ as well as wild type mice presented with an intense suppression of the allergic response when immunised with OVA+PAS-1. In addition the researchers observed that production of anti-OVA IgG1 and anti-OVA IgE and polyclonal IgE were inhibited in wild type mice. The same was true for IL-12 $^{-/-}$ but not IFN- $\gamma^{-/-}$ and IL-10 $^{-/-}$ mice. This suppression correlated with inhibition of IL-4 whereas high levels of IgG1 and IgE and IL-4 were found in IFN- $\gamma^{-/-}$ and IL-10 $^{-/-}$ mice. Similarly, there was no inhibition of IL-5, airway eosinophilia, EPO, eotaxin, IL-13 secretion in wild type, IL-12 $^{-/-}$ IFN $^{-/-}$ and IL-10 $^{-/-}$ C57BL/6 mice models [62].

Wilson and group elucidated that the helminth-driven suppression of effector functions after sensitisation of the animals can be transferred from infected mice to uninfected, pre-sensitised animals by mesenteric lymph node cells. They further proposed that the protection was associated with CD4 $^{+}$ CD25 $^{+}$ T cells. It was found that mice infected with *H. polygyrus* were found to have significantly lower levels of cellular infiltrates including macrophages, lymphocytes, eosinophils and neutrophils after OVA and Der p1 challenge in BALB/c and C57BL/6 models respectively. On staining of the airway epithelium, it was noticed that the inflammation was greatly reduced and there was a decrease in peribronchial and perivascular cellular infiltration along with a reduction in goblet cell numbers. It was noticed that the Th2-driving cytokine IL-4 was unaffected. However, the Th2 effector cytokines IL-5 and IL-13 were diminished, as was the inflammatory phase within the lung. There was an elevation of IL-10 in C57BL/6 mice while TGF- β was increased in BALB/c animals. Therefore, it was postulated that helminth infections down-regulated allergic

reactions through the action of regulatory T cells rather than by altering the Th1–Th2 balance. Furthermore, they observed that the mesenteric lymph node cells from infected mice contained a significantly higher number of CD4⁺CD25⁺Foxp3⁺ cells. In addition, they revealed that despite the prominence of IL-10 production by *H. polygyrus* exposed-T cells, their ability to suppress airway allergy was not mediated by IL-10. This was attributed to the fact that mesenteric lymph node cells from infected IL-10^{-/-} mice were found to mediate suppression. The findings were consistent with the results that anti-IL-10R antibodies did not reverse suppression in the infected animals. On the contrary, they discovered that on the administration of anti-CD25, the airway infiltration was restored in the infected animals [63]. Taken further, they demonstrated that on transfer of both CD4⁺ and CD4⁻ T cells from the infected animals to Der p1 sensitised and challenged animals, there was a reduction in the airway infiltration, eosinophilia, IL-5 levels, and eotaxin levels. The authors also revealed that there was no alteration in the levels of total and Der p1-specific IgE in the control and recipient animals [64].

In studies by Hartmann and team, it was observed that concomitant infection with *H. polygyrus* reduced airway hyper-responsiveness in sensitised and challenged BALB/c mice when compared with uninfected animals. However in the case of atopic dermatitis, there was no infection-induced change in eczematous skin lesions when compared with the control animals [65].

Table 1.2 summarises some studies on animal models of asthma.

Study	Animal	Nematode Species	Observation
Wang C 51	BALB/cByj	<i>Strongyloides stercoralis</i>	↑ in IL-4, IL-5 ↓ IFN- γ , ↓ OVA specific IgE responses, ↓ in eotaxin
Kitagaki 52	BALB/c	<i>Heligosomoides polygyrus</i>	↓ OVA-induced asthma, ↓ in IL-5 ↑ in IL-10
Basher 53	C3H/Hej	<i>H. polygyrus</i>	↓ Ag specific IgE, ↓ IL-13
Wohlleben 54	C57BL/6	<i>Nippostrongylus brasiliensis</i>	↓ Allergen induced airway eosinophilia ↓ airway eotaxin levels ↓ Ova –specific IgG1 and IgE in BAL
Itami 55	BALB/c	<i>Ascaris suum</i> PAS-1(suppressive effect)	↓ airway eosinophilia and hyperresponsiveness ↓ IL-4, IL-5, eotaxin, RANTES, ↓ IgG1 and IgE ↑ in IL-10
Araujo 62	C57BL/6	<i>A. suum</i> PAS-1(suppressive effect)	↓ airway eosinophils, eosinophil peroxidase activity. ↓ IL-4, IL-5, IL-13, eotaxin, ↓ IgG1 and IgE IL-10 and IFN- γ dependent effects
Wilson 63	BALB/c C57BL/6	<i>H. polygyrus</i>	↓ macrophages, lymphocytes, eosinophils and neutrophils in airways. ↓ IL-5, IL-13
Wilson 64	BALB/c C57BL/6	<i>H. polygyrus</i>	↓ airway infiltration, eosinophilia, IL-5 levels, and eotaxin
Hartmann 65	BALB/c	<i>H. polygyrus</i>	↓ airway hyper-responsiveness ↓ OVA-specific IgE ↑ in IL-10

Table 1.2 Table showing animal models of asthma

1.7 Host responses towards helminth infections

The protective effect of helminths in models of allergy and autoimmunity clearly reflects their effects on the immune system. This section considers examples of these effects in more detail.

1.7.1 Classical Th2 response

As opposed to chronic infection, an acute infection with helminths generates a classical CD4⁺ Th2 response that incorporates various effector mechanisms to control the infection. Th2 cells induce the activation and expansion of leukocytes through the production of cytokines such as IL-4, IL-5, IL-9 and IL-13. Studies have shown that IL-4 and IL-13 could directly affect cell populations that express the IL-4R. In addition, IL-4R signaling is dependent on the action of signal transducer and activator of transcription 6 (STAT6). In the BALB/c mouse model infected with *H.polygyrus*, STAT6 influenced changes in epithelial cell function, increased smooth muscle contractility, increased mucus production and increased fluid in the gut lumen through increases in PGE2 and histamine. An increase in the permeability of mucosal epithelial cells and a decrease in sodium dependent glucose absorption, along with increased smooth muscle contractility, contributed towards an inhospitable environment for the parasite, leading to expulsion of worms into the gut lumen [66]. Studies have also shown that IL-4 producing T cells could directly mediate worm expulsion and amplify IL-5, IL-9 and IL-13 generating Th2 cells [67]. IL-5 production aids in the stimulation of eosinophils [57] and IL-3 (along with IL-4), facilitates the growth of mast cells in the gut [57,68,69]. Further studies have shown that infection with *T. spiralis* leads to mast cell degranulation, inducing mediator

release, which facilitated the infiltration of the gut with macrophages and dendritic cells, causing inflammation and oedema in the gut [70].

Furthermore, the role of IgE in the expulsion of *T.spiralis* from the gut in BALB/c mice was elucidated by Gurish *et al.* A vigorous IgE response to the infection was reported in the normal mice, in contrast to the IgE^{-/-} animals. An increase in the number of mast cells was noted in the spleen and jejunum of the control animals, while mast cell numbers were reduced in the spleen of mice lacking IgE [71]. Overall, it can be suggested that the classical response is distinct to the immunomodulatory response elicited in the case of chronic infections with helminths.

1.7.2 Immunomodulatory response

Parasitic helminths are often long-lived organisms. For example, infection with filarial nematodes is usually life long and individual worms live up to 30 years [72]. It is to the advantage of the host to produce an immune response that will control the parasite but it must also limit immune system-mediated damage to itself while preserving the ability to effectively respond to other pathogens. From the standpoint of the parasite, it is advantageous to keep the host alive long enough to complete its lifecycle, possibly by suppressing the host immune response or alternatively subverting it into an ineffective response. The popular opinion now is that the helminths are directly involved in promoting this latter state through molecular secretions that interact with and undermine the host immune system. In the case of lymphatic filarial nematodes, there is a consensus that immuno-modulation incorporates impairment of lymphocyte proliferation and a bias in the production of both cytokines and antibodies [73]. The specific mechanism by which the filarial

helminths down-regulate antigen-specific immune responses in chronically infected patients is not known.

Immuno-modulatory pathways proposed by various studies are.

1.7.2.1 Regulatory T- cell (T_{reg}) induction depending on IL-10 and TGF- β

T regulatory (Treg) cells play crucial roles in the induction of peripheral tolerance to self and foreign antigens. Treg cells are expanded and induced in nematode infections, suggesting a role in helminth-induced modulation of inflammatory diseases in humans and mice [52]. Studies suggest that the two most relevant classes of Tregs described within the CD4⁺ subset are regulatory T cells (Tr1/Th3), and CD4⁺CD25⁺Treg cells. Natural regulatory T cells are usually CD4⁺CD25⁺Treg cells. They express Foxp3, which is member of forkhead/ winged-helix family of transcriptional regulators that functions as master regulator in their development. In contrast, inducible regulatory T cells, also known as Tr1/Th3 cells have variable CD25 expression, lack Foxp3 expression and can be generated *in vitro* and *in vivo* upon priming of naive T cells with antigen in the presence of IL-10. These CD4⁺Tr1 cells are characterised by a unique pattern of cytokine production, which is distinct from that of classical Th1 and Th2 cells because they produce low amounts of IL-2, no IL-4 and high levels of IL-10 and TGF- β . These cytokines play a key role in suppression of antigen-specific effector T-cell responses [74-77].

Some of the studies on animal models revealed that helminthic infection with *H.polygyrus* induced the regulation of the immune system through the production of T regulatory cells that were dependant on IL-10 secretion. Kitagaki *et al* noticed that cells isolated from spleen, lung, parenchyma, and thoracic lymph nodes from infected mice had an increased expression of Foxp3 in the CD4⁺T cells. There was also an

increase in the expression of CD4⁺CD25⁺Treg cells among the cells isolated from thoracic lymph nodes. In addition, they found that the protective effects against airway hyperresponsiveness and airway eosinophilia were abrogated in IL-10^{-/-} mice. Similarly, Bashir and team found in their experiments that the down-regulation of plasma histamine levels and systemic anaphylaxis due to helminth infection was ablated upon treatment with anti-IL-10 [52, 53]. Therefore they too concluded that IL-10 was important for the immunomodulatory effects of the helminths.

In the study by Wilson *et al* in BALB/c mice with *H.polygyrus* infection, it was discovered that the adoptive transfer of mesenteric lymph node cells from the infected mice to naïve hosts induced a down regulation of inflammatory cell infiltrates in the lungs, mediated by T cells. These cells were mainly of CD4⁺CD25⁺ phenotype with raised levels of IL-10 and TGF-β cytokines [63]. A study by McSorley *et al* in BALB/c mice deduced that an infection with *B.malayi* led to the production of Foxp3CD4⁺T cells as compared to uninfected controls. In fact they found that both larval as well as adult stage implantation of the parasite into the animal model generated an immuno-regulatory response. They also found an increase in CD25, CTLA-4 and CD103 (a marker associated with stronger suppressor activity) [76] within the Foxp3CD4⁺ cell population [78]. They demonstrated that both larvae and adults were able to induce Foxp3 expression in adoptively transferred DO11.10 T cells, implying that filarial infection could manipulate the development of T cells and that induction was not restricted to the parasite-specific cells. Furthermore, they noticed that Foxp3 expression in IL4R^{-/-} mice was equivalent to wild type animals in the L3-infected mice. From the above data it was concluded that filarial infections skewed and modulated the immune responses that depended on live parasites and independent of concomitant Th2 responses [78]. Liu and team demonstrated that *H.*

polygyrus infection protected NOD mice against Type 1 diabetes (T1D). The protective effect was more pronounced in the animals which were administered *H. polygyrus* early at 5-7 weeks of age, although significant protection was incurred at 12 weeks of age as well. This was associated with reduced lymphoid infiltration in the islets and an increased frequency of CD4⁺CD25⁺ Foxp3 Tregs along with generation of AAMφs and IL-10 mRNA in the pancreatic lymph nodes. It was also noticed that the protective effect was not abrogated upon the administration of anti CD25⁺ monoclonal antibodies and anti-IL-10 receptor antibodies. Therefore it was concluded that *H. polygyrus*-treated NOD mice maintained their protection against T1D through CD25⁺ and IL-10 independent mechanisms [79]. The authors suggested an IL-4 dependent mechanism could be responsible for the down-modulation. This was supported by the increased expression of IL-4 and IL-13 mRNA in PLN and the production of IL-4 instead of IFN-γ by splenocytes after inoculation with *H. polygyrus*.

A study conducted by Mitre *et al* found that peripheral blood mononuclear cells (PBMC) from 17 filaria-infected patients produced more IL-10 than uninfected control subjects. It was also observed that frequencies of IL-10 -producing CD4⁺Treg cells did not increase after stimulation with parasite antigen, which was not typical for inducible regulatory T cells. Furthermore, IL-10-producing cells did not co-release either IL-4 or IFN-γ, which was consistent with findings of a previous study that isolated T cell clones from the subcutaneous tissue surrounding onchocercomas in patients infected with *O. volvulus* [80]. In that study, 106 of 130 T cell clones released IL-10, no IL-4, and low amounts of IFN-γ, if any. It was also noted that CD8⁺T cells, CD19⁺ B cells, CD14⁺ monocytes, and CD56⁺ NK cells accounted for 27%, 10%, 8%, and 7%, respectively, of all IL-10 -producing cells in filaria-infected

patients and it was considered that some of these cell types also played an important role in the IL-10-mediated down-regulation observed in filarial infections. It was found that PBMC of filaria-infected patients released IL-10 with a greater frequency than PBMC of uninfected patients. Although a definite conclusion could not be reached, on the origins of these cells, the findings suggested that most IL-10-producing cells in filaria-infected patients were Tr1 cells (Th3) [81] rather than natural regulatory T cells and that some originated from a Th2 subset of CD4⁺ cells [80].

The mechanisms mediating hypo-responsiveness in generalised onchocerciasis (GEO) were analysed by Doetze *et al* in 2000. In patients with GEO who were characterised by a turn over rate of microfilariae of more than 50,000/day; spontaneous secretion of IL-10 was significantly elevated compared to individuals resistant to infection (PI). They found that PBMC from GEO patients had higher levels of IL-10 although these PBMC proliferated less than PBMC from PI individuals. They revealed that T cell proliferative hypo-responsiveness could be reversed by the simultaneous addition of anti-IL-10 and anti-TGF- β antibodies to PBMC from patients with GEO. This effect was not observed in the absence of either one of the antibodies or in the absence of antigen against *O.vovulus* (OvAg). From this observation they concluded that patent infection was required to modulate active cellular responses to parasites. They determined the source of IL-10 and TGF- β by obtaining T cell clones from T cell lines from GEO that proliferated strongly in the presence of OvAg. In addition, it was seen these cells could be further divided into two groups; with elevated levels of IL-2 and lack of IL-10 and TGF- β in one and high levels of IL-10 and TGF- β and low levels of IL-2 in the second group. They surmised that the second group were Tr1/Th3 T cells while the earlier group was Th0.

However, they observed that both the groups produced IL-5 but little IFN- γ and IL-4 [81]. From these data they concluded that there was preferential production of cytokines by the T cells from GEO and although there were some T cells producing IL-2, their effect was nullified by IL-10 and TGF- β .

Recently, the activity of Tregs in response to BCG and *Plasmodium falciparum* parasitised red blood cells was investigated in Indonesian school children by Wammes and team. On examining the proliferation and cytokine activity, it was observed that in GEO-infected children, there was a reduction in the proliferation of T cells *in vitro*. In addition, they discovered that although the frequency of CD4⁺ CD25^{Hi} Foxp3⁺ T cells was similar in both the infected and uninfected children, the Ag-specific proliferative responses increased upon CD4⁺ CD25^{Hi} Foxp3⁺ T cell depletion in children with GEO only. Moreover, there was an increase in the production of IFN- γ to both BCG and parasitised red blood cells in children with GEO. This study revealed an inherent effect of helminth modulation not only on co-endemic infections but also on vaccine efficacy [82].

1.7.2.2 Activation of T-cells by alternatively activated macrophages

In the paraphernalia of immune system modulation exerted by helminths, macrophages activated during Th2 type responses have been shown to exhibit a distinct phenotype which is different from classically activated macrophages associated with Th1 immunity. Treatment of murine peritoneal exudates macrophages with IL-4, a Th2 cytokine, resulted in increased mannose receptor expression; cellular responses associated with collagen deposition and reduced iNOS (inducible nitric oxide synthase) production. These cells have thus been aptly named as alternatively

activated macrophages (AAM ϕ) as compared with classically activated macrophages engaged in bacteria and protozoa killing responses [83].

It was found by Allen *et al* that AAM ϕ were generated by the daily injection of excretory/secretory material (ES) products into male CBA/Ca mice from adult *B.malayi* but not when dead worms were implanted [84]. On the contrary, Taylor *et al* showed that dead/dying worms induced the release of pro-inflammatory mediators by macrophages, attributed to the presence of *Wolbachia* bacteria [85]. In a study by Semnani *et al*, mosquito-borne *B. malayi* L3 larvae were able to down-regulate expression of MHC class I and class II on human Langerhans cells and inhibited their ability to activate T cells *in vitro* [86]. Moreover, when the same parasites were injected into the murine peritoneal cavity by MacDonald and team, they realised that these parasites induced suppressive nematode-elicited macrophages (NeM ϕ) that blocked T cell proliferative responses [87]. Furthermore, experiments in CBA/Ca mice revealed that on implanting L3 parasites in the mouse model, there was a generation of adherent peritoneal cells (PEC) that induced significant suppression of cellular proliferation in cultured T cells in an IL-4 dependent manner. They also revealed that Abs to TGF- β did not restore the proliferative property of primary T cells obtained from C57B/6 mice either alone or in conjunction with Abs to IL-10 [87]. Loke and team proposed that the dissemination of suppressive activity to the lymph nodes only occurred when microfilariae released from gravid adult females, exited the pleural cavity and circulated through the blood and draining lymph nodes. The researchers demonstrated that the presence of NeM ϕ , peripheral to the infection site was triggered by the systemic nature of infection, though they could not fully explain their function. They also noticed that T cells were able to recover their full functionality once NeM ϕ had been removed from culture, proving the transient nature

of the inhibitory effect of the NeM ϕ [88]. They also established NeM ϕ as a source of *in vivo* derived AAM ϕ . Several markers for AAM ϕ were identified by them including an increased expression for arginase 1, Ym1/ ECF-L, Fizz1/RELM α and suppression of MIP-1 α and MIP-1 β [89]. It was also seen that there was an increase in the production of IL-10 and TGF- β . The same group verified that the suppressive activity was dependent on IL-4 as the mice lacking IL-4 were unable to induce AAM ϕ , whereas IL10^{-/-} sustained both AAM ϕ induction and immuno-suppressive activity during *B.malayi* infection [87, 89]. Nair and team further added that Fizz1 and Ym1 were secreted in the peritoneal lavage fluid of the mouse models after implantation with *B.malayi* in an IL-4 dependent manner. In addition, Nair *et al* suggested that its expression was increased in the tissue nematode *L.sigmodontis* as well as in the gastric nematode *N.brasiliensis*. It was further noted that at the sites of infection with *N.brasiliensis*, AAM ϕ s expressed certain chitinase and Fizz1 (found in inflammatory zone) family member proteins (ChAFFs), including Fizz1/RELM α , Ym1, Fizz2 and acidic mammalian chitinase [90]. Experiments by Taylor and team using *Litomosoides sigmodontis* in BALB/c mice revealed that the hyporesponsiveness at the infection site was restricted to CD4⁺ T cells. Beyond the site of infection, F4/80⁺ population of NeM ϕ macrophages induced the suppressive effects. They revealed that before the infection becomes patent in *L. sigmodontis*, NeM ϕ are restricted to the infection site, resulting in localised suppressive activity. On the other hand, when the Mf were released and spread systemically, the suppressive activity of NeM ϕ was extended peripherally into the draining lymph nodes. It was found that beyond the site of infection, immune regulation was mediated by a suppressive F4/80⁺ population of NeM ϕ which were phenotypically similar to AAM ϕ , acting through a partially TGF- β -dependent, but IL-10 and CTLA-4-independent mechanism. Thus, at patency,

two independent mechanisms of suppression operated in the pleural cavity; an intrinsic defect in the Ag responsiveness of the CD4⁺ T cell population and inhibition of proliferation by NeMφ [91].

Experiments by Lin and Faunce, in an anterior chamber-associated immune deviation (ACAID) model of peripheral tolerance, disclosed that adoptive transfer of F4/80⁺ APC resulted in suppression of the delayed type hypersensitivity responses in F4/80^{-/-} mice. These APC were generated *in vitro* by treatment of peritoneal exudate cells from BALB/c mice, with soluble protein Ag such as BSA, in the presence of supernatants harvested from cultured iris and ciliary body cells. This indicated an important role of F4/80 glycoprotein in the generation of efferent Treg cells [92]. IL-4 and IL-5 cytokine responses remained relatively unaffected even though NeMφ inhibited the proliferative responses of T cells. These cytokines are known to be important for protective immunity toward both adult parasites and Mf [93,94], suggesting that the generation of NeMφ *in vivo* may not have a direct impact on parasite survival. Interestingly, it was discovered that killing of adult *L. sigmodontis* parasites induced through the neutralisation of regulatory T cell activity occurred despite the presence of the suppressive NeMφ. This indicated that, although multiple levels of suppression did exist, specifically targeting T cell-mediated regulation was sufficient to restore protective immunity. Anthony *et al* observed that during memory responses in enteric *H. polygyrus* infection, AAMφ accumulated at the sites of larval invasion in the sub-mucosa as early as four days after implantation. Adoptive transfer of memory CD4⁺ T cells into STAT6-deficient or wild type mice given a primary *H. polygyrus* inoculation indicated that IL-4R signaling on macrophages mediated their alternative activation. It further suggested that IL-4/IL-13 production by memory CD4⁺ T cells induced AAMφ recruitment and differentiation at the host–parasite

interface [95]. By contrast, in the experiment conducted by Reece *et al*, rapid increases of AAM ϕ were detected in the lung by four days after *N. brasiliensis* infection in SCID mice lacking T cells, as indicated by an increase in the expression of Ym1, Fizz1/RELMa, and arginase-1 gene products associated with AAM ϕ . However after day 4, the expression of these genes decreases markedly in the lungs of *N. brasiliensis*-infected SCID but not in infected wild type mice [96], suggesting that innate cells may make sufficient IL-4/IL-13 to induce initial differentiation of AAM ϕ . A study by Hunter and colleagues found that AAM ϕ produced an anti-colitic effect in mice infected with the rat tapeworm *H.diminuta* and suffering dinitrobenzene sulphonic acid (DNBS) induced colitis. They observed increased colonic expression of Fizz1, arginase-1 and CD14 mRNA in the mice infected with *H.diminuta*. They further noticed that after the depletion of intestinal macrophages using clodronate-liposomes, there was a reduction in the anticolic effect of *H.diminuta*. This was however restored with the injection of AAM ϕ . Mitogen activated spleen cells from the mice given AAM ϕ produced more IL-10 than control and DNBS-only treated animals. This was accompanied by an increase in IL-10 production from mitogen stimulated spleen cells from the mice *ex vivo*. In addition they observed that *in vivo* neutralisation of IL-10 partially reduced the effects of AAM ϕ transfer [97].

1.7.2.3 Increased expression of cytotoxic T lymphocyte antigen-4 (CTLA-4) on T- cells

Another possible pathway in the suppression of parasite-specific responses could be through the engagement of the T cell co-stimulatory molecule CTLA-4. CTLA-4 is stored in endosomal compartments and expressed on the cell surface following

activation [98]. It delivers an inhibitory signal to T cells in contrast to its homologue CD28 which can provide a potent co-stimulatory signal for the production of various interleukins such as IL-2 and IL-6. The role of CTLA-4 in controlling immune responses has also been documented, particularly in animal models of autoimmunity [99-101]. Kuhns and associates studied the regulation of CD4⁺ T cells induced by CTLA-4 in a SJL/J mouse model of experimental autoimmune encephalitis. They used disease incidence and severity as a measure of *in vivo* CD4⁺ T cell responses. Their results indicated that blockade of CTLA-4 during immunisation with proteolipid protein PLP-139-151 (disease agonist) resulted in 100% disease incidence and exacerbation of the disease. It was demonstrated by Takahashi *et al* [101] that *in vivo* blockade of CTLA-4 in normal mice lead to spontaneous development of chronic organ-specific autoimmune diseases, immuno-pathologically similar to diseases in humans. They explained that CTLA-4 was a key co-stimulatory molecule for activating CD25⁺CD4⁺ regulatory T cells to exert suppression. Hence it controlled self-reactive T cells. They verified their study by administering anti-CTLA-4 monoclonal antibody (mAb), anti-CD25 mAb as well as a mixture of both to normal BALB/c mice. The results revealed that all the mice treated with high doses of anti-CTLA-4 mAb developed spontaneous autoimmune gastritis, oophoritis, and sialadenitis that were evident both serologically and histologically. However, low doses of anti-CTLA-4 mAb and anti-CD25 mAb induced only low levels of the autoimmune diseases that could not be recorded histologically. It was also shown that a mixture of higher doses of the two produced autoimmune gastritis in ~ 85% of mice. Similarly, the study by Steinbrink *et al* [102] demonstrated that blocking antibodies to CTLA-4 restored the T-cell activity by about 70% in anergic alloantigen-specific CD4⁺ T cells in humans.

It has been shown by Steel *et al* that long term T cell anergy was induced in children born to filaria-infected Mf⁺ mothers [103]. It was later demonstrated that these children also demonstrated increased mRNA expression of CTLA-4 in response to Mf Ag, but not to the other parasite stages tested. The tolerance to the Mf has been attributed to an early *in-utero* exposure to this stage of the parasite in many infected individuals from endemic areas. It has been explained as being due to the effect of specific Mf Ag on an immature immune system (i.e., one that has immature APC with low expression of CD80 and CD86). Studies with soluble fusion protein have indicated that CTLA-4 binds to both B7 family members with an affinity ~ 20-50 folds higher than that of CD28 [104-106]. CD28 engagement via antibodies augments the proliferation of T cells in response to immobilised anti-TCR antibodies [107]). Hence the binding to B7 family members of co-stimulatory ligands instead of CD28, accounted for the ability of the CTLA-4 Ig fusion protein to block co-stimulation *in vitro* [108,109]. Chronic *in utero* exposure to parasite Ag may alter both the memory/naive T cell ratio and increase the expression of CTLA-4 as more cells become activated. The fact that CTLA-4 expression continued to increase in response to Mf Ag even many years later in uninfected children born to Mf⁺ mothers suggested that those changes experienced *in utero* continued later in life if the individual was under constant environmental exposure to the parasites or parasite Ag.

It was shown by studies in humans that Th2 clones expressed higher percentages of CTLA-4 [110] and that blockade of CTLA-4 *in vitro* enhanced the secretion of Th2 cytokines such as IL-4 [111]. Similar findings were seen with regard to Th1/Th2 dichotomy in the study conducted by Steel et al (2002) in which blocking CTLA-4 led to increased production of IL-5, but decreased secretion of IFN- γ in response to Mf Ag [112]. Their study indicated that CTLA-4 played an important role

in immune modulation although they could not indicate a single unifying mechanism that completely explained the cellular hypo-responsiveness seen in filaria-infected individuals [112]. Chronic infections by human filarial parasites are related to long term down regulation of hosts' immune responses. Using the BALB/c model with *L. sigmodontis* infection, Taylor and colleagues revealed that CD4⁺ T cell regulation was the main factor in parasite survival. It was suggested that filarial infection up-regulated the expression of regulatory and activation markers. On analysis of the phenotype of CD4⁺ T cells from the thoracic cavity of mice, an increase in the levels of CTLA-4 GITR (glucocorticoid induced TNF receptor family related gene) ^{high} was seen with the progression of infection. The workers further noticed that during the later stages of infection, CTLA-4, GITR ^{high} expressing cells increased in numbers even at distal sites. It was thus concluded that the most dominant phenotype responsible for hyporesponsiveness in the cells from the thoracic cavity was CD25⁻ GITR^{high}CTLA-4, which was more frequent in sites peripheral to the nidus of infection [113]. Similar studies using *B.pahangi* L3-infected BALB/c mice indicated that CD4⁺CD25⁺CTLA-4⁺ T cells increased only in the splenocyte cultures from L3-infected animals restimulated with parasite Ag. In addition, all CTLA-4⁺ cells were found to be CD25⁺. There was no difference in the expanded regulatory population obtained from splenocyte cultures of IL-4^{-/-} or wild type mice, thus confirming that their differentiation was IL-4 independent. These cells were also not found in the cultures obtained from microfilariae-transplanted mice or control animals. This was in contrast to human studies where CTLA-4⁺ CD4⁺ cells are in higher frequency in microfilaraemic patients [114].

Investigations by Wohlleben *et al* using C57BL/6 and BALB/c mice infected with *N.brasiliensis* indicated that after 1 week of infection, 12 % of CD4⁺ T cells

produced IL-10, out of which 74 % of CD4⁺ IL-10⁺ cells also produced IL-4, and 94% expressed CD25 while 99% of cells produced CTLA-4. They further elucidated that after 4 weeks of infection about 55-67 % of cells expressed CTLA-4. These results suggested that these cells obtained from the BAL fluid had phenotypic characteristic of Treg cells. This result added to the previous studies by the same group where it was elucidated that infection with *N.brasilienses* suppressed the allergen induced airway eosinophilia via IL-10 [54]. As alluded to previously, upon inoculation of L3 larvae of *B.malayi* into BALB/c mice, by McSorley's team, there was a significant increase in CD4⁺ Foxp3⁺ T cells in the peritoneal lavage cells. Furthermore, there was a sharp increase in the expression of CTLA-4 and CD25 within this T cell population, which indicated that this phenotype was associated with anergy [78].

In chronic filariasis patients with lymphoedema, Babu *et al* investigated the factors responsible for serious pathology. In a group of 12 filarial lymph oedema patients (CP) and 10 asymptomatic but infected (INF) controls, they observed that filaria antigen did not induce differential Th2 or IL-10 responses in the CP patients. Furthermore, they noticed that there was an increase in the production of Th-17 cells with an increase in IL-17A, IL-17F and IL-21 induced at significantly higher level than in the controls. Finally their results revealed that there was a marked down-regulation of immunosuppressive markers of Treg cells such as Foxp3, GITR, TGF- β and CTLA-4 in the patients with lymphoedema. These results indicate that during helminth infections, CTLA-4 up-regulation may play an important role in induction of hypo-responsiveness of the immune system [115]. Therefore, it can be assumed from the above studies that CTLA-4 expression in filarial infections may function to down-regulate inflammatory responses that could lead to the debilitating effects of

these diseases or it may also prevent the elimination of the parasite by altering cytokine profiles and modulating T cell activation.

1.8 ES-62

The previous sections indicate that helminth infection can protect against the development of allergy and autoimmunity in mouse models and discusses some of the mechanisms involved. This raises the idea of using helminthes for therapeutic purposes but clearly it would be better if the actual molecules responsible for immunomodulation, could be defined, characterized and employed. This section focuses on one such molecule, ES-62, which is arguably the best characterized of all helminth-derived immunomodulators.

ES-62 is an immunomodulatory molecule secreted by *Acanthocheilonema viteae*. It was discovered in 1989 in the laboratory of Prof. W. Harnett [116]. The most receptive host for filarial nematodes was discovered to be the gerbil. *A.viteae* is a filarial nematode whose life cycle can be reproduced in the laboratory using the tick *Ornithodoros moubata* as vector/intermediate host and the jird *Meriones libycus* as a final host [117]. This molecule has an overabundance of immunomodulatory activities, which can be classified as anti-inflammatory [118]. ES-62 has a molecular mass of 62kDa when analysed by SDS-PAGE under reducing conditions. Sedimentation equilibrium data demonstrated that ES-62 is tetrameric and self interaction occurs with high affinity [119]. It is a 'stage specific' protein i.e. it can only be detected in certain stages of the parasite life cycle (L-4-adult stage). Although it is not present in the earlier stages, the mRNA can be detected in all the life-cycle stages of *A.viteae* (L3 larvae ~5% of adult levels and microfilariae <0.2% of adult levels). The same was found in the case of *B.pahangi*. This was studied by

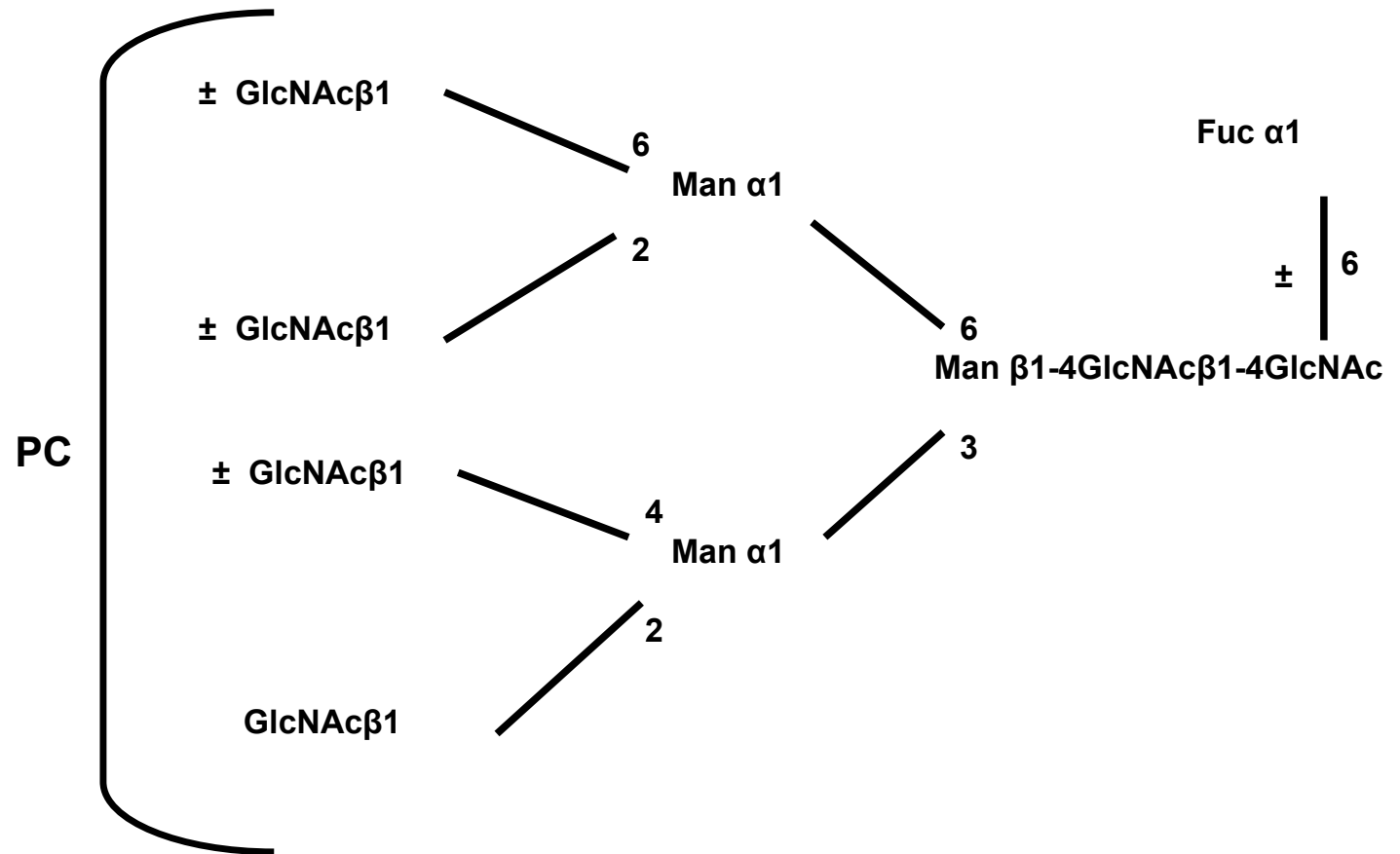
comparing the levels of ES-62 transcribed in the different stages of these two nematodes [120,121].

1.8.1 Structure

The secreted form of ES-62 consists of 474 amino acids verified by cDNA sequence analysis, N-terminal amino acid sequencing and Q-TOF sequencing. It has a molecular mass of 52.8kDa and an iso-electric point of 5.96 [116]. Analysis of the protein-coding sequence revealed the presence of four potential N-linked glycosylation sites (using PRINTS/PROSITE scanner). Fast atom bombardment mass spectroscopy shows ES-62 to contain three different types of *N*-glycan structure. These have been demonstrated as – 1) high mannose type structures ($\text{Man}_{5-9}\text{GlcNAc}_2$), 2) trimannosyl core and sub stoichiometrically fucosylated glycans ($\text{Fuc}_{0-1}\text{Man}_3\text{GlcNAc}_2$) and 3) those with a trimannosyl core with or without core fucosylation carrying between one and four additional *N*-acetylglucosamine residues ($\text{Fuc}_{0-1}\text{Man}_3\text{GlcNAc}_{3-6}$). A second post-translational substitution present on a number of filarial nematode proteins is phosphorylcholine (PC), which is covalently attached to the third type of *N*-glycan [122,123]. PC is a molecular pattern associated with various pathogen products from varied range of organisms consisting of bacteria, fungi, protozoa, and filarial as well as gastrointestinal nematodes [124]. PC is a potent immuno-modulator and many immunomodulatory properties of ES-62 have been attributed to the PC component of the molecule [117, 125]. Blast search showed that ES-62 shared 67% identity and 80% positives with leucyl aminopeptidase of *B.malayi*. It also shares 37% and 36% identity and 57% and 54% of positives with plasma glutamate carboxypeptidase in humans and mouse respectively. Incubation of ES-62 with leucine-7-amino-4-methylcoumarin as substrate confirmed that ES-62

possessed weak aminopeptidase activity [126]. Fig 1.4 represents the structure of the PC-N-glycan of ES-62.

Fig 1.4 represents the structure of the PC-N-glycan of ES-62.



Fuc = fucose, PC= phosphorylcholine, GlcNAc β = N-acetylglucosamine β , Man β = mannose β ,

1.8.2 Immuno-modulatory properties of ES-62

ES-62 modulates immune responses via a number of cells including dendritic cells, macrophages, B-lymphocytes and mast cells as a consequence of interaction with signal transduction pathways. The modulation of the activity of signal transduction molecules including MAP-kinases, P-I-3 kinase and NF- κ B is dependent on complexing of ES-62 with TLR4 [125].

1.8.2.1 ES-62 and its influence on antibody subclasses

It was revealed by Houston *et al* that subcutaneous injection of ES-62 into BALB/c mice resulted in generation of high levels of IgG1 Ab (Th2) but no IgG2a (Th1), which was directed against the non-PC epitopes of the molecule [117]. It was found that ES-62 free of PC had no significant effect on the IgG1 response but it induced a substantial IgG2a response. PC-free ES-62 was produced by adding either 1-deoxymannojirimycin (dMM) [127] or hemicholinium-3 to the culture medium [128]. The experiment was repeated comparing PC attached to BSA (bovine serum albumin) with BSA alone and it was found that PC moiety blocked the IgG2a response to BSA. It was also established that the polarising effects of ES-62 were independent of IL-4. This was shown by measuring the effects of ES-62 and PC-free ES-62 in IL-4^{-/-} mice. The results revealed that along with elimination of the IgG1 response there was no production of specific IgG2a, although there was a slight increase in IFN- γ levels (required for class switching to IgG2a [127]) induced by the PC-free ES-62. These results confirmed that IL-4 did not influence the Th1 response. In addition, it was considered that PC was blocking production of IgG2a Abs by inducing production of IL-10. This was confirmed by measuring the response to ES-62 in IL-10^{-/-} BALB/c mice. On injection of ES-62, there was generation of an IgG2a response against the

molecule. Hence, from these results it was concluded that PC on ES-62 could be down-regulating Th1 responses by activating IL-10 production [117].

1.8.2.2 Effects of ES-62 on B cells and B cell signaling

The effect of ES-62 on B cell activation was investigated on mouse derived spleen cells. It was seen that ES-62 was able to inhibit signaling through the B cell receptor (BCR) induced using F(ab')₂ fragments of anti-IgM [129]. The analysis of the data indicated that B cells exposed to ES-62 were hyporesponsive to subsequent BCR-induced proliferation in a concentration dependent manner [130]. The inhibition via BCR was further investigated by injecting BALB/c mice with ES-62 at concentrations (0.2– 2 µg/ml) comparable to those found for PC-containing molecules in the blood stream of infected humans [131]. Furthermore, the same effect was observed when B cells were exposed to ES-62 *in vivo* by release from subcutaneously implanted osmotic pumps and were subsequently activated *ex vivo* [130]. This inhibition appeared to be direct (not through other cells or mechanisms) and not through apoptosis or induction of commitment to apoptosis following further stimulation. These results were mimicked by PC alone or by PC conjugated to BSA, thus implying that the PC moiety of ES-62 may be responsible for this immunomodulatory effect [130]. Moreover, B cells from mice exposed to PC *in vivo* are hypo-responsive to BCR cross-linking compared to B cells from control animals [132]. However B1 cells from the same animals, showed an increase in proliferation *ex vivo* when stimulated with F(ab')₂. This elucidated the fact, that interaction of ES-62 with the two B cell types (peritoneal B cells and conventional splenic B cells) was very distinct [133, 134]. The research on the effects of ES-62 on B cells indicated that ES-62 did not target the BCR-coupled phospholipase C- γ -mediated hydrolysis of

phosphatidylinositol 4,5-bisphosphate that generated inositol 1,4,5-trisphosphate and diacylglycerol and activated protein kinase C isoforms, but rather selectively downregulated the expression of α , β , ζ , δ and ι/λ PKC isoforms by proteolytic degradation in murine splenic cells while upregulating PKC- γ and PKC- ϵ in the same cells [135]. It was also discovered that ES-62 modulated BCR signaling by upregulating SHP-1. SHP-1 is an inhibitor of the signaling cascade in that it prevents the activation of the BCR complex by de-phosphorylating the Ig α/β -ITAMs. This prevents the recruitment of the ShcGrb2Sos complexes needed for the activation of RasErk MAP kinase signaling cascade [136]. In addition, ES-62 induced the BCR mediated recruitment of RasGAP to stop Ras signals, and targeted the activation of MAP kinase by down modulating PKC isoforms [136]. Further evidence suggested that ES-62 did not mediate its uncoupling of the BCR from PI-3-K or RasErk MAP kinase cascades by targeting the activation of Syk, Lyn or Blk. ES-62 also reduced the levels of dually phosphorylated, active p38 MAP kinase observed in resting or activated B cells [129, 135]. Similarly, BCR-mediated stimulation of p46 and p54 JNK MAP kinase was desensitized by pre-treatment with ES-62, although stimulation with ES-62 alone selectively activated p54 JNK [137]. It was seen that Rac-1 (a small GTPase implicated in the regulation of JNK and p38) constitutively active in B cells was abrogated on pre-treatment with ES-62 [137]. The mechanism underlying the deactivation was unclear because there was no effect of ES-62 on Vav, which is a GDP/GTP exchange factor required for Rac-1 activation. However additional experiments exposed that ES-62 down-modulated Shc, a BCR-associated adaptor molecule which is related to Vav in an antigen-receptor-mediated capacity [137]. Taken together, these results suggested that the BCR modulated p38 and JNK

signaling in a Vav- and Rac-dependent manner and this regulatory mechanism is a target for ES-62 [137].

1.8.2.3 Effects of ES-62 on T cell signaling

The effects of ES-62 on T cell signaling were determined by using the human leukaemic T cell line, Jurkat. The results indicated that co-culture with ES-62 not only suppressed anti-CD3-mediated stimulation of proliferation, but also reduced the threshold for growth arrest effects in response to Con-A [138]. These effects were due to desensitisation of T cell receptor (TCR) signaling. This resulted in disruption of TCR coupling to phospholipase-D (PLD), protein kinase C (PKC), PI-3-K, and RasErk MAP kinase signaling [132]. The effects of ES-62 on T cell signaling were attributed to the PC moiety as culture with PC or PC-BSA had similar effects to ES-62 on the coupling of the TCR to tyrosine kinase activation (ZAP-70, Lck and Fyn) and the PLC, Ras and MAP kinase signaling cascades [135].

ES-62 has also been found to modulate heterologous Ag-specific responses *in vivo*. This was demonstrated using a CD4⁺ tg (transgenic) TCR T cell adoptive transfer system in which BALB/c mice were given ovalbumin-specific TCR tg CD4⁺ T cells from DO.11.10 BALB/c mice along with subcutaneous injection of ES-62 [139]. Thus, in contrast to the mixed IgG1-IgG2a response observed in control animals, ES-62 treated mice demonstrated an increase in anti-OVA IgG1 and decrease in OVA-specific IgG2a. Furthermore, there was a decrease in the production of IFN- γ by T-cells from ES-62-treated mice although there was an increase in IL-5. The response was not completely biased towards Th2 but a modified one as there was decreased production of IL-4 and IL-13 cytokine responses when re-challenged with Ag *ex vivo*. The response was neither Th1/pro-inflammatory as there was a decrease

in IL-2, IL-6, IL-12, IL-17, TNF- α , and MIP-1 α . Utilising the adoptive transfer system, it was revealed that pre-exposure to ES-62 *in vivo* inhibited the clonal expansion of transferred Ag-specific CD4⁺T cells and inhibited the rate and extent of migration of T cells into B cell follicles in the lymph nodes [140].

The adoptive transfer system was used in double transfer using OVA-specific tg TCR CD4⁺ T cells and HEL (hen egg lysosyme)-specific tg BCR B cells followed by immunisation with conjugated OVA-HEL/CFA to promote cognate interactions between B- and T- cells. This study demonstrated that the presence of activated B cells not only restored clonal T cell expansion and division, but it also prevented skewing of immune response towards Th2. However, there was a generalised suppression of both Th1 and Th2 cytokines and a lack of anti-OVA IgG Abs which indicated that ES-62 inhibited the helper and effector functions of T cells [141].

1.8.2.4 Effects of ES-62 on APC (macrophages and dendritic cells)

It was demonstrated by Goodridge *et al* [142] that pre-treatment of macrophages with ES-62 alone briefly stimulated the production of low levels of IL-12, IL-6, and TNF- α but later there was a reduction in these cytokines when cells were stimulated with their classic inducers IFN- γ and lipopolysaccharide (LPS). This hypo-responsive state of macrophages was due to direct interaction with ES-62 because there was inhibition of IL-12 p40 in the macrophages even after washing of cells before stimulation with LPS and IFN- γ . This was established further by the fact that the transfer of culture supernatants from ES-62 pre-treated cells to resting macrophages before stimulation with IFN- γ +LPS resulted in normal levels of IL-12 p40. Furthermore, it was concluded that simultaneous addition of ES-62 with IFN- γ +LPS also resulted in suppression of macrophage cytokine production. It was observed that there was no

production of IL-10 by peritoneal macrophages in the presence of ES-62 alone or in the presence of IFN- γ +LPS. This was an interesting observation because in previous experiments ES-62 induced IL-10 production in dendritic cells and dendritic-T cell co-cultures *in vitro* and in *in vivo* experiments where IL-10 regulated ES-62 dependent IgG class switching [117, 143]. On investigating the level of ES-62's effect on suppression of cytokine production, it was discovered that pre-treatment with ES-62 reduced the level of IFN- γ +LPS-induced IL-12 p40 and p35 transcripts. Thus it was suggested that ES-62 achieved inhibition of bioactive IL-12 p70 by inhibiting production of both of its subunits. It was also observed that the levels of TNF- α mRNA were not significantly affected. Therefore, it was assumed that TNF- α modulation might be occurring at a translational/posttranslational level. When macrophages were exposed to ES-62 by osmotic pumps *in vivo*, it resulted in *ex vivo* suppression of IFN- γ +LPS induced IL-12 and TNF- α levels. There was no effect on NO production. Also cell viability was not affected by the presence of ES-62.

By employing CD4⁺T cells from DO.11.10 tg mice expressing TCR specific for OVA peptide, Whelan *et al* showed that pathogen derived products were capable of inducing bone marrow derived dendritic cells towards a Th1 or Th2 phenotype [143]. The results showed that when naïve CD4⁺T cells were cultured with bone marrow derived dendritic cells (bm-DC) in the presence of OVA peptide, they secreted both IFN- γ and IL-4, which reflected their ability to generate either a Th1 or Th2 response, providing a simple model of immuno-modulation. It was discovered that co-culturing of immature bm-DC with OVA-specific CD4⁺T cells in the presence of LPS, induced a Th1 response, as shown by increased production of IFN- γ along with suppression of IL-4. On the other hand, Th2 responses with increased production of IL-4 and decreased production of IFN- γ were elicited in the presence of ES-62.

The results also indicated an increase in the expression of various co-stimulatory molecules such as CD40, CD80, CD86 and CD54 in the presence of LPS. There was no such increase in the presence of ES-62. On measuring various cytokines in co-cultures of bm-DC-CD4⁺T cells in the presence of LPS, an increased production of IL-12 p70 was revealed. Surprisingly, a small but significant increase in the level of IL-12p70 was observed in the presence of ES-62 co-culture as well. Also on testing the levels of IL-10, there was no difference found in the cultures with LPS and ES-62. Thus it was concluded that ES-62 induced the production of immature bm-DC that drove Th2 responses and induced its immuno-modulatory function through an unknown mechanism.

The receptors/signaling molecules used by ES-62/PC to modulate the activity of macrophages and DC were identified using knockout mice. It was discovered that ES-62 responses of macrophages and DC were dependent on myeloid differentiation primary response gene (88) MyD88, a key TLR adaptor molecule [124] using wild type and MyD88 KO mice [144]. It was shown by Goodridge *et al* that low level induction of IL-12p40 and TNF- α cytokines by ES-62 was inhibited in MyD88 KO mice. Furthermore, with respect to the PC moiety of ES-62, PC-OVA induced modulation was also absent in the MyD88 KO mouse. There was a reduction in the expression of CD40 in the DC after exposure to either LPS or ES-62 in the MyD88 KO mice, although there was little effect on the level of CD54, CD80, or CD86 expression [145]. These results indicated that that some LPS responses were independent of MyD88 [146], as shown previously where in response to LPS, MyD88^{-/-} DC up-regulated co-stimulatory molecule expression and enhanced their T cell stimulatory activity and induced the production of IL-4 instead of IFN- γ . The same reasoning held true for ES-62, but collectively, the data indicated that other

immuno-modulatory effects of ES-62 were dependent on MyD88. It was also observed that in TLR2 KO mice, ES-62-induced low level induction of IL-12 p40 and TNF- α , as well as suppression of LPS-induced IL-12 p40 and TNF- α production were intact in peritoneal macrophages, bmMs, and bmDCs. Similarly, the phenotypes of bm-DCs induced in response to LPS or ES-62 were essentially identical in wild type and TLR2 KO mice indicating that TLR2 was not required for modulation of cytokine production by ES-62. In contrast, ES-62 failed to stimulate low level IL-12 or TNF- α production by macrophages from LPS-unresponsive TLR4 KO mice. Similarly, LPS- and ES-62-mediated modulation of the bmDC phenotype was lost in TLR4 KO mice. It was also found that the interaction of ES-62 with TLR4 was distinct from that with LPS as evidenced from an experiment which showed that unlike LPS, ES-62 was fully active against APC derived from HeJ mice that have a mutation in the TIR domain of TLR4 [125, 144], indicating a novel use for the TLR4 receptor since ES-62 did not require TLR4 to be fully functional.

1.8.3 ES-62 and mast cells

Mast cells and basophils play an important role in the inflammatory and immediate allergic reactions. Mast cells are distributed throughout the mammalian tissues, specially the peri-vascular spaces and the connective tissues of the skin, respiratory and gastrointestinal tracts [147].

Aggregation of high affinity Fc receptors for IgE (Fc ϵ RI) on mast cell surfaces elicits the release of preformed granule-associated inflammatory mediators, including histamine, neutral proteases, preformed cytokines and proteoglycans. The same stimulus triggers the rapid synthesis and release of lipid mediators that are the products of endogenous arachidonic acid metabolism, such as prostaglandin D₂,

leukotrienes LTB₄, and LTC₄, the parent molecule of cysteinyl leukotrienes LTC₄, LTD₄ and LTE₄. Activated mast cells also synthesise and secrete a host of pro-inflammatory, chemo-attractive, growth promoting and immuno-modulatory cytokines and chemokines over a period of several hours [147]. The regulatory mechanisms governing mast cell degranulation and calcium release from internal stores are only partially understood although some of the signaling cascades triggered by FcεRI have been characterised. FcεRI is a heterotrimeric receptor complex (αβγ₂) that contains immuno-receptor tyrosine-based activation motifs in both β and γ subunit cytoplasmic domains [148]. The protein-tyrosine kinase Lyn is associated with the β subunit in resting cells [149], and its activation is promoted by FcεRI cross-linking [150]. Activated Lyn phosphorylates immunoreceptor tyrosine-based activation motifs of β and γ subunits, resulting in the recruitment of other Src-like as well as Syk protein tyrosine kinases through Src homology 2 domain-mediated interactions with phosphotyrosine residues [151, 152]. Activation of these newly recruited protein tyrosine kinases, in turn, facilitates the translocation and phosphorylation of multiple signaling molecules, including phospholipase C (PLC) γ isoforms and phosphoinositide 3-kinases. Activated PLCγ hydrolyses phosphatidylinositol 4,5-bisphosphate to *D-myo*-inositol 1,4,5-trisphosphate and diacylglycerol, which induce the release of Ca²⁺ from intracellular stores and the activation of protein kinase C isoforms, respectively. The amplitude and duration of the Ca²⁺ response potentially modulates the activation of different transcription factors [153], regulating different gene expression. Ca²⁺ signals are also indispensable for the release of histamine-containing granules [154], the synthesis of arachidonic acid-derived mediators, and the release and generation of various cytokines, which together are responsible for the major symptoms of immediate hypersensitivity

reactions. Thus, an understanding of mast cell activation and Ca^{2+} signaling therefore has obvious therapeutic implications.

The diverse chemical mediators are generated and released by mast cells after allergen exposure in sensitised hosts through IgE dependant mechanisms and depending upon route of exposure provoke plasma extravasation, tissue oedema, broncho-constriction, mucous secretion, leukocyte recruitment and inflammation. Clinically, these pathological changes are the basis of medical conditions such as anaphylaxis, urticaria, angioedema, and acute exacerbations of asthma and rhinoconjunctivitis. The responsible mediators often have overlapping functions, and therefore blockade of one mediator might not completely prevent any one biological consequence. Therefore it was considered to be prudent to consider the development of a novel drug that would inhibit the overall functioning of mast cells.

Pre-exposure of human mast cells to ES-62 substantially inhibited FcεRI-triggered generation of TNF-α and interleukin IL-6 and IL-3, but not IL-5 or IL-13. This indicates that ES-62 can inhibit pro-inflammatory, but not certain type 2 helper T cell (Th2, IL-4), cytokine production by human mast cells [155].

ES-62 inhibited the initial peak of Ca^{2+} mobilisation triggered by FcεRI, but not the delayed, more sustained response. Pre-treatment of cells with ES-62 inhibited FcεRI-coupled PLD and SPHK activities, whereas PLC-γ1 translocation and inositol trisphosphate generation proceeded as normal. Earlier work [156, 157] demonstrated that protein kinase C-α (PKC-α) expression was essential for FcεRI coupling to PLD in monocytes, and exposure of mast cells to ES-62 led to down-regulation of several PKC isoforms, with PKC-α being the most strongly affected isoforms. By reducing PKC-α levels by 80% by an anti-sense oligonucleotide it was shown that PKC-α expression was not only required for FcεRI-coupling to PLD, but also for

degranulation in mast cells. This result was consistent with reports that PKC- α is an important regulator of Fc ϵ RI-mediated mast-cell responses [158, 159]. Collectively, these findings indicated that down-regulation of PKC- α provided a mechanism for ES-62-mediated inhibition of PLD and SPHK and the consequent calcium mobilisation. ES-62 inhibits Fc ϵ RI-initiated mast cell activation. a) In normal mast cells PKC- α couples Fc ϵ RI to a pathway that results in increased calcium concentration and cell activation. b) In the presence of ES-62, which binds to TLR4, PKC- α is sequestered away from Fc ϵ RI and targeted for degradation and key mast cell activities are blocked (Fig 1.5).

It has been shown that ES-62-mediated modulation of macrophage pro-inflammatory cytokine production is depended on TLR4 [125]. It was found that signaling mediated by ES-62 had unique features as compared to signaling induced by LPS, which is a known ligand for TLR4. The mechanism of subversion of TLR4 signaling by ES-62 was described by Melendez *et al* (2007) by antisense reduction of TLR4 expression in mast cells which blocked the ES-62-mediated inhibition of degranulation and the consequent release of eicosanoids and pro-inflammatory cytokines. The use of TLR4 as a receptor by ES-62 was assessed by the localisation of both molecules in mast cells by confocal microscopy. Mast cells were incubated with FITC conjugated ES-62 and its localisation with respect to TLR4 was examined at various timepoints. It was observed that the trafficking of ES-62-TLR4 complexes drove ES-62-mediated down regulation of PKC- α expression. Analysis of the composition of TLR4-containing immune complexes by western blotting revealed the presence of ES-62 in these complexes. There were low levels of PKC- α at time 0, but within 15 min, the amount of bound PKC- α was greatly increased corresponding to the entry of ES-62-TLR4 complexes into the vesicular compartment. Furthermore, on

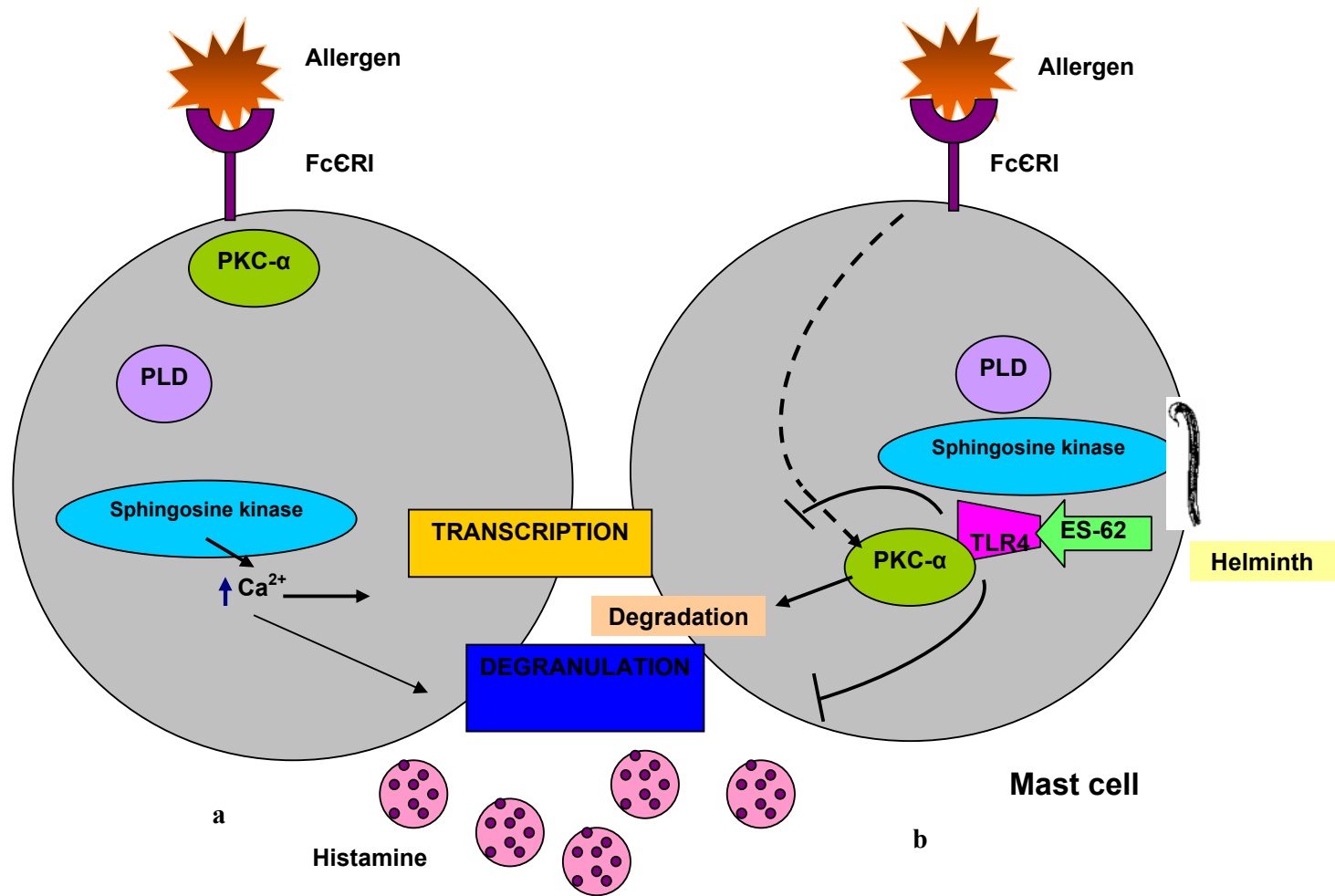
analysis of the TLR4-depleted lysates, it was discovered that all the ES-62 had been depleted from the time 0 lysate consistent with its association at the plasma membrane. PKC- α was depleted with kinetics that corresponded to its association with ES-62–TLR4. These results suggested that ES-62–TLR4 complexes might sequester PKC- α from Fc ϵ RI and PLD at the plasma membrane [160], and the subsequent internalisation of ES-62–TLR4 complexes might drive trafficking of PKC- α to the perinuclear region, where it could be targeted for degradation [161]. It was also observed that PKC- α was not sequestered by TLR4 when the cells were exposed to LPS emphasising the fact that interactions between TLR4 and the bacterial product are different from those between TLR4 and ES-62. It was suggested that other PKC isoforms (β , ζ , δ , ι) targeted by ES-62 might also be sequestered in a TLR4-dependent manner, which might contribute through reduced NF- κ B activation, to suppressed mast cell function. However, by reducing PKC- α levels (~ 80 % reduction) using antisense knockdown, it was shown that PKC- α is required for Fc ϵ RI-coupling to PLD as well as degranulation in mast cells. Thus, the sequestration and degradation of PKC- α by ES-62–TLR4 complexes provided a mechanism for the disruption of key PLD-SPHK-dependent pathways of calcium, PKC and NF- κ B activation. The disruption of these pathways was associated with the consequent failure of ES-62–treated mast cells to degranulate in response to cross-linking of Fc ϵ RI.

The activity of ES-62 against mast cells *in vivo* was demonstrated by the use of a mouse model of immediate-type hypersensitivity to oxazolone [162]. As indicated by knockout mouse studies, the immediate hypersensitivity response in this model is crucially dependent on functional mast cells [162]. It was discovered that mast cells obtained from the ears of sensitised and challenged mice degranulated in

response to FcεRI cross-linking *ex vivo*, but the degranulation was considerably reduced if animals had been inoculated with ES-62. Inhibition of degranulation correlated with the lack of production of TNF-α, IL-3 and IL-6 (but not IL-5 and IL-13) and suppression of NF-κB activation in response to FcεRI cross-linking *ex vivo*. ES-62 also inhibited the mast cell-dependent hypersensitivity reaction *in vivo* as determined by measurement of ear swelling. The ability of ES-62 to be active at other sites of mast cell-mediated inflammation was demonstrated by inhibition of degranulation in the lungs of mice sensitised to and challenged with OVA. ES-62 was active in these experiments, which demonstrated the differences between ES-62- and LPS-mediated TLR4 signaling, as it has been shown that LPS increased mast cell-dependent airway inflammation [163]. Also, mast cells, but not T cells or eosinophils, localise within bronchial smooth muscle in individuals with asthma, where mast cell mediators promoted tissue remodelling leading to hyper-reactive lung function [164]. It was therefore assessed whether ES-62 could prevent airway remodelling and hence disease progression by using unrestrained barometric plethysmography to quantify changes in lung function in response to the broncho-constricting agent methacholine [165]. ES-62 clearly suppressed such airway hyper-responsiveness. Moreover, it was also found that disease severity and progression were reduced by ES-62 in the murine model, as measured by histological analysis of lung pathology, lung eosinophilia and the release of IL-4, the signature cytokine necessary for the development of airway inflammation. Figure 1.5 represents mechanism of action of ES-62 on mast cells [166].

Figure 1.5 represents mechanism of action of ES-62 on mast cells.

Mechanism of action of ES-62



1.9 AIMS:

The side effects caused by the conventional asthma medications including corticosteroids are manifold. Reaction caused by drugs such as leukotriene antagonists and Omalizumab can even be life threatening. Moreover, considering the immunomodulatory role of helminths, it was decided to try and produce a drug to be used as novel treatment for asthma. In addition, it has also been elucidated that ES-62 has been highly effective both *in vitro* and *in vivo* as an immunomodulatory molecule and hence it represents a good starting point.

ES-62 reduced the severity of collagen induced arthritis in DBA/1 mice. There was reduction in collagen-specific IFN- γ , TNF- α and IL-6 and increase in IL-10 produced *ex vivo* by draining lymph node cells from the mice receiving ES-62 [252]. Pretreatment with ES-62 inhibited degranulation and prevented the initial peak of Ca²⁺ mobilisation triggered by Fc ϵ RI in human mast cells. Furthermore, it was demonstrated that ES-62 prevented oxazolone induced skin hypersensitivity and reduced OVA-induced airway hyperresponsiveness in a mouse model [155]. However, ES-62 is very large and hence immunogenic and its immunomodulatory activity is dependent on PC attachment to the molecule by a nematode-specific synthetic pathway. Hence, it would be difficult to consider ES-62 as a drug. Therefore, based on PC, 65 small molecule analogues were manufactured by the team of Prof. Collin Suckling in the Department of Pure and Applied Chemistry at the University of Strathclyde. It was hypothesized that the molecules based on the PC moiety of ES-62 would be able to mimic its immunomodulatory properties. It was decided to screen these molecules and compare them with ES-62 for effects on mast cells. Various analyses were employed to test these SMAs, namely measurement of

effects on degranulation, calcium mobilisation, cytokine release and PKC- α , PLD1 and SPHK1 expression.

To further this end, degranulation assay was performed in the BMMC and later conducted in a mast cell line, RBL 2H3 cells to see whether these SMAs caused any reduction in the degranulation similar to the effect of ES-62 in human and murine mast cells [155].

Calcium mobilisation assays were performed to test for the effect of the SMAs on SPHK induced Ca²⁺ mobilisation in the BMMC. These were undertaken to test the ability of SMAs to induce any inhibition in the mobilisation, which would in turn influence degranulation in the mast cells.

The degranulation in mast cells is accompanied by the *de novo* production of various cytokines. Thus the effects of the SMAs on the release of pro-inflammatory cytokines TNF- α and IL-6, in the BMMC were performed. Any inhibition in the release of these cytokines would help in amelioration of the pathology associated with chronic asthma.

ES-62 had prevented degranulation in human mast cells by proteasome-independent degradation of PKC- α which further prevented the sequential activation of PLD and SPHK. Consequently, the effects of SMAs on the signaling molecules PKC- α , PLD1 and SPHK1 were determined by laser scanning cytometry. These analyses were conducted on BMMC which were sensitised and crosslinked with the antigen and then stained with immunofluorescent antibodies to determine the expression, degradation and translocation of the signaling molecules in these mast cells.

CHAPTER II

MATERIALS AND METHODS

2.1 Reagents

RPMI-1640 (without L-glutamine) was obtained from PAA Laboratories, Yeovil, Somerset, UK. Penicillin, streptomycin and L-glutamine were all purchased from Lonza Biologics plc, (Slough, Berkshire, UK). Sodium azide, fetal bovine serum, lipopolysaccharide (LPS) derived from *E.coli* 0111, B4, sodium bicarbonate, citric acid, Triton X-100 1% (v/v), p-Nitrophenyl N-acetyl β -D-glucosaminide, tyrode's salt solution, monoclonal anti-DNP produced in mouse (IgE-isotype), dinitrophenyl albumin (DNP-HSA), ionomycin calcium salt, Fura-2AM, sodium chloride, potassium chloride, magnesium chloride, hepes, calcium chloride, trypan blue, glucose, bovine serum albumin (BSA), EDTA, ammonium chloride, disodium hydrogen orthophosphate dodehydrate, potassium dihydrogen orthophosphate, saponin, formaldehyde 36.5% (v/v), 4',6-diamidino-2-phenylindole (DAPI), phosphorylcholine, sodium nitrite, boric acid, toluidine blue and Tris were obtained from Sigma-Aldrich Company Limited, (Dorset, UK). Minimum essential medium (MEM) was obtained from Invitrogen limited, (Inchinnan Business Park, Paisley, U.K.). The cytokine ELISA kits for TNF- α and IL-6, high binding Corning costar 96 well ELISA plates and purified mouse anti-PKC- α were obtained from BD Biosciences, (Oxford Science Park, Oxford, UK). Mouse monoclonal antibody to TLR4 (Phycoerythrin-conjugate) was bought from Abcam plc, (Cambridge Science Park, Cambridge, UK). P.E mouse IgG2b κ isotype control, mouse IgG2a isotype, (A Becton Dickinson, Oxford UK) and rabbit IgG isotype were bought from BD Pharmingen, (Oxford Science Park, Oxford, UK). Endosafe kits were obtained from Charles River Laboratories (Edinburgh, Scotland). SMAs of phosphorylcholine were provided by Prof. Collin Suckling, Department of Pure and Applied Chemistry, University of Strathclyde. IL-3 and SCF were produced by PeproTech House,

(London, UK). PE anti-mouse c-kit and PE conjugate rat IgG2b isotype control were obtained from BD Biosciences, (Oxford Science Park, Oxford, UK). FITC anti-mouse FcεRI and FITC Armenian Hamster Isotype IgG were produced by eBiosciences. Rabbit polyclonal anti-PLD1 was procured from Insight Biotechnology limited, Middlesex UK. Rabbit polyclonal anti-SPHK1 was bought from Exalpa Biologicals, Shirley, Massachusetts, USA. Anti-rabbit IgG-HRP conjugate and Alexa Fluor-488 were purchased from Cell Signaling Technology of Massachusetts, USA who are distributed by New England Biolabs, Hertfordshire, UK. Highly purified endotoxin-free ES-62 was produced from spent culture medium of adult *Acanthocheilonema viteae* [134] in the laboratory of Prof. W. Harnett, University of Strathclyde, UK.

2.2 Preparation of bone marrow derived mast cells (BMMC)

(i) Animals

The animals used were 6-8 weeks old BALB/c male mice that were no less than 20 grams (gms) in weight. They had been bred in the University of Strathclyde animal unit.

(ii) Mast cell culture medium

RPMI-1640 (without L-glutamine) was employed as medium. 100U/ml penicillin, 100 mg/ml (v/v) streptomycin, 2mM L-glutamine, 1% (w/v), fetal bovine serum 10% (v/v), β-mercaptoethanol, 0.1% (v/v) and cytokines IL-3 (5ng/ml) and SCF (50ng/ml), were added to the medium which was stored at 4° C.

(iii) Culturing of mast cells

The femurs of the BALB/c mice were taken and the flesh cleaned off. They were immersed in 70% ethanol for 3-4 minutes to remove fibroblasts and connective

tissue. The femurs were cut from both ends and bone marrow was flushed out using a 23 gauge needle. The resulting cell suspension was mixed very gently using a 1 ml Gilson to obtain a uniform mixture and remove any clumps of cells. Shards of bone and other debris were removed by passing the sample through sterile Nitex mesh. The mixture was centrifuged at 483 g for 5 minutes. The supernatant was discarded and the cells were re-suspended in fresh medium and then counted. To 75ml culture flasks, 1×10^6 cells per ml of progenitor cells (bone marrow cell suspension) were added. These bone marrow derived haemopoietic cells are capable of differentiation into all blood cell types under the influence of various cytokines [167]. The cytokines, IL-3 (5ng/ml) and SCF (50ng/ml) were added to this suspension of cells. The flasks were maintained at 37°C in 5% CO_2 in an incubator. Daily inspection of cells was undertaken to ensure sterility of the culture. On the fourth day, the cells were provided with fresh medium and cytokines. On the seventh day, the cells were again provided with fresh medium and transferred into a new sterile flask to get rid of any adherent cells. They were fed every third day and checked for infection. In the third week the cells were no longer transferred to a new flask as after the third week, the majority of cells are immature mast cells. After 4 weeks maturation, the cells were tested for expression of various markers e.g. c-kit, Fc ϵ RI to ascertain their identity.

(iv) Staining of BMMC

The maturity of BMMC was ascertained by toluidine blue staining of the mast cells. 100ml of 1×10^6 BMMC were added to a cytofunnel, assembled with slide and filter paper. BMMC were cytocentrifuged for 4 min at 40 g in a Shandon Cytospin 2 at a high-medium speed setting. The slide was removed and the area with the cells was marked with a hydrophobic pen and allowed to air dry. 0.01% (v/v) of toluidine blue

stain in 1XPBS was added to the slide for 5 minutes and washed with distilled water. Presence of metachromatic granules observed under 10x Olympus inverted microscope confirmed the cells to be mast cells.

2.3 Preparation of PC-conjugate to BSA and BSA

PC-conjugated to BSA was obtained from the laboratory of Prof. Harnett, which had been prepared previously according to the protocol mentioned by Pery *et al* [168] and further adopted by Goodridge *et al* [125]. According to Goodridge *et al*, diazoniumphenyl-PC was prepared by dissolving 1 mmol of aminophenyl-PC (v/v) in 3ml of 1N HCl (v/v) and adding 1mmol of sodium nitrite (w/v). 125µmol of diazoniumphenyl-PC was coupled to 1.5µmol of BSA (v/v) by incubation in 5ml of 0.1M borate buffer with 0.15M sodium chloride, pH 9.0, for 12 hrs at 4°C, followed by dialysis against 10mM phosphate buffer (v/v), pH 7.2. The absence of endotoxin from the PC-BSA was confirmed using an Endosafe kit.

Sham treated BSA was prepared according to the method mentioned above but without PC. The solutions were filter sterilised for the use in the experiments.

2.4 Fluorescence activated cell sorting (FACS) analysis:

FACS analysis of the BMMC was undertaken to confirm the presence of high affinity FcεRI and c-kit receptor on the cells. Mast cells (mature at 4 weeks) were incubated with PE conjugated-anti-mouse c-kit, PE-conjugated rat IgG2b isotype control, FITC conjugated anti-mouse FcεRI or FITC conjugated Armenian hamster isotype IgG to confirm the presence of c-kit and FcεRI on the cells. Staining buffer was prepared with PBS pH 6.5, fetal calf serum 5% (v/v), and sodium azide 0.05% (w/v). 50µl of staining buffer was added to 0.5×10^6 cells in FACS tubes. The antibodies were added

at a concentration of 0.5µg/tube. The tubes were placed on ice at 4°C in the dark for 20 min and then analysed for the markers of mast cells.

2.5 Determination of β-hexosaminidase release in BMMC

1x10⁶ BMMC were incubated overnight in the wells of an ELISA plate at 37°C in the presence or absence of mouse IgE anti-DNP (1µg/ml) and ES-62 (2µg/ml) in Tyrode's salt solution with fetal calf serum 1% (v/v). The BMMC were then incubated with dinitrophenyl human serum albumin (DNP-HSA) or ionomycin calcium salt (1µg/ml) for 1 hr at 37°C. After removing the culture supernatant, the BMMC were solubilised with 100µl of 1% v/v Triton X-100, to obtain the total β-hexosaminidase released by the cells. Razin *et al* determined that sensitisation of BMMC with monoclonal IgE leads to the release of β-hexosaminidase and histamine, sulfidopeptide leukotrienes and proteoglycans [199]. Release of β-hexosaminidase on addition of the substrate p-nitrophenyl *N*-acetyl β-*d*-glucosaminide was used as a marker to confirm degranulation. Therefore, 200µl of 1mM p-Nitrophenyl *N*-acetyl β-*d*-glucosaminide in 0.5M citrate buffer with pH 4.5 was added to samples and the ELISA plate incubated for 1 hr at 37°C. Adding 0.1M sodium bicarbonate buffer pH 10.4 terminated the reaction between enzyme and substrate. The plate was read at an optical density of 405 nm.

The % β hexosaminidase release was calculated by the formula

$$= \frac{\text{optical density of the supernatant}}{\text{optical density of the supernatant} + \text{optical density of the pellet}} \times 100$$

(Optical density of the supernatant + optical density of the pellet).

2.6 Determining the effects of SMAs on cytosolic calcium ion concentration in

BMMC

(i) Materials

Buffers: Calcium buffer (pH 7.4) was made in 500ml of distilled water (dH₂O). NaCl 145mM, KCl 5mM, MgCl₂ 1mM, Hepes 10mM and CaCl₂ 1mM were added to the calcium buffer. Glucose (1.8mg/ml) and BSA (2mg/ml) were added to the calcium buffer immediately before the assay. EDTA was used at a concentration of 500mM in 50ml of dH₂O. EDTA was dissolved with the help of 1g of NaOH in 50ml of distilled water. BMMC were sensitised with monoclonal anti-DNP (100ng/ml) and the antibody cross-linked with DNP-HSA (1µg/ml). 50µl of 1% Triton X-100 was used for solubilisation of cells. Fura-2AM was employed at a concentration of 5mM. The mast cells were stimulated with the SMAs at a concentration of 1µg/ml.

(ii) Method

1x10⁶ BMMC were incubated with anti-DNP IgE, 1µg/ml of SMAs 1-65, 2µg/ml of PC-BSA and BSA. After 18 hrs incubation the cells were re-suspended in 500µl of the calcium buffer and Fura-2 AM and incubated at 37°C for 30 minutes in the dark. Thereafter, the cells were washed twice with calcium buffer and re-suspended in 1.5 ml of calcium buffer. They were allowed to rest for 15 minutes in the dark and then analysed.

Each sample of 500µl was added to 1.5ml of the calcium buffer in the cuvette and examined at the single, fixed emission of 510nm and variable excitation emission wavelengths of 340 and 380nm. The bound calcium was calculated at 340nm and the unbound calcium at 380nm.

A baseline was obtained and then the sample was added with 50µl of the DNP-HSA antigen. At 150 sec, 1% Triton X-100 was added to lyse the cells to obtain R_{max} and

then EDTA was added at 250 sec to obtain R_{min}.

The ratio of these 2 fluorescence intensities was obtained and was used to calculate the calcium ion concentration by the formula:

$$Ca^{2+} = K^d \times \frac{R - R_{MIN}}{R_{MAX} - R} \times \frac{S_{f2}}{S_{b2}}$$

K^d is the dissociation constant for Fura-2 and calcium ion. R is the ratio of fluorescence intensities at 340 and 380 nm. R_{max} is the maximum ratio value between the two fluorescent intensities when Fura-2AM binds all calcium ions. R_{min} is the minimum ratio value between the two fluorescent intensities when Fura-2AM is in a completely free state. S_{b2} and S_{f2} represent the fluorescence at 380nm associated with the bound and free forms of the dye, respectively.

2.7 Culturing of RBL-2H3 cell line

Rat basophilic cells were first obtained by Eccleston *et al* by treating Wistar rats with the potent carcinogen 2-(a-chlor-b-isopropylamine)ethyl naphthalene [169]. Barsumian and colleagues cloned the various sublines of RBL cells by injecting them into 2-4 days old Wistar rats [170]. Stable cell lines were later produced by transfecting RBL-2H3 cell lines with human FcεRI by Gilfillan and team [171].

RBL-2H3 cell lines and clones are cultured as a single layer. When the cell layer is approaching confluency, the culture has to be replated at a lower density.

(i) Preparation of RBL-2H3 cell line

The RBL-2H3 cell line was a kind gift from Dr. Susanne Hartmann, Department of Molecular parasitology, Humboldt University, Berlin, Germany.

(ii) RBL-2H3 cell culture medium

The cells were grown in Minimum Essential Medium (MEM), 2mM L-glutamine 1%

(v/v), 100 U/ml penicillin (v/v), 100 mg/ml, streptomycin (v/v), and fetal bovine serum 10% (v/v). The medium was stored at 4°C.

(iii) Maintenance of the cell line

RBL cells were passaged every third day with the change of the medium and seeded at the concentration of 1×10^6 cells/ml. The cells were split 30 times after which they were frozen down and fresh cells were thawed and a new culture started in the same way.

2.8 FACS analysis for determination of TLR4 receptor on RBL-2H3 cells

FACS analysis was performed to determine the presence of TLR4 on RBL cells to determine their effectiveness as a screening tool for SMAs of ES-62. Spleen cells were employed as a positive control.

(i) Harvesting spleen cells

The spleen of a rat was aseptically removed and placed in 5ml of RPMI-1640 medium containing 2mM L-glutamine 1% (v/v) (as RPMI lacks L-glutamine, this essential amino acid is added to make complete RPMI), 100 U/ml penicillin (v/v), 100 mg/ml, streptomycin (v/v), and fetal bovine serum 10% (v/v). Cell suspensions were prepared by teasing the spleen apart and placing it in two sterile (autoclaved) Nitex mesh pieces and mashing with the help of the plunger end of a sterile syringe in a Petri dish with medium. The suspension obtained was centrifuged at 400 g for 5 min at 4°C.

To remove the erythrocytes, the cell suspension was added to 3ml of Boyles Solution (5ml Tris. 0.17M, 45ml ammonium chloride 0.16M in distilled water) and incubated for 3min at 4°C in a refrigerator. Viable cell numbers were estimated by trypan blue exclusion.

(ii) Procedure for FACS

1x10⁶ cells of each of RBL cells and spleen cells were added to P.E. conjugated mouse monoclonal antibody to TLR4 (0.5mg/ml) and P.E conjugated Mouse IgG2b, isotype control (0.2mg/ml) in 100µl of staining buffer. Staining buffer was made with PBS (phosphate buffered saline) pH 6.5, fetal bovine serum 5% (v/v), and sodium azide 0.05% (w/v). The cells were incubated on ice for 20 min. after which cells were analysed for the presence of TLR4.

2.9 Degranulation of RBL-2H3 cells

(i) Materials

RBL-2H3 cells were added to Tyrode's salt solution containing fetal calf serum 1% (v/v) and monoclonal anti-DNP antibody (100ng/ml) (IgE-isotype). DNP-HSA (100ng/ml), ionomycin calcium salt (1µg/ml), PMA (1µg/ml), 0.1M sodium bicarbonate pH 10.4, 0.5M citrate buffer, pH 4.5 1x PBS, Triton X-100 1%, and p-nitrophenyl *N*-acetyl β-*d*-glucosaminide were employed.

(ii) Procedure

0.15x10⁶ cells were incubated for 2 hrs at 37°C in the presence or absence of mouse IgE anti DNP (100ng/ml) and ES-62 (2µg/ml). The RBL cells were then incubated with antigen DNP-HSA (2µg/ml) for 1 hr at 37°C in Tyrode's buffer. After obtaining the culture supernatant, the cells were solubilised with 100µl of 1% Triton X-100 to release the total β-hexosaminidase. The samples were incubated with 200µl of 1mM p-Nitrophenyl *N*-acetyl β-*d*-glucosaminide in citrate buffer in an ELISA plate and incubated for 1 hr at 37°C. The reaction was terminated by adding sodium bicarbonate buffer pH 10.4. The plate was read at an optical density of 405nm.

The % β -hexosaminidase was calculated by the formula

$$= \frac{\text{optical density of the supernatant}}{\text{optical density of the supernatant} + \text{optical density of the pellet}} \times 100$$

(Optical density of the supernatant + optical density of the pellet).

2.10 Effects of SMAs on degranulation of RBL-2H3 cells after 4 hrs incubation

The RBL-2H3 cells were sensitised with 100ng/ml of IgE for 2 hrs at 37°C, stimulated with 2 μ g/ml of ES-62 or 1 μ g/ml of SMAs 1,3,4,6,9,25,27,28,33,35,39,52,54,63,64 and 65 or 1 μ g/ml of either PC-BSA or BSA. The cells were crosslinked with 100ng/ml DNP-HSA during incubation for 1 hr at 37°C. Degranulation was assessed by release of β -hexosaminidase. This was undertaken by incubating the culture supernatants containing enzyme with 200 μ l of 1mM p-nitrophenyl N acetyl β -D-glucosaminide (substrate) in 0.5M citrate buffer for 1 hr at 37°C. Remaining β -hexosaminidase in cells was also measured following extraction with 1% Triton X-100 and the % β -hexosaminidase release subsequently calculated after stopping the reaction using sodium bicarbonate buffer. 1 μ M Ionomycin/PMA were used as a positive control.

2.11 Cytokine analysis of BMMC after incubation with SMAs by Enzyme-Linked ImmunoSorbent Assay, (ELISAs).

1 \times 10⁶ BMMC were sensitised and incubated for 18 hrs with 1 μ g/ml of SMAs 1,3,4,6,9,25,27,28,33,35,39,52,54,63,64 and 65 or 1 μ g/ml of PC-BSA or BSA and in the case of IL-6, 2 μ g/ml of ES-62. The samples were cross-linked with 1 μ g/ml DNP-HSA for 6 and 24 hrs or incubated with 1 μ M ionomycin/PMA for 6 hrs.

The concentration of TNF- α and IL-6 in the supernatants obtained from BMMC was ascertained with cytokine detection kits according to manufacturer's (as described

below in the methods section) protocols. The cytokines were detected by biotinylated monoclonal antibodies, Streptavidin horseradish peroxidase (SAv-HRP) and TMB substrate. The reactions were measured at 450nm in an Elisa plate reader.

(i) Materials and methods

All the solutions were made in distilled water unless stated otherwise.

High binding Corning costar 96 well ELISA plates from BD Biosciences were used for the cytokine assays.

PBS wash buffer was made 10 times to the concentration required and diluted immediately before performing the ELISA. For the wash buffer, 160gms of sodium chloride, 4gms of potassium chloride, 58.02gms disodium hydrogen orthophosphate dodehydrate and 4gms of potassium dihydrogen orthophosphate were dissolved in distilled water to make up to 2 litres of this solution. The solution was diluted to 1 time its concentration before the assay and the pH was adjusted to 7 using HCl/NaOH. 0.05% (v/v) Tween-20 was added to complete the washing buffer solution.

The coat buffer for TNF- α is 0.1 M sodium carbonate buffer, pH 9.5. The pH was adjusted by adding 8.40gms of NaHCO₃, 3.56gms of Na₂CO₃ to 1L of distilled water and stored at 2-8°C. The assay diluent for IL-6 and TNF- α was made by adding 10% (v/v) fetal calf serum to 1X PBS and stored at 4°C.

The standards were used at the starting concentration of 1000pg/ml for TNF- α and IL-6 and prepared in assay diluent. Anti-TNF- α and anti-IL-6 capture antibodies were used at a concentration of 1 in 250 dilution in coating buffer. The detection antibody, biotinylated anti-mouse TNF was used at a concentration of 1 in 250 dilution in assay diluent. Biotinylated anti-mouse IL-6 detection antibody was used at the same concentration. The enzyme SAv-HRP was used at a concentration of 1 in 250 dilution

in assay diluent according to the instructions provided in the kit from BD biosciences. The substrate for the reaction was TMB solution provided by the manufacturer at the working concentration. The reaction was terminated by stop solution, 2N H₂SO₄.

(ii) Procedure

At every stage of incubation, the ELISA plates were covered using cling film. The ELISA plates were coated with 50µl/ well capture antibody in coating buffer and incubated overnight at 4°C. The plates were washed three times with wash buffer after 18 hrs incubation and then dried by blotting on blotting paper. 75µl/well of assay diluent was used to block the plates and then they were incubated for 1 hr at room temperature. Post incubation, the plates were washed with the wash buffer (1XPBS/Tween) and blotted to remove the washing buffer. 50µl of sample was then added to each well. Standards that had been serially diluted with assay diluent were added, 100µl/well, to generate a standard curve. The plates were incubated for 2 hrs at room temperature and later washed 5 times with the wash buffer and blotted to remove any residual wash buffer. 50µl/well of the detection antibody were added to the plates in the case of TNF-α, which were then incubated for 1 hr at room temperature. Detection antibody and SA_v-HRP were added together in 50µl/well in the case of IL-6 and incubated for 1hr at room temperature. The plates for TNF-α were washed for 5 times and blotted dry. SA_v-HRP was added, 50µl/well and incubated for 30 minutes at room temperature. Following incubation, the plates were soaked for 30 seconds to 1 minute in wash buffer, washed 7 times and then blotted dry. TMB substrate 50µl/well was added to the plates, which were then incubated for 10 minutes in the dark avoiding overdevelopment of the assay. The reactions were subsequently stopped with 2N H₂SO₄. The plates were read at 450nm and the data analysed.

2.12 Preparation of slides for signaling studies

(i) Protocol for plating of cells for immunofluorescence analysis and preparation of BMNC for staining

BMNC (2×10^6) were sensitised with $1 \mu\text{g/ml}$ of IgE and incubated with $1 \mu\text{g/ml}$ of SMAs 3, 25, 33, 39, 63, 64 and 65 or PC-BSA or BSA. The cells were incubated overnight in an incubator at 37°C with $5\% \text{CO}_2$. The cells were washed the next morning and fresh medium with $1 \mu\text{g/ml}$ of DNP-HSA added for 1-2 min to the cross-linked samples.

The reaction was stopped after 1-2 minutes by placing the cells on ice and washing them again and then adding fresh medium. Medium was added with the required amount of cytokines (IL-3 and SCF).

(ii) Materials and Method

A stock of 1M TRIZMA base (pH 7.5) was made by adding 12.1gms Tris base to 70 ml of dH_2O . Stock of 1.5M NaCl was made by adding 8.77gms of NaCl to 100 ml of dH_2O . These stocks were used to make TNT wash buffer in the ratio of 1:1: 8 adding TRIZMA base, NaCl, and dH_2O respectively with 0.05% Tween-20.

All samples were kept in a darkened, humidified chamber at room temperature (RT) throughout.

(iii) Procedure

BMNC (2×10^6 cells/ml in $75 \mu\text{l}$) were added to a cytofunnel assembled with slide and filter paper. BMNC were cytocentrifuged for 4 min at 40 g in a Shandon Cytospin 2. The cells were fixed in 4% (v/v) formaldehyde in PBS for 15 min. Cold PBS was used to wash the cells for 5 min. Thereafter, the cells were permeabilised in 2% FCS, 2mM EDTA (pH 8.0), 0.1% w/v saponin in PBS for 5 min. The slides were then washed in PBS for 10 s. This step was repeated twice. The slides were incubated in

1% blocking reagent (BR)/0.1% w/v saponin in PBS for 10-15 min. Cells were then incubated with Primary Abs at 1 in 50 concentration - purified mouse anti-PKC- α (0.25mg/ml), rabbit polyclonal anti-PLD1 (0.2mg/ml) and rabbit polyclonal anti-SPHK1 (0.5mg/ml), diluted appropriately in 1% BR/0.1% w/v saponin for 30 min. At the same time mouse IgG2a isotype for anti-PKC- α and anti-rabbit IgG isotype control for anti-PLD1 and anti-SPHK1 antibodies were employed after adjusting the dilutions according to the primary Abs in 1% BR/0.1% w/v saponin for 30 min. The slides were washed in TNT wash buffer for 3 min, twice. The cells were incubated with anti-mouse IgG-HRP for PKC- α and goat anti-rabbit IgG-HRP conjugate for PLD1 and SPHK1, diluted 1:100 in BR/0.1% saponin for 25 min. Another wash was given for 3 min and repeated. The slides were incubated with Alexa Fluor 488-labelled tyramide (green), diluted 1:100 in 0.0015% H₂O₂/amplification buffer for 10 min. Another wash was given to the slides in TNT wash buffer for 1-3 min. DAPI (300nM in PBS/0.1% saponin) was added for 1-5 mins (30-50 μ l per slide). The slides were allowed to dry for 5 min after the final wash with TNT wash buffer. The slides were mounted with Vectashield and sealed with clear nail varnish and stored in aluminium foil at 4°C.

2.13 Analysis of Data for Laser Scanning Cytometry using Wincyte software

(i) LSC Data collection

Instrument settings: the appropriate .DPR and .PRO files were set for the collection from the green and blue sensors which enabled the detection of the Alexa Fluor 488 labelled antibodies and DAPI labelled nuclei respectively. The cells were detected by detection of the nucleus set at the threshold value of 8000 pixels. The integration contour (i.e. cell surface) in green was set on cell size with minimum area of the cell

set at $30\mu\text{m}^2$. The peripheral contouring depicted the area between the threshold contour and the integration contour. This area was set between 1 and 9 pixels outside the threshold contour. The area to be scanned was highlighted using the Scan Area option, and the optimal settings for analysis of BMMC were adjusted accordingly. The Photomultiplier tube (PMT)-Voltage was set with Offset and Gain settings to 35%, 2100 and 255 for Green (AF488), and 29%, 2048 and 255 for blue (DAPI).

(ii) Data Analysis

The data were analysed using Wincyte version 3.6 software (Compucyte). The .DPR files were generated which produced histograms that allowed the following analysis:

- Max Pixel versus count, to determine the intensity of foci of fluorescence representing expression of PKC- α , PLD1 and SPHK1 in individual BMMC.
- integral versus count, reflecting fluorescence levels of PKC- α , PLD1 and SPHK1 expression within individual cells.
- Peripheral integral versus count to identify the levels of fluorescence representing PKC- α , PLD1 and SPHK1 expression in the cytoplasm (between the nuclear and cell surface contours) in individual cells.
- The Isotype/rabbit IgG control samples were used to set negative staining regions on the Max pixel plot and hence, allowing determination of the parameters PKC- α , PLD1 and SPHK1 positive cells. These regions were connected with total and peripheral integral plots depicting PKC- α , PLD1 and SPHK1 expression by the BMMC on the total integral versus Count and Peripheral integral versus Count histograms. The percentage and number of cells together with mean fluorescence value for every region was then calculated.

2.14 Statistics

The statistical analysis was done by student *t*-test.

CHAPTER III

RESULTS

3.1 Small Molecules Analogues

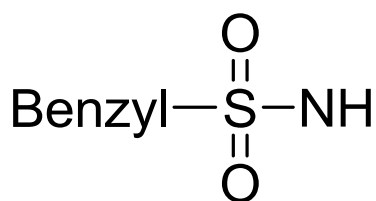
It has been shown previously that many immuno-modulatory properties of ES-62 have been attributed to the PC component of the molecule [117, 125]. Similar to ES-62, PC attached to OVA modulated the production of pro-inflammatory cytokines in macrophages and dendritic cells. This was accomplished in a TLR4/ MyD88-dependent manner, which appears unique to ES-62 as compared to signaling induced by lipopolysaccharide (LPS), which is considered to be a classical TLR4 ligand [125]. Furthermore, previous studies indicated that compounds such as oxidised 1-palmitoyl-2-arachidonoyl-*sn*-glycerol-3-phosphocholine (OxPAPC) induced protective effects against the inflammatory cascade induced by LPS. This action was accomplished by competitively blocking the ability of LPS to bind to TLR4, thereby preventing the injury to lungs induced due to oxidative stress caused by peroxidation of phospholipids in cases of acute and chronic inflammatory conditions of the lung, including acute respiratory distress syndrome and asthma [172,173]. A choline-deficient diet is known to induced hepatocarcinoma and non-alcoholic steatotic hepatitis in rats [174-176]. In the study by Kwaratani *et al* [176] a choline-deficient diet also lead to an increase in the TNF- α levels in the serum and liver of male F344 rats along with an increase in the gene expression for TLR4 and CD14, a co-receptor for LPS. Furthermore, a study by Detapoulou *et al* concluded that subjects, whose diets were rich in choline and betaine, had the lowest levels of inflammatory markers including C-reactive protein, homocysteine, IL-6 and TNF- α [177]. Based on these studies, it could be assumed that compounds containing PC would have immuno-modulatory and anti-inflammatory potential.

As the ES-62 molecule itself is very large and hence immunogenic, it is unlikely to be suitable for therapeutic use. Thus, small molecule analogues (SMAs)

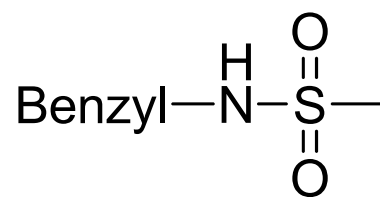
of ES-62 based on the PC moiety were developed and a total of 65 of these were tested for immuno-modulatory effects on the mast cells. These molecules were developed by Dr. Judith Huggan and Dr. Abedawn Khalaf, under the supervision of Prof. Colin Suckling, all of University of Strathclyde. Out of these 65 SMAs, 62, made by Dr. Abedawn Khalaf, contained sulphonamide and amide. The remaining three compounds made by Dr. Judith Huggan resembled phosphorylcholine more closely. It was assumed that the 'transition state', in this case "phosphoryl", could be mimicked by alternative moieties such as sulphonamide, sulphone and amide. The SMAs thus consisted of sulphonamide, sulphone and amide group-containing molecules. These groups were attached to the benzyl group through the sulphur atom or the nitrogen atom (Fig. 3.1.1 a and b) with resultant modifications to the structure of choline (Fig 3.1.2). The right hand side of the SMA molecule (yellow background) is dimethylamine and it was assumed that the analogue of choline (Fig 3.1.3) would protonate (in the buffer or in the body) to generate a compound very similar to choline itself with respect to charge, even though it lacked one methyl group. On this basis, many compounds were prepared as "free bases"; i.e. with two methyl groups attached to the nitrogen atom. In one, SMA 64, a quaternary amine compound (i.e. three methyl groups attached to the nitrogen atom) was prepared. Also, the oxygen atom of the hydroxyl group of choline was substituted with nitrogen in some cases. Replacing dimethylamine with morpholine or pyrrolidine also generated further compounds. The core structure of all the SMAs was very much similar to choline, with CH₂-CH₂ forming the basis in each case.

It was assumed that the addition of the aromatic benzyl group to the SMAs enabled them to be lipophilic and hence assist their entry into the phospholipid-containing cell membrane (Fig 3.1.4). It is possible that the extra two methylene groups in the case

of pyrrolidine and extra two methylene groups and oxygen in morpholine, could bring benefits as it is thought that in medicinal chemistry it is advantageous to have a bulkier material, which may fill empty spaces and hence increase vital contacts with the active sites on cell membrane receptors. In comparing the ClogP (computed logarithm of the 1-octanol/water partition coefficient), which is a measure of lipophilicity, it was found that choline and morpholine had almost similar values (CLogP: -0.3974 and -0.4078 respectively). However the value for pyrrolidine was increased marginally at (ClogP: 0.2472). Furthermore, it was seen that chemically the SMAs are basic in character and are easily soluble in water. This readily enabled their use in *in vitro* experiments. The solubility of SMAs will also facilitate their use in an injectable form for *in vivo* use for further analysis. It was also ascertained that the salts of the SMAs would also be water soluble, when manufactured for further experiments and analysis.



a)



b)

Fig.3.1.1 Sulphonamide attachment to the benzyl group (a) *via* the sulphur atom, (b) *via* the nitrogen atom.

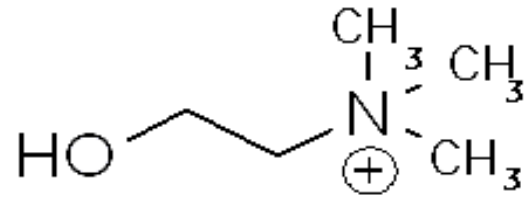


Fig 3.1.2 Basic structure of Choline

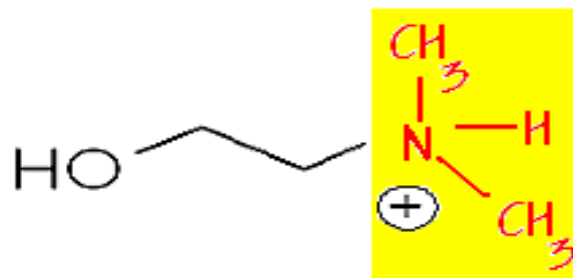


Fig 3.1.3 Structure of Analogue of Choline

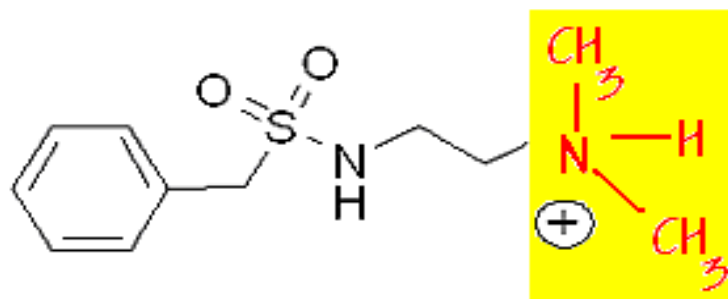


Fig 3.1.4 Basic structure of SMAs

Modifications to the structure of choline were achieved by the substitution of methyl groups with 1) Dimethylamine 2) Morpholine 3) Pyrolidine to the sulphonamide moiety.

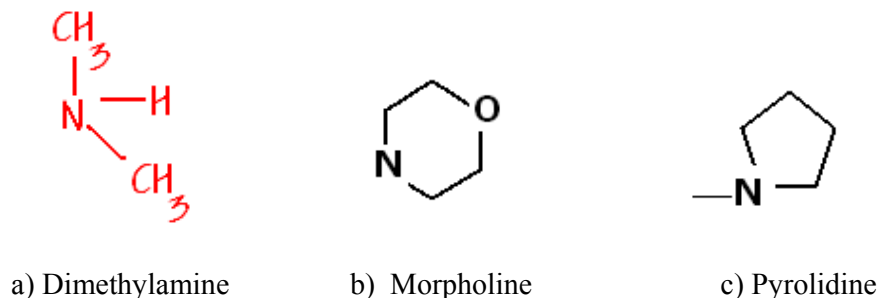


Fig. 3.1.5 Structures of the various substituents of methyl groups in choline.

Dimethylamine is an analogue of choline (Fig 3.1.5a). SMAs 1, 2, 3, 10, 13, 16-20, 23, 26, 29, 32, 35, 38, 39, 42, 45-49, 52, 53, 56, 57 and 61-64 are examples of compounds with the dimethylamine group. Of relevance, there is an excretory-secretory product first discovered by Harnett *et al* in 1986, that is released by juvenile female *Litomosoides sigmodontis*[178]. This molecule was later studied by Hintz *et al* and called Juv-p120. It was observed that parasitaemic hosts (*Mastomys coucha*; *Sigmodon hispidus*) failed to mount any antibody response to two microfilarial sheath surface antigens of 40 and 120kDa (shp3a and shp3) that cross-reacted with Juv-p120, suggesting that Juv-p120 may be able to induce hyporesponsiveness in these animal models. The biological and biochemical characterisation of Juv-p120 revealed that the protein contained large amounts of N, N-dimethylethanolamine (DMAE). The similarity with choline could be assumed to be responsible for the immunosuppressive property of Juv-p120 in inducing anergy in lymphocytes, even in the presence of high microfilaraemia [179]. Further studies by Houston *et al* suggested the source of DMAE in Juv-p120 to be choline [180]. DMAE is very similar in

structure to dimethylamine and is synthesised using equimolar amounts of ethylene oxide and dimethylamine [181]. Therefore, in the light of DMAE, dimethylamine could be assumed to possess immunomodulatory properties. One of the derivatives of dimethylamine, 2-(diphenylmethoxy)-N,N-dimethylethanamine also called diphenhydramine is a histamine H1 antagonist used for the control of allergic symptoms. It is also employed as an anti-emetic in motion sickness, an anti-tussive for irritant cough, a hypnotic and an ingredient in common cold preparations. Diphenhydramine is also used for the treatment of dermatosis e.g. atopic dermatitis (AD) caused due to immune-mediated inflammation of skin arising from an interaction between genetic and environmental factors, irritant contact dermatitis due to chemicals, soaps, plants and body fluids and allergic contact dermatitis due to type IV hypersensitivity to various allergens. It is able to relieve pruritus in dermatosis by actively competing with free histamine for binding at histamine receptor sites leading to reduction in the adverse symptoms which consist of redness, inflammation, itching, blisters, dryness and lichenification of the skin [182, 183].

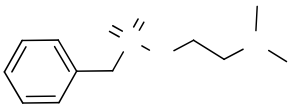
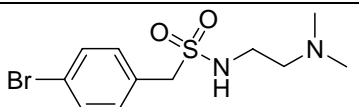
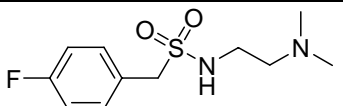
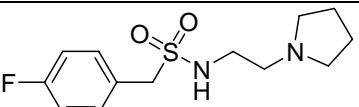
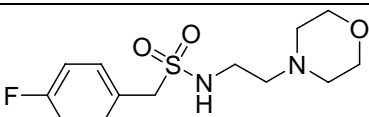
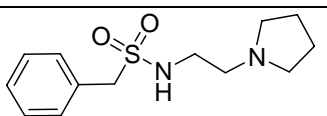
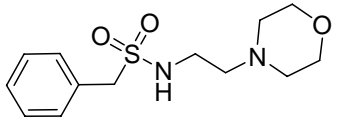
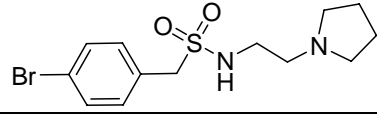
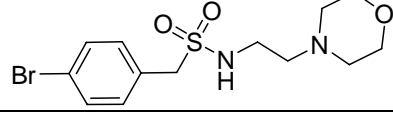
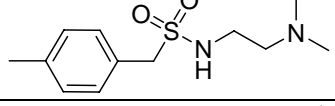
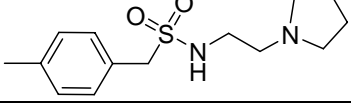
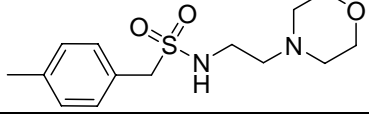
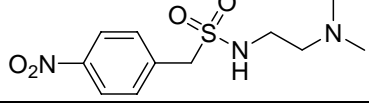
Morpholine (Fig 3.1.5b) is an aliphatic compound. The methyl groups of dimethylamine were substituted with morpholine to obtain SMAs 5, 7, 9, 12, 15, 22, 24, 27, 30, 33, 36, 37, 41, 44, 51, 55 and 59. Commercially, it has already been used as an ingredient in the production of Gefitinib, N-(3-chloro-4-fluorophenyl)-7-methoxy-6-(3-morpholin-4-ylpropoxy)quinazolin-4-amine, a compound that inhibits epidermal growth factor receptor (EGFR) tyrosine kinase by binding to the adenosine triphosphate (ATP)-binding site of the enzyme. Clinically it is used for the continued treatment of patients with locally advanced or metastatic non-small cell lung cancer [184, 185]. As seen above, compounds of morpholine, were shown to inhibit EGFR signaling and hence this property can be utilised in the lungs to control the pathology

of asthma. Its aliphatic nature would enable it to penetrate the cellular membrane, which may contribute towards the effects of the SMAs.

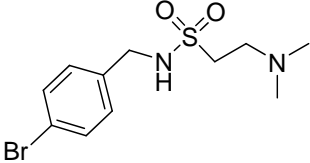
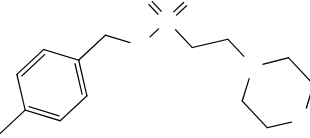
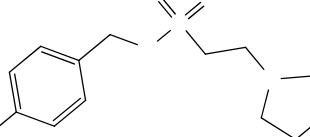
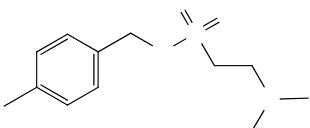
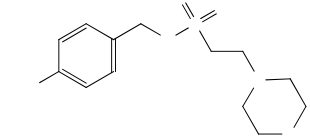
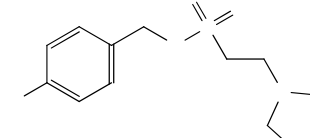
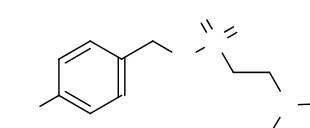
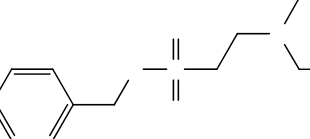
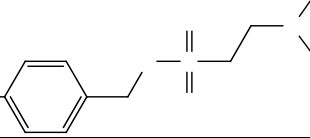
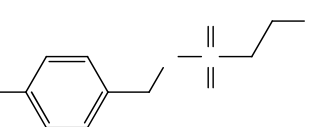
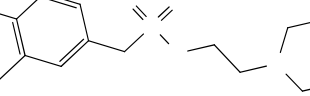
Pyrolidine (Fig. 3.1.5c) is also an aliphatic compound. The SMAs modified by substitution of methyl groups are 4, 6, 8, 11, 14, 21, 25, 28, 31, 34, 40, 43, 50, 54, 60 and 65. Its derivative with the formula 1-cyclohexyl-1-phenyl-3-pyrrolidin-1-ylpropan-1-ol is known clinically as procyclidine. It is thought to act by blocking central cholinergic receptors [186, 187]. Its derivative, bepridil with the formula N-[3-(2-methylpropoxy)-2-pyrrolidin-1-ylpropyl]-N-(phenylmethyl) aniline, acts as a calcium channel blocker in cardiac and vascular smooth muscles, interfering with calcium binding to calmodulin, and blocking both voltage and receptor operated calcium channels [188, 189]. The use of pyrolidine for substituting methyl groups in choline could thus be beneficial in ways other than having potential to modulate TLR4 signalling. The derivatives could not only possibly act as anti-cholinergics by relaxing the smooth muscles of the lungs in asthma but could also block calcium signaling in mast cells.

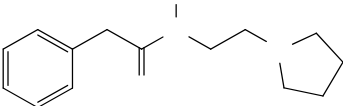
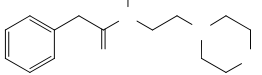
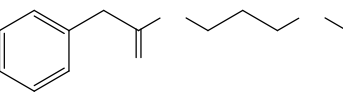
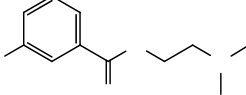
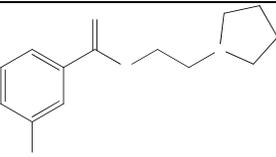
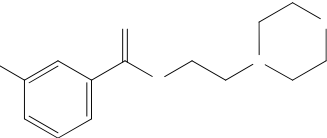
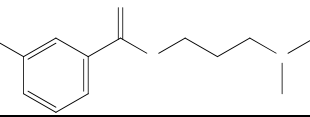
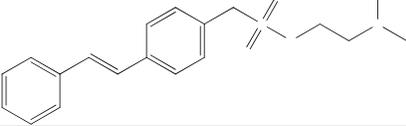
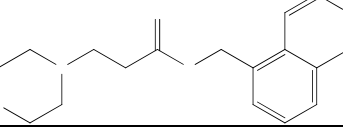
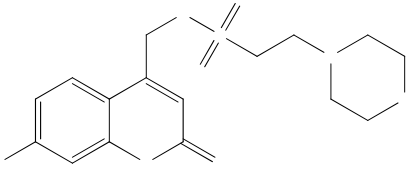
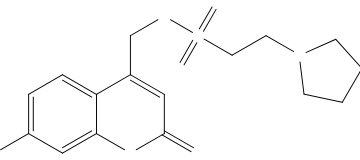
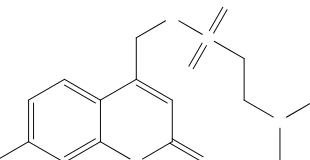
To investigate the future use of these SMAs as therapeutic agents, various assays and techniques were employed to assess their effects on mast cells. These are described subsequently.

3.1.2 List of small molecule analogue formulae

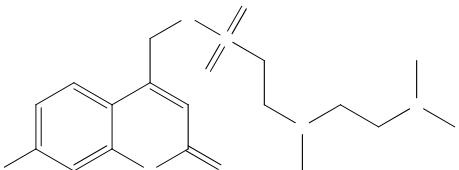
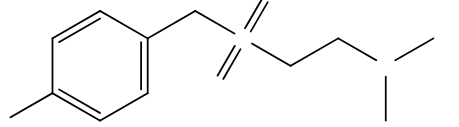
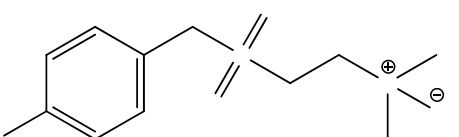
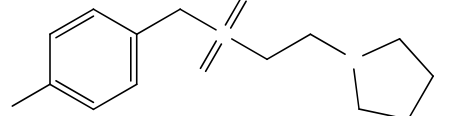
No	STRUCTURE	FORMULA/ MW
1		C ₁₁ H ₁₈ N ₂ O ₂ S 242.3
2		C ₁₁ H ₁₇ BrN ₂ O ₂ S 321.2
3		C ₁₁ H ₁₇ FN ₂ O ₂ S 260.3
4		C ₁₃ H ₁₉ FN ₂ O ₂ S 286.4
5		C ₁₃ H ₁₉ FN ₂ O ₃ S 302.4
6		C ₁₃ H ₂₀ N ₂ O ₂ S 268.4
7		C ₁₃ H ₂₀ N ₂ O ₃ S 284.4
8		C ₁₃ H ₁₉ BrN ₂ O ₂ S 347.3
9		C ₁₃ H ₁₉ BrN ₂ O ₃ S 363.3
10		C ₁₂ H ₂₀ N ₂ O ₂ S 256.4
11		C ₁₄ H ₂₂ N ₂ O ₂ S 282.4
12		C ₁₄ H ₂₂ N ₂ O ₃ S 298.4
13		C ₁₁ H ₁₇ N ₃ O ₄ S 287.3

O
S
O
N

26		$C_{11}H_{17}BrN_2O_2S$ 321.2
27		$C_{14}H_{12}N_2O_3S$ 298.4
28		$C_{14}H_{22}N_2O_2S$ 282.4
29		$C_{12}H_{20}N_2O_2S$ 256.4
30		$C_{13}H_{19}N_3O_5S$ 329.4
31		$C_{13}H_{19}N_3O_4S$ 313.4
32		$C_{11}H_{17}N_3O_4S$ 387.4
33		$C_{13}H_{19}FN_2O_3S$ 302.4
34		$C_{13}H_{19}FN_2O_2S$ 286.4
35		$C_{11}H_{17}FN_2O_2S$ 260.3
36		$C_{17}H_{22}N_2O_3S$ 334.4 O_2N

50		C ₁₄ H ₂₀ N ₂ O 232.3
51		C ₁₄ H ₂₀ N ₂ O ₂ 248.3
52		C ₁₃ H ₂₀ N ₂ O 220.3
53		C ₁₂ H ₁₈ N ₂ O ₂ 222.3
54		C ₁₄ H ₂₀ N ₂ O ₂ 248.3
55		C ₁₄ H ₂₀ N ₂ O ₃ 264.3
56		C ₁₃ H ₂₀ N ₂ O ₂ 236.3
57		C ₁₉ H ₂₄ N ₂ O ₂ S 344.5
58		C ₁₉ H ₂₂ F ₃ N ₂ O ₂ 413.2
59		C ₁₇ H ₂₂ N ₂ O ₆ S 382.4
60		C ₁₇ H ₂₂ N ₂ O ₅ S 366.4
61		C ₁₅ H ₂₀ N ₂ O ₅ S 346.4

O
H
N
O
H
N
O
O
O
NH
O
NH
O

62		$C_{18}H_{27}N_3O_5S$ 397.5
63		$C_{11}H_{16}BrNO_2S$ 306.2
64		$C_{12}H_{19}INO_2S$ 368.3
65		MeO $C_{14}H_{21}NO_2S$ 267.4

Br

Me

Me

3.2 Selection of Assays for Measuring Mast Cell Degranulation

It has been suggested that cross-linking of antigen-specific IgE bound to cell surface FcεRI initiates the phosphorylation of Lyn [190], which is a protein tyrosine kinase of the Src family. Lyn phosphorylates the tyrosines in the ITAMs (immunoreceptor tyrosine based activation motifs) of β and γ chains, initiating a further phosphorylation reaction involving Lyn, Syk and Fyn as well as the phosphorylation of PLC-γ [191-195]. PLCγ hydrolyses phosphatidylinositol-4, 5 biphosphate (PIP2) to inositol 1, 4, 5-triphosphate (IP3) and diacylglycerol (DAG). These second messengers mediate the process of degranulation. It is thought that IP3 increases intracellular Ca²⁺ levels. This increased level of Ca²⁺ and DAG leads to activation of PKC [195, 196]. The increase in intracellular Ca²⁺ concentration and activated PKC leads to degranulation. Also, it has been assumed from the previous studies that ionophores such as ionomycin stimulate the hydrolysis of inositol phospholipids. This hydrolysis induces an increase of calcium in the mast cells by mobilisation of calcium extracellularly and intracellularly from the endoplasmic reticulum and helps in the fusion of the granules laden with mediators with the plasma membrane to induce degranulation [197, 198]. Similarly, PMA acts like DAG, a PKC stimulator for the initiation of the degranulation [199, 200].

3.2.1 Degranulation assay using β-hexosaminidase

An assay involving measurement of release of β-hexosaminidase, induced via cross-linking of bound DNP-specific IgE antibodies, had been previously used successfully to show ES-62-mediated inhibition of degranulation of human BMMC. It was thus decided to test whether the assay could also be employed with mouse BMMC. If this

was the case then the more readily available mouse BMMC could be used to test the effects of SMAs on mast cell degranulation.

3.2.2 Degranulation assay employing BMMC

BMMC were obtained from femurs of BALB/c mice that were 6-8 weeks old. The progenitor cells were grown in RPMI-1640 complete culture medium, in the presence of recombinant IL-3 and SCF cytokines for four weeks, to obtain mature mast cells. The cells were analysed to confirm their identity as mast cells by testing for the presence of c-kit receptor (CD117), and Fc ϵ RI (Fig. 3.2.1 a, b, and c) [201]. Their identity was also confirmed by staining with toluidine blue. The figures show that the majority of cells stained positive for the presence of metachromatic granules thereby identifying them as mast cells [202] (Fig 3.2.2). These cells were analysed for degranulation following sensitisation with, and cross-linking of, IgE antibodies by measuring the release of β -hexosaminidase on addition of the substrate p-nitrophenyl *N*-acetyl β -*D*-glucosaminide. The ideal level of degranulation in the absence of ES-62 was expected to be 30-40% β -hexosaminidase release on addition of the antigen [203]. However, the desired level of degranulation was not observed in these experiments (Fig 3.2.3). Similar results were obtained when ionomycin and PMA were employed for degranulation. Upon repeated undertaking of the assay (n=3), the percentage of degranulation was in general very low, as indicated by the degree of enzyme release. This was subsequently attributed to the fact revealed by electron-microscopic studies that the ultra-structures of mouse BMMC consisted mainly of cytoplasmic granules that are immature as compared to peritoneal mast cells [204]. This immaturity of the granules was considered to be a reason for the poor

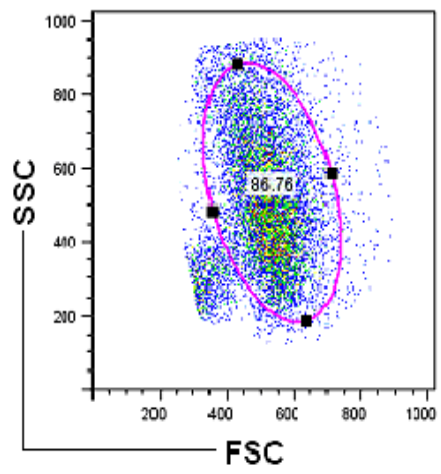
degranulation observed after the addition of cross-linking antigen or PMA/ionomycin.

Therefore, as an alternative, it was decided to investigate calcium mobilisation as a procedure for investigating the effects of SMAs on activation of BMMC.

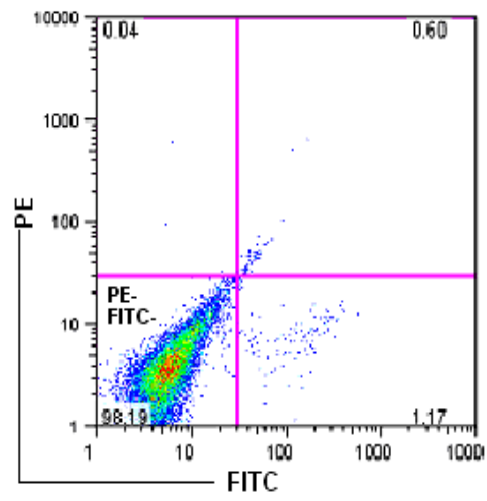
Fig 3.2.1

The phenotype of bone-marrow derived cells was assessed by flow cytometric analysis for the co-expression of CD117 (also called c-kit) and FcεRI receptors [197].

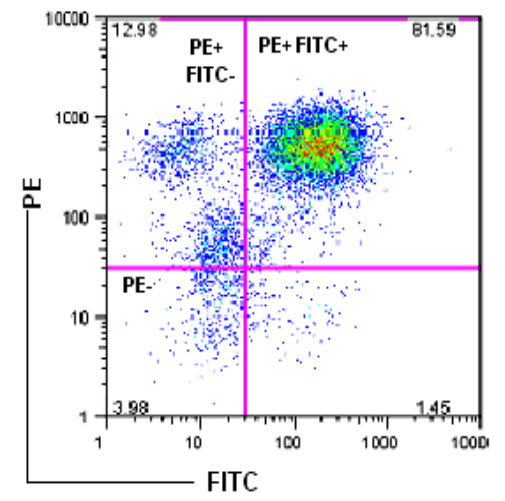
- a) Dot plots of forward scatter (FSC) versus side scatter (SSC) analysis giving the measure of cell size and granularity, respectively, reveal the cell population to be of a size and granularity associated with mast cells
- b) Gating on the cells deemed healthy by their position on these plots shows the position of isotype controls. Analysis for expression of CD117 indicated by staining with a Phycoerythrin (PE)-conjugated rat anti-mouse c-kit IgG2b antibody relative to its isotype control (PE-conjugated rat anti-mouse IgG2b) and FcεRI, indicated by staining with a FITC-conjugated Armenian Hamster anti-mouse FcεRI IgG antibody relative to its isotype control.
- c) Dot plots showing the staining of CD117/FcεRI relative to isotype controls (b) are presented with the 81.59 % of CD117⁺FcεRI⁺ double positive mast cells shown in the upper right hand side quadrant.



a)



b)



c)

Fig 3.2.2

Toluidine blue staining of BMMC showing morphology of cells. The majority of cells showed purple staining of metachromatic granules indicating the cells to be mast cells.

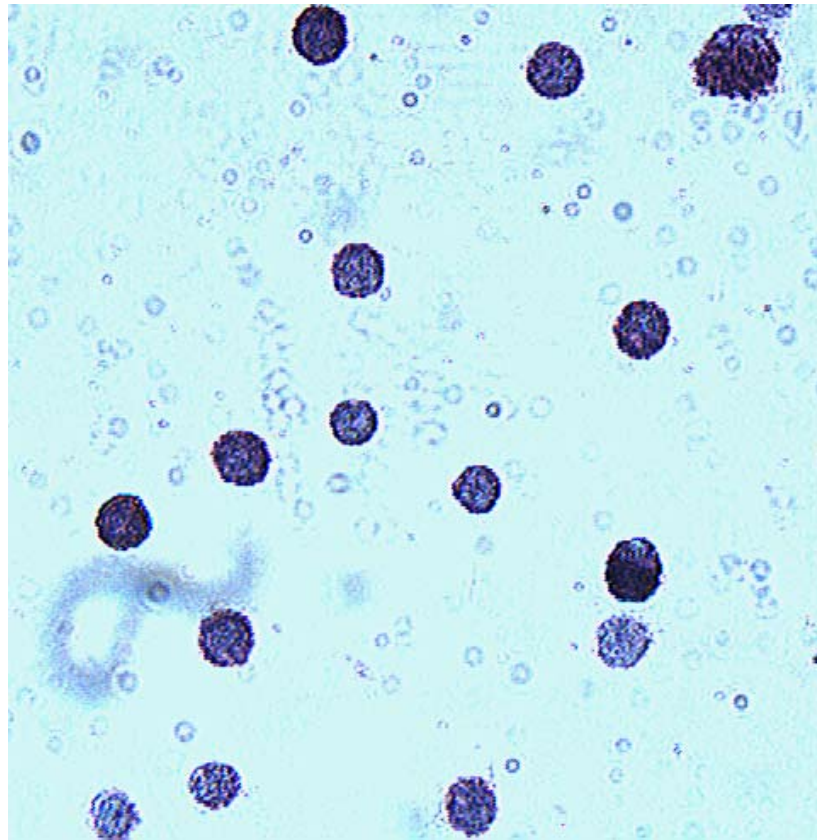
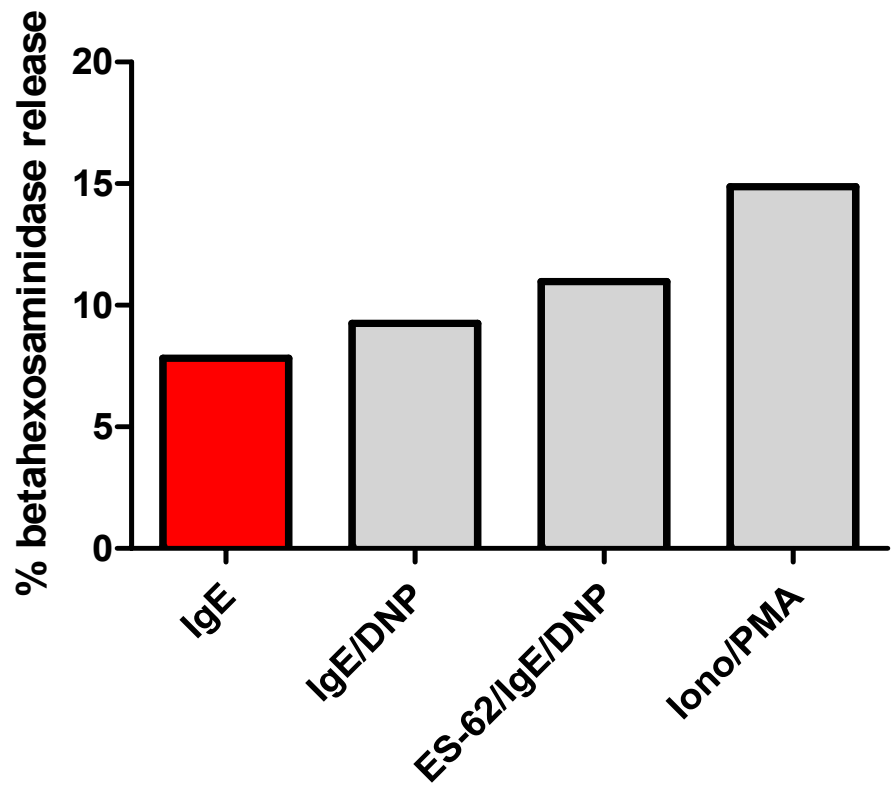


Fig 3.2.3

BMMC were sensitised with 1µg/ml of anti-DNP IgE, stimulated with ES-62 (2µg/ml), crosslinked with 1µg/ml of antigen (DNP-HSA) and incubated for 1hr at 37°C. Degranulation was assessed by release of β-hexosaminidase, a marker for mast cell degranulation. This was undertaken by incubating the culture supernatants containing enzyme with 200µl of 1mM p-nitrophenyl N acetyl β-D-glucosaminide (substrate) for 1 hr at 37°C before measuring the optical density at 405nm. Remaining β-hexosaminidase in cells was also measured following extraction with 1% Triton X-100 and the % β-hexosaminidase release subsequently calculated. 1µM ionomycin/PMA were used as a positive control. The data are the average of triplicate readings in a single experiment. IgE = sample consisting of BMMC sensitised with anti-DNP IgE to examine any spontaneous degranulation. IgE/DNP = sample sensitised and cross-linked with antigen. ES-62/IgE/DNP = sample pre-incubated with ES-62 and anti-DNP IgE before cross-linking with antigen. Iono/PMA = sample exposed to ionomycin and PMA as a positive control.



3.3 Calcium Mobilisation Studies

When there is cross-linking of a multivalent allergen in a sensitised individual, the high affinity receptor for IgE (FcεRI) on mast cells triggers the Ca²⁺-dependent release and production of a wide range of mediators responsible for the major symptoms of immediate hypersensitivity reactions. The amplitude and duration of the Ca²⁺ response modulates the activation of various transcription factors [205], thereby regulating expression of different genes.

It has been shown by Melendez and Khaw in 2002 that the initial rapid release of calcium from the mast cells is triggered by sequential activation of PLD and SPHK [156]. Conversely, the later slow release of calcium is triggered by phospholipase Cγ. In a study performed on human mast cells, it has also been shown by Melendez *et al* [155] that ES-62 prevents the initial peak of Ca²⁺ mobilisation dependent on SPHK. Therefore, the latter experiment was undertaken to observe whether similar results could be obtained using mouse BMDC. These cells were considered fully grown after four weeks in culture and their maturity was confirmed by Toluidine blue staining where 99% of the cells stained positive for the dye. These cells were loaded with the flurophore, Fura-2AM for analysis. Fura-2AM is the cell-permeable acetoxymethyl (AM) ester form of Fura-2. On addition of Fura-2AM to the extracellular medium, the ester (acetoxymethyl) is taken up by the cell and is hydrolysed by the action of an intracellular esterase. Removal of the acetoxymethyl esters regenerates "Fura-2". Fura-2AM is a ratiometric fluorescent dye which binds to free intracellular calcium that is excited at 340nm and 380nm of light, and the ratio of the emissions at those wavelengths is directly correlated to the amount of intracellular calcium. The use of the ratio automatically cancels out confounding variables, such as variable dye concentration and cell thickness, making Fura-2 an ideal tool to

quantify calcium levels. The use of such ratiometric analysis is particularly beneficial as alteration of excitation wavelengths is more practical than the detection of multiple emission wavelengths. Upon binding Ca^{2+} , the excitation spectrum of Fura-2 shifts to shorter wavelengths between 300 and 400nm, while the peak emission remains steady around 510nm. Thus, calcium binding is associated with an increase in the ratio of the 340/380 fluorescence intensity at a fixed emission of 510nm. Maximal levels of calcium are determined by adding 1% Triton-X-100 to lyse cells and allow binding of all free Ca^{2+} to Fura-2AM whilst chelation with 0.5M EDTA strips the calcium from Fura-2AM to provide minimum calcium concentration values.

Calcium ion concentration was calculated by the formula:

$$\text{Ca}^{2+} = K^d \times \frac{R - R_{\text{MIN}}}{R_{\text{MAX}} - R} \times \frac{S_{f2}}{S_{b2}}$$

K^d is the dissociation constant for Fura-2 and calcium ion. R is the ratio of fluorescence intensities at 340 and 380nm. R_{max} is the maximum ratio value between the two fluorescent intensities when Fura-2AM binds all calcium ions. R_{min} is the minimum ratio value between the two fluorescent intensities when Fura-2AM is in a completely free state. S_{b2} and S_{f2} represent the fluorescence at 380nm associated with the bound and free forms of the dye, respectively.

In the present investigation, the results obtained were similar to the results shown for human mast cells by Melendez and colleagues [155]. Thus, it was observed that ES-62 inhibited the initial peak of Ca^{2+} influx triggered by sequential activation of PLD and SPHK (Fig 3.3.1). Consequently, it was decided to analyse the effects of SMAs of PC using mouse BMMC. The assay was performed by incubating BMMC with SMAs, sensitising the cells with anti-DNPIgE and then assessing the amount of Ca^{+} ion concentration after cross-linking with the antigen.

The assay was run in triplicate using one batch of cells treated with each SMA and the values obtained were normalised against the control. It was observed that the basal values were offset in the experiments, meaning that the basal values of Ca^{2+} ion concentrations obtained at the same time point were not uniform even for the same sample. Therefore the values had to be normalised against their respective controls. This was performed by obtaining the difference between the basal value and the peak value of the control activated sample. This value was then divided by the difference between the peak and the basal values obtained with SMAs. This quotient was referred to as the normalised value, depicted in percentage. Table 3.3.1 represents the effects of SMAs on the peak intracellular calcium mobilisation mediated by activation of SPHK. The assay revealed some interesting results. It was found that some molecules increased the calcium mobilisation while other molecules inhibited it. The representative figures (Fig 3.3.2 a, b and c) show an increase in the peak intracellular Ca^{2+} concentration in BMBC associated with certain SMAs. SMA 1 demonstrates clear stimulation of peak intracellular (SPHK-dependent) calcium mobilisation as well as an apparent slight increase in secondary influx. SMA 65 shows clear stimulation of peak intracellular (SPHK-dependent) calcium mobilisation. There is stimulation of peak intracellular calcium mobilisation and an increase in secondary influx in the case of SMA 27.

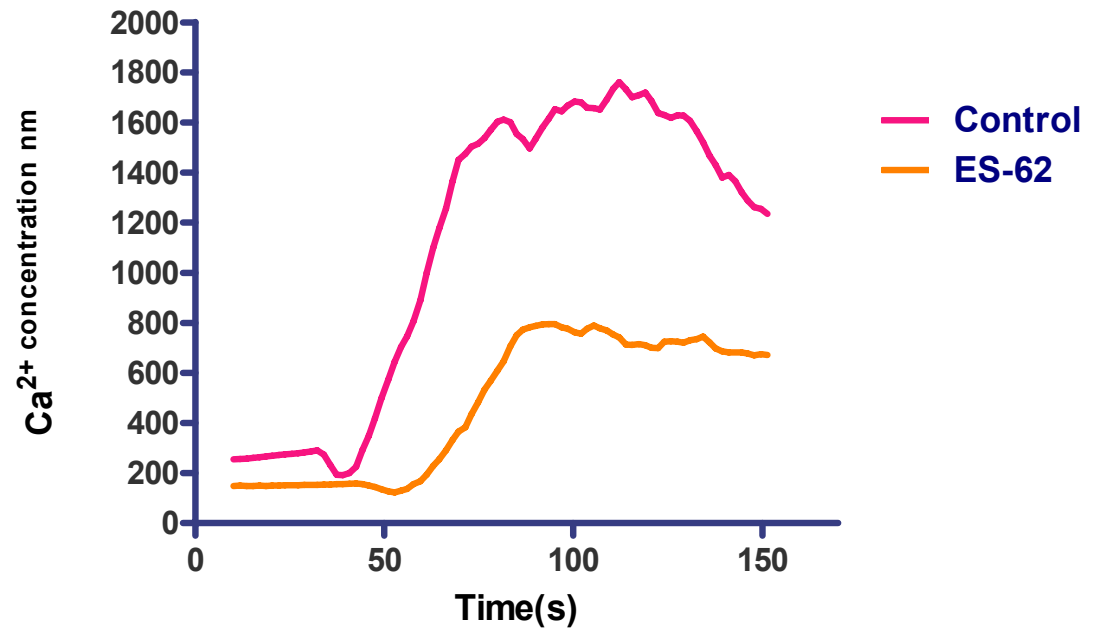
Conversely, Fig. 3.3.3 a, b, and c depict the effects of SMAs that inhibit SPHK-dependent Ca^{2+} mobilisation. SMA 63 demonstrates inhibition of peak intracellular (SPHK-dependent) calcium mobilisation while SMAs 64 and 25 indicate clear inhibition of peak intracellular (SPHK-dependent) calcium mobilisation and also show some evidence of a decrease in the secondary influx. Finally, there was no change in the peak intracellular Ca^{2+} mobilisation associated with most SMAs, as

demonstrated by the examples in Fig. 3.3.4 a, b and c. It was decided to select some molecules which inhibited Ca^{2+} mobilisation and a few that increased Ca^{2+} mobilisation for further studies outlined in subsequent chapters. Table 3.3.2 represents SMAs chosen for further analysis. The SMAs were chosen depending upon their ability to increase or decrease the initial peak of Ca^{2+} mobilisation based on SPHK activation. In the case of SMA 1, as mentioned above, it was discovered that the percentage of Ca^{2+} mobilisation obtained was substantially more as compared to its control. Similarly, SMAs 4, 6, 27, 33, 35 and 65 demonstrated an increase in obtained Ca^{2+} values. SMAs 3, 9, 25, 28, 39, 63, and 64 showed a decrease in peak Ca^{2+} mobilisation values calculated in percentages compared to their controls. SMA 52 was chosen as a control because it demonstrated no significant change in peak Ca^{2+} concentration. It should be noted that some SMAs did not show consistent data in the analysis described above (see Table 3.3.1) and these were omitted from the selection.

Fig 3.3.1

Representative figure of peak intracellular Ca^{2+} mobilisation due to activation of SPHK in BMMC incubated with ES-62 as compared to control cells. It depicts a decrease in Ca^{2+} concentration in the presence of ES-62 as compared to control cells. BMMC were sensitised with $1\mu\text{g/ml}$ of anti-DNP IgE and incubated overnight with $2\mu\text{g/ml}$ of ES-62. The cells were cross linked with $1\mu\text{g/ml}$ of DNP-HSA. R_{MAX} was obtained by adding 1% Triton X-100 and R_{MIN} was obtained by chelating Ca^{2+} with 0.5M EDTA

The data are representative of triplicate determinations in one experiment.



Tab 3.3.1

The table depicts the effects of the SMAs on the peak intracellular calcium mobilisation that is mediated by activation of SPHK. The percentages of Ca^{2+} concentration values released by SMAs after normalising against the Ca^{2+} concentration in the sensitised BMBC control are shown in triplicate. 1×10^6 BMBC were incubated with each SMA at a concentration of $1 \mu\text{g/ml}$ overnight and treated with Fura-2AM for 30 min in the dark. Each of the SMA samples was centrifuged and diluted in 1.5 ml of calcium buffer containing 1mM external Ca^{2+} . Thereafter, three samples were taken from one treated batch of cells for each SMA. The values for some experiments were not considered because calcium influx with antigen was not obtained as indicated by a blank in the table. Each value given in the table is the average of the three determinations in a single experiment and where there are blanks; data from two rather than three experiments were considered.

SMA	1	2	3	MEAN
1		279	333	306
2	80	111	265	152
3	88	63	68	73
4	160	160		160
5	194	102	160	152
6	178		189	183.5
7	100		93	96.5
8	76	94		85
9	87	81		84
10	115	107		111
11	129	121	66	105.3
12	123	71	93	95.6
13	111	87	92	96.6
14	124	141		132.5
15	106	111		108.5
16		118	137	127.5
17	87	118	103	102.6
18	144	67	137	116
19	159	103		131
20		135	84	109.5
21	100	136	59	98.3
22	104	98	84	95.3
23	109	109	60	92.6
24	112	84		98
25	94	70	45	69.7
26		97	193	145
27		268	197	232.5
28	87	65	93	81.7
29	98	107	85	96.7
30	105	106	93	101.3
31	87	108	82	92.3
32		155	148	151.5
33	132	141	135	136
34	125	128	149	134
35	139	160	90	129.7
36	125	129	155	136.3
37	88	103	108	99.7
38	114	108	119	113.6
39	97	82	81	86.7
40	74	138	122	111.3
41	93	133	110	112
42	91	114	88	97.7
43		126	97	111.5
44	107	144	112	121

45		101	88	945
46	120	170	97	129
47		105	127	116
48	147	118	144	136.3
49		110	93	101.5
50		115	107	111
51	124	57	155	112
52	91	91	97	93
53	123	114	90	109
54	129	122	131	127.3
55	87	114	129	110
56	118	107	110	111.7
57	115	148	117	126.7
58	113	113	117	114.3
59	133	94	93	106.7
60	139	101	88	109.3
61	105	131	86	107.3
62	168	106	118	130.7
63	76	74		75
64	61	87		74
65	114	151		132.5

Table 3.3.1

Table 3.3.2

SMA s selected for further analysis. The SMA s were chosen depending upon their ability to increase or decrease the initial peak of Ca^{2+} mobilisation based on SPHK activation. In the case of SMA 1, it was discovered that the percentage of Ca^{2+} mobilisation obtained was substantially more as compared to its control. Similarly, SMA s 4, 6, 27, 33, 35 and 65 demonstrated an increase in Ca^{2+} values obtained. SMA s 3, 9, 25, 28, 39, 63, and 64 showed a decrease in peak Ca^{2+} concentration values calculated in percentages as compared to their controls. SMA 52 was chosen as a control because it demonstrated no change in peak Ca^{2+} concentration. The SMA s were also chosen because consistent or near consistent values were obtained with respect to the triplicate determinations of the experiment. The values for some experiments were not considered because calcium influx with antigen was not obtained as indicated by a blank in the table.

SMA	1	2	3	MEAN
1		279	333	306
3	88	63	68	73
4	160	160		160
6	178		188	183.5
9	87	81		84
25	94	70	45	69.7
27		268	197	232.5
28	87	65	93	81.7
33	132	141	135	136
35	139	160	90	129.7
39	97	82	81	86.7
52	91	92	97	93
63	76	74		75
64	61	87		74
65	114	151		132.5

Table 3.3.2

Fig 3.3.2 a, b and c

Representative figures of peak intracellular Ca^{2+} mobilisation due to activation of SPHK in BMMC incubated with SMAs as compared to control cells. An increase in Ca^{2+} concentration is depicted in the presence of SMAs as compared to control cells. BMMC were sensitised with $1\mu\text{g/ml}$ of anti-DNP IgE and incubated overnight with $1\mu\text{g/ml}$ of SMAs. The cells were cross linked with $1\mu\text{g/ml}$ of DNP-HSA. R_{MAX} was obtained by adding 1% Triton X-100 and R_{MIN} was obtained by chelating Ca^{2+} with 0.5M EDTA. The data are representative of triplicate determinations in one experiment.

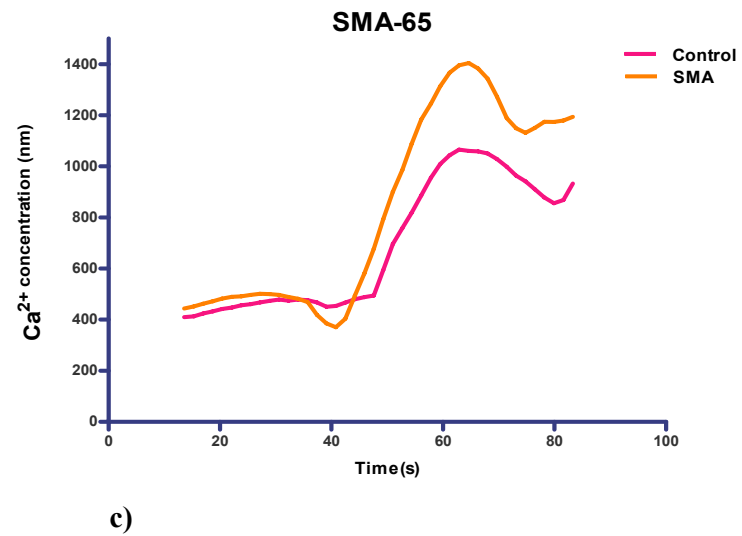
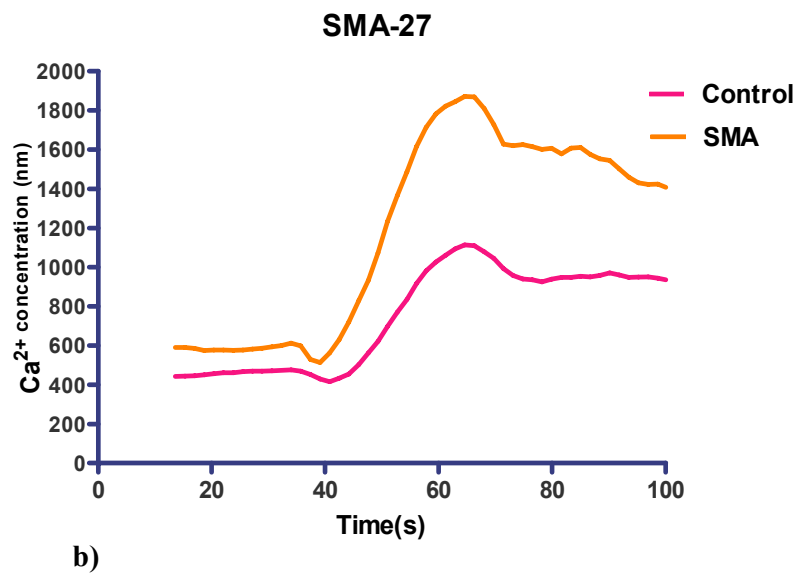
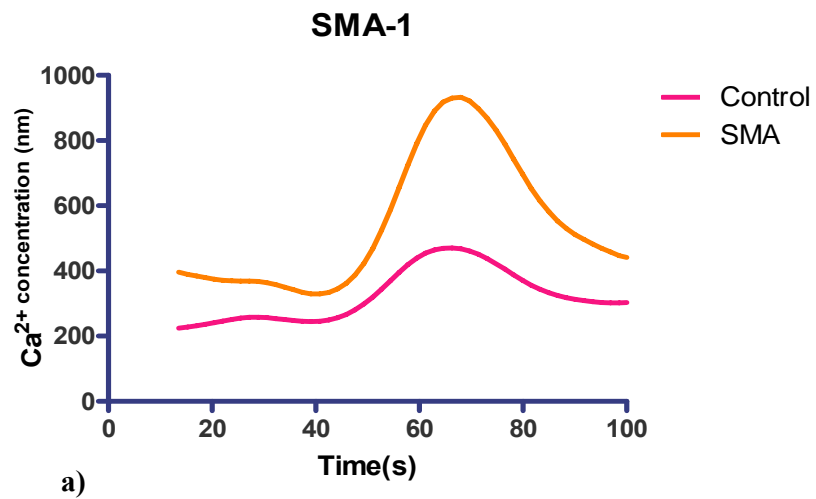
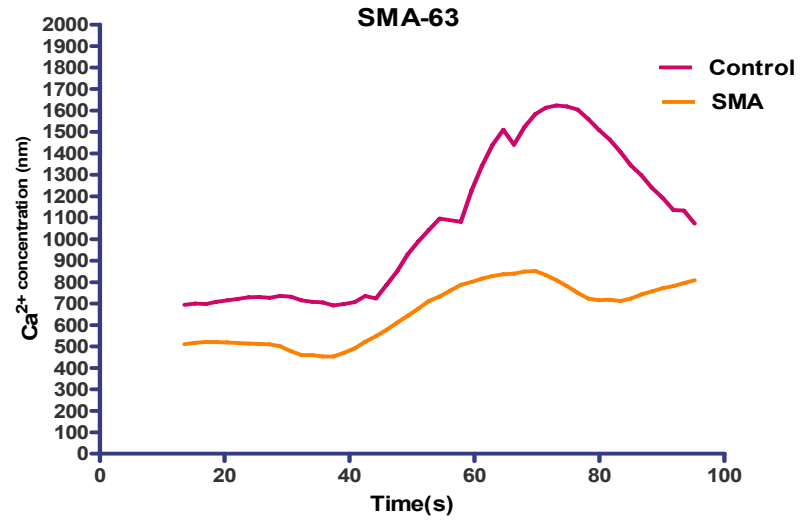


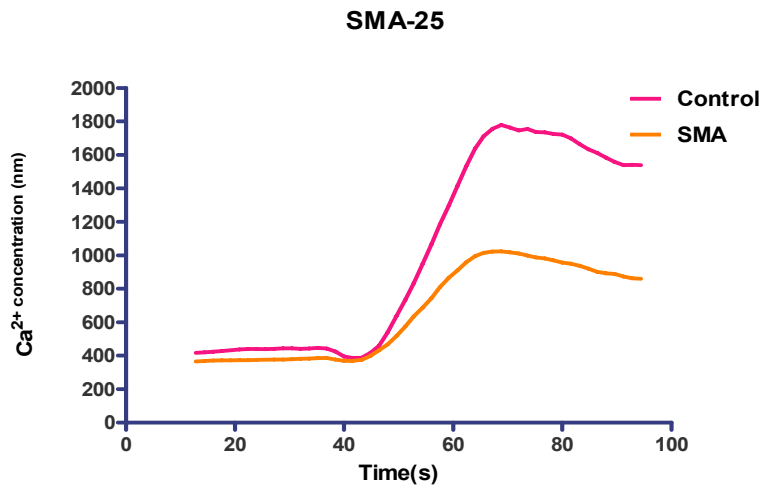
Fig 3.3.3 a, b and c

Peak intracellular Ca^{2+} mobilisation due to activation of SPHK in BMMC incubated with SMAs as compared to control cells. A decrease in Ca^{2+} ion concentration in the presence of SMAs as compared to control cells is depicted in these figures. BMMC were sensitised with $1\mu\text{g/ml}$ of anti-DNP IgE and incubated overnight with $1\mu\text{g/ml}$ of SMAs. The cells were cross linked with $1\mu\text{g/ml}$ of DNP-HSA. R_{MAX} was obtained by adding 1% Triton X-100 and R_{MIN} was obtained by chelating Ca^{2+} with 0.5M EDTA.

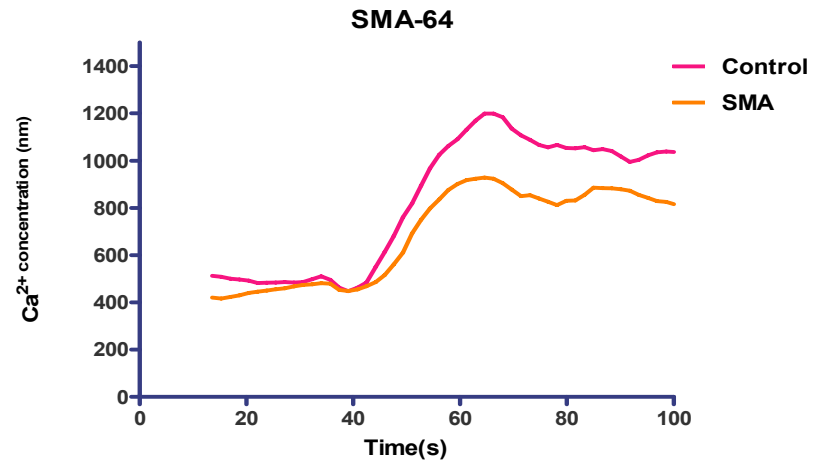
The data are representative of triplicate determinations in one experiment.



a)



b)

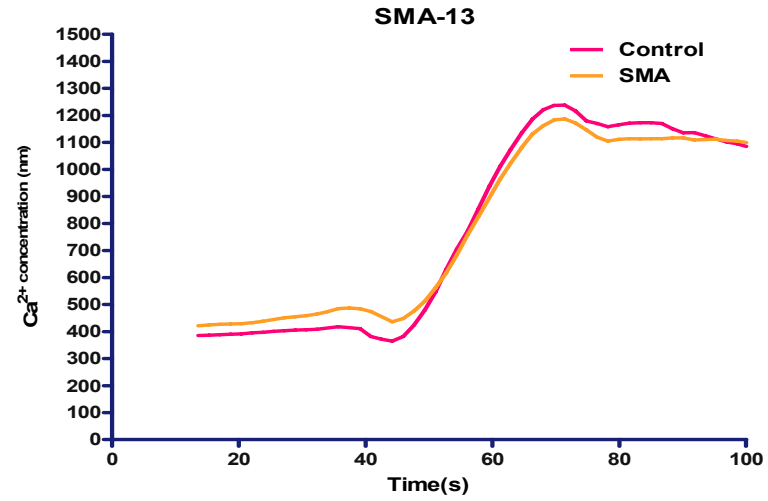


c)

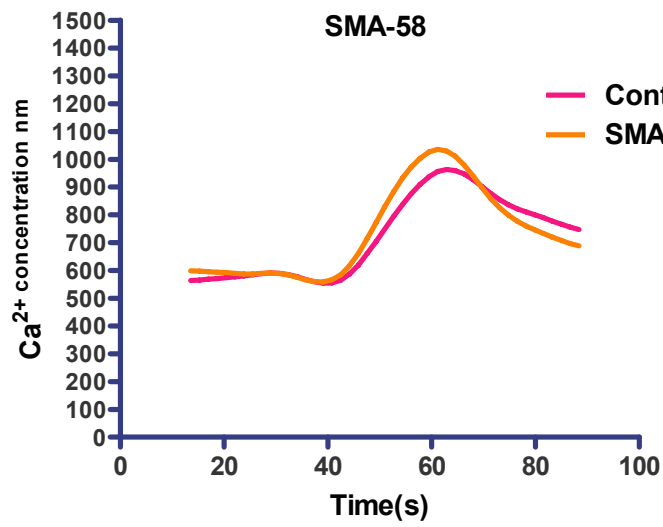
Fig 3.3.4 a, b and c

Representative figures of peak intracellular Ca^{2+} mobilisation due to activation of SPHK in BMMC incubated with SMAs as compared to control cells. The figures depict no change in Ca^{2+} ion concentration in the presence of SMAs as compared to control cells. BMMC were sensitised with $1\mu\text{g/ml}$ of anti-DNP IgE and incubated overnight with $1\mu\text{g/ml}$ of SMAs. The cells were cross linked with $1\mu\text{g/ml}$ of DNP-HSA. R_{MAX} was obtained by adding 1% Triton X-100 and R_{MIN} was obtained by chelating Ca^{2+} with 0.5M EDTA.

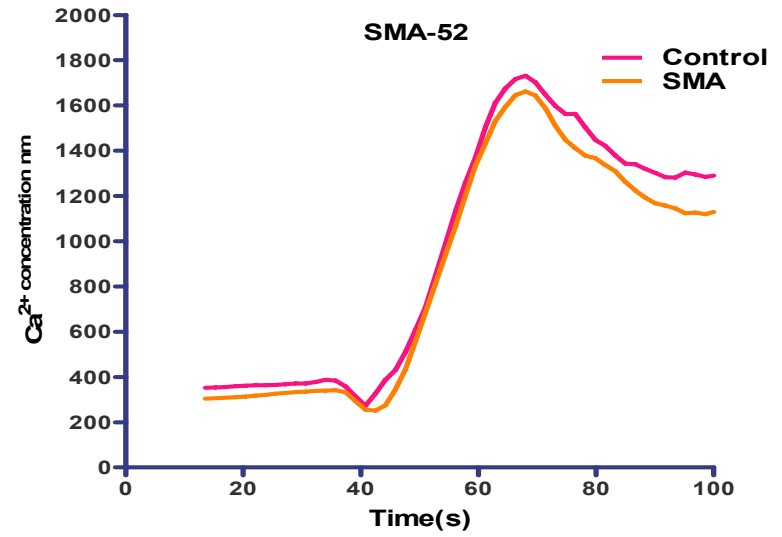
The data are representative of triplicate determinations in one experiment.



a)



b)



c)

3.4 Degranulation Assay using the RBL-2H3 cell line

The calcium mobilisation assay was employed as a screening system to select SMAs, pre-exposure to which could modulate subsequent mast cell activation. However there was still a need to demonstrate that the active SMAs actually had effects on mast cell degranulation. Thus, as an alternative to mouse BMMC, the rat basophilic leukaemia cell line RBL-2H3 was considered.

RBL is a misnomer, as this cell line is more mast cell-like than basophil-like [154, 206]. The RBL-2H3 cell line has been invaluable for the delineation of the structure of, and immediate signaling events associated with, FcεRI. In addition, RBL-2H3 cells also provide a suitable model for high-throughput screening of potential inhibitors of mast cell activation. As shown in previous studies with RBL-2H3 cells, MyD88 and TRAF6 act as key regulators in the LPS/TLR4 signal transduction pathway resulting in production of TNF-α and IL-13 [207]. As ES-62 was shown to act through the TLR4 receptor [125], RBL-2H3 cells expressing TLR4 were considered appropriate for the planned experiments. However, it was decided to confirm TLR4 expression by FACS analysis. As assumed, positive staining of PE-conjugated mouse monoclonal antibody to TLR4 on the RBL-2H3 cells can be seen in Fig. 3.4.1(a, and b).

The degranulation assay employing RBL-2H3 cells was performed to demonstrate that RBL-2H3 cells degranulated when sensitised with anti-DNP IgE and challenged with antigen. The release of β-hexosaminidase was measured by adding the substrate p-nitrophenyl *N*-acetyl β-*D*-glucosaminide as shown for BMMC (section 3.2). The degranulation assay was optimised before analysing the SMAs.

The results indicated, as assessed by measuring the release of β-hexosaminidase, that there was almost 33% degranulation obtained in response to cross-linking of bound

anti-DNP IgE antibodies with RBL-2H3 cells (Fig 3.4.2). Thus, RBL-2H3 cells could be used for demonstrating degranulation and hence further screening of SMAs. The degranulation obtained with ionomycin/PMA was 30%. These reagents can be employed as an additional positive control as ascertained by previous studies, which showed that RBL-2H3 cells degranulated in the presence of ionomycin/PMA, which act as second messengers to induce degranulation [199, 208, 209].

3.4.1 Degranulation assay with stimulation in the presence of small molecular analogues of ES-62

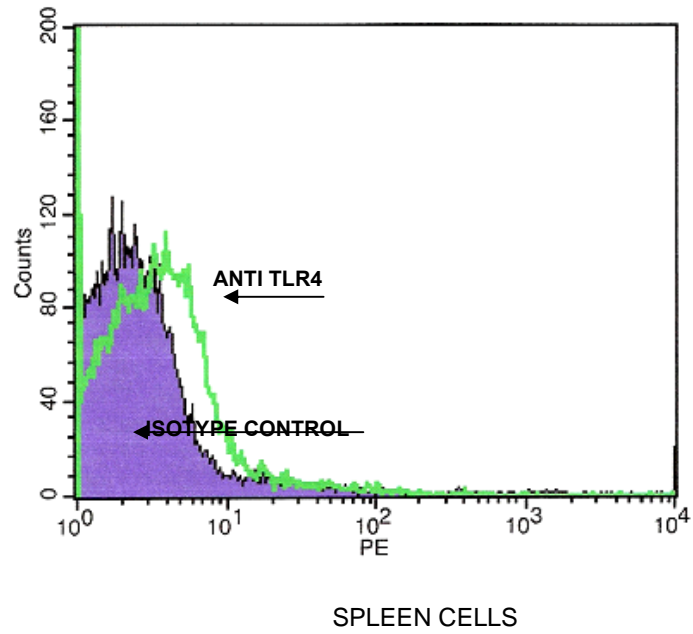
A set of three identical experiments with RBL-2H3 cells involved incubation with ES-62 and the SMAs selected for further study. Phosphorylcholine attached to bovine serum albumin (PC-BSA) and bovine serum albumin (BSA) were also incorporated into the experiments. PC conjugated to BSA (PC-BSA) was used to confirm that any inhibitory effects were due to ES-62's covalently attached PC moiety, which has previously been shown to play a major role in facilitating its immuno-modulatory effects [210] and on whose structure the SMAs are of course designed. Sham-conjugated BSA (BSA) was employed as a negative control for PC-BSA and on showing no modulatory effect on mast cell degranulation in preliminary experiments (not shown), was used in place of the medium control in subsequent experiments. The results obtained indicated that similar to ES-62, three of the SMAs, namely SMA 63, SMA 64 and SMA 65 (and PC-BSA) were able to inhibit Fc ϵ RI-mediated degranulation of RBL-2H3 cells (Fig. 3.4 3). None of the other SMAs had any significant reproducible effect on degranulation (results not shown). Furthermore, each of the molecules found to inhibit Fc ϵ RI-mediated degranulation was also found to reduce the level of spontaneous degranulation observed in the assay (Fig. 3.4.3).

When it came to examining the effects on degranulation induced by ionomycin/PMA, the overall results were not as clear. It was observed that SMA 64 in particular, did not follow the common trend of inhibition. On the contrary, it tended if anything to increase degranulation with ionomycin/PMA (Fig.3.4.3). The mean values obtained from the three experiments (Fig. 3.4.3 a, b, and c) were compared to the normalised control samples (Fig. 3.4.4), which revealed that ES-62 exposure induced 43% of spontaneous degranulation as compared to control (taken as 100%). In the case of SMA 63, the spontaneous degranulation obtained was 41.56%, for SMA 64 it was 50%, for SMA 65, 41.34%, and for PC-BSA it was 38.34% of the BSA control.

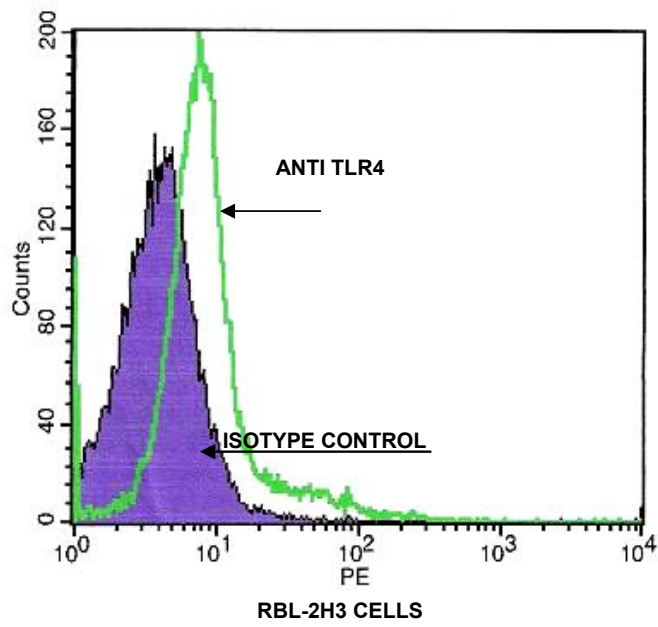
In the sensitised samples cross-linked with antigen, ES-62 exhibited 50%, SMA 63 showed 48%, SMA 64, 57%, SMA 65, 45%, and PC-BSA 47% of degranulation as compared to the control. With respect to the samples that employed ionomycin/PMA as the degranulation agent, ES-62 showed 56% degranulation relative to the control, SMA 63, 33%, SMA 64, 101%, SMA 65, 46%, and PC-BSA 77% of the BSA control.

Fig.3.4.1 a and b

Determination of the presence of TLR4 on RBL-2H3 cells by FACS analysis. Spleen cells were used as a positive control. Phycoerythrin (PE)-conjugated mouse IgG2b was used as an isotype control. PE-conjugated mouse monoclonal antibody to TLR4 was used to determine expression of the TLR4 receptor on RBL cells. Fig a) spleen cells, b) RBL-2H3 cells



a)



b)

Fig. 3.4.2

The RBL-2H3 sample used as a negative control was sensitised with 100ng/ml of anti-DNP IgE for 2 hrs at 37°C, the sample used for cross-linking was sensitised with 100ng/ml of anti-DNP IgE for 2 hrs at 37°C and then incubated with antigen (DNP-HSA) and the other sample used as a positive control was incubated with 1µM each of Ionomycin/PMA. These samples were then incubated for 1 hr at 37°C. Degranulation was assessed by the release of β -hexosaminidase, a marker for mast cell degranulation. This was undertaken by incubating the culture supernatants containing released enzyme with 200µl of 1mM p-nitrophenyl N acetyl β -D-glucosaminide (substrate) for 1 hr at 37°C before measuring the optical density at 405nm. The remaining β -hexosaminidase in cells was also measured following extraction with 1% Triton X-100 and the % β -hexosaminidase release subsequently calculated. Con= BSA control, XL = cross-linking with 100ng/ml of DNP-HSA and I/P = ionomycin and PMA.

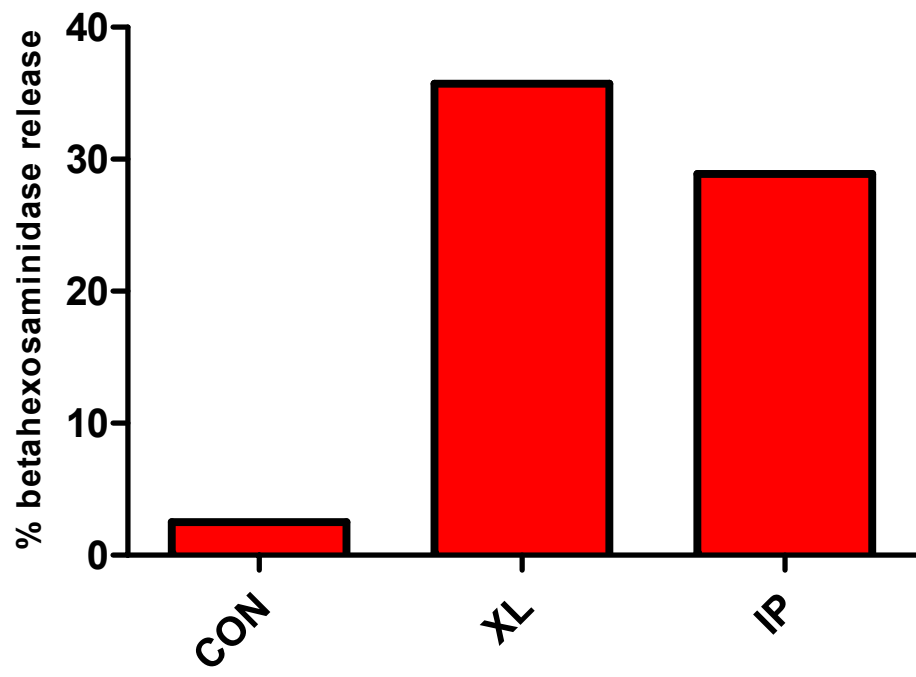


Fig 3.4.3 a, b, and c

The histogram represents data for three separate experiments (a, b and c). The RBL-2H3 cells were sensitised with 100ng/ml of anti-DNP IgE for 2 hrs at 37°C, stimulated with 2µg/ml of ES-62 or 1µg/ml of SMAs or 1µg/ml of PC-BSA or 1µg/ml BSA for 2 hrs and incubated with 100ng/ml DNP-HSA or 1µM Ionomycin/PMA for 1 hr at 37°C. Degranulation was assessed by the release of β-hexosaminidase, a marker for mast cell degranulation. This was undertaken by incubating the culture supernatants containing enzyme with 200µl of 1mM p-nitrophenyl N acetyl β-D-glucosaminide (substrate) for 1 hr at 37°C before measuring the optical density at 405nm. The remaining β-hexosaminidase in cells was also measured following extraction with 1% Triton X-100 and the % β-hexosaminidase release subsequently calculated. XL = cross-linking with DNP-HSA and I/P = incubation with ionomycin and PMA.

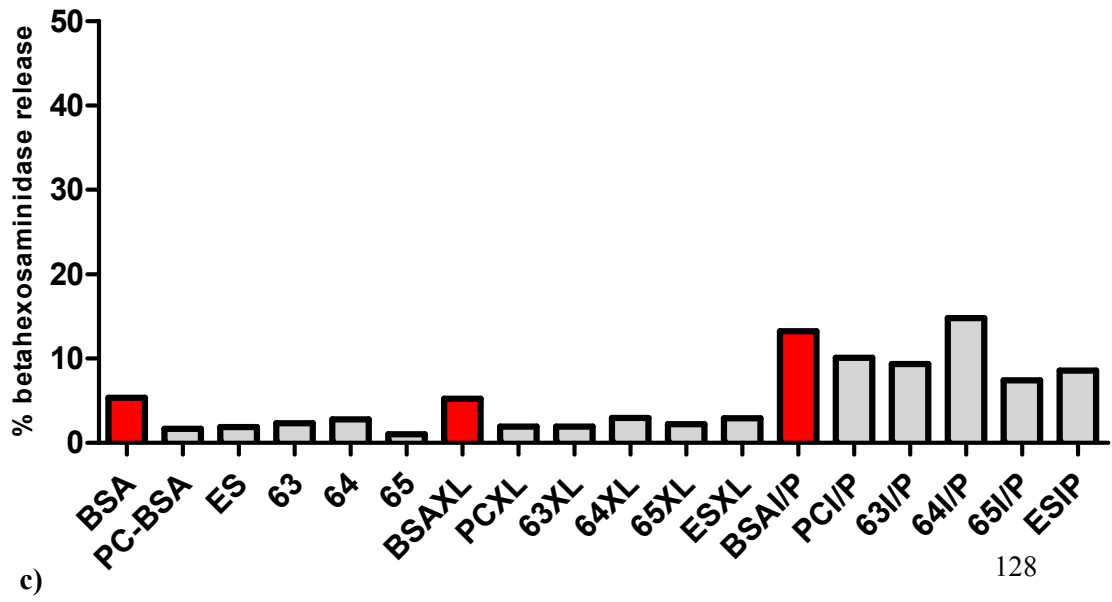
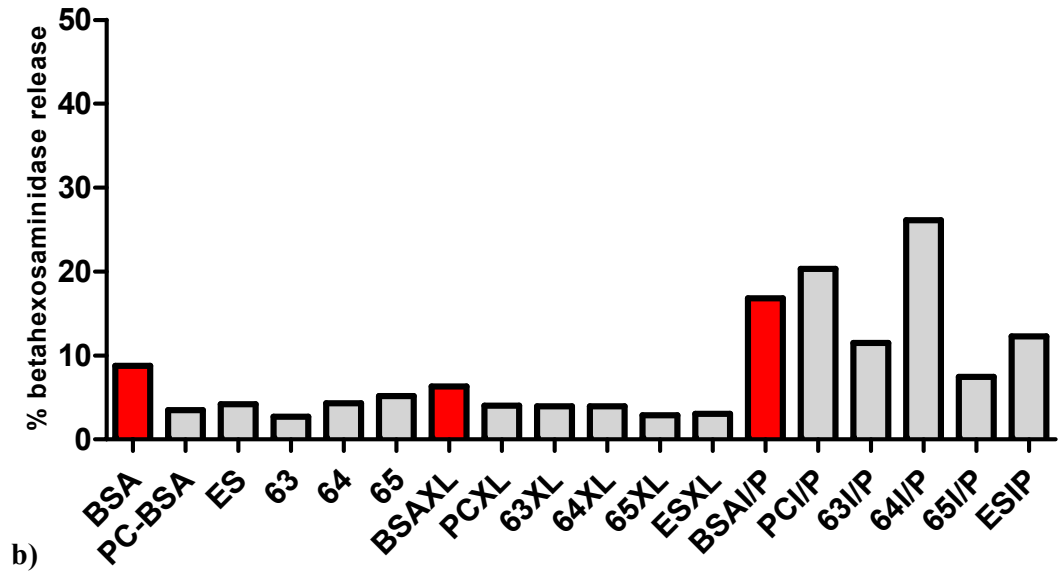
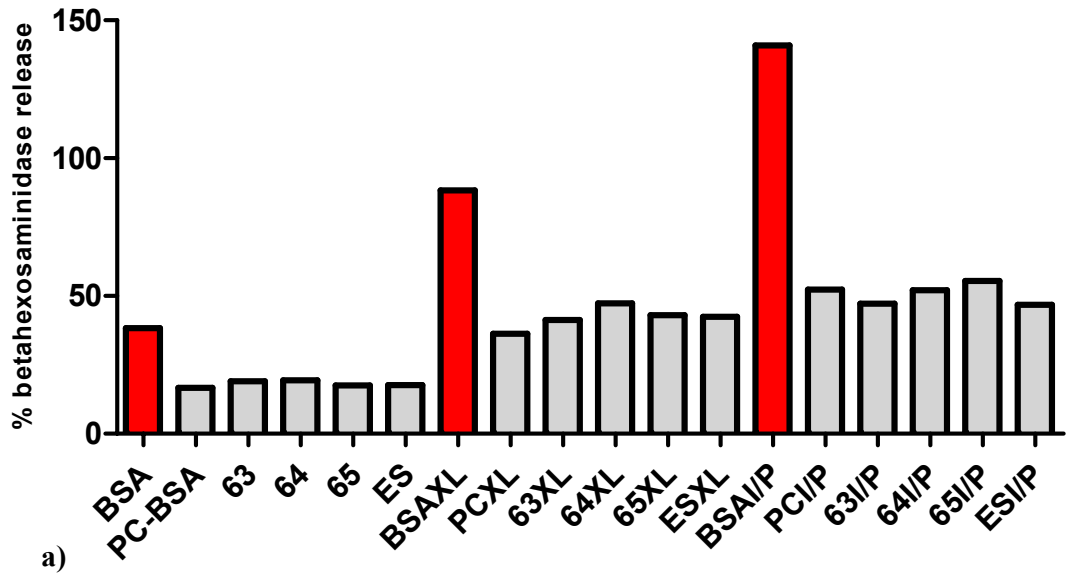


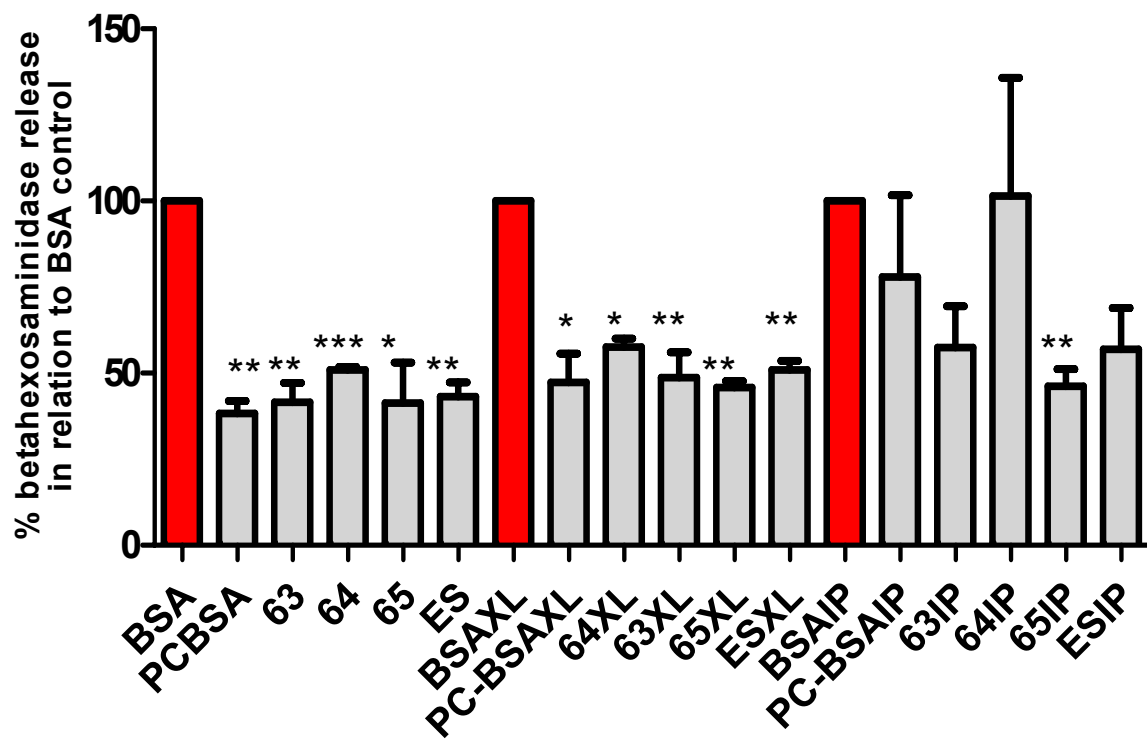
Fig 3.4.4

Comparison of the mean degranulation values normalised with respect to the BSA control. The diagram represents the mean value of three experiments (Fig 3.3 a, b and c). $p=0.05=*$, $p=0.005=**$, $p=0.0005=***$. XL= cross-linking with DNP-HSA and I/P = incubation with ionomycin and PMA.

For no induced degranulation: BSA versus ES-62**, BSA versus 63**, BSA versus 64***, BSA versus 65*, BSA versus PC-BSA**,

For cross-linking with DNP-BSA: BSA versus ES-62**, BSA versus 63*, BSA versus 64**, BSA versus 65**, BSA versus PC-BSA*

For incubation with ionomycin and PMA: BSA versus 65 **



p= 0.05=*
 p=0.005=**
 p=0.0005=***

3.5 Cytokine Analysis of BMMC after Incubation with SMAs

There is a cascade of cytokine production upon activation of mast cells induced by cross-linking of IgE bound to FcεRI, via a multivalent antigen. These cytokines include IL-4 and IL-13, which have been implicated in IgE production [211, 212], IL-3 and IL-9, which are known to aid mast cell development [213-217], IL-5 and GM-CSF, which are involved in eosinophil accumulation and survival leading to airway hyper-responsiveness as well as airway re-modelling of the lungs [218-221], and IL-6 and TNF-α, which play a major role in inflammatory pathology associated that with allergy and asthma [222-224]. An experiment by Gordon *et al* [222] revealed that TNF-α production by murine peritoneal mast cells contributed towards its bioactivity as measured by its cytotoxicity and granule content. It was further added that there was a difference in TNF-α production in BMMC when compared to peritoneal mast cells as more TNF-α was noted in the case of unstimulated peritoneal mast cell when compared with unstimulated BMMC. It was also demonstrated that IgE-dependent activation of these mast cells (both peritoneal and cultured) induced extracellular release of TNF-α and augmented TNF-α messenger RNA production and bioactivity. These findings identified murine mast cells as an important source of preformed and immunologically inducible TNF-α, and suggested that the release of TNF-α by mast cells is important for host defence and pathophysiology of allergic diseases and other mast cell-dependent processes such as inflammation. Studies in C57BL/6J mice by Nakae *et al* [223] showed that TNF-α contributed to pathogenesis of mast cell-dependent and IgE-dependent OVA-induced allergic inflammation and airway hyper-reactivity in mice. In addition to producing TNF-α, it was demonstrated by Hultner *et al* that bone marrow derived IL-3-dependent mast cells were able to produce IL-6 *in vitro*. Peters *et al* verified that there were elevated levels of IL-6 and its signaling

components in patients with chronic rhinosinusitis and nasal polyps. This showed that IL-6 is an important cytokine associated with inflammation of the airways [225]. Moreover, the role of mast cells in the mobilisation of dendritic cells to inflamed lymph nodes in an IL-6- and histamine-dependent manner in response to peptidoglycan (a component of bacterial cell wall) was shown by Dawicki in C57BL/6 mice [226]. In addition, it has been demonstrated by Melendez *et al*, that pre-treatment of human mast cells with ES-62 inhibited the production of FcεRI-induced production of TNF-α, IL-6 and IL-3 [169]. In lieu of these studies, it was decided to investigate the effects of the selected SMAs on TNF-α and IL-6 production by mast cells.

The BMDC were sensitised with anti-DNP-IgE and then cross-linked with the antigen DNP-HSA (1μg/ml) for 6 and 24 hrs to measure preformed as well as *de novo* production of TNF-α and *de novo* production of IL-6 by the mast cells. BMDC were also stimulated with Iono/PMA for the same time. The activation of mast cells by the antigen/Iono/PMA was stopped by simply collecting the culture supernatant and storing it at -20°C for subsequent analysis of the cytokines. The experiment was undertaken three times and measurement of secreted IL-6 and TNF-α was performed according to procedures described in the Materials and Methods section. After 6 hours incubation, the analysis revealed that routinely, there was no release of IL-6 and TNF-α following cross-linking of surface-bound IgE with the antigen but there was some production of IL-6 when cells were exposed to ionomycin/PMA (results not shown). Thereafter the analysis was performed after incubation of the cells for 24 hrs for measurement of both IL-6 and TNF-α. BSA and PC-BSA were employed as negative and positive controls in the experiments as described in the last section.

Preliminary experiments indicated no statistically significant differences in results obtained between the BSA negative control and a medium control.

3.5.1 Spontaneous IL-6 release

Initially work was carried out to determine whether there was any effect of the SMAs on spontaneous cytokine release. A total of three experiments were undertaken and IL-6 levels were measured in all of the samples exposed to SMAs and compared to the BSA negative control. It was discovered that after 24 hrs, spontaneous IL-6 release was only detected in one of the experiments. The data are plotted in Fig 3.5.1: IL-6 release in samples with SMAs was not found to be statistically significantly different when compared to the BSA control.

3.5.2 IL-6 release after cross-linking of bound IgE

On antigenic stimulation of BMMC for 24 hrs after sensitising with anti-DNP IgE (1µg/ml) for 18 hrs at 37°C, it was discovered that there was inhibition of IL-6 release with SMA 64 in three distinct experiments (Fig. 3.5.2 a, b and c). There was also reduction with SMA 63 in two of three experiments (Fig. 3.5.2 a and c). Pre-incubation of BMMC with ES-62 was also undertaken in one of the three experiments whereupon an inhibition of 80% was found as compared to the BSA control. In addition, SMAs 3 and 35 showed an increase in IL-6 release in all three experiments whereas 27, 28 and 39 exhibited an increase in only two of the three experiments. Table 3.5.1 shows the results (increase/decrease in percentage control) of the three different experiments depicting the effects of SMAs on the release of IL-6 following cross-linking of bound anti-DNP IgE antibodies by antigen. The value obtained for the BSA control was taken as 100%. The symbols ↔, ↓ and ↑ represent

no change, decrease and increase, respectively, for the release of IL-6 as compared with the control. It should be noted that only the data showing statistical significance were inserted as numerical values in the table.

3.5.3 IL-6 release with Ionomycin/PMA

On incubating the BMMC with 1 μ M each of Ionomycin/PMA for 24 hrs, it was observed that there was inhibition of IL-6 in all three experiments with SMAs 63 and 64 (Fig. 3.5.3 a, b and c). An increase in IL-6 levels with Ionomycin/PMA was observed with SMAs 3, 25, 27, 28, 35 and 52 in two out of three experiments. The overall results can be seen in Table 3.5.2, which shows the results (in percentage increase/decrease of control) of three different experiments depicting the effects of SMAs on the release of IL-6 in the presence of ionomycin/PMA. The value obtained for control was considered to be 100%. The symbols \leftrightarrow , \downarrow and \uparrow represent no change, decrease and increase, respectively, in the release of IL-6 as compared with the control. Only the data showing statistical significance were inserted as numerical values in the table. It is clear that the results obtained for many SMAs are not consistent for the three experiments.

3.5.4 Spontaneous TNF- α release

Spontaneous TNF- α release could only be detected in one out of three experiments. In this experiment a 52% decrease in its level was observed with SMA 63 as compared to the BSA control and an increase with SMAs 27, 28, 35 and 39 was noted as depicted in Fig 3.5.4.

3.5.5 TNF- α release after cross-linking of IgE

The analysis of the BMMC for TNF- α release following cross-linking of bound anti-DNP IgE antibodies with antigen after 24 hrs was performed in three separate experiments. TNF- α could not be detected in the first experiment. However, the other two experiments revealed that there was a reduction with PC-BSA, as well as slight reduction with SMAs 63 and 64 (Fig 3.5.5 a and b). There was an increase obtained with SMAs 1, 25, 27, 28, 35, and 52 in one experiment and with SMAs 3 and 39 in both experiments. The results were presented in a tabulated form in Table 3.5.3 where the value for the BSA control was taken as 100%. The symbols \leftrightarrow , \downarrow and \uparrow represent no change, decrease and increase, respectively, in the release of TNF- α as compared with the BSA control. Only the data showing statistical significance were inserted as numerical values in the table.

3.5.6 TNF- α release with ionomycin/PMA

Analysis was also performed to establish the effects of SMAs on the release of TNF- α in BMMC stimulated with 1 μ M each of ionomycin and PMA for 24 hrs. It was not clear with many molecules as to whether they inhibited or stimulated the production of TNF- α , as the results obtained were not consistent across the three experiments. However it can be mentioned that SMA 63 showed a decrease in the levels of TNF- α in two experiments along with SMA 6. Similarly, SMA 65 revealed an increase in levels in at least two experiments. Table 3.5.4 shows the results of the data (Fig 3.5.6 a, b and c) in a tabulated form where the BSA control value was taken to be 100%. The symbols \leftrightarrow , \downarrow and \uparrow represent no change, decrease and increase, respectively, in the release of TNF- α as compared with the control. Only the data showing statistical significance were inserted as numerical values in the table.

Fig 3.5.1

Measurement of the effects of ES-62 and SMAs on IL-6 release. 1×10^6 BMMC were incubated with ES-62 or SMAs and sensitised with anti-DNP IgE ($1 \mu\text{g/ml}$) for 18 hrs at 37°C . BSA was employed as the control. ELISA for IL-6 was performed using the resulting supernatants. Results are expressed as means \pm s.d. Each data are indicative of triplicate determinations in one experiment. The detection limit for IL-6 was taken to be $\geq 4\text{pg/ml}$ according to manufacturer's protocol.

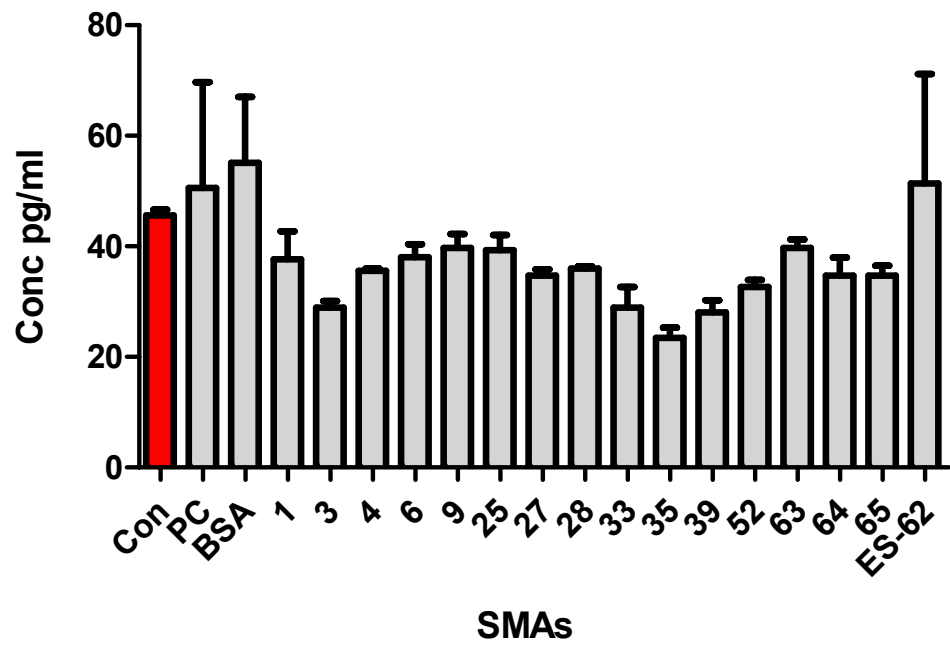


Fig 3.5.2 a, b and c

Measurement of the effects of ES-62 and SMAs on IL-6 release. 1×10^6 BMDC were incubated with ES-62 or SMAs and sensitised with anti-DNP IgE ($1 \mu\text{g/ml}$) for 18 hrs at 37°C . The cells were then cross-linked with the antigen DNP-HSA ($1 \mu\text{g/ml}$) for 24 hrs. BSA was taken as the control. ELISA for IL-6 was performed using the resulting supernatants. The detection limit for IL-6 was taken to be $\geq 4 \text{pg/ml}$ according to manufacturer's protocol.

Results are expressed as means \pm s.d. Each data are indicative of triplicate determinations in one experiment. $n=3$. $p=0.05=*$, $p=0.01=**$, $p=***=0.001$.

a) (BSA versus 3**, BSA versus 35*, BSA versus 64*,
BSA versus ES-62**)

b) (BSAXL versus 1*, BSA versus 3*, BSA versus 27*,
BSA versus 28*, BSA versus 35*, BSA versus 39***, BSA versus 52***, BSA
versus 63*, BSA versus 64**)

c) (BSA versus 3*, BSA versus 25*, BSA versus 27*,
BSA versus 28*, BSA versus 35*, BSA versus 39**,
BSA versus 63***, BSA versus 64**)

BSAXL= BSA Cross-linked with antigen, XL= Cross-linked with antigen

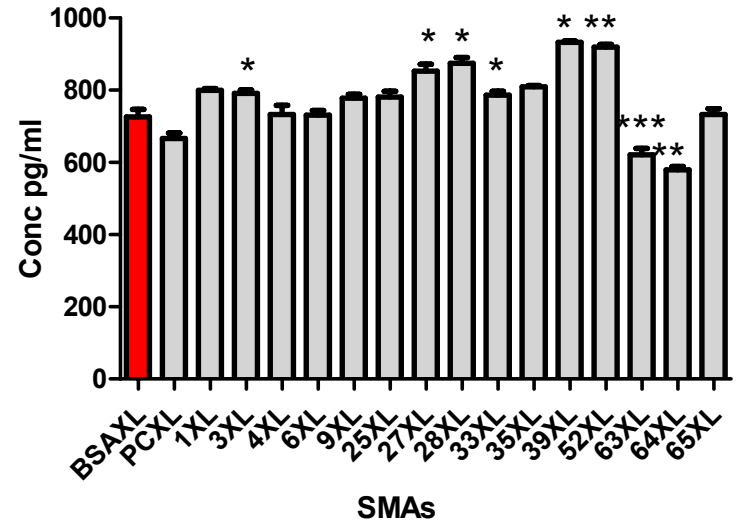
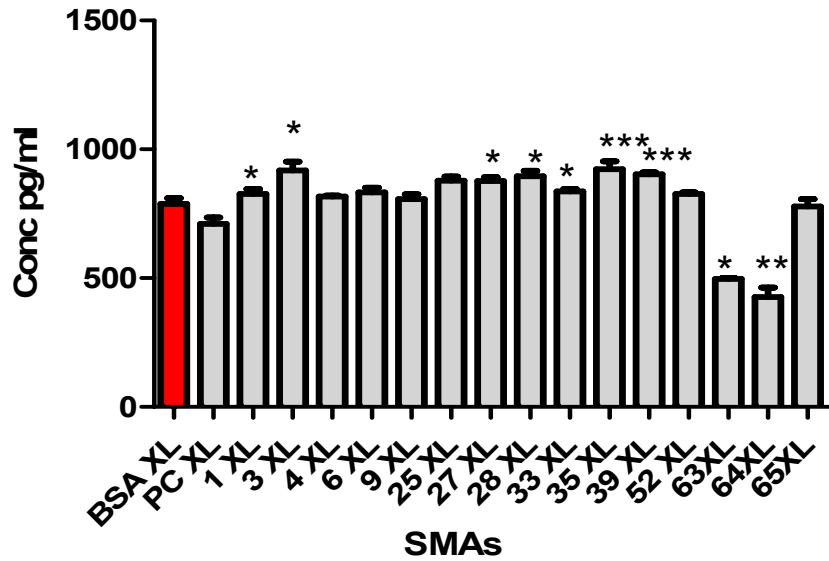
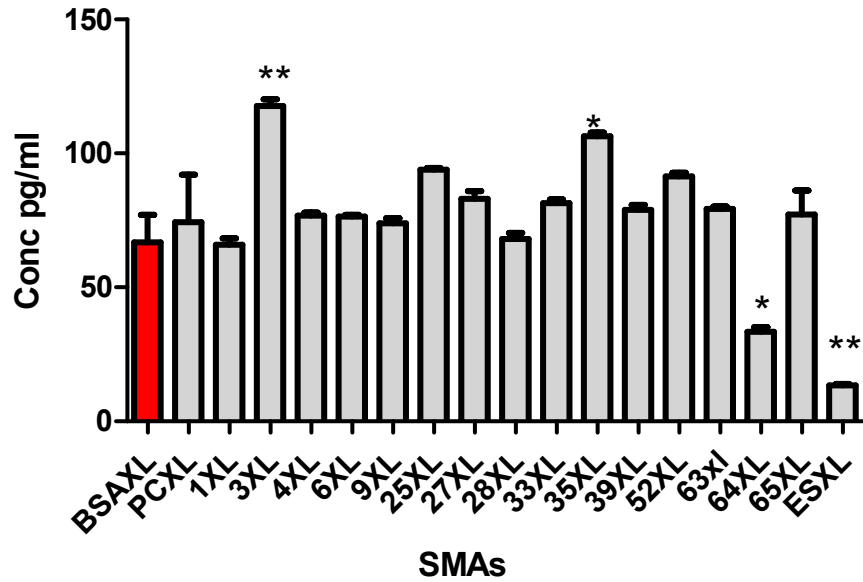


Fig 3.5.3 a, b and c

Measurement of the effects of SMAs on IL-6 release. 1×10^6 BMDC were incubated with SMAs. The cells were stimulated with $1 \mu\text{M}$ Ionomycin/PMA for 24 hrs. BSA was taken as the control. ELISA for IL-6 was performed using the resulting supernatants. The detection limit for IL-6 was taken to be $\geq 4 \text{ pg/ml}$ according to manufacturer's protocol.

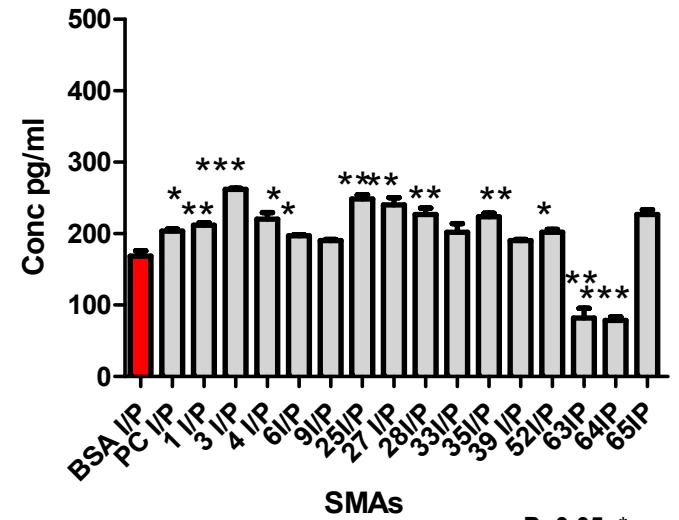
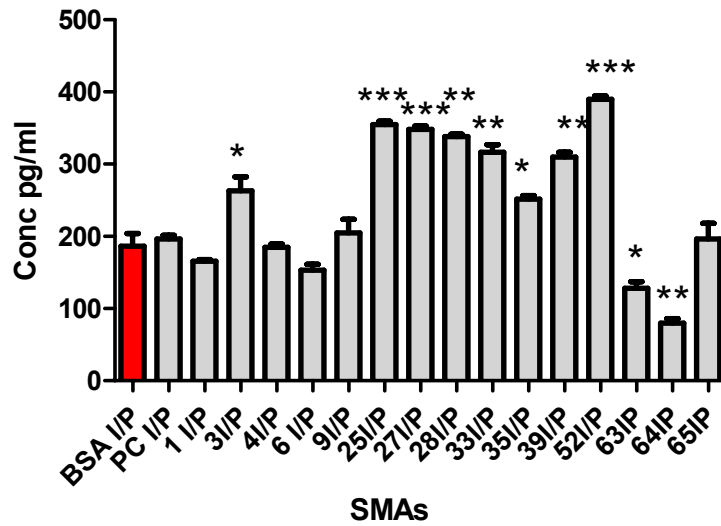
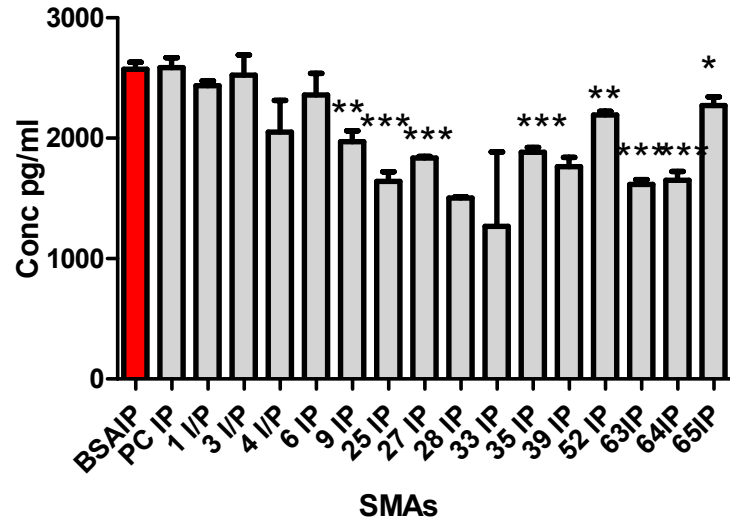
Results are expressed as means \pm s.d. Each data are indicative of triplicate determinations in one experiment. $n=3$. $p=0.05=*$, $p=0.01=**$, $p=***=0.001$.

a) (BSA versus 9**, BSA versus 25***, BSA versus 27***, BSA versus 28***, BSA versus 35***, BSA versus 39**, BSA versus 52**, BSA versus 63***, BSA versus 64***, BSA versus 65*)

b) (BSA versus 3*, BSA versus 25***, BSA versus 27***, BSA versus 28**, BSA versus 33**, BSA versus 35*, BSA versus 39**, BSA versus 52***, BSA versus 63* BSA versus 64**)

c) (BSA versus PC*, BSA versus 1**, BSA versus 3***, BSA versus 4*, BSA versus 6*, BSA versus 25**, BSA versus 27**, BSA versus 28**, BSA versus 35**, BSA versus 52*, BSA versus 63**, BSA versus 64*** BSA versus 65**)

BSAIP= BSA with Ionomycin/PMA, IP= Ionomycin/PMA.



P=0.05=*
P=0.01=**
P=0.001=***

Table 3.5.1 shows the results (increase/decrease in percentage control) of three different experiments depicting the effects of SMAs on the release of IL-6 in the presence of the antigen. The value obtained for BSA control was taken as 100%. The symbols ↔, ↓ and ↑ represent no change, decrease and increase, respectively, in the release of IL-6 as compared with the control. Only the data showing statistical significance were inserted as numerical values in the table.

IL-6 RELEASE WITH ANTIGEN TABLE COMPARED TO BSA CONTROL (%)

SMA	Experiment-1	Experiment-2	Experiment-3
PC-BSA	↔	↔	↔
1	10 ↑	↔	↔
3	8 ↑	77↑	16↑
4	↔	↔	↔
6	↔	↔	↔
9	↔	↔	↔
25	↔	↔	11↑
27	17↑	↔	11↑
28	20 ↑	↔	13↑
33	↔	↔	↔
35	11 ↑	60 ↑	17↑
39	28↑	↔	14↑
52	26 ↑	↔	↔
63	14 ↓	↔	37 ↓
64	20 ↓	50 ↓	45 ↓
65	↔	↔	↔
ES-62	80↓	-	-

Table 3.5.1

Table 3.5.2 shows the results (increase/decrease in percentage control) of three different experiments depicting the effects of SMAs on the release of IL-6 in the presence of Ionomycin/PMA. The symbols ↔, ↓ and ↑ represent no change, decrease and increase, respectively, in the release of IL-6 as compared with the control. Only the data showing statistical significance were inserted as numerical values in the table.

IL-6 RELEASE WITH IONOMYCIN/PMA TABLE COMPARED TO BSA CONTROL (%)

SMA	Experiment-1	Experiment-2	Experiment-3
PC-BSA	↔	↔	20↑
1	↔	↔	25↑
3	41 ↑	↔	55↑
4	↔	↔	30↑
6	↔	↔	16↑
9	↔	23↓	↔
25	90 ↑	36↓	47↑
27	87 ↑	28↓	42↑
28	81 ↑	41↓	34↑
33	69↑	↔	↔
35	34↑	26↓	32↑
39	66↑	31↓	↔
52	109↑	14↓	19↑
63	31↓	37↓	51 ↓
64	57 ↓	35↓	↓
65	↔	11↓	34↑

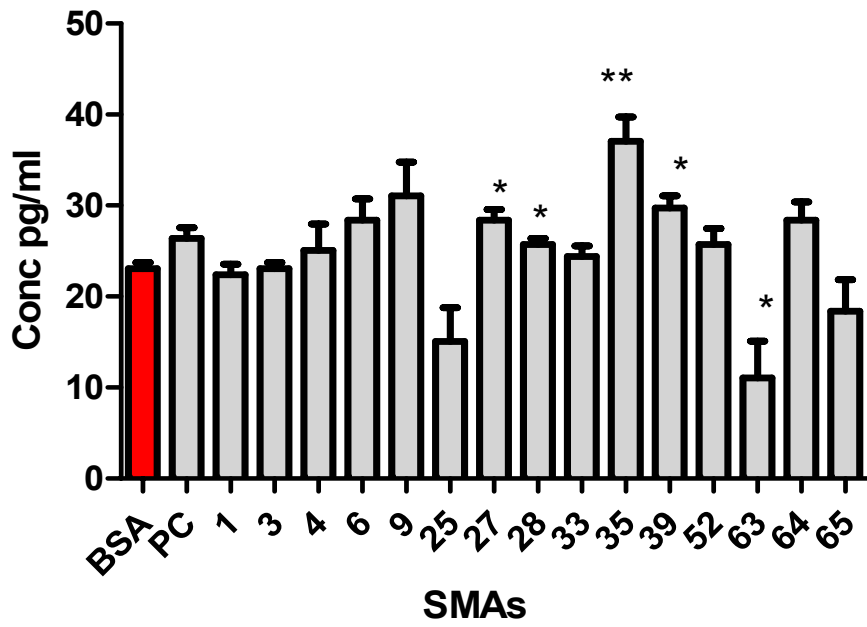
Table 3.5.2

Fig 3.5.4

Measurement of the effects of SMAs on the release of TNF- α in BMDC. 1×10^6 BMDC were incubated with SMAs and sensitised with anti-DNP IgE ($1 \mu\text{g/ml}$) for 18 hrs at 37°C . BSA was taken as the control. ELISA for TNF- α was performed using the resulting supernatants. Results are expressed as means \pm s.d. The detection limit for TNF- α was $\geq 15\text{pg/ml}$

Each data are indicative of triplicate determinations in one experiment. $n=3$.
 $p=0.05=*$, $p=0.01=**$, $p=***=0.001$.

(BSA versus 27*, BSA versus 28*, BSA versus 35**, BSA versus 39*,
BSA versus 63*)



P=0.05=*
P=0.01=**
P=0.001=***

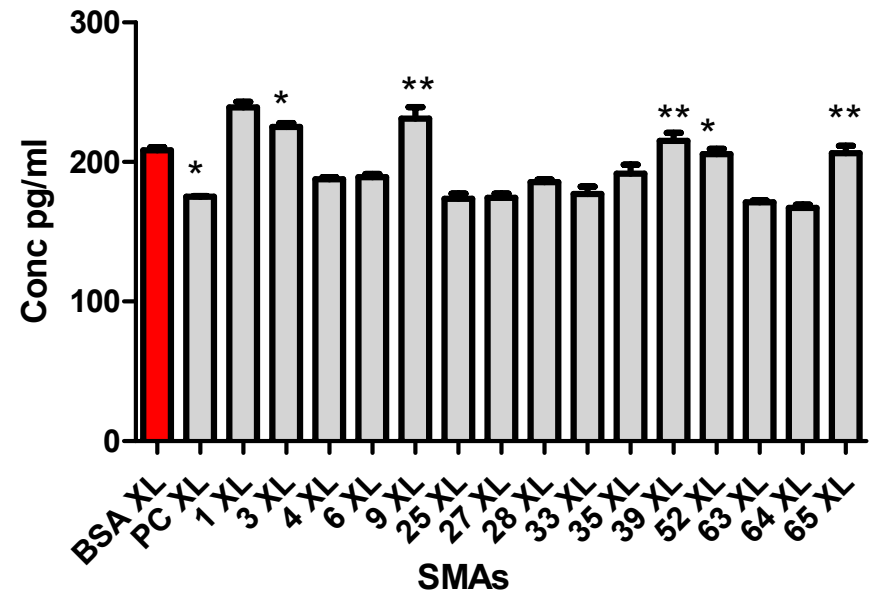
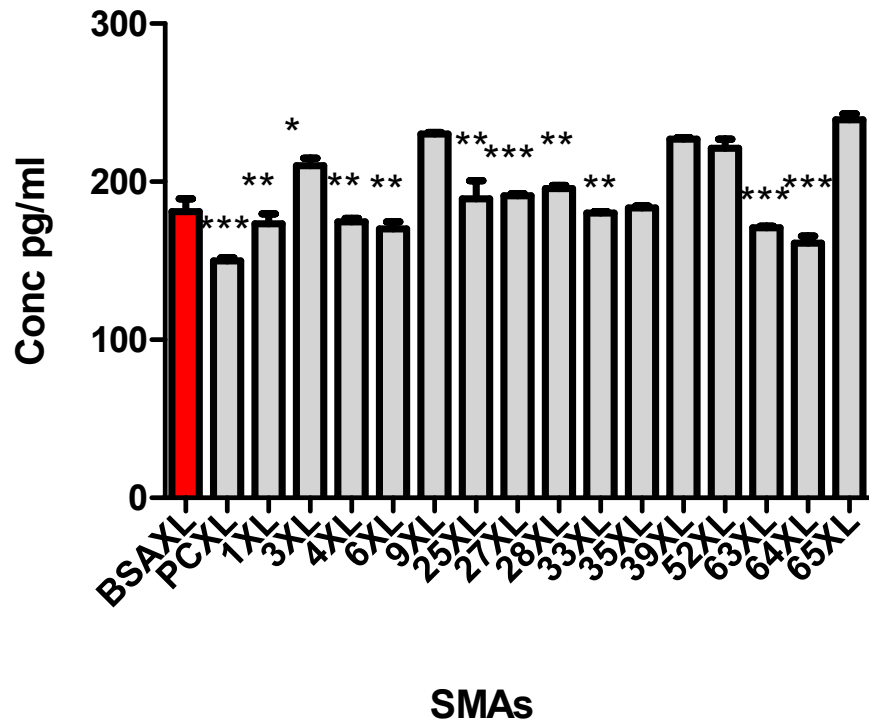
Fig 3.5.5 a and b

Measurement of the effects of SMAs on TNF- α release. 1×10^6 BMMC were incubated with SMAs and sensitised with anti-DNP IgE (1 μ g/ml) for 18 hrs at 37°C. The cells were then cross-linked with the antigen DNP-HSA (1 μ g/ml) for 24 hrs. BSA was taken as the control. ELISA for TNF- α was performed using the resulting supernatants. The detection limit for TNF- α was taken to be ≥ 15 pg/ml according to manufacturer's protocol.

Results are expressed as means \pm s.d. The data are indicative of triplicate determinations in one experiment. n=3. p=0.05=*, p=0.01=**, p=***=0.001.

a) (BSA versus 4**, BSA versus 6**, BSA versus 25**,
BSA versus 27***, BSA versus 28**, BSA versus 33**,
BSA versus 63***, BSA versus 64***)

b) (BSA versus PC*, BSA versus 3*, BSA versus 9**,
BSA versus 39**, BSA versus 52*, BSA versus 65**)



P=0.05=*
P=0.01=**
P=0.001=***

Fig 3.5.6 a, b and c

Measurement of the effects of SMAs on TNF- α release. 1×10^6 BMMC were incubated with SMAs. The cells were stimulated with $1 \mu\text{M}$ Ionomycin/PMA for 24 hrs. BSA was taken as the control. ELISA for TNF- α was performed using the resulting supernatants. The detection limit for TNF- α was taken to be $\geq 15 \text{pg/ml}$ according to manufacturer's protocol.

Results are expressed as means \pm s.d. The data are indicative of triplicate determinations in one experiment. n=3. p=0.05=*, p=0.01=**, p=***=0.001.

a) (BSA versus 65**)

b) (BSA versus PC***, BSA versus 3*, BSA versus 4*, BSA versus 6***, BSA versus 9*, BSA versus 27*, BSA versus 33**, BSA versus 35**, BSA versus 52*, BSA versus 63***, BSA versus 64***, BSA versus 65**)

c) (BSA versus PC*, BSA versus 6**, BSA versus 9**, BSA versus 25**, BSA versus 27**, BSA versus 28***, BSA versus 33**, BSA versus 35**, BSA versus 63** BSA versus 65**)

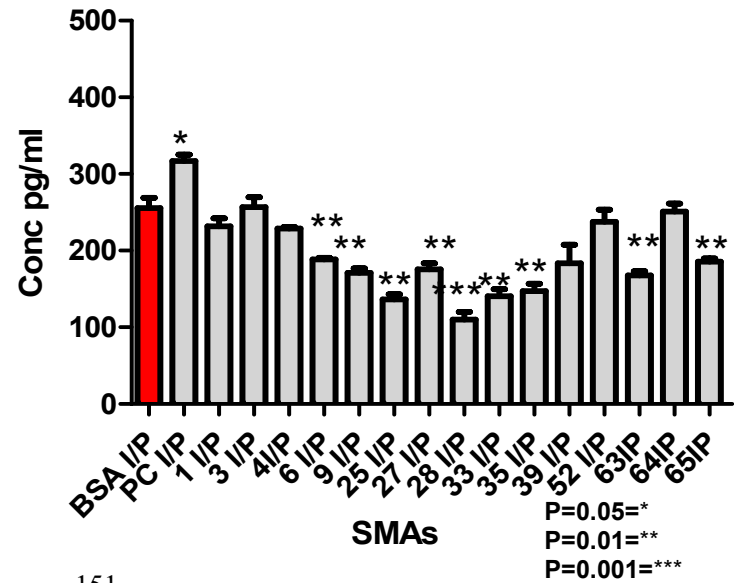
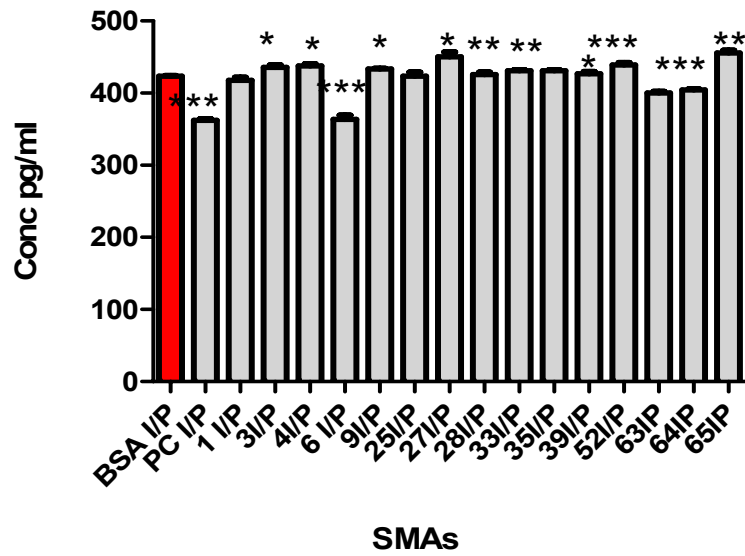
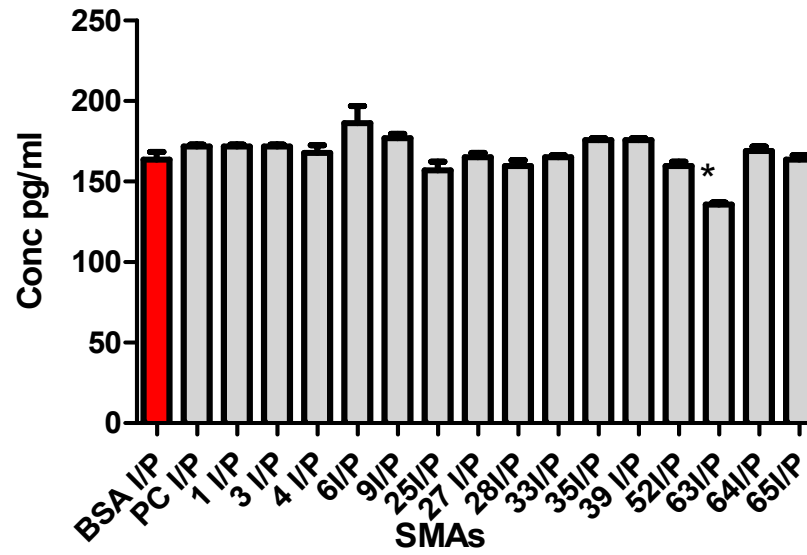


Table 3.5.3 shows the results (increase/decrease in percentage control) of three different experiments depicting the effects of SMAs on the release of TNF- α in the presence of the antigen. The value obtained for BSA control was taken as 100%. The symbols \leftrightarrow , \downarrow and \uparrow represent no change, decrease and increase, respectively, in the release of TNF- α as compared with the control. Data showing statistical significance when compared to BSA control were only considered in the table.

TNF- α RELEASE WITH ANTIGEN AS COMPARED TO BSA CONTROL
(%)

SMA	Experiment-1	Experiment-2	Experiment-3
PC-BSA	↔	17 ↓	15 ↓
1	↔	4 ↑	↔
3	↔	16 ↑	8 ↑
4	↔	↔	↔
6	↔	↔	↔
9	↔	↔	11 ↑
25	↔	4 ↑	↔
27	↔	5 ↑	↔
28	↔	7 ↑	↔
33	↔	↔	↔
35	↔	1 ↑	↔
39	↔	24 ↑	3 ↑
52	↔	22 ↑	1 ↓
63	↔	5 ↓	↔
64	↔	9 ↓	↔
65	↔	↔	↔

Table 3.5.3

Table 3.5.4 shows the results (increase/decrease in percentage control) of three different experiments depicting the effects of SMAs on the release of TNF- α in the presence of ionomycin/PMA. The value obtained for BSA control was taken as 100%. The symbols \leftrightarrow , \downarrow and \uparrow represent no change, decrease and increase, respectively, in the release of TNF- α as compared with the control. Data showing statistical significance when compared to BSA control were only considered in the table.

TNF- α RELEASE WITH IONOMYCIN/PMA COMPARED TO BSA CONTROL (%)

SMA	Experiment-1	Experiment-2	Experiment-3
PC-BSA	14↓	23↑	↔
1	↔	↔	↔
3	2↑	↔	↔
4	3↑	↔	↔
6	14↓	10↓	↔
9	2↑	32↓	↔
25	↔	46↓	↔
27	6↑	31↓	↔
28	↔	56↓	↔
33	↔	45↓	↔
35	↔	42↓	↔
39	↔	↔	↔
52	3↑	↔	↔
63	5↓	34↓	↔
64	4↓	↔	↔
65	7↑	27↓	25↑

Table 3.5.4

3.6 Determination of the effect of SMAs on Protein Kinase C- α , Phospholipase-D and Sphingosine Kinase in BMMC

Pretreatment of human mast cells with ES-62 inhibited the Fc ϵ RI-triggered release of β -hexosaminidase, a marker of mast cell degranulation. However, the expression of Fc ϵ RI on the cell surface was not affected. It was further seen that ES-62 treatment of mast cells did not affect Fc ϵ RI-induced tyrosine phosphorylation of proteins required for the associated signaling cascade [155]. It was also observed that ES-62 inhibited the β -hexosaminidase release induced by ionomycin/PMA. The experiments revealed that the Fc ϵ RI-triggered initial peak of Ca⁺ mobilisation dependent on sequential activation of PLD and SPHK was inhibited by treatment of cells with ES-62. The sequestration and degradation of PKC- α by ES-62–TLR4 complexes provided a mechanism for the disruption of key PLD-SPHK-dependent pathways of calcium, PKC and NF- κ B activation. The disruption of these pathways was associated with the consequent failure of ES-62–treated mast cells to degranulate in response to cross-linking of Fc ϵ RI. Therefore, it was decided to analyse the effects of SMAs on the signaling molecules-PKC- α , PLD and SPHK in BMMC [155].

3.6.1 Laser scanning cytometry

Quantitative and qualitative analysis of signaling molecules-PKC- α , PLD and SPHK in BMMC was performed by the technique of Laser Scanning Cytometry (LSC), which combines the quantitative aspects of flow cytometry with the assessment of morphological and cell-cell interaction capabilities of slide-based cytometric platforms [227]. Fig 3.6.1 shows a diagrammatic representation of how LSC detects and analyses fluorescence associated with individual cells. Emitted fluorescence is collected by photomultiplier tubes (PMT) and digitised by the propriety Wincyte

software as pixels, with those above a certain designated threshold (threshold contours; indicated by red rim: Fig. 3.6.1) recognised as cells and analysed. The threshold contour is usually set on nuclear staining, such as that provided by 4'6'-diamidino-2-phenylindole (DAPI), to identify all cells in the population whilst the cells of interest can be analysed by setting integration contours based on cell size and/or cell surface staining of lineage markers (green rim). Non-specific background staining is corrected by applying a background contour (two blue rims). Data can be represented in terms of fluorescence integral or maximum pixel (max pixel), the latter of which calculates regions of the highest intensity of fluorescence within the contour. Peripheral contours can also be set between the threshold and integration contours to allow analysis of the area between the nucleus and the cell membrane in terms of either peripheral fluorescence integrals or max pixels.

Quantitative analysis of the effects of SMAs was performed and the results were plotted as graphs after calculating the mean fluorescence intensity (MFI) for the total and peripheral fluorescence integrals, following gating of specific staining of the signaling element of choice relative to the relevant isotype control. The peripheral fluorescence contours quantified fluorescence between the nucleus and the plasma membrane of the cell i.e. the cytoplasmic space. In addition, the maximum pixel fluorescence facility was used to measure the areas of brightest fluorescence localisation within the analysis contour. The values obtained clearly quantified the fluorescence associated with the signaling enzymes thereby suggesting this approach could be of value in providing evidence of immunomodulation by the SMAs.

On cross-linking of FcεRI by antigen, there is translocation of the signaling molecules towards the plasma membrane or towards the perinuclear region indicating activation of the signaling molecules. With respect to the effects of SMAs on the

degradation/translocation of the signaling molecules, the immunofluorescence obtained at various regions could provide valuable information regarding the activation and expression of PKC- α , PLD and SPHK in the mast cells. Difference in degradation/translocation of these molecules from the nuclear region towards the plasma membrane (between sensitised and sensitised/cross-linked samples) would indicate activation or inhibition of the signaling molecule. The increase or decrease in the value of Max pixel would indicate the strength of expression of the signaling molecules. Non cytoplasmic fluorescence obtained by the difference of peripheral fluorescence from the total fluorescence would also suggest whether the effect is induced by degradation or translocation of the signaling molecules in the cytoplasm towards the plasma membrane or the perinuclear region.

The SMAs selected for analysis based on the data obtained from the previous experiments were SMAs 3, 25, 33, 39, 63, 64 and 65. PC-BSA and BSA were employed as positive and negative controls respectively. From the calcium mobilisation studies described in section 3.3, the data revealed that pre-exposure to SMAs 1, 4, 6, 27, 33, 35, and 65 enhanced the Fc ϵ RI-mediated increase in free Ca²⁺ ion concentration in mast cells. On the other hand, pre-treatment with SMAs 3, 9, 25, 28, 39, 63 and 64 caused a marked decrease in calcium mobilisation and this inhibition was especially marked with SMAs 63 and 64. With respect to degranulation studies, SMAs 3, 25, 33 and 39 were found to generate data that were not reproducible. However, SMAs 63 and 64 reduced Fc ϵ RI-mediated degranulation in RBL-2H3 cells as opposed to treatment with SMA 65, which resulted in an increased response. In the case of cytokine analysis, the data obtained appeared to be dependent on the stimulus (DNP-HSA or Ionomycin/PMA) used. The data revealed inconsistent results when cells were stimulated with either DNP-HSA or

Ionomycin/PMA with all of the SMAs, except 63 and 64, which showed a significant decrease in the production of IL-6 and TNF- α by the BMDC in response to either DNP-HSA or Ionomycin/PMA. Therefore, it was decided to select SMAs 63 and 64, as they showed a consistent decrease in the data obtained for Ca²⁺ mobilisation, the degranulation assay and cytokine analysis. Similarly, SMA 65 showed an increase in the values obtained for the aforementioned analyses. The data obtained for SMAs 3, 25, 33 and 39 showed differential effects depending on the particular analysis, but in each individual analysis, the results obtained were significant enough to warrant further analysis via signaling experiments.

3.6.2 The effects of SMAs on PKC- α signaling

PKC constitutes a family of at least 12 phospholipid-dependent serine-threonine kinases that are subdivided into three categories. The classical/conventional category consists of PKC- α , - β 1, - β 2 and - γ , which are Ca²⁺ dependent enzymes and activated by both DAG and phosphatidylserine (PS) [228]. The second category is represented by the novel PKC isoforms: PKC- ϵ , - δ and - θ that are Ca²⁺ independent and regulated by DAG and PS [229]. The third category comprises the atypical PKCs, PKC- ξ , - ι and - λ which are also Ca²⁺ independent and do not require DAG but are dependant on PS [230, 231]. Previous studies have revealed that on cross-linking of Fc ϵ RI, phospholipase C- γ (PLC- γ) hydrolyses phosphatidylinositol 4, 5 biphosphate (PIP₂) to generate two second messengers; inositol 1, 4, 5 triphosphate (IP₃) and DAG which, via IP₃-mediated mobilisation of Ca²⁺, lead to the activation of PKC- α resulting in exocytosis of various preformed granules consisting of serine proteases such as tryptases, histamine, serotonin and proteoglycans, mainly heparin, in mast cells [191, 192, 232-235].

In mouse splenic B cells, ES-62 was found to modulate B cell receptor signaling through the down regulation of PKC isoforms α , β , ζ , δ and ι/λ and up-regulation of PKC- γ and $-\epsilon$ [129, 141]. Likewise, in human mast cells, ES-62 reduced the expression of PKC- α , β , δ , ι (which is the human homologue of mouse λ) and ξ . Moreover, the sequestration of PKC- α by ES-62-TLR4 complexes from the cell surface into the vesicular compartments and further into a perinuclear region that resulted in its subsequent degradation, led to the disruption of key Fc ϵ RI-coupled PLD-SPHK-dependent pathways of calcium mobilisation and NF- κ B activation. The disruption of these pathways was found to be associated with the consequent failure of ES-62-treated mast cells to degranulate in response to cross-linking of Fc ϵ RI [155]. Therefore, it was decided to investigate the effects of SMAs on the expression, degradation and translocation (as a measure of its activation) of PKC- α in resting and Fc ϵ RI-stimulated mouse BMMC.

BMMC were incubated overnight with SMAs and sensitised with anti-DNP IgE. The cells were then activated by the cross-linking of Fc ϵ RI by DNP-HSA for 2 minutes. Redistribution of enzymes from the perinuclear region and cytoplasm towards the plasma membrane was expected following cross-linking of Fc ϵ RI. The timepoint of 2 minutes was chosen for analysis because earlier studies by Jolly *et al* [236] had shown that the SPHK activity generated by cross-linking of Fc ϵ RI and then measured *in vitro*, showed an increase within 2 min that reached a plateau within 10 min in BMMC harvested from SV129 X C57/B16 mice. Similarly, degranulation experiments by Pushparaj *et al* performed on BALB/c-derived BMMC revealed that SPHK1 (an isoenzyme of SPHK) activity peaked at 5 min and stabilised at 15 min [235]. Thus, as SPHK1 is activated downstream of Fc ϵ RI-mediated PKC- α signaling in human mast cells, it was decided to observe whether PKC- α expression,

degradation or translocation kinetics had been modified within 2 minutes. Immunofluorescent staining of the cells was undertaken as described in the Materials and Methods section with PKC- α expression being detected by a commercially available mouse monoclonal anti-PKC- α antibody that had been purified by affinity chromatography. An Alexa488-labelled anti-mouse IgG antibody was used to detect anti-PKC- α by means of green fluorescent staining. The cells were also counterstained with DAPI (blue) to demonstrate the presence of the nuclei. For qualitative analysis of such PKC- α expression in BMMC using LSC, representative images at 40x magnification were taken without (Fig. 3.6.1.1) and with (Fig. 3.6.1.2) 2 min cross-linking with DNP-HSA.

It was observed that in the sensitised only samples, there seemed to be a downregulation of expression of PKC- α in the case of SMAs 39, 63 and 64 (Fig. 3.6.1.1 f, g, h) while in case of SMA 3 (Fig. 3.6.1.1.c), there seemed to be a slight increase in expression. On observation of the samples cross-linked for 2 min (Fig. 3.6.1.2 a-j), it was found that the loss of expression in response to SMAs 39, 63 and 64 was maintained while there was not much evidence of a change in expression with SMA 3 as compared to the sensitised only sample. Interestingly, it was observed that there did not appear to be much PKC- α translocation from the cytosol to the plasma membrane following cross-linking of Fc ϵ RI. Rather, most of the PKC- α expression appeared to be present at/close to the plasma membrane even in the sensitised only samples (Fig. 3.6.1.1a and 3.6.1.2a). A similar observation was noted by Melendez *et al* with respect to U937 cells (a human monocyte cell line), where it was demonstrated that in non-stimulated IFN- γ primed cells, all of the PKC- α expression seemed to be present in the plasma membrane. However, by contrast, the novel PKCs δ , ϵ and atypical ζ isoenzymes were translocated to the membrane following Fc γ RI

cross-linking in such cells [236]. Furthermore, it was also observed by Evans *et al* that allergen challenge had no effect on expression and subcellular distribution of conventional PKC isoforms α , β I and β II in eosinophils of asthmatic patients [237]. Moreover, earlier work by Kuo *et al* on acute myeloid leukemic cells obtained from human patients revealed that the 80-kDa fraction of PKC that is now known to likely represent PKC- α was distributed in various locations (including plasma membrane, cytoplasm, periphery of nucleus and Golgi apparatus) [238].

Quantitative LSC analysis of PKC- α expression and subcellular localisation was performed using Wincyte software version 3.6 (Compucyte). Figure 3.6.1.3 depicts the gates used for quantitation of the fluorescence obtained from the qualitative data in the form of histograms. The quantitation of data obtained from more than 2×10^3 BMNC revealed that in the sensitised only samples, there was marked reduction in the % of cells expressing PKC- α in the case of cells exposed to PC-BSA and SMAs 39, 63 and 64 as compared to the BSA control (Fig. 3.6.1.4a). Moreover, in the samples cross-linked for 2 min it was revealed that the % of BMNC expressing PKC- α was also reduced in PC-BSA, and SMAs 3 and 33 samples as compared to the BSA control but not to such a marked extent as observed with those exposed to SMAs 39, 63, 64 and 65 (Fig. 3.6.1.4b). It was also observed that the mean total level of fluorescence per cell following sensitisation was reduced in cells exposed to all SMAs or PC-BSA (Fig. 3.6.1.5a) as compared to the BSA control although there appeared to be no reduction in expression relative to the BSA control by PC-BSA, and only slight effects by SMAs 3, 25 and 33, following cross-linking of Fc ϵ RI for 2 min (Fig. 3.6.1.5b). However with respect to the latter and consistent with the data presented in Fig. 3.6.1.4, it was noticed that the mean level of fluorescence per cell was strikingly reduced following exposure to SMAs 39, 63, 64

and 65. Furthermore, when the total fluorescence in the sensitised only BMMC was compared with the cross-linked samples, it was observed that SMAs 64 and 65 induced a further decrease in PKC- α expression. On studying the peripheral fluorescence integral to examine cytosolic PKC- α levels, it was noticed that the fluorescence detectable in the cytoplasmic space of the sensitised only cells, generally revealed a rather similar pattern to that observed with the total mean fluorescence integral analysis with PC-BSA (although only marginally in the cross-linked samples) and all the SMAs reducing PKC- α expression (Fig. 3.6.1.6 a and b). Thus comparing the peripheral fluorescence between the sensitised and cross-linked samples revealed that SMAs 64 and 65 also further reduced “peripheral” PKC- α expression on cross-linking samples. Nuclear (Non-cytoplasmic space) fluorescence was obtained by subtracting the peripheral fluorescence values from the total fluorescence values (Figures 3.6.1.7a and b). This calculation revealed that in the sensitised only samples, such non-cytoplasmic fluorescence was also reduced in all the samples as compared to the BSA control. The values obtained were remarkably reduced with PC-BSA, SMAs 39, 63, 64 and 65 and 25 (Figures 3.6.1.7a), suggesting exclusion of PKC- α from the nucleus in these samples. Additionally, in sensitised/cross-linked samples, it was observed that the fluorescence obtained was again reduced in all the samples except PC-BSA, and SMA 25 in relation to the BSA control (Figures 3.6.1.7b). In the case of PC-BSA, SMAs 3, 25 and 33, the results obtained were strikingly different from those in the sensitised only samples. In the case of PC-BSA, it was seen that in the sensitised only samples, there was a remarkable reduction of non-cytoplasmic fluorescence and some reduction with SMA 25, while for the sensitised/ cross-linked samples; non-cytoplasmic fluorescence was more than the BSA control, which showed a net translocation of PKC- α out of the

nucleus following cross-linking. As these observations also indicated that subsequent FcεRI-signaling could overcome the PC-dependent block on nuclear PKC-α translocation, it could be seen that BSA-and PC-BSA-treated cells tended to show differential ratios of nuclear/cytoplasmic PKC-α expression in both sensitised and cross-linked cells. However, an opposite scenario was observed with SMAs 3 and 33, where only a slight reduction was observed in the sensitised samples, but there was a conspicuous reduction in the case of sensitised/cross-linked samples. It was also observed that the reduction in nuclear fluorescence obtained in the case of SMAs 39, 63, 64 and 65 was profoundly reduced relative to the BSA control, in both the sensitised only and cross-linked samples (Figures 3.6.1.7a and b). The Max pixel data, which by measuring intensity of staining indicates clustering of signal, revealed a slightly more disperse localisation of signal with PC-BSA and SMAs 39, 63 and 64 following sensitisation relative to the rest of the SMA samples, which were more focused and similar to the BSA control (Figure 3.6.1.8a). These values did not change substantially following cross-linking perhaps providing further evidence that most of the PKC-α was already focused at the plasma membrane: however it was noted that the Max pixel fluorescence recovered in the case of PC-BSA, suggesting that FcεRI-signaling could drive some additional PKC-α translocation (either to the plasma membrane or nucleus) even following exposure to these molecules. However, only in the case of SMA 65, was the Max pixel fluorescence reduced in the sensitised/cross-linked more than the sensitised only sample (Fig. 3.6.1.8b). This can be more clearly appreciated in the images (both sensitised and cross-linked) in (Figures 3.6.1.1 and 3.6.1.2 a, b and i) where in the case of PC-BSA the signal obtained is more focussed in the cytoplasm and in the case of SMA 65, it is less focused and more dispersed.

It can be thus deduced from the data that SMAs 39, 63 and 64 reduce the % cells expressing PKC- α and of those where expression remains, it is at a reduced level, both globally and at the periphery, the latter being corroborated by the more disperse nature of the signal as indicated by the reduced max pixel value. Similarly, with SMA 65, although the % cells expressing PKC- α is more in the sensitised samples, there is reduction obtained after cross-linking again both globally and at the periphery as indicated by Total fluorescence and Peripheral fluorescence values.

Fig 3.6.1

Diagrammatic representation of the various contours used for the analysis in Laser Scanning Cytometry.

The threshold contour in red was DAPI set at 8000 pixels. The integration contour (i.e. cell surface) in green was set on cell size with minimum area of the cell set at 30 μm^2 . The peripheral contours were set with one immediately outside of the threshold contour and another immediately inside the integration contours. The background contour (blue) was set outside the integration contour.

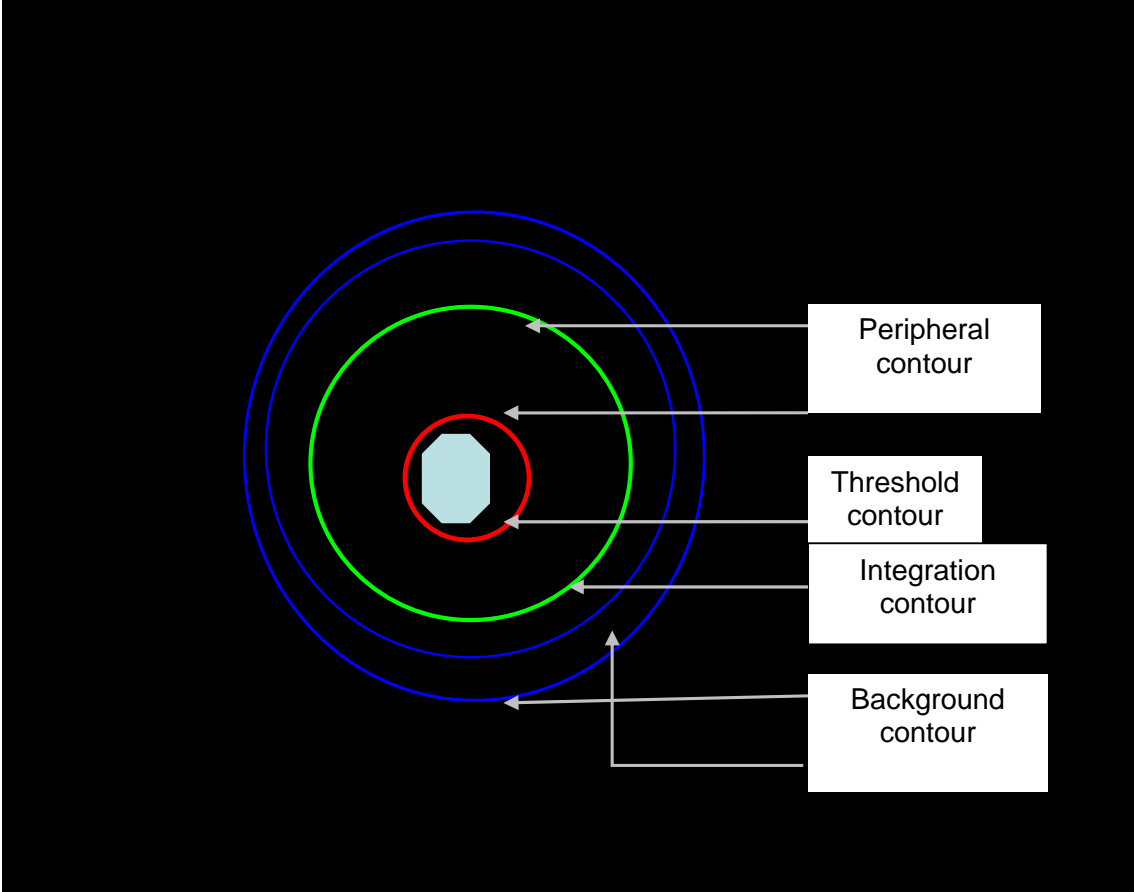


Figure 3.6.1.1 a-j

Representative images (40x magnification) of BMMC incubated with mouse anti-PKC- α (an IgG2a subclass antibody). Anti-mouse IgG2a was used as an isotype control for measurement of non-specific staining and an Alexa488-labelled rabbit anti-mouse IgG antibody was used to indirectly detect binding of the primary antibody by means of green fluorescent staining. The cells were also counterstained with DAPI (blue) to identify the cell nucleus. The cells were incubated with BSA (negative control), PC-BSA (positive control) and SMAs and sensitised with anti-DNP-IgE overnight. Images were captured using a connected Hamamatsu Orca ER digital camera and Openlab version 3.0.9 digital imaging program (Improvision).

a=BSA, b=PC-BSA, c= SMA 3, d= SMA 25, e= SMA 33, f= SMA 39, g= SMA 63, h= SMA 64, i= SMA 65, j=Anti-PKC- α isotype.

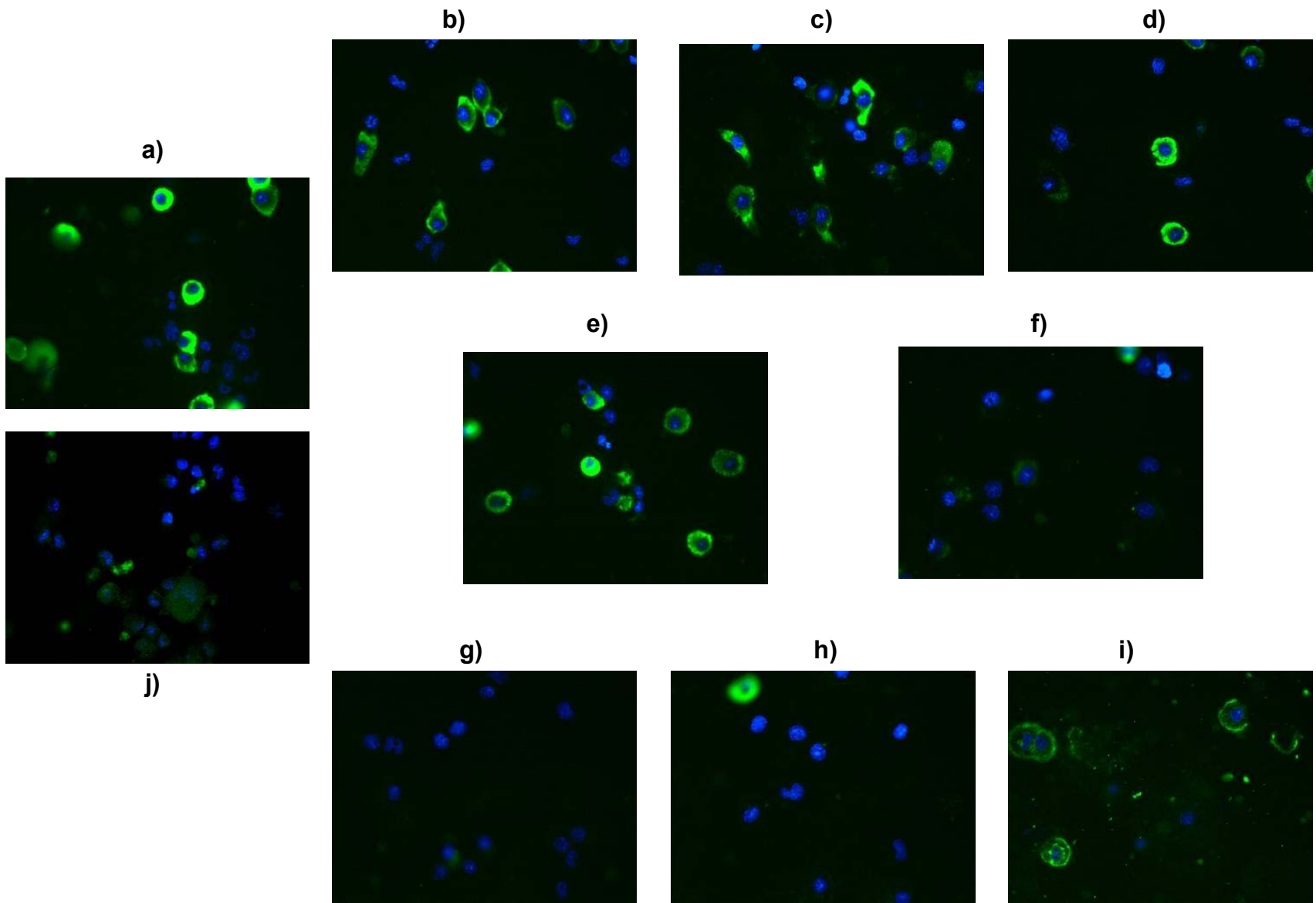


Figure 3.6.1.2 a-j

Representative images (40x magnification) of BMMC incubated with mouse anti-PKC- α (an IgG2a subclass antibody). Anti-mouse IgG2a was used as an isotype control for the measurement of non-specific staining and an Alexa488-labelled rabbit anti-mouse IgG antibody was used to indirectly detect the binding of the primary antibody by means of green fluorescent staining. The cells were also counterstained with DAPI (blue) to identify the cell nucleus. The cells were incubated with BSA (negative control), PC-BSA (positive control) and SMAs and sensitised with anti-DNP-IgE overnight and cross-linked with DNP-HSA for 2 minutes. Images were captured using a connected Hamamatsu Orca ER digital camera and Openlab version 3.0.9 digital imaging program (Improvision).

a=BSA, b=PC-BSA, c= SMA 3, d= SMA 25, e= SMA 33, f= SMA 39, g= SMA 63,
h= SMA 64, i= SMA 65, j=Anti-PKC- α isotype.

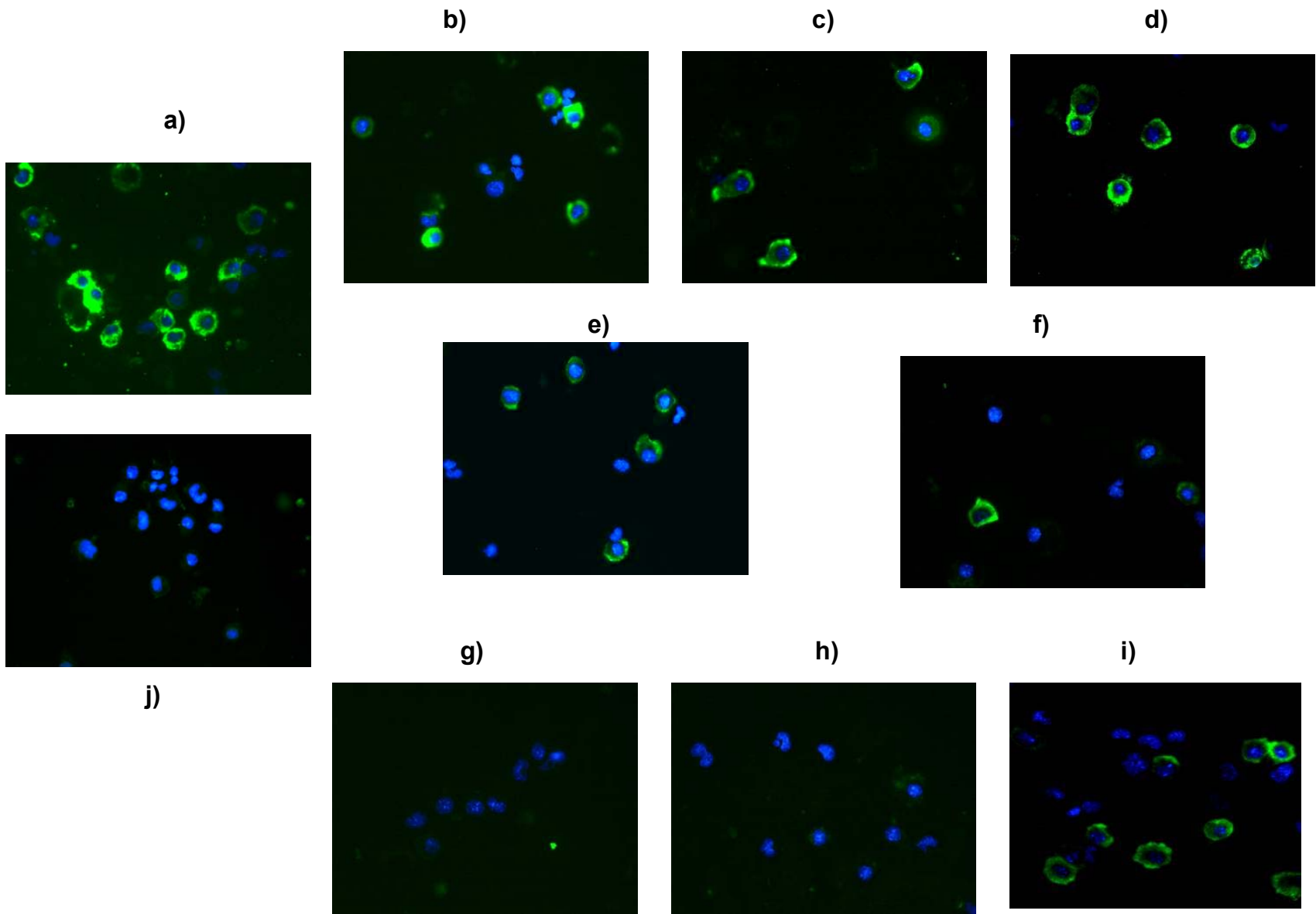


Figure 3.6.1.3 a-e

The figure represents the gating used for the quantitative analysis of immunofluorescence staining with mouse anti-PKC- α of BMMC exposed to SMAs for sensitised and sensitised/cross-linked samples. a) The gating depicts the cell population taken for analysis on the basis of threshold contours. This population is then analysed for PKC- α expression (c) relative to Isotype control (b) allowing calculation by Wincyte software of mean fluorescence integral (c) and mean peripheral fluorescence integral (d). Mean fluorescence integral relates to the level of staining throughout the whole cell whilst peripheral fluorescence depicts the value for the area between the nucleus and the cell membrane. By contrast, (e) max pixel fluorescence gives the value for regions of highest intensity of fluorescence within the cell. The cells were incubated with BSA, PC-BSA or SMAs and sensitised with Anti-DNP-IgE overnight and in some cases cross-linked with DNP-HSA for 2 minutes.

The data are the results of staining in one experiment.

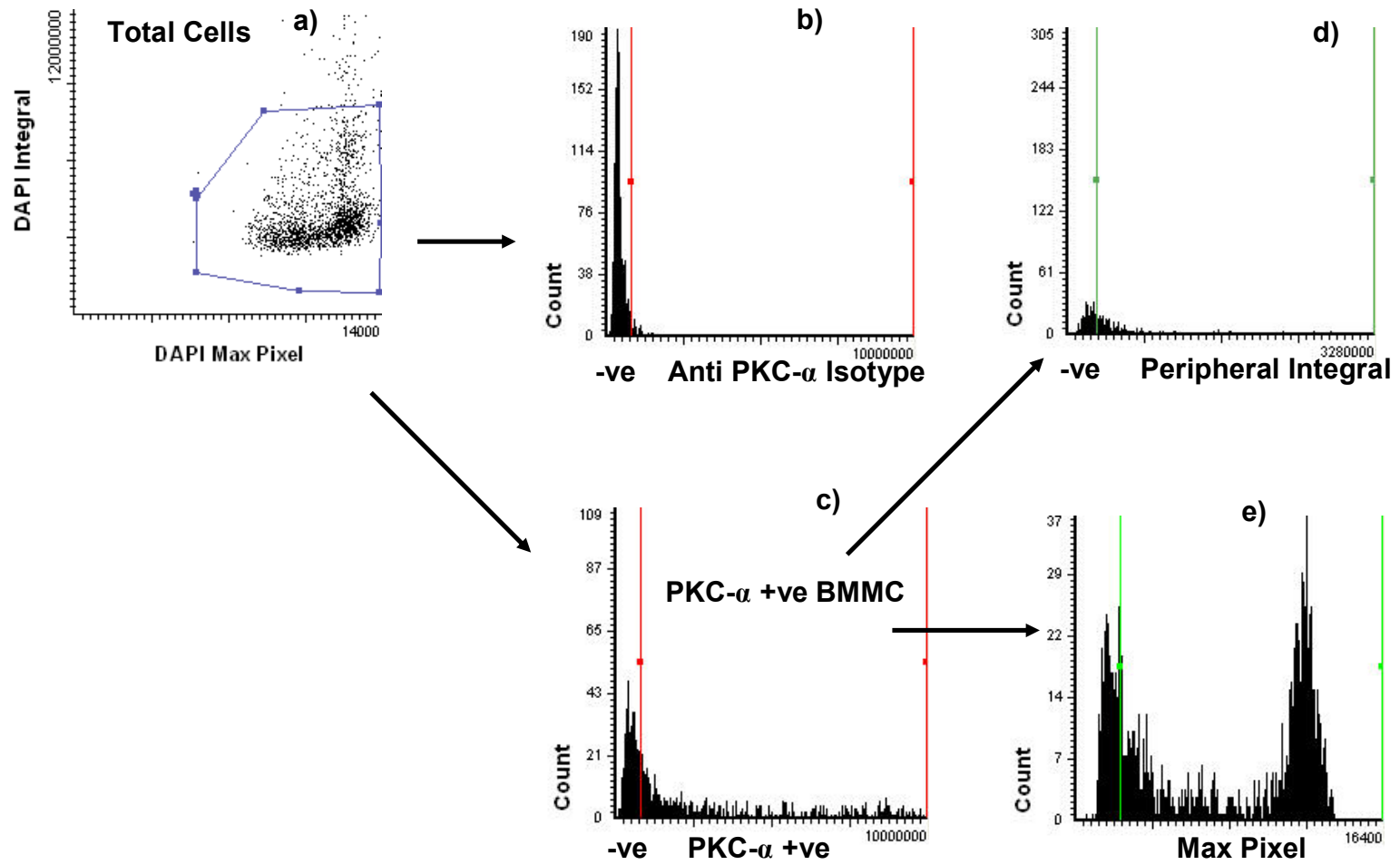
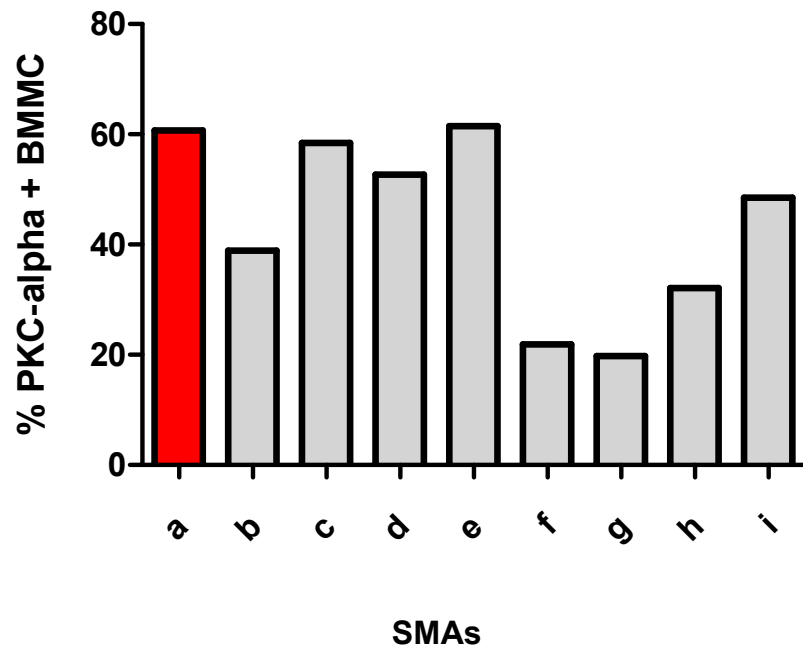


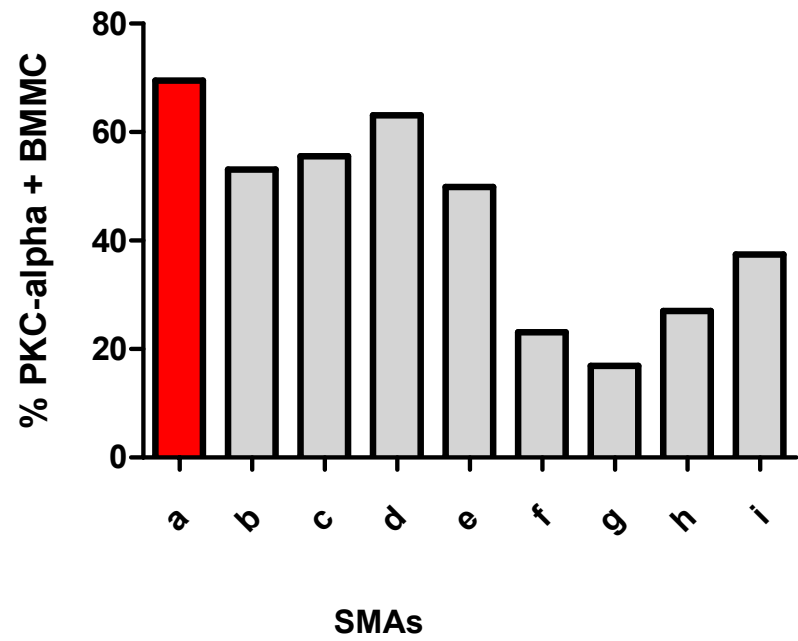
Figure 3.6.1.4 a and b

The figures represent the % of BMBC expressing detectable levels of PKC- α relative to the isotype control. The cells were incubated with BSA, PC-BSA and SMAs and anti-DNP-IgE overnight and then left for a further 2 minutes (a) or cross-linked with DNP-HSA for 2 minutes (b). The quantitative analysis of immunofluorescence associated with binding of mouse anti-PKC- α to BMBC for sensitised and sensitised/cross-linked samples was performed using Wincyte software. The data are indicative of the results obtained from more than 2×10^3 BMBC in each sample from one experiment.

a=BSA, b=PC-BSA, c= SMA 3, d= SMA 25, e= SMA 33, f= SMA 39, g= SMA 63,
h= SMA 64, i= SMA 65



a)

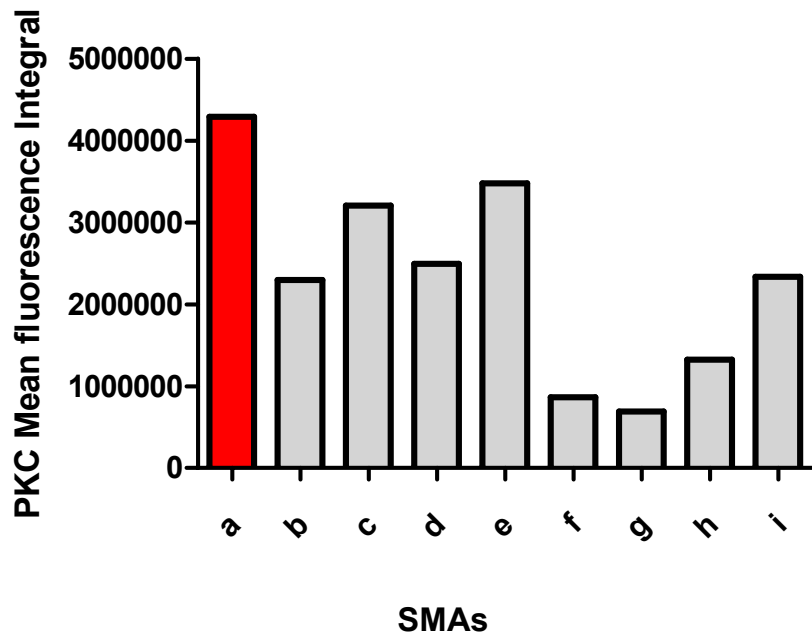


b)

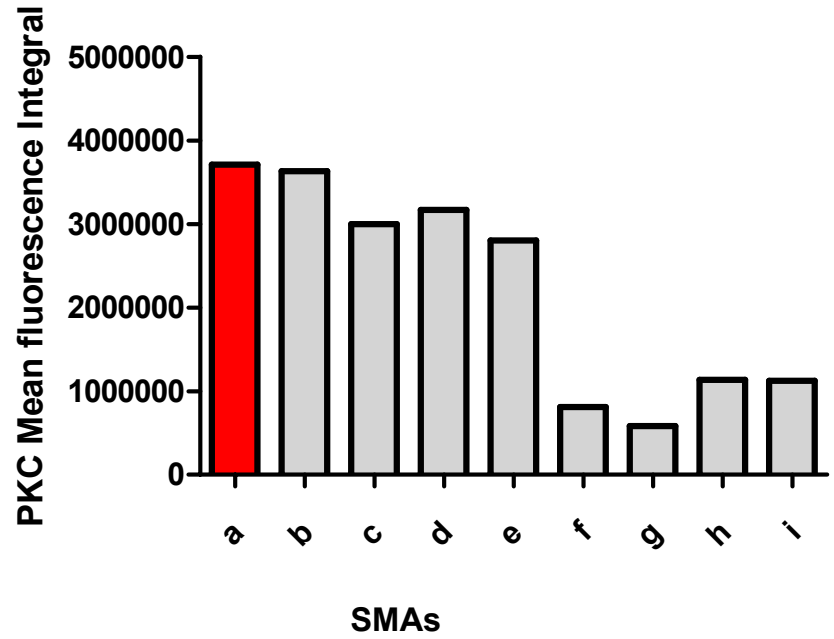
Figure 3.6.1.5 a and b

The figures represent the quantitative analysis of immunofluorescence staining associated with mouse anti-PKC- α binding to BMDC for sensitised and sensitised/cross-linked samples after calculation of Mean Total Fluorescence integral (Wincyte software) following gating of specific staining relative to the isotype control. Mean fluorescence integral relates to the level of staining throughout the whole cell. The cells were incubated with BSA, PC-BSA or SMAs and sensitised with anti-DNP-IgE and then left for a further 2 minutes (a) or cross-linked with DNP-HSA for 2 minutes (b). The data are the results of staining in one experiment.

a=BSA, b=PC-BSA, c= SMA 3, d= SMA 25, e= SMA 33, f= SMA 39, g= SMA 63,
h= SMA 64, i= SMA 65



a)

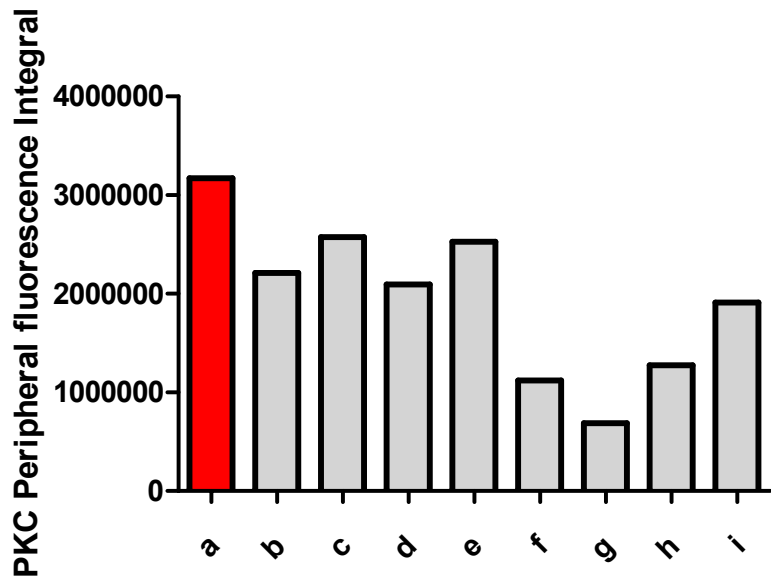


b)

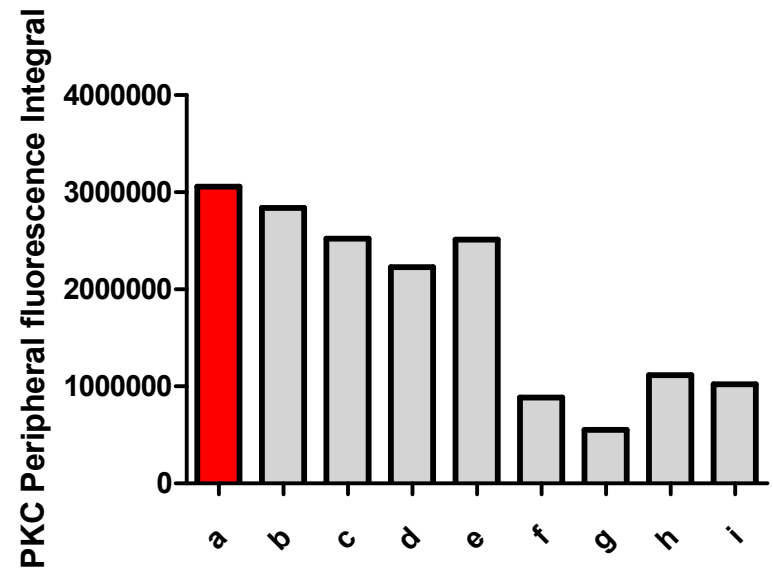
Figure 3.6.1.6 a and b

The figures represent the quantitative analysis of immunofluorescence staining associated with mouse anti-PKC- α binding to BMBC for sensitised and sensitised/cross-linked samples after calculation of Peripheral Fluorescence integral (Wincyte software) following gating of specific staining relative to the isotype control. Peripheral fluorescence depicts the value for the area between the nucleus and the cell membrane. The cells were incubated with BSA, PC-BSA or SMAs and sensitised with anti-DNP-IgE and then left for a further 2 minutes (a) or cross-linked with DNP-HSA for 2 minutes (b). The data are the results of staining in one experiment.

a=BSA, b=PC-BSA, c= SMA 3, d= SMA 25, e= SMA 33, f= SMA 39, g= SMA 63,
h= SMA 64, i= SMA 65



a) SMAs

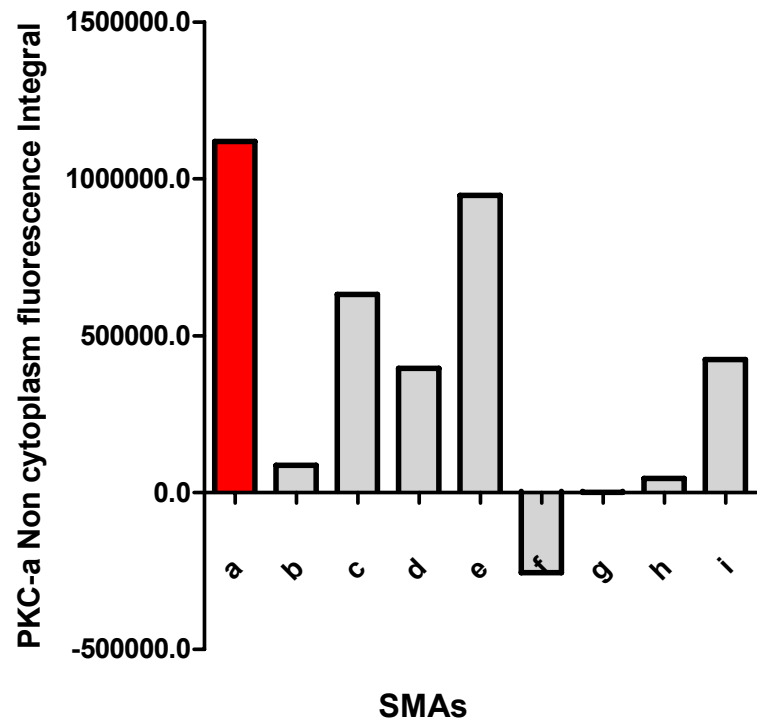


b) SMAs

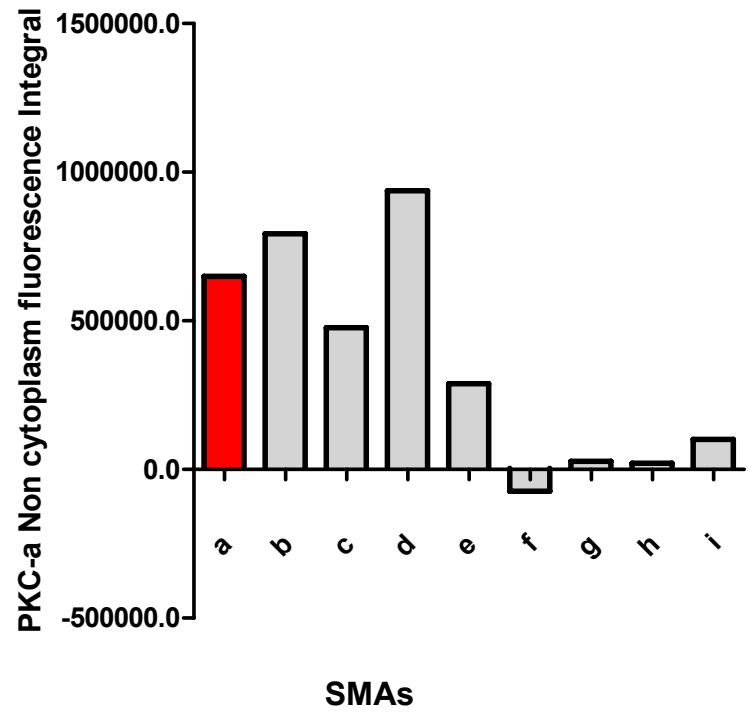
Figure 3.6.1.7 a and b

The figure represents the comparison of the quantitative analysis of immunofluorescence staining between the sensitised and sensitised/cross-linked samples associated with binding of mouse anti-PKC- α of BMMC. Non Cytoplasmic fluorescence was obtained by subtracting the Peripheral fluorescence values from the Total Fluorescence within the cell. The cells were incubated with BSA, PC-BSA or SMAs and sensitised with anti-DNP-IgE and then left for a further 2 minutes (a) or cross-linked with DNP-HSA for 2 minutes (b). The data are the results of staining in one experiment.

a=BSA, b=PC-BSA, c= SMA 3, d= SMA 25, e= SMA 33, f= SMA 39, g= SMA 63,
h= SMA 64, i= SMA 65



a)

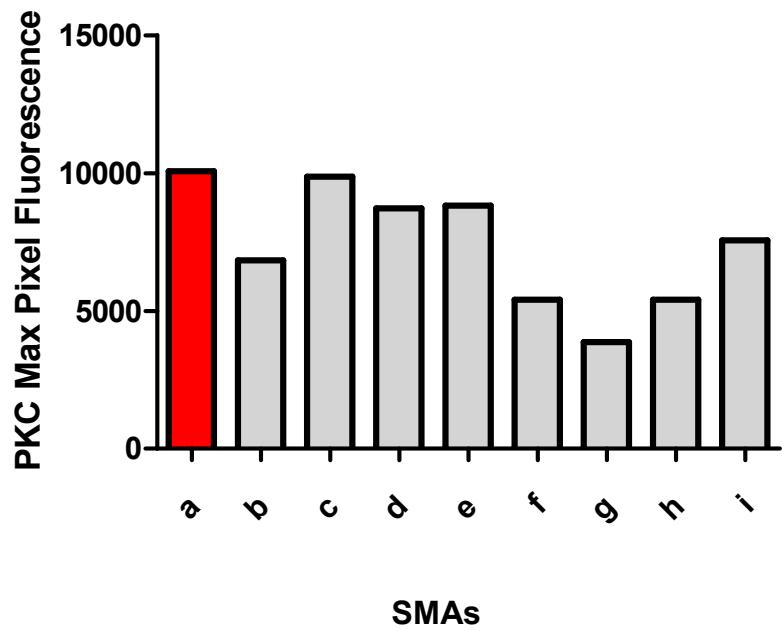


b)

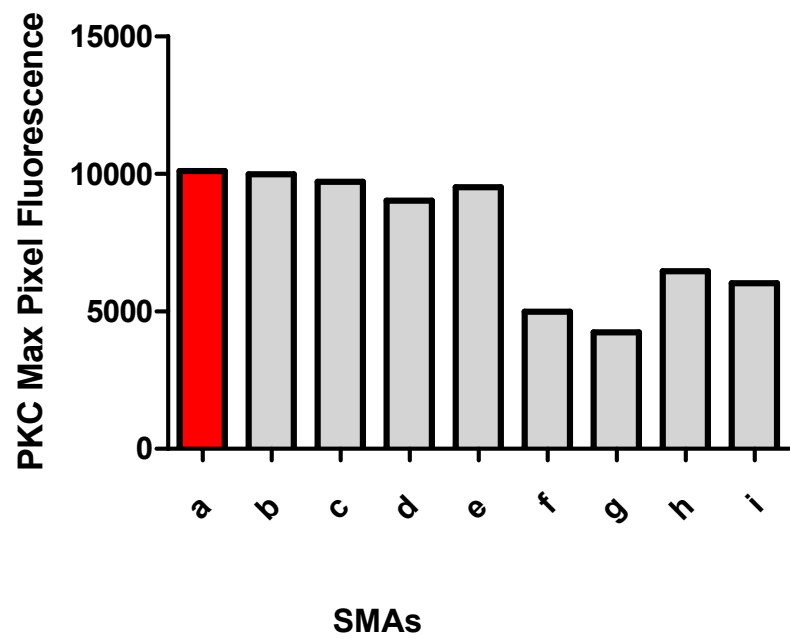
Figure 3.6.1.8 a and b

The figure represents the comparison of the quantitative analysis of immunofluorescence staining between the sensitised and sensitised/cross-linked samples associated with binding of mouse anti-PKC- α of BMMC. Max pixel fluorescence gives the value for highest intensity of fluorescence within the cell. The cells were incubated with BSA, PC-BSA or SMAs and sensitised with anti-DNP-IgE and then left for a further 2 minutes (a) or cross-linked with DNP-HSA for 2 minutes (b). The data are the results of staining in one experiment.

a=BSA, b=PC-BSA, c= SMA 3, d= SMA 25, e= SMA 33, f= SMA 39, g= SMA 63,
h= SMA 64, i= SMA 65



a)



b)

3.6.3 The effects of SMAs on PLD1 signaling

PLD is considered to regulate a variety of cellular functions, particularly those relating to membrane processes, including vesicle transport, membrane reorganisation, membrane budding and endocytosis. PLD catalyses the hydrolysis of phosphatidylcholine (PtdCho), to generate phosphatidic acid and choline. Multiple PLD activities have been characterised in mammalian cells but only two genes encoding PtdCho-specific PLDs, *PLD1* and *PLD2* have been identified. PLD1 has been reported to be preferentially associated with cytosolic granule membranes and intracellular vesicles, and PLD2 with the plasma membrane, although this differential distribution may be receptor- and cell type-specific [239-241].

It has been previously shown by Melendez *et al* that the rapid rise in FcεRI-mediated Ca²⁺ mobilisation in mast cells is triggered by sequential activation of PLD1 and SPHK1, and eventually leads to degranulation [156]. It has also been elucidated that there was inhibition of the initial peak of Ca²⁺ mobilisation within human mast cells in the presence of ES-62 and this reflected sequestration and degradation of the upstream regulator of PLD1, PKC-α [155].

In accordance with these studies, it was decided to investigate the effects of SMAs on PLD1 expression and translocation. Immunofluorescence staining of BMDC with anti-PLD1 for both the sensitised and sensitised and cross-linked samples was therefore undertaken. An Alexa488-labelled anti-rabbit IgG antibody was used to indirectly detect PLD1 by means of green fluorescent staining. The cells were also counterstained with DAPI (blue) to identify them by their nuclei.

Similar to the experiments investigating PKC-α, expression of PLD1 was measured following exposure to SMAs/sensitisation with anti-DNP IgE on BMDC and also following antigenic cross-linking of sensitised FcεRI for 2 minutes

respectively (Figures 3.6.2.1-3.6.2.2 a-j). The sensitised only samples revealed a generalised down-regulation of expression of PLD1 relative to the BSA control (Fig 3.6.2.1 a-j), although a clustering of signal with punctate fluorescence can be appreciated in the cytoplasm in the case of PC-BSA, SMAs 33 and 63 (Fig 3.6.2.1 b, e and g). With respect to the samples cross-linked for 2 minutes, the BSA control revealed small bright fluorescent foci in the cytoplasm along with SMAs 33, 63 and 65, while there was a generalised inhibition of expression with all the SMAs (Fig 3.6.2.2). SMA 64 revealed a near complete obliteration of PLD expression (Fig 3.6.2.2 h).

Quantitative LSC analysis of these samples using Wincyte software version 3.6 (Compucyte) was performed. The cells were gated according to the required fields which were used for quantitation of the fluorescence obtained from the qualitative data in the form of histograms (Figure 3.6.2.3). The quantitation of data obtained from 1×10^3 BMBC revealed that in the sensitised only samples, there was a reduction in the % of BMBC expressing PLD1 in the case of PC-BSA and all the SMAs and marked reduction with SMA 64 as compared to the BSA control (Figure 3.6.2.4a). Moreover, in the samples cross-linked for 2 minutes it was revealed that the % of BMBC expressing PLD1 was reduced in all the samples as compared to the BSA control with very minor reduction with SMA 39 and markedly so in the case of SMA 64 (Figure 3.6.2.4b).

In addition, on comparison of the Mean total fluorescence obtained per cell, it was observed that in the sensitised cells, all the SMAs showed a reduction in the level of PLD expression. This reduction was again most evident in the case of SMA 64. PC-BSA, however, showed an increase in the immunofluorescence in the cell (Figure 3.6.2.5a). Nevertheless, following cross-linking even PC-BSA showed a reduction in

the levels of PLD expression per cell as compared to the BSA control. SMA 64 again revealed particularly significant reduction in the levels of immunofluorescence (Figure 3.6.2.5b). On observation of the peripheral fluorescence depicting the fluorescence in the cytoplasm in the sensitised only samples, not much change was observed in immunofluorescence of experimental samples when compared with the control, except in the cases of PC-BSA and SMA 63, which revealed an increase in expression (Figure 3.6.2.6a). As there was not much change in the expression of PLD1 in the samples as compared with the control, it can be assumed that SMAs were particularly targeting non-cytoplasmic expression of PLD. These marginal changes in cytoplasmic PLD expression were also observed following cross-linking with only slight decrease in immunofluorescence obtained with PC-BSA, SMAs 3, 25, 33, 39 and 64 (Figure 3.6.2.6b), whilst SMAs 63 and 65 revealed no change when compared with the BSA control. Consistent with this, on calculation of Nuclear (non cytoplasmic space) fluorescence for the sensitised only samples (Figure 3.6.2.7a), whilst it was noted that there was no change in fluorescence obtained with PC-BSA and SMA 33 with respect to the control value, treatment with SMAs 3, 25 and 39 lead to a substantial decrease in fluorescence. However the most remarkable reduction was observed with SMAs 63, 64 and 65. For the sensitised/ cross-linked samples, it was observed that the values were strikingly reduced for all the SMAs and PC-BSA. However, SMA 65 showed an increase as compared to its sensitised sample, although it was still less than the BSA control. Perhaps rather surprisingly, the data for Max pixel measuring intensity of staining indicating clustering of signal, in the sensitised and cross-linked samples did not show any significant change between the various samples although there was a slight generalised decrease with all the SMAs (Figure 3.6.2.8 a and b).

Thus, it can be assumed that with SMA 64, there is an overall trend for down regulation of expression and desensitisation of activation as evidenced from the data showing reduction in % of cells expressing PLD1. In these experiments, the distribution of expression of PLD did not reveal significant information about the activation of the signaling molecules as it was seen that the inhibitory SMAs induced a global reduction in the immunofluorescence. For example there was a decrease in the total immunofluorescence with SMA 64, along with a decrease in expression, both in the nuclear and cytoplasmic fluorescence. The data from the remainder of the molecules show a general inhibitory trend for the expression of PLD1. From the above data, it can thus be assumed that although the effects with SMA 64 are the most profound, SMAs 3, 25, 33, 39 and 63 are also suppressing the response as evident from the total fluorescence obtained per cell (Figure 3.6.2.5a and b) and nuclear fluorescence (Figure 3.6.2.7 a and b).

Figure 3.6.2.1 a-j

Representative images (40x magnification) of BMMC incubated with polyclonal anti-PLD1. Anti-rabbit IgG was used as an isotype control for the measurement of non-specific staining and an Alexa488-labelled rabbit anti-mouse IgG antibody was used to indirectly detect the binding of primary antibody by means of green fluorescent staining. The cells were also counterstained with DAPI (blue) to identify the cell nucleus. The cells were incubated with BSA (negative control), PC-BSA (positive control) and SMAs and sensitised with anti-DNP-IgE overnight. Images were captured using a connected Hamamatsu Orca ER digital camera and Openlab version 3.0.9 digital imaging program (Improvision).

a=BSA, b=PC-BSA, c= SMA 3, d= SMA 25, e= SMA 33, f= SMA 39, g= SMA 63,
h= SMA 64, i= SMA 65, j=Anti-PLD isotype

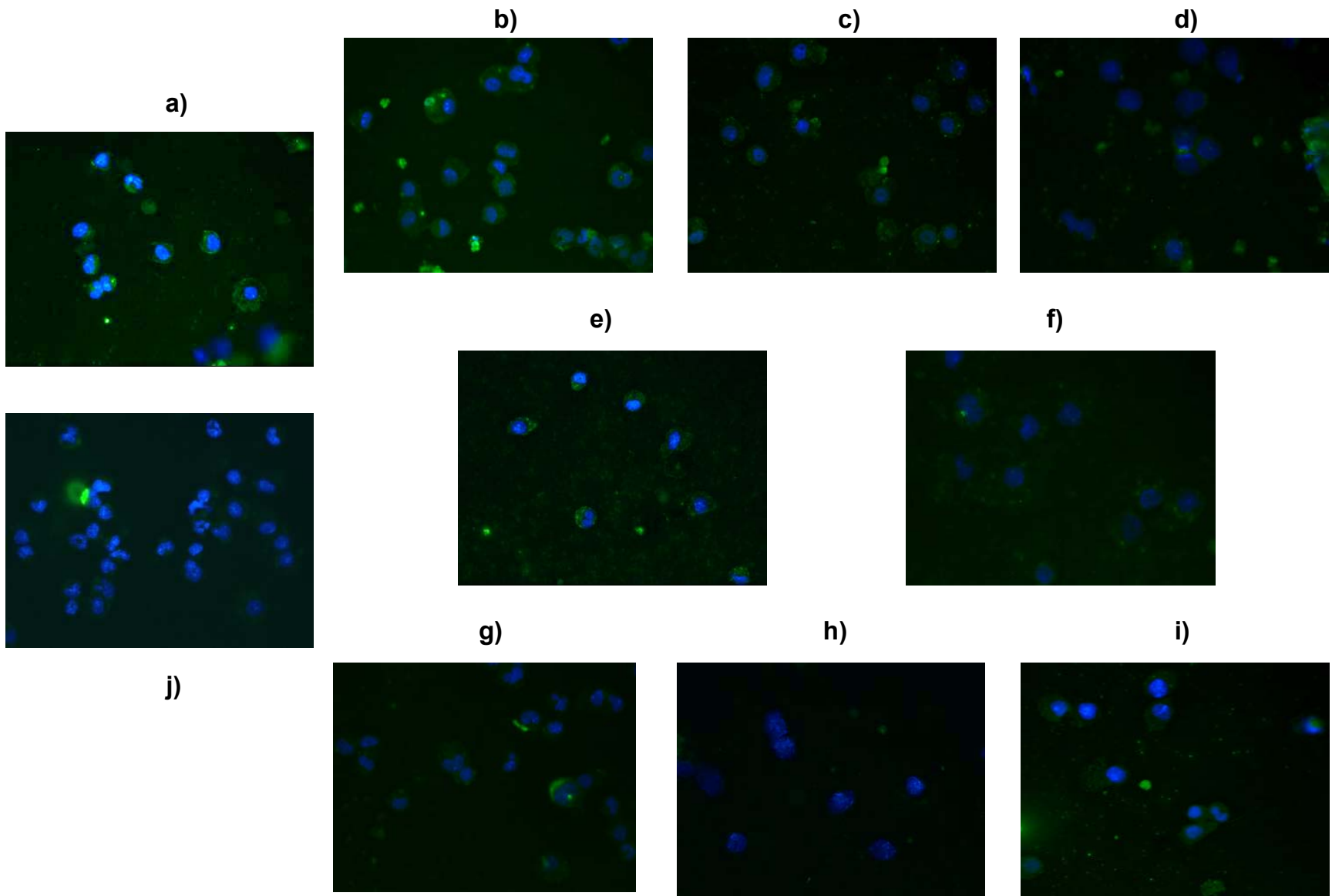


Figure 3.6.2.2 a-j

Representative images (40x magnification) of BMMC incubated with polyclonal anti-PLD1. Anti-rabbit IgG was used as an isotype control for the measurement of non-specific staining and an Alexa488-labelled rabbit anti-mouse IgG antibody was used to indirectly detect the binding of the primary antibody by means of green fluorescent staining. The cells were incubated with BSA (negative control), PC-BSA (positive control) and SMAs and sensitised with anti-DNP-IgE overnight and cross-linked with DNP-HSA for 2 minutes. Images were captured using a connected Hamamatsu Orca ER digital camera and Openlab version 3.0.9 digital imaging program (Improvision).

a=BSA, b=PC-BSA, c= SMA 3, d= SMA 25, e= SMA 33, f= SMA 39, g= SMA 63,
h= SMA 64, i= SMA 65, j=Anti-PLD isotype

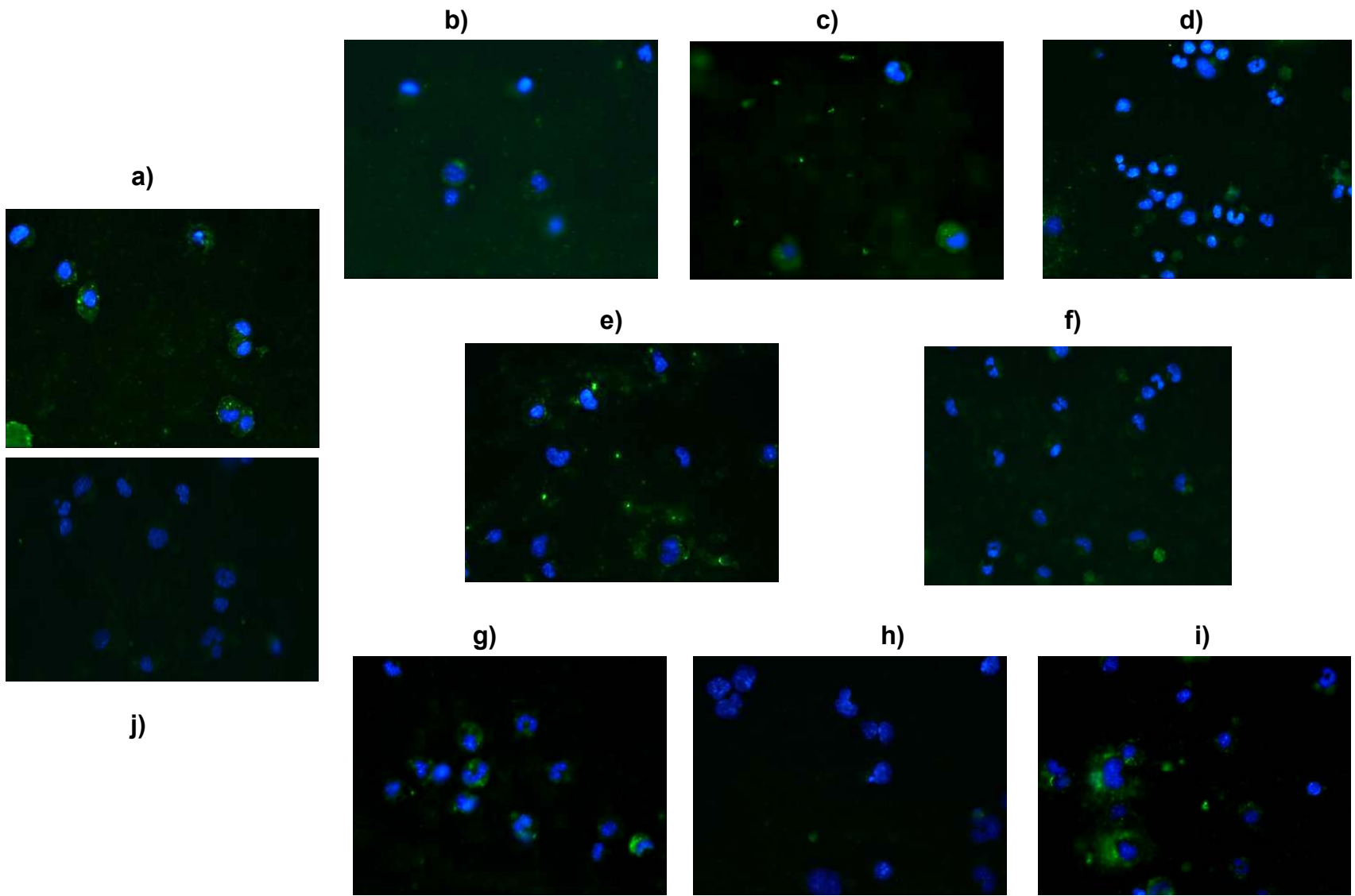


Figure 3.6.2.3 a-e

The figures represent the gating used for the quantitative analysis of immunofluorescence staining with polyclonal rabbit anti-PLD1 of BMMC exposed to SMAs for sensitised and cross-linked samples. a) The gating depicts the cell population taken for analysis on the basis of threshold contours. This population is then analysed for PLD1 expression relative to Isotype control (b) allowing calculation by Wincyte software of mean fluorescence integral (c) and mean peripheral fluorescence integral (d). Mean fluorescence integral relates to the level of staining throughout the whole cell whilst peripheral fluorescence depicts the value for the area between the nucleus and the cell membrane. By contrast, (e) max pixel fluorescence gives the value for highest intensity of fluorescence within the cell. The cells were incubated with BSA (negative control), PC-BSA (positive control) and SMAs and sensitised with anti-DNP-IgE overnight and cross-linked with DNP-HSA for 2 minutes.

The data are the results of staining in one experiment.

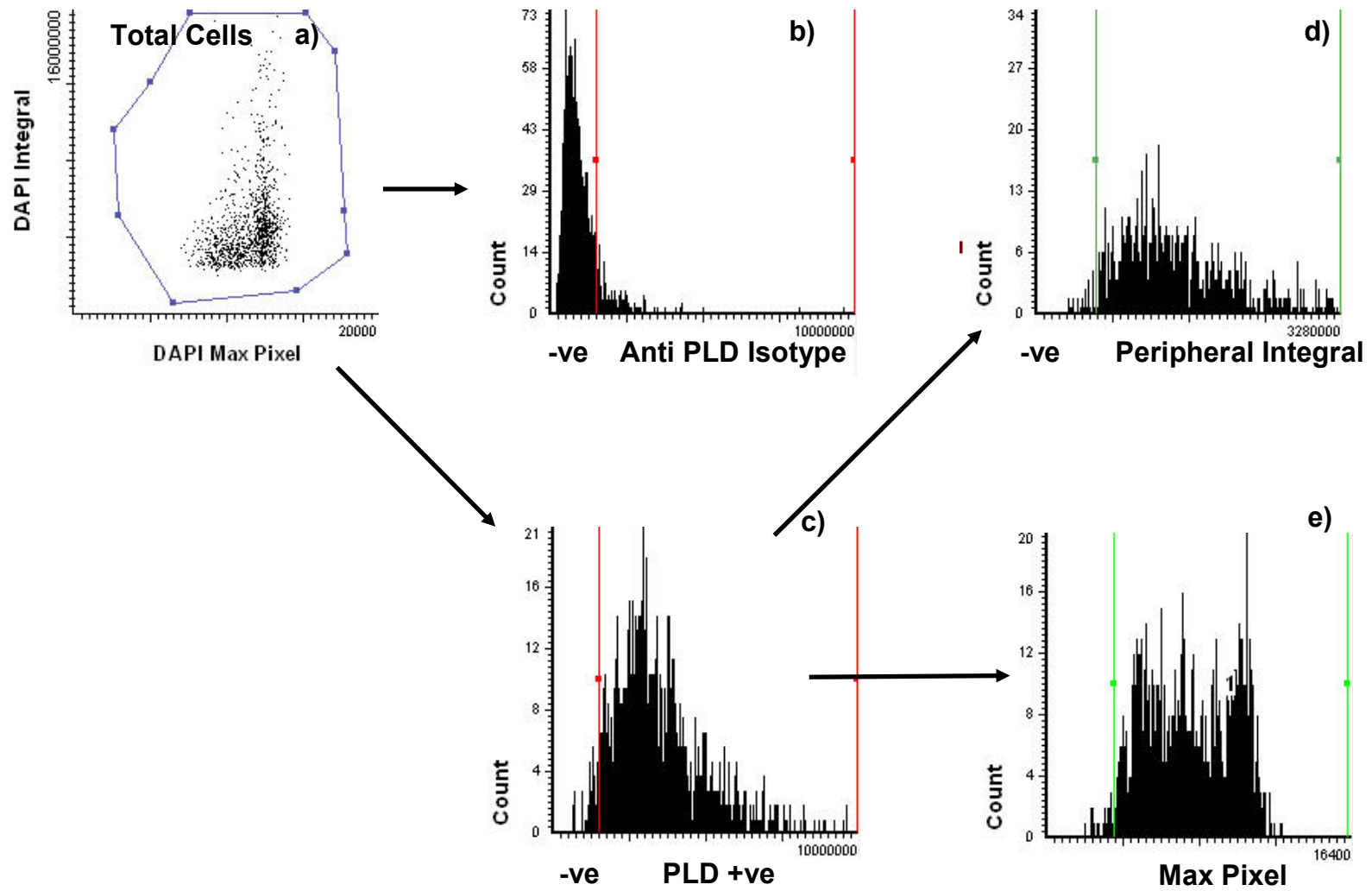
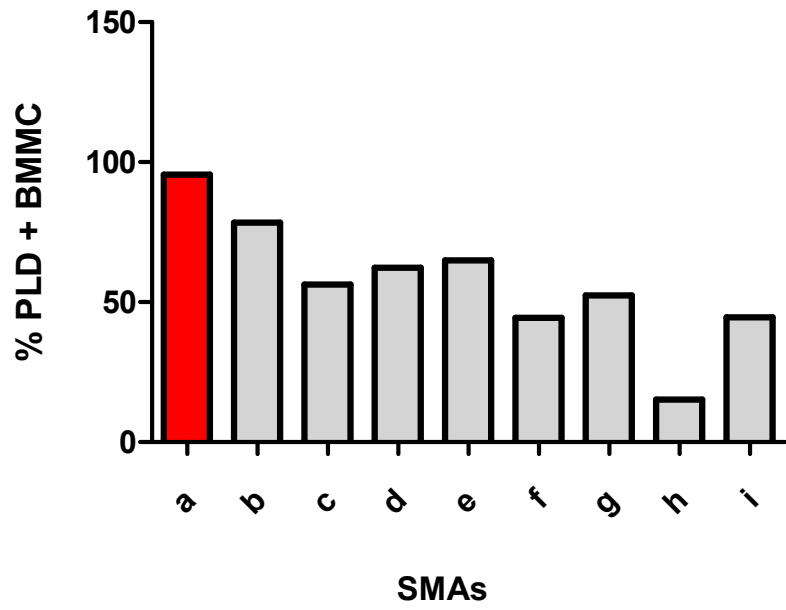


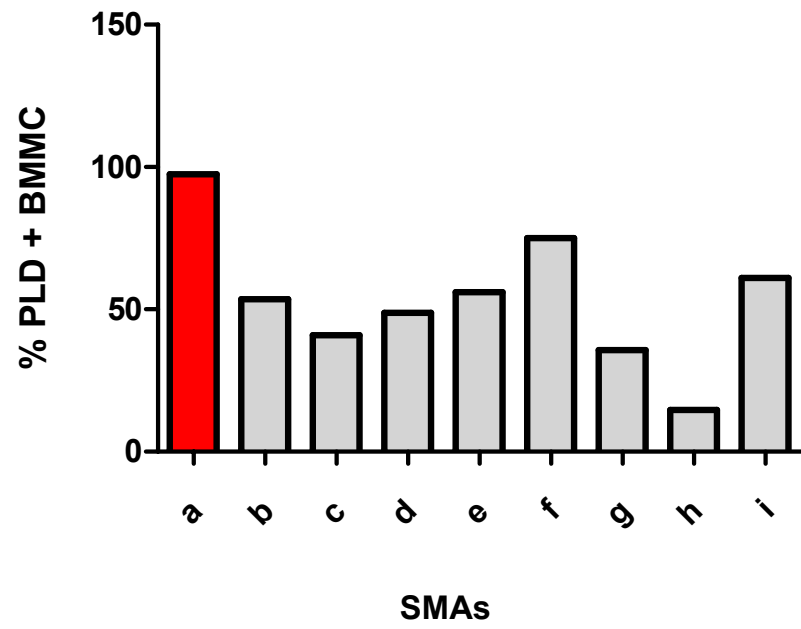
Figure 3.6.2.4 a and b

The figures represent the % of BMMC expressing detectable levels of PLD1 relative to isotype control. The cells were incubated with BSA, PC-BSA or SMAs and anti-DNP-IgE overnight and then left for another 2 minutes (a) or cross-linked with DNP-HSA for 2 minutes (b). The quantitative analysis of immunofluorescence associated with binding of polyclonal anti-PLD1 to BMMC for sensitised and sensitized/cross-linked samples was performed using Wincyte software. The data are indicative of the results of analysis of more than 1×10^3 BMMC in each sample from one experiment.

a=BSA, b=PC-BSA, c= SMA 3, d= SMA 25, e= SMA 33, f= SMA 39, g= SMA 63,
h= SMA 64, i= SMA 65



a)

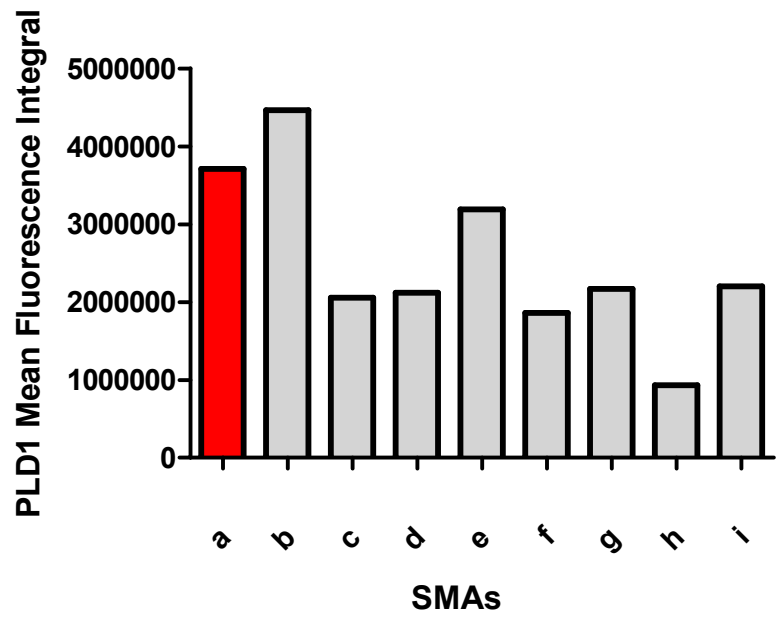


b)

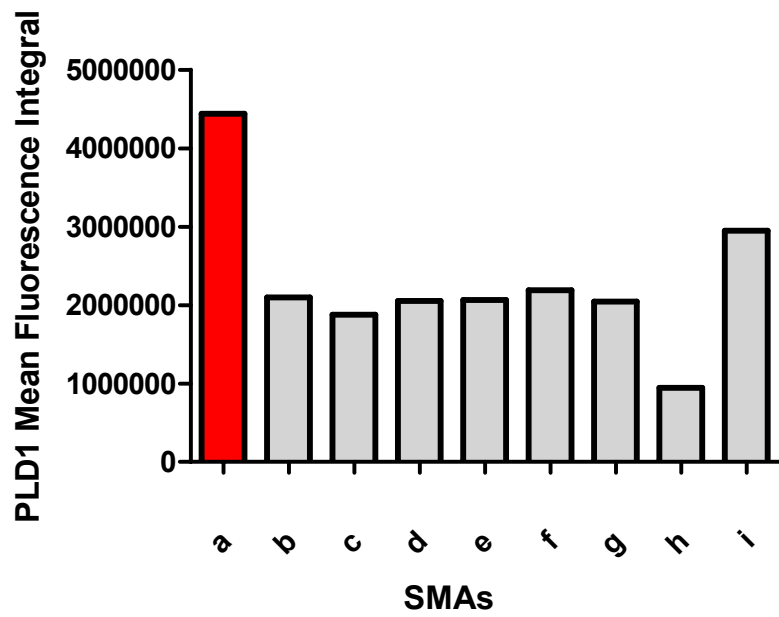
Figure 3.6.2.5 a and b

The figures represent the quantitative analysis of immunofluorescence staining associated with polyclonal rabbit anti-PLD1 binding to BMMC for sensitised and sensitised/cross-linked samples after calculation of Mean Total fluorescence integral (Wincyte software) following gating of specific staining relative to the isotype control. Mean fluorescence integral relates to the level of staining throughout the whole cell. The cells were incubated with BSA, PC-BSA or SMAs and sensitised with anti-DNP-IgE and then left for a further 2 minutes (a) or cross-linked with DNP-HSA for 2 minutes (b). The data are the results of analysis of at least 1×10^3 cells.

a=BSA, b=PC-BSA, c= SMA 3, d= SMA 25, e= SMA 33, f= SMA 39, g= SMA 63,
h= SMA 64, i= SMA 65



a)



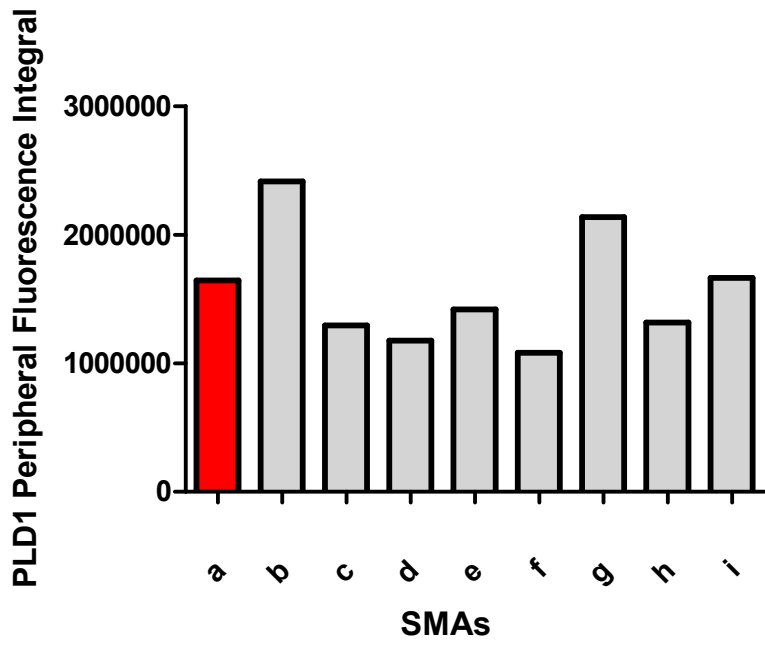
b)

Figure 3.6.2.6 a and b

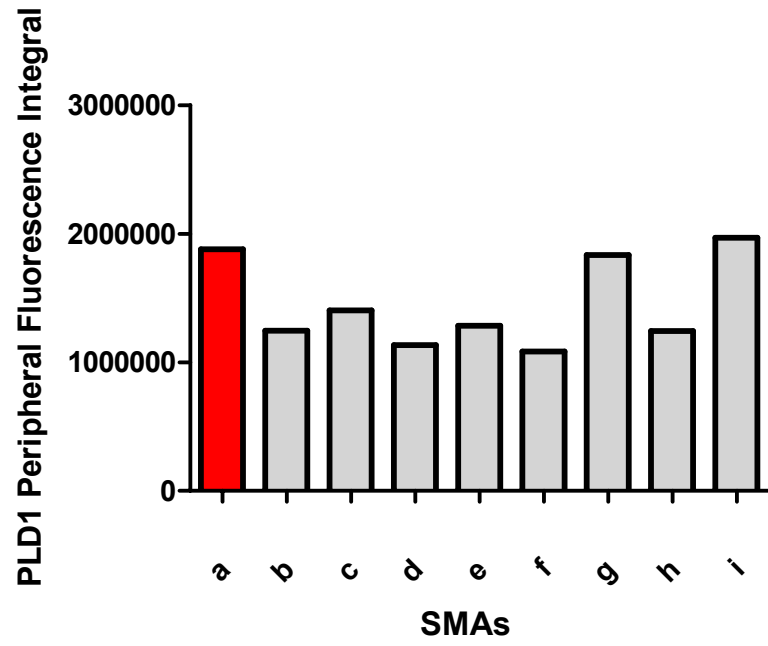
The figures represent the quantitative analysis of immunofluorescence staining associated with polyclonal rabbit anti-PLD1 binding to BMMC for sensitised and sensitised/cross-linked samples after calculation of Peripheral Fluorescence integral (Wincyte software) following gating of specific staining relative to the isotype control. Peripheral Fluorescence integral depicts the value for the area between the nucleus and the cell membrane. The cells were incubated with BSA, PC-BSA or SMAs and sensitised with anti-DNP-IgE and then left for a further 2 minutes (a) or cross-linked with DNP-HSA for 2 minutes (b). The data are the results of analysis of 1×10^3 cells.

a=BSA, b=PC-BSA, c= SMA 3, d= SMA 25, e= SMA 33, f= SMA 39, g= SMA 63,

h= SMA 64, i= SMA 65



a)

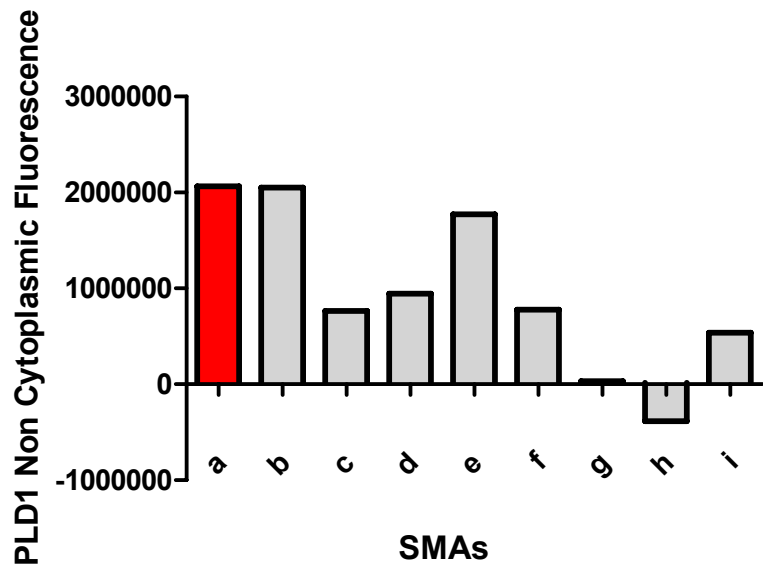


b)

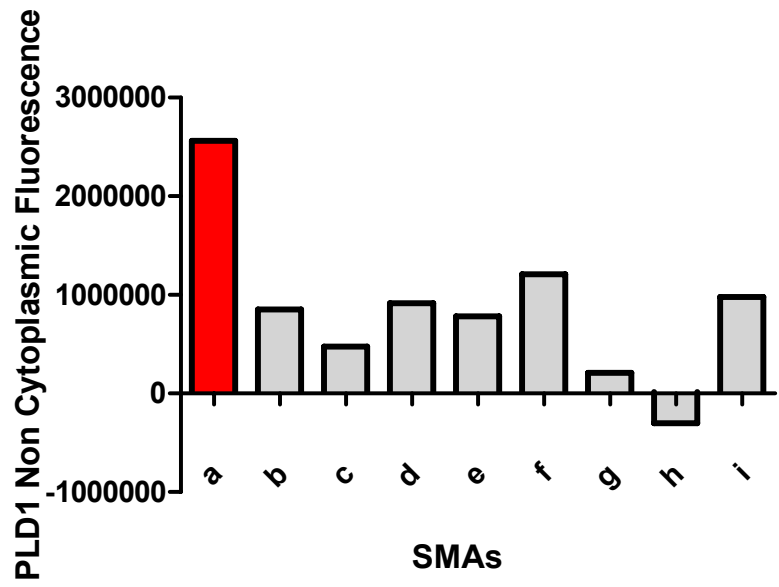
Figure 3.6.2.7 a and b

The figure represents the comparison of the quantitative analysis of immunofluorescence staining between the sensitised and sensitised/cross-linked samples associated with binding of rabbit anti PLD1 of BMMC. Nuclear (Non-cytoplasmic fluorescence) was obtained by subtracting the Peripheral fluorescence values from the Total Fluorescence within the cell. The cells were incubated with BSA, PC-BSA or SMAs and sensitised with anti-DNP-IgE and then left for a further 2 minutes (a) or cross-linked with DNP-HSA for 2 minutes (b). The data are the results of analysis of at least 1×10^3 cells

a=BSA, b=PC-BSA, c= SMA 3, d= SMA 25, e= SMA 33, f= SMA 39, g= SMA 63,
h= SMA 64, i= SMA 65



a)



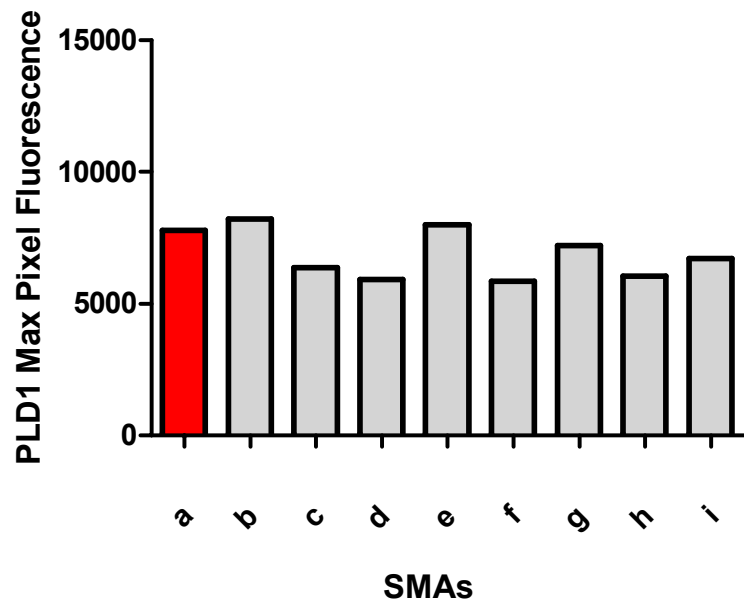
b)

Figure 3.6.2.8 a and b

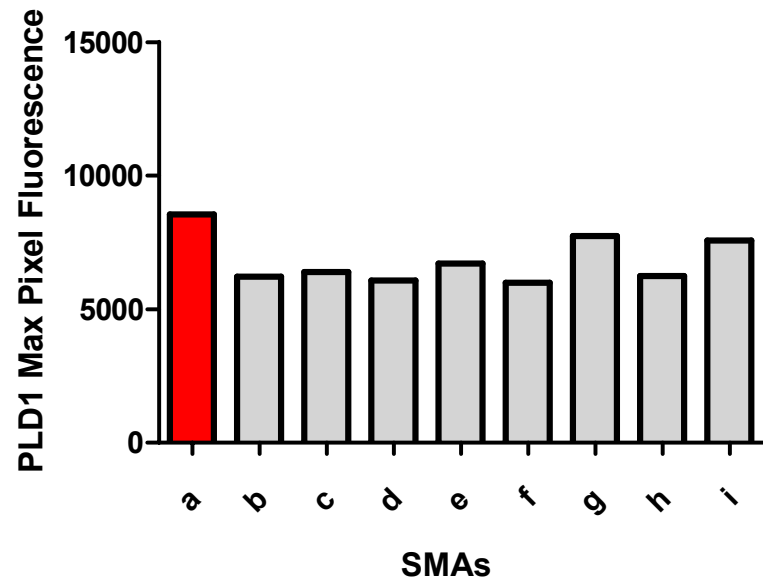
The figure represents the comparison of the quantitative analysis of immunofluorescence staining between the sensitised and sensitised/cross-linked samples associated with binding of polyclonal rabbit anti-PLD1 of BMMC. Max pixel fluorescence gives the value for highest intensity of fluorescence within the cell.

The cells were incubated with BSA, PC-BSA or SMAs and sensitised with anti-DNP-IgE and then left for a further 2 minutes (a) or cross-linked with DNP-HSA for 2 minutes (b). The data are the results of analysis of at least 1×10^3 cells

a=BSA, b=PC-BSA, c= SMA 3, d= SMA 25, e= SMA 33, f= SMA 39, g= SMA 63,
h= SMA 64, i= SMA 65



a)



b)

3.6.4 The effects of SMAs on SPHK1 signaling

It has been revealed by Melendez *et al* that SPHK1 is downstream of PLD1 activity in FcεRI-triggered signal transduction pathways in mast cells. In their experiments, an anti-sense oligonucleotide to PLD1 blocked FcεRI-triggered SPHK1 activity, though it had no effect on SPHK1 expression [156]. Melendez and colleagues also demonstrated that in human BMMC, SPHK1 is present in the cytosolic fraction of mast cells and that it translocated to the periphery upon aggregation of FcεRI. The cross-linking of FcεRI by DNP-HSA was repeated on mouse BMMC sensitised with anti-DNP IgE, by Pushparaj *et al* [235], whereupon they demonstrated that SPHK1 rather than SPHK2 was essential for the generation of the signaling events in mast cells that lead to production of various cytokines and chemokines. In addition, an anti-sense oligonucleotide to SPHK1 blocked FcεRI-triggered sphingosine kinase activity but had no effect on PLD activity or expression of PLD1 levels. As mentioned earlier, it has also been demonstrated that ES-62 abrogated the initial rise in Ca²⁺ mobilisation dependent on the sequential activation of PLD and SPHK and that consequent to its downregulation of PKC-α, exposure to ES-62 inhibited FcεRI-mediated PLD1 and SPHK1 activation.

In accordance with the above experiments, and under the aforementioned conditions, BMMC were incubated with the selected SMAs and on sensitising and cross-linking with the antigen the cells were stained for immunofluorescent analysis of SPHK1 expression and/or activation. BMMC were stained with rabbit polyclonal anti-SPHK1 in the case of both the sensitised and sensitised/cross-linked samples. The cells were also stained with an Alexa488-labelled anti-rabbit IgG antibody, used to indirectly detect SPHK1 by means of green fluorescent staining. The cells were counterstained with DAPI (blue) to identify the cells by their nuclei. The data were

analysed and quantitative analysis was performed on the cells after 2 min of cross-linking with the antigen.

In the sensitised only samples, it was observed that the immunofluorescence obtained was almost similar to the BSA control in most of the samples (Figure 3.6.3.1 a-j); although small areas of fluorescence of greater intensity than that seen with the BSA control were observed with PC-BSA and SMAs 3, 33 and 64. It was observed that for the cross-linked samples, fluorescent foci could be appreciated in the cytoplasm for the BSA control, PC-BSA and SMAs 33, 39 and 65 (Figure 3.6.3.2 a, b, e, f and i).

Figure 3.6.3.3 represents the gating performed for the quantitative analysis using Wincyte software for the data collected on BMBC cross-linked for 2 minutes. Figure 3.6.3.4a shows that in the sensitised only samples, the % of BMBC expressing SPHK1 was decreased in samples with PC-BSA, SMAs 25, 39, 63 and particularly so with 65. The expression was increased with SMAs 3, 33 and with 64 as compared to the BSA control. On the other hand Figure 3.6.3.4b illustrated that in the cross-linked samples, except for SMA 33, where no change was observed, there was a decrease in the % of BMBC expressing SPHK1 with all the SMAs and also PC-BSA. The mean of total immunofluorescence obtained per cell in the sensitised only samples was somewhat reduced with SMAs 25, 39 and substantially more reduced with 65 relative to the BSA control (Figure 3.6.3.5a). There was not much change compared to the BSA control in the case of the rest of the samples except for PC-BSA and SMAs 3, and 64, which showed a small increase. In the case of sensitised/cross-linked samples, no change was observed in all the samples with the exception of SMAs 3, 25, 39, 63 and 64 (Figure 3.6.3.5b), where a slight decrease was observed. It was noticed that there was an increase in the immunofluorescence in

the cross-linked samples when compared to their respective sensitised only sample in the case of SMA 65, although the immunofluorescence obtained in the sensitised samples was less than the BSA controls both for sensitised and cross-linked samples. In the case of most of the SMAs, there was an increase in the sensitised samples more than the sensitised/cross-linked samples thereby implying a reduction in expression of SPHK after cross-linking. For the data on peripheral immunofluorescence obtained from the cytoplasm, it was seen that there was no change as compared to the BSA control in the case of most the SMAs, except SMAs 63, 64 and 65 and also PC-BSA, which exhibited an increase with respect to the sensitized only samples. The trend was again very similar in all the cross-linked samples, where PC-BSA and SMAs 63, 64 and 65 revealed a minor increase relative to the BSA control (Figure 3.6.3.6 a and b). It was also seen that the immunofluorescence was almost similar for all the SMAs in the sensitised only and sensitised/cross-linked samples. The calculation of the nuclear fluorescence revealed that in the sensitised only samples, SMAs 3, 33 and 64 had values that were slightly more than the BSA control. SMA 65 was strikingly decreased and PC-BSA and SMAs 25, 39 and 63 also demonstrated a reduction (Figure 3.6.3.7a) On observation of the sensitised/cross-linked samples, the value obtained for SMA 33 was found to be almost the same as the control (Figure 3.6.3.7b) The non-cytoplasmic fluorescence values for SMAs 3 and 64 that were more than the control in the sensitised samples were now reduced and there was a marked reduction in the case of SMAs 64 and also 63 and 65. However, in the case of SMA 65 the value that was more reduced in the sensitised only sample, was less so in the sensitised/cross-linked one, although the reduction was still very significant relative to the BSA control. The values for the Max pixel obtained for sensitised-only samples did not show much change with respect to the BSA control. The same was

seen in the case of the cross-linked samples when compared to their control (Figure 3.6.3.8 a and b).

Thus it can be concluded that the % of cells expressing SPHK1 was reduced with SMAs 39, 63, 64 and 65. This was more significant in the case of SMA 64 where although the expression is increased in the sensitised only samples, the expression was reduced after FcεRI cross-linking. This can be observed in the graphs representing % of cells expressing SPHK1 (Figure 3.6.3.4 a and b), mean total fluorescence (Figure 3.6.3.5 a and b) and non- cytoplasmic fluorescence in the cell indicating a global reduction in SPHK1 levels (Figure 3.6.3.7 a and b). This was a potentially significant finding in view of the results obtained in the case of ES-62 where cross-linking of FcεRI led to the internalisation of PKC- α from the plasma membrane to the perinuclear region which prevented the sequential activation of PLD and SPHK. However, the results from the peripheral immunofluorescence and Max pixel data did not give a clear indication of the effect of SMAs on the translocation of SPHK1 from the cytoplasm to the plasma membrane. A general trend for down regulation of expression both at the non-cytoplasmic and cytoplasmic level could not be recognized with most of the SMAs. However, PC-BSA induced a decrease in non cytoplasmic fluorescence for both the sensitised and sensitised/cross-linked samples (Figure 3.6.3.7 a and b) although a small increase was noticed in mean total fluorescence for the sensitised only samples while no change was observed in the mean total fluorescence in the cell for the sensitised/cross-linked ones (Figure 3.6.3.5 a and b).

Figure 3.6.3.1 a-j

Representative images (40x magnification) of BMDC incubated with polyclonal anti-SPHK1. Anti-rabbit IgG was used as an isotype control for the measurement of non-specific staining and an Alexa488-labelled anti-rabbit IgG antibody was used to indirectly detect the binding of primary antibody by means of green fluorescent staining. The cells were also counterstained with DAPI (blue) to identify the cell nucleus. The cells were incubated with BSA (negative control), PC-BSA (positive control) and SMAs and sensitised with anti-DNP-IgE overnight. Images were captured using a connected Hamamatsu Orca ER digital camera and Openlab version 3.0.9 digital imaging program (Improvision).

a=BSA, b=PC-BSA, c= SMA 3, d= SMA 25, e= SMA 33, f= SMA 39, g= SMA 63, h= SMA 64 and i= SMA-65, j=Anti-SPHK isotype.

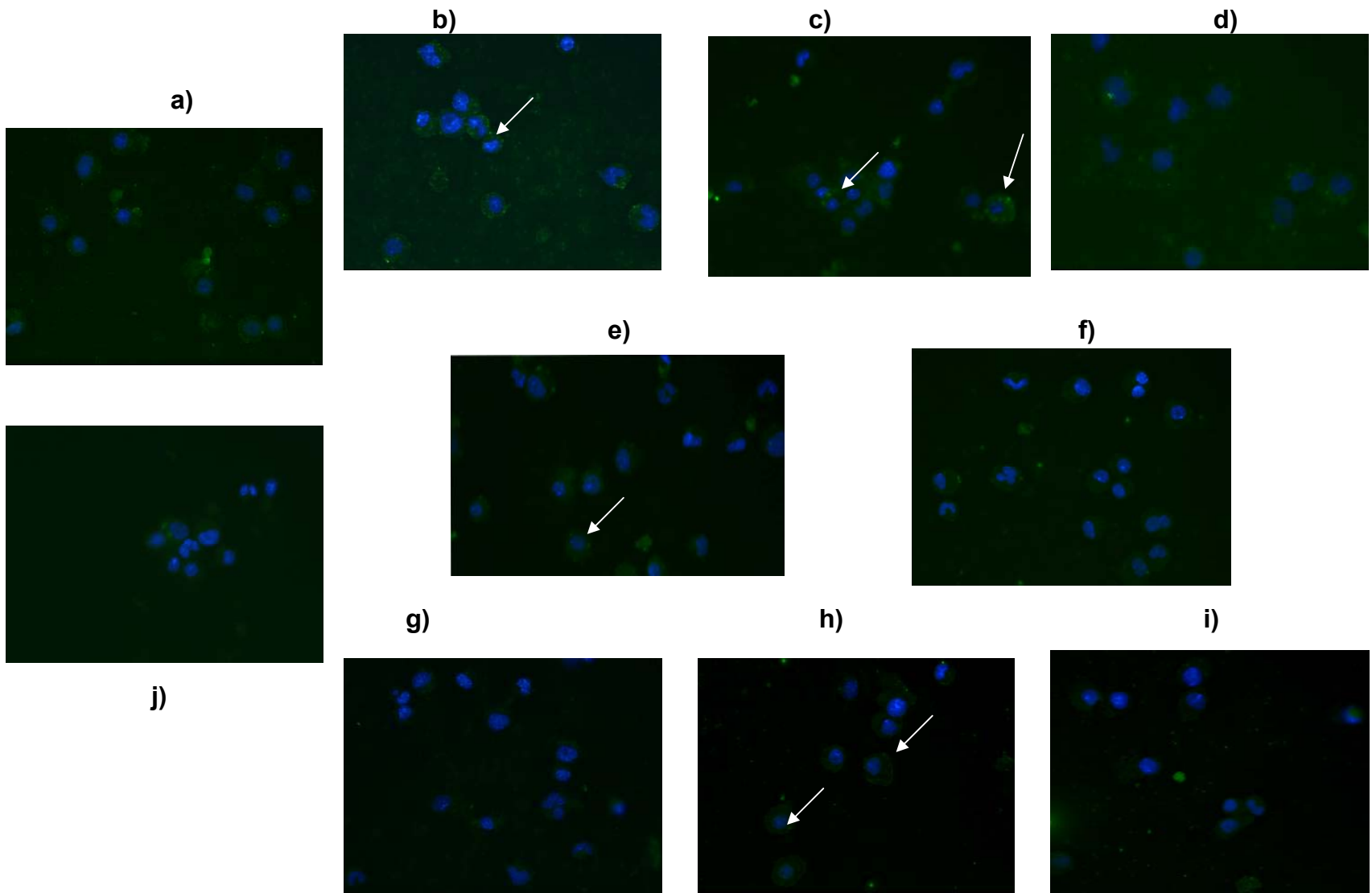


Figure 3.6.3.2 a-j

Representative images (40x magnification) of BMMC incubated with polyclonal anti-SPHK1. Anti-rabbit IgG was used as an isotype control for the measurement of non-specific staining and an Alexa488-labelled anti-rabbit IgG antibody was used to indirectly detect the binding of the primary antibody by means of green fluorescent staining. The cells were incubated with BSA (negative control), PC-BSA (positive control) and SMAs and sensitised with anti-DNP-IgE overnight and sensitised and cross-linked with DNP-HSA for 2 minutes. Images were captured using a connected Hamamatsu Orca ER digital camera and Openlab version 3.0.9 digital imaging program (Improvision).

a=BSA, b=PC-BSA, c= SMA 3, d= SMA 25, e= SMA 33, f= SMA 39, g= SMA 63, h= SMA 64 and i= SMA-65, j=Anti-SPHK isotype.

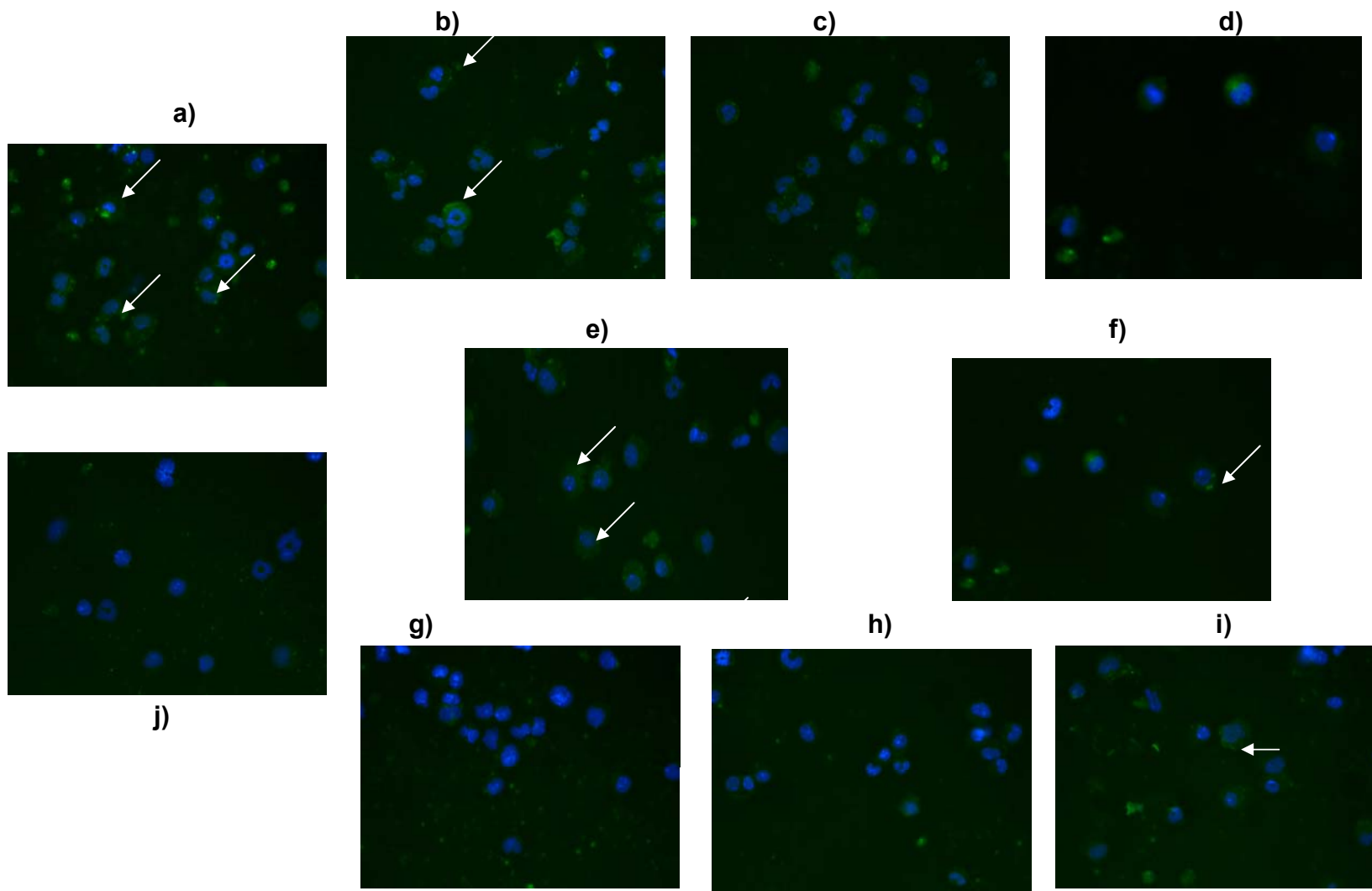


Figure 3.6.3.3 a-e

The figures represent the gating used for the quantitative analysis of immunofluorescence staining with polyclonal anti-SPHK1 of BMMC exposed to SMAs for sensitised and cross-linked samples. a) The gating depicts the cell population taken for analysis on the basis of threshold contours. This population is then analysed for SPHK1 expression relative to Isotype control (b) allowing calculation by Wincyte software of mean fluorescence integral (c) and mean peripheral fluorescence integral (d). Mean fluorescence integral relates to the level of staining throughout the whole cell whilst peripheral fluorescence depicts the value for the area between the nucleus and the cell membrane. By contrast, (e) max pixel fluorescence gives the value for highest intensity of fluorescence within the cell. The cells were incubated with BSA, PC-BSA or SMAs and sensitised with anti-DNP-IgE overnight and cross-linked with DNP-HSA for 2 minutes.

The data are the results of staining in one experiment.

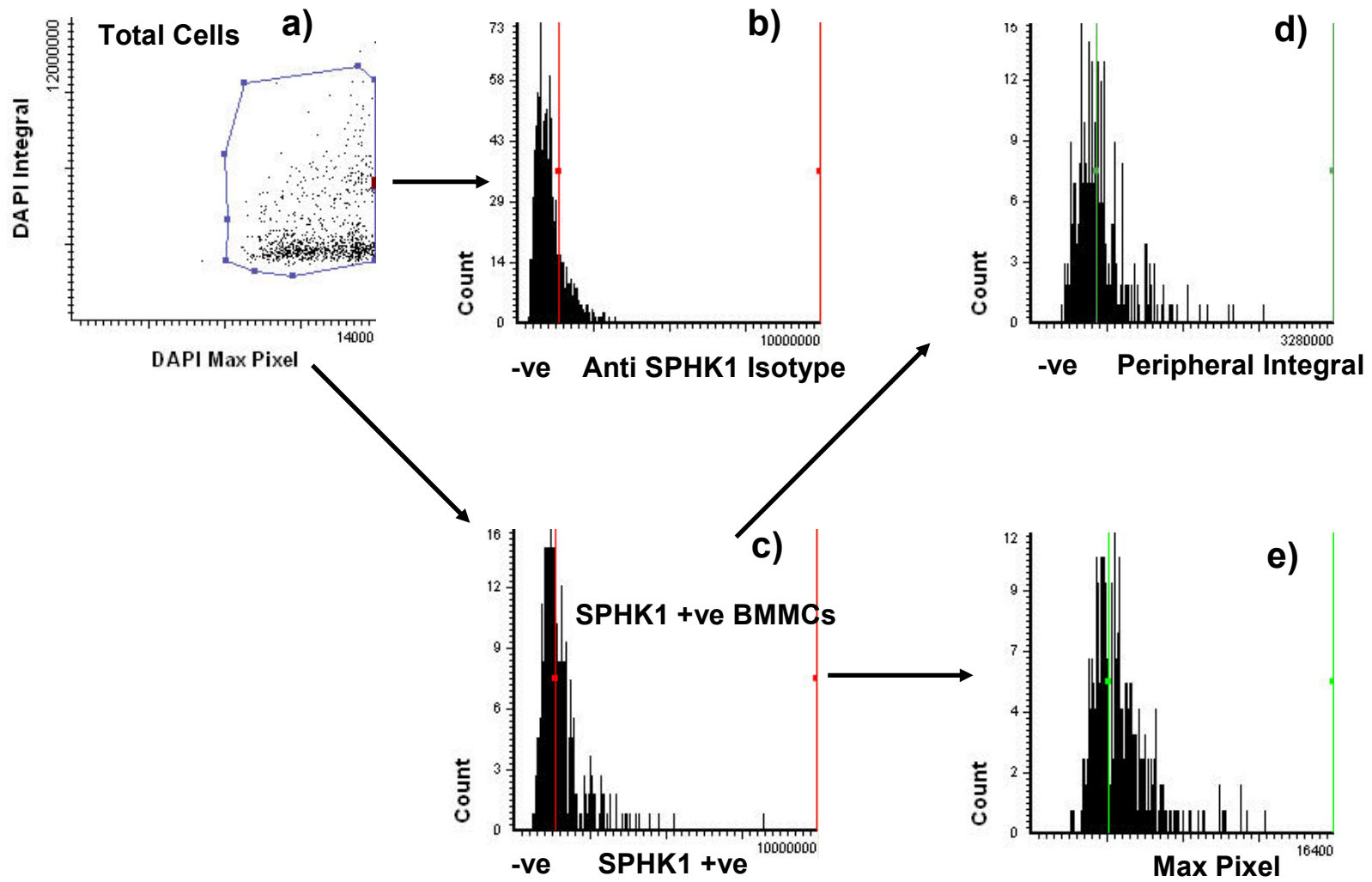
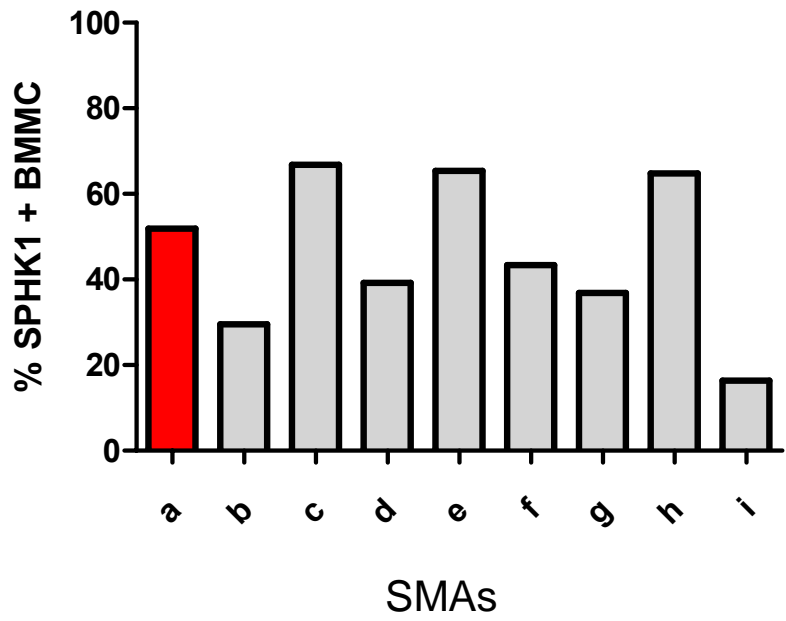


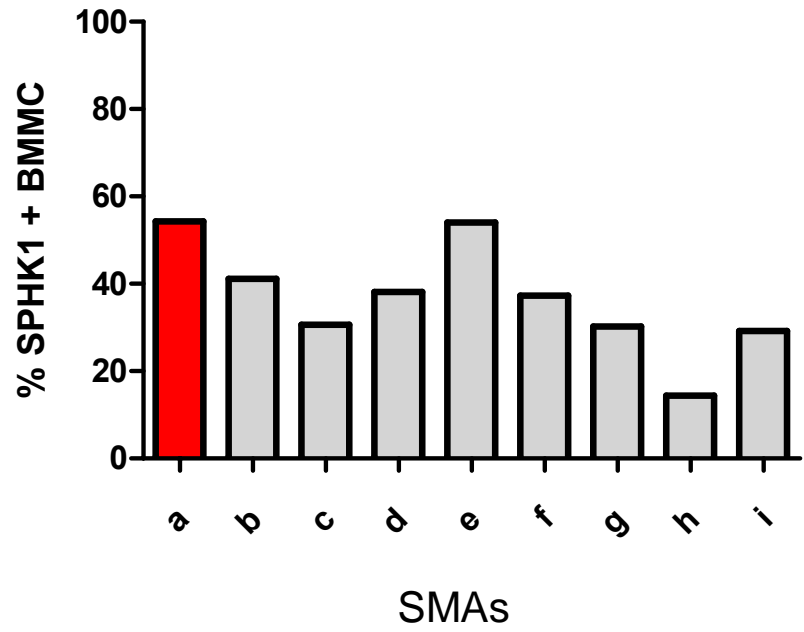
Figure 3.6.3.4 a and b

The figures represent the % of BMBC expressing detectable levels of SPHK1 relative to isotype control. The cells were incubated with BSA, PC-BSA and SMAs and anti-DNP-IgE overnight and then left for another 2 minutes (a) or cross-linked with DNP-HSA for 2 minutes (b). The quantitative analysis of immunofluorescence associated with binding of polyclonal anti-SPHK1 to BMBC for sensitised and cross-linked samples was performed using Wincyte software. The data are indicative of the results of more than 1×10^3 BMBC in each sample from one experiment.

a=BSA, b=PC-BSA, c= SMA 3, d= SMA 25, e= SMA 33, f= SMA 39, g= SMA 63,
h= SMA 64 and i= SMA 65



a)

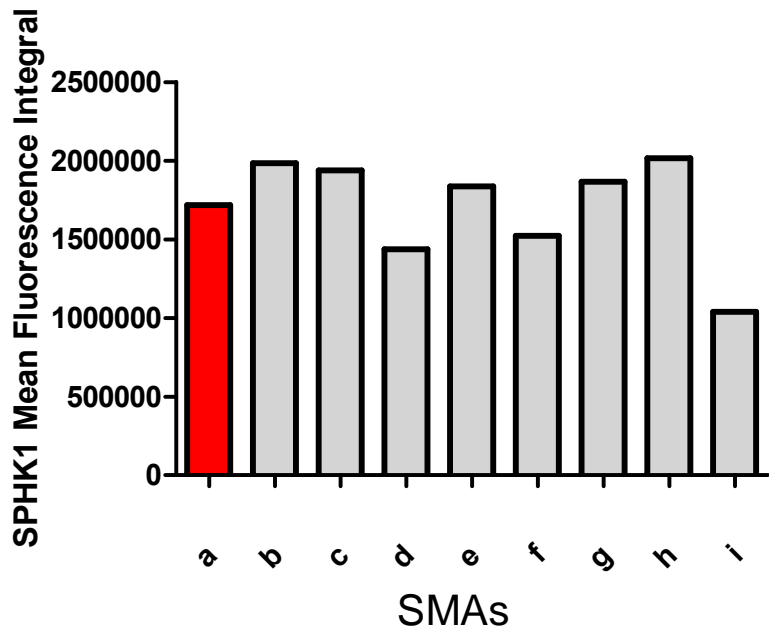


b)

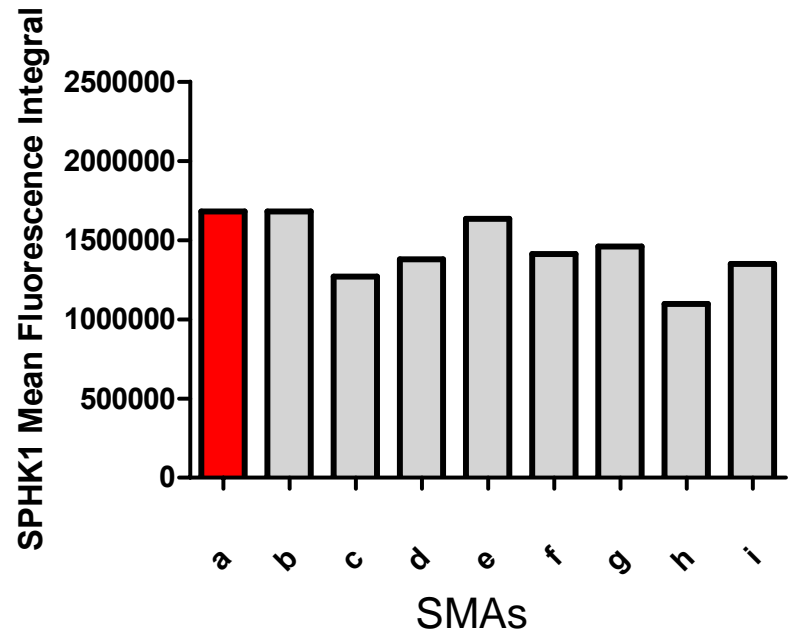
Figure 3.6.3.5 a and b

The figures represent the quantitative analysis of immunofluorescence staining associated with polyclonal anti-SPHK1 binding to BMMC for sensitised and sensitised/cross-linked samples after calculation of Mean Total fluorescence integral (Wincyte software) following gating of specific staining relative to the isotype control. Mean fluorescence integral relates to the level of staining throughout the whole cell. The cells were incubated with BSA, PC-BSA or SMAs and sensitised with anti-DNP-IgE and then left for a further 2 minutes (a) or cross-linked with DNP-HSA for 2 minutes (b). The data are the results of analysis of at least 1×10^3 cells.

a=BSA, b=PC-BSA, c= SMA 3, d= SMA 25, e= SMA 33, f= SMA 39, g= SMA 63,
h= SMA 64 and i= SMA 65



a)

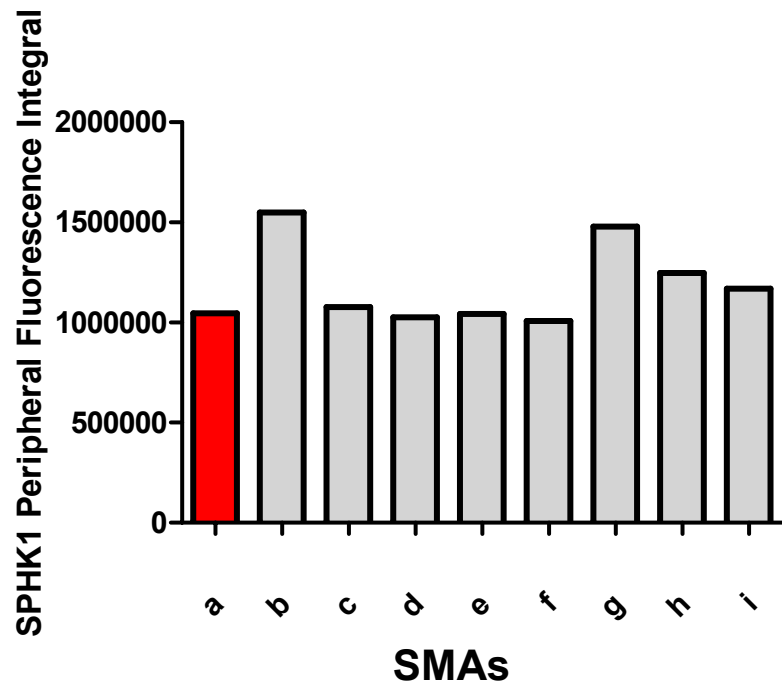


b)

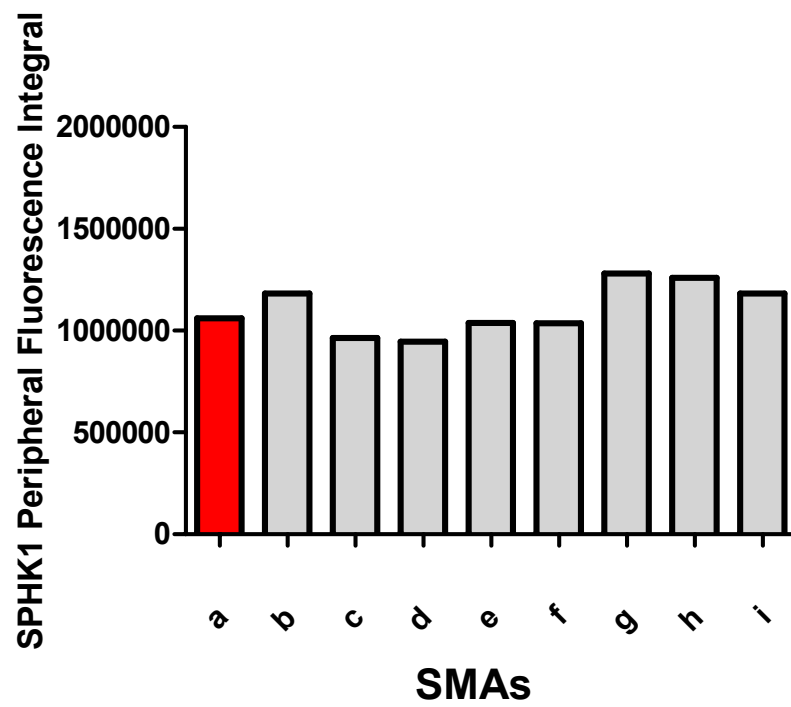
Figure 3.6.3.6 a and b

The figures represent the quantitative analysis of immunofluorescence staining associated with polyclonal anti-SPHK1 binding to BMMC for sensitised and sensitised/cross-linked samples after calculation of Peripheral Fluorescence integral (Wincyte software) following gating of specific staining relative to the isotype control. Peripheral Fluorescence integral depicts the value for the area between the nucleus and the cell membrane. The cells were incubated with BSA, PC-BSA or SMAs and sensitised with anti-DNP-IgE and then left for a further 2 minutes (a) or cross-linked with DNP-HSA for 2 minutes (b). The data are the results of analysis of at least 1×10^3 cells.

a=BSA, b=PC-BSA, c= SMA 3, d= SMA 25, e= SMA 33, f= SMA 39, g= SMA 63,
h= SMA 64 and i= SMA 65



a)

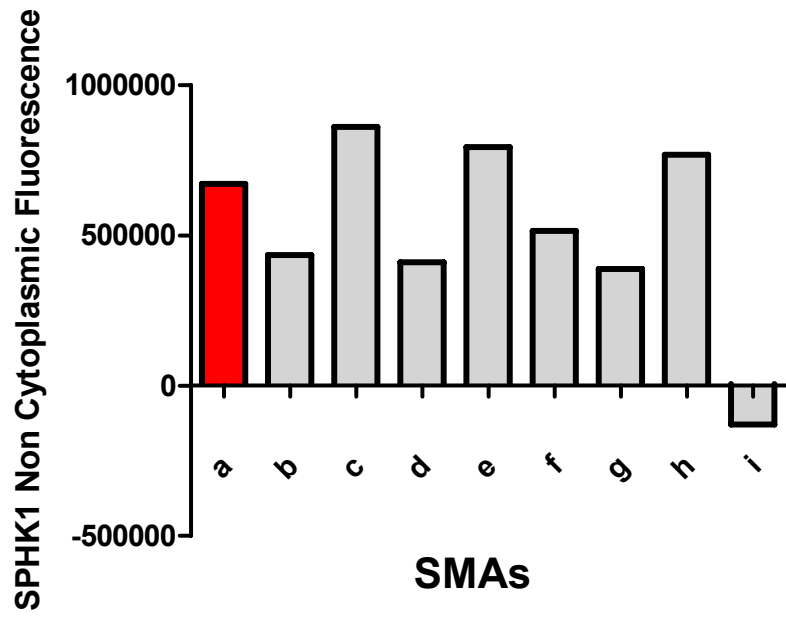


b)

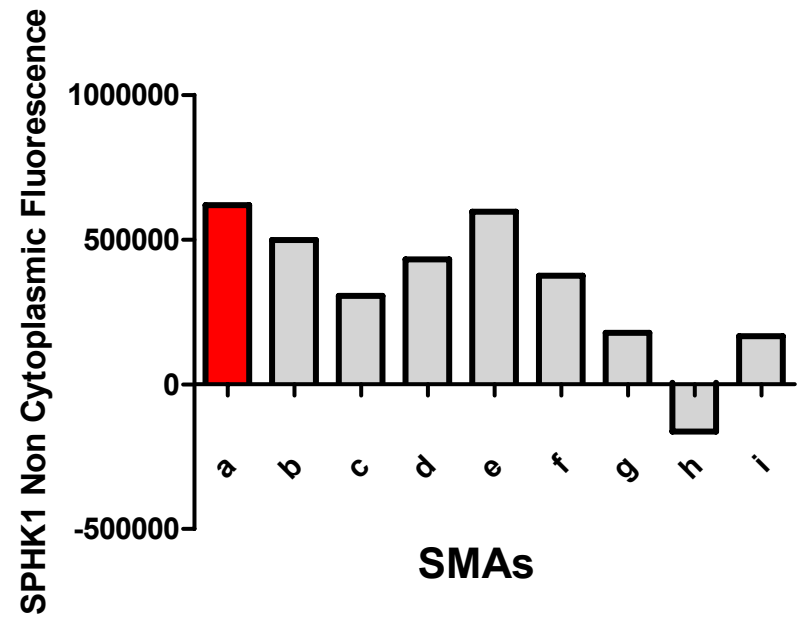
Figure 3.6.3.7 a and b

The figure represents the comparison of the quantitative analysis of immunofluorescence staining between the sensitised and sensitised/cross-linked samples associated with binding of anti-SPHK1 of BMMC. Nuclear (Non-cytoplasmic space) fluorescence was obtained by subtracting the Peripheral fluorescence values from the Total Fluorescence within the cell. The cells were incubated with BSA, PC-BSA or SMAs and sensitised with anti-DNP-IgE and then left for a further 2 minutes (a) or cross-linked with DNP-HSA for 2 minutes (b). The data are the results of analysis of at least 1×10^3 cells.

a=BSA, b=PC-BSA, c= SMA 3, d= SMA 25, e= SMA 33, f= SMA 39, g= SMA 63,
h= SMA 64 and i= SMA 65



a)

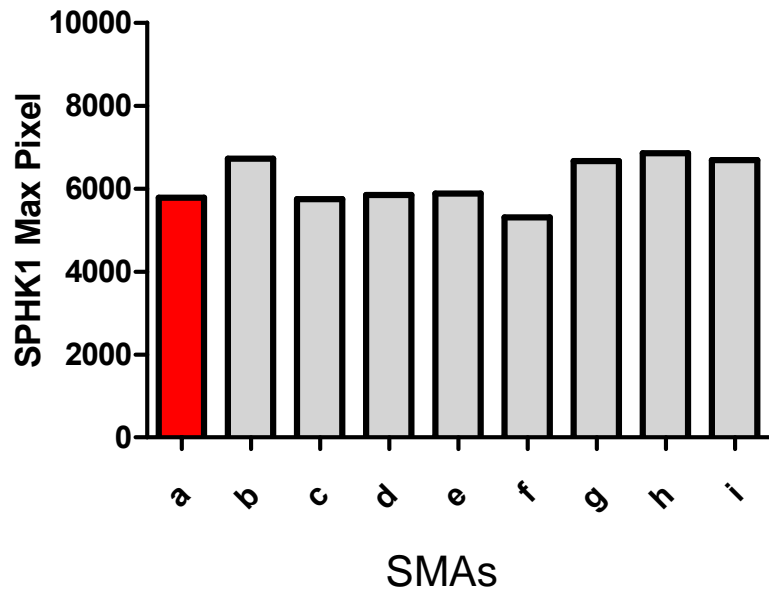


b)

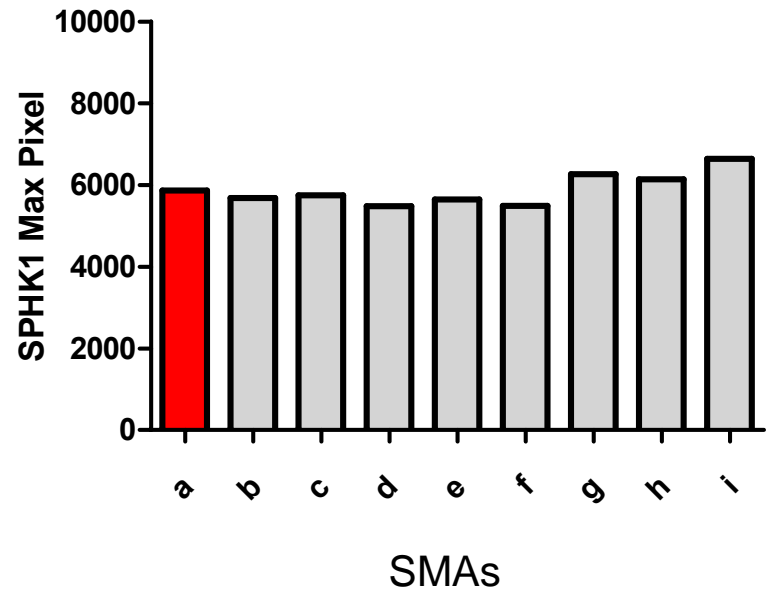
Figure 3.6.3.8 a and b

The figure represents the comparison of the quantitative analysis of immunofluorescence staining between the sensitised and sensitised/cross-linked samples associated with binding of polyclonal anti-SPHK1 of BMMC. Max pixel fluorescence gives the value for highest intensity of fluorescence within the cell. The cells were incubated with BSA, PC-BSA or SMAs and sensitised with anti-DNP-IgE and then left for a further 2 minutes (a) or cross-linked with DNP-HSA for 2 minutes (b). The data are the results of analysis of at least 1×10^3 cells.

a=BSA, b=PC-BSA, c= SMA 3, d= SMA 25, e= SMA 33, f= SMA 39, g= SMA 63,
h= SMA 64 and i= SMA 65



a)



b)

CHAPTER IV

DISCUSSION

4.1 Introduction

ES-62 has been highly effective both *in vitro* and *in vivo* as an anti-inflammatory, immunomodulatory molecule. As ES-62 is large and hence immunogenic, it would be difficult to consider it as a drug. However, the majority of the immunomodulatory properties of ES-62 have been attributed to its phosphorylcholine (PC) moieties. Therefore, it was decided to produce molecules based on the structure of PC to evaluate whether they possessed immuno-modulatory effects similar to the parent molecule. Hence, around 65 small molecule analogues (SMAs) were screened and assessed for their immunomodulatory potential. Degranulation analysis, measurement of calcium mobilisation, cytokine measurements and studies to observe the signaling molecules PKC- α , PLD1 and SPHK1 were conducted in BMMC or the RBL-2H3 mast cell line. The results revealed some interesting information and potential for the use of SMAs as therapeutic agents for the control of allergic and inflammatory disorders.

4.2 The Hygiene hypothesis and helminths as a link to immune modulation

The Hygiene hypothesis states that there has been an increase in autoimmune and allergic diseases like asthma, dermatitis, inflammatory bowel disease, multiple sclerosis and diabetes in the West [46-50], associated with an increase in hygiene and lack of infections. This hypothesis has been the foundation for my work relating to testing of SMAs based on the parasitic helminth molecule ES-62, for anti-allergy activity.

Various studies conducted in the past have supported the role of helminths in protection against allergies. van de Biggelaar and team noted an increase in allergic skin sensitivity after treatment of children chronically infected with *A.lumbricoides* and

T.trichiura [46], while Cooper *et al* observed that an active infection with geohelminths (*A.lumbricoides* or *Ancylostoma duodenale*) was protective against allergen skin test reactivity [47]. Similarly, Rodrigues and colleagues noticed that children who had heavy infections with *T.trichiura* in early childhood had a significantly low prevalence of allergen skin reactivity later in childhood even in the absence of *T. trichiura* infection at the time of skin testing [48]. Furthermore, it was seen that infections with *Ascaris lumbricoides* and *Necator americanus* offered protection against wheeze in young children in Ethiopia [49]. Also, infection with *Schistosoma mansoni* resulted in reduction in the severity of course of asthma in a rural group endemic for the infection [50]. Therefore, the hygiene hypothesis emphasises a role for worms in protection against allergic diseases.

4.2.1 Studies showing experimental use of worm therapy

The use of novel immunomodulatory mechanisms has already been tested in the treatment of autoimmune diseases. Summers *et al* in 2003 [242] conducted an experiment for treatment of Ulcerative colitis and Crohn's disease by the use of *Trichuris suis*, a porcine whipworm. In this experiment, 3 out of 4 patients entered remission, while clinical improvement was noted in all 4 patients. The same experiment was repeated in 2005 [243] where 29 patients of Crohn's disease were recruited with the required criteria including Crohn's disease activity index (CDAI) between 220 and 450. A decrease in CDAI of less than 150 out of 220 was labeled as a response in the Crohn's disease whereas a remission was defined as a decrease in CDAI of 100 or less out of 220. Dramatic results with a response rate of 80% and remission rate of 73% were reported in

24 out of the 29 patients, who continued with the treatment for 24 weeks with *T. suis* ova. In addition it was noted that the therapy was more effective in patients on immunosuppressive drugs and with intact ileum as it aided in the colonisation of the gut. Thus it was concluded that *T. suis* was well tolerated and was efficacious for the open labelled trial. This was an interesting finding as helminth therapy could be combined with the current medication to achieve longer and faster remissions for the disease. However, in the above experiments, infection with *T. suis* required repeated inoculation and there was concern regarding aberrant migration of the parasites. Croese *et al* proposed that such migration could be minimised by using *Necator americanus* larvae (L3) as an alternative to *T. suis*. It was suggested that as human beings are the natural hosts of *N. americanus*, this worm will follow its normal migration pattern thereby preventing aberrant migration and hypobiosis. Thus, *N. americanus* larvae from reservoir donors (healthy volunteers with established infections) were inoculated in patients with established Crohn's disease. It was observed that there were no detectable respiratory symptoms and no aberrant migration of the larvae. The improvement in the CDAI was observed after 20 weeks. Disease re-activation as indicated from CDAI was observed in 2 patients after the doses of long term immune suppressive drugs had been reduced. In summary, the team deduced that *N. americanus* may be used as an alternative treatment or as an adjunct to immune suppressive therapy for the treatment of Crohn's disease [244].

Furthermore in this regard, in 2006 Mortimer *et al* [245] conducted a dose ranging study to identify the number of hookworm larvae necessary to achieve a load of 50 eggs per g in human stool to enable therapeutic trials with respect to asthma. 10 healthy

subjects without asthma or airway hyperresponsiveness to inhaled methacholine were employed for the double blind study. They were administered with 10, 25, 50 or 100 *N. americanus* in a drop of water to the skin of the non-dominant arm. The subjects were studied for 12 weeks and the experiment was ended after the treatment of the subjects with anti-helminthic drugs. It was found that skin itching at the site of entry and gastrointestinal distress was common especially at higher doses, due to which one subject had to leave the trial due to very bad symptoms. In the 8 subjects that finally completed the study, it was concluded that infection with 10 *N. americanus* larvae was well tolerated and could be used for further clinical therapeutic trials.

As indicated in the studies mentioned above, helminths offer protection against various allergic and autoimmune diseases. Therefore, it would be logical to further explore this phenomenon in order to define the actual molecules involved in the immunomodulation. In accordance with this, some of the molecules generated by the helminths and their mechanisms of action are described in the following sections.

4.2.2 Helminth molecules with anti-allergy activity

4.2.2.1 PAS-1

It was discovered that a protein (PAS-1) secreted by *A.suum* decreased antibody production induced by another *A. suum* protein (APAS-3) and also reduced cytokine and chemokine release, cellular migration and airway hyperresponsiveness (AHR) in an IL-10 dependent manner in an APAS-3 induced asthma model [55]. On analysis of BAL fluid obtained from BALB/c mice, it was seen that total cellular infiltrate was significantly lower in PAS-1+APAS-3 sensitised mice when challenged with APAS-3 as

compared with APAS-3 sensitised and challenged animals. It was also observed that eosinophil peroxidase activity (EPO) in the BAL induced by APAS-3 challenge was again significantly lower in PAS-1+APAS-3 mice as compared with control animals. Furthermore, there was suppression of IgE and IgG1 antibodies in PAS-1+APAS-3 exposed mice while APAS-3 alone induced an increase in these antibodies. PAS-1 downregulated the production of Th2 cytokines (IL-4 and IL-5) in the APAS-3 group, when compared with the control groups. A decrease in the production of eotaxin and RANTES was also observed following the injection of PAS-1. However there was an increase in IL-10 in mice immunised and challenged with PAS-1+ APAS-3 in relation to the APAS-3 group and control groups that were just challenged with PAS-1+APAS-3. Methacholine-induced hyperreactivity was also reduced in mice immunised with PAS-1. In this study, the researchers suggested that the reduction in IL-4 and IL-5 and an increase in IL-10 contributed towards the immunosuppressive properties of PAS-1. They speculated that the production of high levels of IL-10 indicated that PAS-1 produced its effects through the generation of CD4⁺CD25⁺ regulatory T cells. In addition, the decrease in APAS-3-induced IgE and IgG1 antibodies was attributed to the reduction in IL-4, which along with IL-13, which is held responsible for the production of antigen specific IgE and IgG1 [211, 212].

4.2.2.2 Cystatin (Av-17)

A.vitae derived recombinant cystatin Av-17 was shown to inhibit ovalbumin (OVA) induced airway hypersensitivity and dextran sulphate sodium (DSS) induced colitis in BALB/c and C57BL/6 mouse models in an IL-10 dependent manner [246].

Intraperitoneal injection with Av-17 resulted in reduction of eosinophil infiltrate in the BAL fluid of the mice sensitised and challenged with OVA. This was further corroborated histologically where the lung tissue section revealed a decrease in the cellular infiltrate. The effect of cystatin on allergen-induced sensitisation and airway inflammation was accompanied by a significant reduction in the development of *in vivo* airway hyperreactivity (AHR) in treated mice, both in the preventive (during sensitisation) as well as in the pre-challenge (after sensitisation) models. Moreover, reduced levels of total IgE and OVA-specific IgE in response to Av-17 were also observed in the preventive model. The reduction was specific to IgE, as serum levels of OVA specific-IgG1 and IgG2a did not change significantly when compared with sensitised and challenged controls. The significant inhibition of IgE was also accompanied with reduced capacity of serum from OVA/cystatin-treated animals to induce degranulation of basophils. However, cystatin treatment in the pre-challenge model showed only minor reduction of total IgE, although OVA-IgE levels decreased significantly. Therefore, it was concluded from the above data that the immunomodulatory effect was caused by the action of cystatin on the recruitment of inflammatory cells and IgE production in the mouse models.

Further experiments revealed that BAL fluid of mice treated with OVA/cystatin contained less IL-4 as compared with animals treated with OVA only. The reduction in IL-4 was extended to the spleen cells of OVA/cystatin treated animals after allergen stimulation *in vitro*, when compared with control mice. Treatment with cystatin also reduced DSS induced colitis in C57BL/6 mice as shown by a decrease in erosions and cellular infiltrate in the colon. The researchers demonstrated in the BALB/c mouse

model of OVA-induced airway inflammation, that the modulation induced by cystatin Av-17 was dependent on macrophages. Depletion of macrophages (using clodronate containing liposomes) in cystatin-treated animals led to an increase in total cell numbers and eosinophils in the BAL fluid, similar to the level found in the OVA-sensitised and challenged control group. The treatment also partially restored the production of total IgE and OVA-specific IgE in OVA/cystatin treated mice with no change in IL-4 production. AHR in macrophage-depleted, OVA/cystatin-treated mice increased significantly. These results indicated that macrophages facilitated the immunomodulatory effects of cystatin via inhibition of airway inflammation, airway hyperreactivity, and IgE production.

It was further revealed that there was a significant increase in T regulatory (Treg) cells in OVA/cystatin treated animals as compared with OVA-sensitised and challenged controls. The OVA-sensitised animals were treated with anti-CD25 Abs to analyse the nature of the immunomodulation induced by cystatin. The depletion of Treg cells led to restoration of the total cell levels and eosinophils in cystatin-treated mice with an increase in total IgE and OVA-specific IgE. No such change was observed in the cystatin-treated animals in which the Treg cells had not been depleted. In addition, no change was observed in the allergen-specific IL-4 and AHR in cystatin-treated mice with depleted Treg cells. This finding signified a partial role of CD4⁺CD25⁺ regulatory T cells as depletion of these cells resulted in an increase in the levels of total IgE, OVA-specific IgE and eosinophils, while no change was observed in the levels of IL-4 and AHR. Blocking of the IL-10R in OVA/cystatin-treated animals completely restored total cell numbers in BAL fluid as observed in sensitised and challenged positive control

(OVA/cystatin/anti-IL10R treated) animals. The effect was most pronounced for the eosinophilic airway infiltration. Likewise, the development of AHR and the production of OVA-specific IgE were increased to the levels observed in OVA-sensitised and OVA-challenged control mice. Again, the inhibition of allergen-specific IL-4 production in OVA/cystatin-treated animals was not altered after application of anti-IL-10R Abs. These data indicated that IL-10 was the key cytokine in filarial cystatin-induced modulation of allergic disease, although IL-4 suppression was independent of IL-10. Cystatin-treated animals showed significantly increased levels of IL-10 in the spleen in comparison to OVA-treated animals. However, after depletion of macrophages, IL-10 production was significantly decreased in the OVA/cystatin-treated animals, whereas such an effect was not observed in the animals depleted of Treg cells. Therefore, these data indicated the impact of macrophages in the cystatin-induced modulation of allergic airway inflammation and hyperreactivity.

4.2.2.3 DiAg

The purified *Dirofilaria immitis*-derived antigen (DiAg) is an excretory-secretory protein with a molecular weight of 15kDa obtained from the dog parasite *Dirofilaria immitis*. It is an IgE inducing factor and was found to be considerably stable to various proteases, to periodate digestion and to physiochemical treatment. Experiments in the non-obese diabetic (NOD) mouse demonstrated that injection of recombinant DiAg (rDiAg) prevented the spontaneous development of anti-insulin antibodies, an indicator of overt diabetes. rDiAg was found to impair islet antigen specific Th1 response *in vivo*. The prevention of diabetes was associated with skewing of the Th1 response towards a Th2

profile. In addition, rDiAg prevented relapses in a model of EAE [247]. Experiments in BALB/c mice revealed that rDiAg administered by osmotic mini pumps led to an increase in the level of total and non-specific IgE, while there was no increase in the levels of rDiAg-specific IgE. In addition, IL-4 and IL-10 cytokine levels were increased in the serum of the exposed animals. In contrast, there was a decrease in the levels of IFN- γ . rDiAg induced proliferation of spleen cells, which were later confirmed to be B cells, from naïve BALB/c mice in a dose dependent manner. mRNA expression of CD23 (a marker of B cell differentiation) was up-regulated on stimulation with rDiAg. Moreover, the expression of CD23 was cumulatively increased in the presence of both IL-4 and rDiAg. Culturing of naïve B cells with rDiAg and IL-4 induced significant up-regulation of IgE production in splenic B cells, which suggested a role for rDiAg as a co-stimulatory molecule in IgE class switching.

In previous experiments by Imai *et al*, it had been concluded that DiAg was an agonist of human CD40 [248]. Later experiments revealed that rDiAg directly stimulated a human immune cell line, THP-1 cells, and induced proinflammatory cytokine production. There was induction of IL-12 and TNF- α on stimulation of THP-1 cells with either rDiAg or recombinant human soluble CD40L (rsCD40L), which demonstrated that human antigen presenting cells (APC) showed similar responses to CD40L and rDiAg. Also, the production of IL-12 was inhibited by addition of recombinant human soluble CD40 (rsCD40). In addition, rsCD40L competitively inhibited rDiAg binding to the membrane of these cells. Moreover, rDiAg was not effective in CD40-deficient mice [249]. In addition, the experimental results showed that polyclonal IgE induction by DiAg was also affected in CD40-deficient mice. To this end,

wild-type and CD40-deficient mice were infused with rDiAg or OVA as controls. Total IgE levels in wild-type mice were increased with rDiAg, with a further increase in specific IgE levels after OVA administration. In contrast, total IgE production in CD40-deficient mice was completely absent. The mesenteric lymph node B cells purified from CD40-deficient mice and wild-type mice were stimulated with rDiAg. The cells from wild-type mice revealed enhanced proliferation with rDiAg as compared with CD40-deficient mice. Altogether these results revealed that DiAg stimulated polyclonal IgE production in a CD40 dependent manner [248]. It was also determined that rDiAg stimulated the production of IL-10 in both splenic B cells and peritoneal B cells. In addition, IgE production by splenic B cells activated in the presence of rDiAg-IL-4 was enhanced synergistically in the presence of peritoneal B cells. Almost 50% reduction in the production of IgE by B cells stimulated with rDiAg-IL4 was noticed in the presence of anti-IL10 mAb [250].

In the rat model of passive cutaneous inflammation (PCA), rDiAg suppressed PCA reactions induced by IgE anti-dinitrophenol (DNP) antibodies. The number and viability as well as the histamine content of peritoneal mast cells were similar in the rDiAg group and the control animals. IL-10 content of the plasma, ascitic fluid and supernatant obtained from the spleen cells was markedly increased in rDiAg infused animals. The data further revealed that mRNA expression of the β -subunit of Fc ϵ RI was upregulated in peritoneal mast cells from the rats infused with rDiAg. The results overall indicated that the rDiAg facilitated the production of non-specific IgE and IL-10 that offered protection against unrelated allergies.

4.2.2.4 sm-CKBP

The chemokine binding protein obtained from *S.mansoni* egg secretions (sm-CKBP) was found to inhibit the binding of CXCL8 (IL-8), cc-chemokine ligand 3 (CCL3), CX₃C-chemokine ligand 1(CX₃CL1), CCL2 (MCP1) and CCL5 to their receptors on U937 cells, which constitute a human leukaemic monocyte lymphoma cell line. Purified recombinant sm-CKBP (r-smCKBP), used in a chemotaxis assay, blocked the migration of human neutrophils initiated by CXCL8. Furthermore, it was discovered, that CCL5-induced calcium mobilisation in PBMC was blocked in a dose dependent manner by the helminth product. In the *in vitro* murine air pouch model of inflammation, an injection of r-smCKBP significantly reduced inflammation induced by CXCL8-induced neutrophil infiltration. In a contact hypersensitivity model, hapten-sensitised mice treated with r-smCKBP had notable reduction in ear swelling after the challenge. The extent of inhibition of inflammation was evident on examination of cross sections of ears from r-smCKBP-treated mice. Isolation of the inflammatory infiltrate from the ears of hapten-treated mice showed that r-smCKBP-treated mice were devoid of the marked neutrophilia observed in cells isolated from the ears of the control mice. In the *in vivo* models, intravenous injection of r-smCKBP completely abrogated all the CXCL8 induced pulmonary inflammation in the mouse models as well as improved lung function [251]. As diseases such as asthma and allergies are associated with over activation of chemokines, this molecule exhibits possible therapeutic potential.

4.2.2.5 ES-62

It was revealed by McInnes *et al* that ES-62 reduced the severity of CIA (collagen induced arthritis) in DBA/1 mice. This was correlated with reduction in collagen-specific IFN- γ , TNF- α and IL-6 and increase in IL-10 produced *ex vivo* by draining lymph node cells from the mice receiving ES-62. Significant reduction in the disease progression was evident as reduction in inflammation in synovium in animals given ES-62 [252]. Also, with respect to allergy, ES-62 substantially inhibited Fc ϵ RI-triggered generation of TNF- α and interleukin IL-6 and IL-3 by human mast cells. ES-62 inhibited the initial peak of Ca²⁺ mobilisation triggered by Fc ϵ RI, although it did not affect the delayed, more sustained response. Pre-treatment of cells with ES-62 inhibited Fc ϵ RI -coupled PLD and SPHK activities, whereas PLC- γ 1 translocation and inositol trisphosphate generation proceeded as normal. Also, using barometric plethysmography to measure airway hyperresponsiveness induced by methacholine in an animal model of asthma, it was discovered that there was considerable reduction with ES-62 treatment. Furthermore, on sensitising and challenging with OVA in an AHR mouse model, it was clearly demonstrated that ES-62 reduced the levels of IL-4 and eosinophils in the BAL fluid. In addition, an ES-62-mediated protective effect was noted in a model of allergic skin hypersensitivity in which mice were sensitised and challenged with oxazolone. Namely, treatment with ES-62 resulted in reduction of ear swelling via direct inhibition of mast cell dependent hypersensitivity. In particular, mast cells obtained from the ears of these sensitised and challenged animals degranulated *ex vivo* in response to Fc ϵ RI-cross-linking but this was reduced by ES-62 and this also correlated with reduction in production of TNF- α , IL-3 and IL-6 [155].

The PC moiety of PC has been shown to be responsible for its immunomodulatory activities including protection against CIA [210]. For this reason SMAs based on PC were produced for investigation of anti-inflammatory potential, with reference to asthma in this particular study.

Table 4.0 represents a summary of the mechanisms of action and therapeutic effects of the various immuno-modulators excreted-secreted by helminths described above.

Species	Component	Mechanism of action	Effect	Ref
<i>A.suum</i>	200 kDa PAS-1	Increase in IL-10	Suppression of cellular migration and eosinophil peroxidase activity with reduction in the levels of IL-4, IL-5, eotaxin and RANTES in the BAL fluid	108
<i>A.vitae</i>	Recombinant filarial cystatin (Av17)	IL-10 production by macrophages	Reduction in airway inflammation and hyperreactivity, Reduction in allergy specific IgE and decrease in basophil degranulation, ↓ IL-4. Decrease in DSS induced colitis	245
	ES-62	Inhibition of B2 B cell proliferation and induction of B1 B cell dependent IL-10 secretion; TLR4 dependent activation of macrophages and dendritic cells promoting Th2 type anti-inflammatory responses, TLR4 dependent inhibition of mast cell degranulation and inflammatory mediator production	Reduced Collagen induced arthritis, Decrease in AHR in methacholine induced asthma, ↓ IL-4 and eosinophilia in OVA challenged AHR mouse model, Protection in oxazolone induced hypersensitivity	264 156
<i>D.immitis</i>	<i>Dirofilaria immitis</i> -derived antigen (DiAg)	CD40 dependent polyclonal IgE production	Prevention of diabetes, EAE, passive cutaneous inflammation	246 249
<i>S.mansoni</i>	<i>S.mansoni</i> chemokine binding protein (sm-CKBP)	Chemokine binding protein that binds to and inhibits the binding of CXCL8, CCL3, CX3CL1, MCP1 and CCL5.	Reduction in hypersensitivity, inhibition of neutrophil migration, Reduced CXCL8 induced pulmonary inflammation	250

Table 4.0 Mechanisms of action and therapeutic effects of various immunomodulators excreted-secreted by helminths.

4.3 Reasons for disparity in mouse BMMC degranulation as compared with human mast cells

From the data obtained from my degranulation experiments on mouse BMMC, it was noticed that there was less degranulation (measured by β -hexosaminidase release) when compared to the experiments by Melendez *et al* [155] conducted on human BMMC. This meant that it was not possible to undertake degranulation experiments with mouse BMMC.

This disparity in results was attributed to the following reasons: Electron-microscopic studies have revealed that the ultra-structure of mouse BMMC consisted mainly of cytoplasmic granules that are immature as compared to murine peritoneal mast cells or human mast cells [253, 254]. Gene-expression studies have shown that in both resting and cells activated by Fc ϵ RI aggregation, only some of the genes that are expressed correspond in murine and human mast cells [206]. For instance, human mucosal mast cells and murine mast cells obtained from bone marrow differ in their ability to produce IL-4, IL-5 and TNF- α . Gene-expression and mutation studies also indicated that the cultures of murine mast cells expressed considerable monocytic features [154]. Conversely, murine mast cells have some functional properties in common with human basophils, whereas human mast cells seemed to form a separate cell type lacking a full equivalent in rodents. For instance, some murine mast-cell populations and human basophils responded well to IL-3, whereas human mast cells either lacked the IL-3 receptor or hardly responded to IL-3 [207, 255-257]. This was true not only for cell development but also for the regulation of mature mast cells by cytokines [257]. Trypsases and chymases contribute to inflammation and tissue remodelling through the selective proteolysis of matrix proteins and the activation of protease-activated receptors and matrix metalloproteinases [222, 258-260]. It has been found that in murine mast cells, there is a large number of chymases that have

distinct and narrow proteolytic specificities [222]. However in humans, several tryptases with different specificities have been characterised, but only a single chymase [258, 259]. Human pulmonary and intestinal mast cells express chymase at lower levels than tryptases, whereas murine mucosal mast cells express mucosa-specific chymases [222]. Therefore, the results from the human mast cell studies might not be comparable with the murine system in certain aspects.

4.3.1 Effects of SMAs on calcium mobilisation in BMDC

In the study conducted by Melendez and Khaw (2002) [156], the role of SPHK1 was demonstrated in triggering Ca^{2+} release from intracellular stores on cross-linking Fc ϵ RI in human mast cells. They showed that the Fc ϵ RI coupling to PLD1 resulted in the activation of SPHK-1. This was verified by means of an anti-sense oligonucleotide to PLD1 that blocked both of Fc ϵ RI-triggered PLD and SPHK1 activity. In addition it was noticed that the anti-sense oligonucleotide to SPHK1 blocked Fc ϵ RI-triggered SPHK1 activity but had no effect on PLD1 activity. This demonstrated that SPHK1 was downstream of PLD1 activity. Their team also demonstrated that the anti-sense oligonucleotide to SPHK1 considerably down-regulated the initial rise in Ca^{2+} release from intracellular stores; however, extracellular Ca^{2+} entry was unaffected. Conversely, with pre-treatment with anti-sense oligonucleotide to PLC- γ , the initial rise in Ca^{2+} was unaffected, but calcium entry was reduced. Furthermore, pre-treatment with anti-sense oligonucleotides to both (SPHK1 and PLC- γ) completely blocked the Ca^{2+} response triggered by Fc ϵ RI. In our experiments, the effects of SMAs were analysed on BMDC. It was discovered that SMA 1 demonstrated stimulation of peak intracellular (SPHK-mediated) calcium mobilisation as well as a slight increase in secondary influx dependant on PLC- γ . Similarly, SMA 6 showed clear stimulation of peak intracellular (SPHK-mediated)

calcium mobilisation. There was also stimulation of peak intracellular calcium mobilisation and an increase in the secondary influx in the case of SMA 27. Therefore it can be hypothesised that some of the SMAs stimulated FcεRI triggered release of Ca²⁺ in BMMC. These findings could not be correlated with the expression of the signaling molecules because as discussed later most of the SMAs in signaling experiments caused a generalised inhibition of the expression. Conversely, it was discovered that similar to ES-62, some SMAs inhibited SPHK-dependent Ca²⁺ mobilisation. For example, pre-incubation with SMA 3 demonstrated inhibition of peak intracellular calcium mobilisation. Furthermore, both SMAs 25 and 64 indicated clear inhibition of peak intracellular (SPHK) calcium mobilisation. It was also noted that there was inhibition of the secondary Ca²⁺ influx in the case of SMAs 3, 25 and 64. This inhibition of secondary influx could have some therapeutic implications additional to those associated with the initial influx as it is also responsible for the release of *de novo* mediators from the mast cells following entry of extracellular calcium into the cell [156, 261].

4.3.2 Effects of SMAs on degranulation of RBL-2H3 cells

In RBL-2H3 cells, cross-linking of the IgE-bound FcεRI receptor results in activation of these cells and initiates a biochemical cascade leading to their degranulation and mediator release [192, 262]. On utilising the RBL-2H3 cell line it was discovered that SMAs 63 and 64, reduced degranulation as measured by β-hexosaminidase release. However, in the set of experiments with the rest of the selected SMAs 1, 3, 4, 6, 9, 25, 27, 28, 33, 35 and 52, no significant change in degranulation was observed. It was noticed that inhibitory molecules, SMAs 63 and 64 are very similar in structure which might be a factor in explaining their inhibitory effects (Table 3.1.2).

4.3.3 Effects of SMAs on levels of IL-6 and TNF- α in BMMC

Previous studies with mast cells have demonstrated that there is formation and release of various cytokines including IL-3, IL-4, IL-5, IL-6, IL-10, IL-13, GM-CSF and TNF- α , on the activation of Fc ϵ RI [211-224]. In recent experiments by Pushparaj *et al* [263] using BMMC, it was revealed that Fc ϵ RI triggered the synthesis and release of cytokines including IL-1 β , IL-3, IL-6 and TNF- α . On analysing the effects of SMAs on the production of the pro-inflammatory cytokines IL-6 and TNF- α by BMMC, it was observed that SMAs 3, 27, 28, 35, 39, 51 induced an increase in the production of IL-6 when stimulated both by antigen and ionomycin/PMA. Furthermore, there was a decrease in IL-6 with SMAs 63 and 64. Turning to the release of TNF- α , this was increased in the presence of SMAs 3 and 39. However a decrease was observed in the presence of SMAs 63 and 64. In addition to being generated in mast cells these two cytokines can potentiate inflammatory immune responses through the generation of other inflammatory mediators [264]. Therefore, medications inducing abrogation of these pro-inflammatory cytokines would provide alleviation from allergic and inflammatory disorders such as asthma.

4.3.4 Effects of SMAs on the expression and activation of PKC- α , PLD1 and SPHK1

With regards to the signaling experiments, it can be seen from the data that SMAs 39, 63 and 64 not only induced down-regulation of expression of PKC- α in the sensitised samples, but also led to a degradation and decrease in translocation of PKC- α by causing desensitisation of its activation on cross-linking of cells with the antigen (DNP-HSA). The effects with SMA 64 are the most profound overall with a trend for down regulation of expression and desensitisation of activation also evident from the data showing reduction in % of cells expressing PLD1. Also, the % of cells

expressing SPHK1 was reduced following exposure to SMAs 39, 63, 64 and 65 and this was again more significant in the case of SMA 64 where although the expression is increased in the sensitised only samples, the expression was reduced after FcεRI cross-linking. This result was very similar to the down-modulation induced by ES-62 where by sequestering and degradation of PKC-α, ES-62 inhibited further activation of PLD and SPHK in the human mast cells [155].

Collectively, (Table 4.1) these data suggest that SMAs 63 and 64 may inhibit calcium mobilisation and subsequent mast cell degranulation and cytokine production by uncoupling FcεRI from the PLD/SPHK axis by down-regulating PKC-α, presumably by a manner analogous to that observed with ES-62 (Figure 4.1). SMA 65 however, did not fit the pattern seen with SMAs 63 and 64. This was evident from the fact that although it induced similar effects in reducing degranulation and decreasing the expression of SPHK1, in the BMMC stimulated with antigen and ionomycin/PMA, SMA 65 stimulated calcium mobilisation while the led to equivocal results with respect to IL-6 and TNF-α. Without a more detailed examination of the signaling modulation associated with SMA 65, the reason for this must remain unclear.

Similar to the earlier results, where ES-62 not only down-regulated PKC-α expression but also inhibited BCR-mediated PKC-α translocation to the nucleus in B cells and influenced down modulation of PKC-α in human mast cells [135, 155], SMAs down-modulated the expression of signaling molecules especially globally in the case PKC-α. Moreover, an inhibition in the *de novo* production of proinflammatory cytokines was obtained on the treatment of BMMC with the SMAs. In the light of these findings, it's tempting to assume that SMAs (particularly SMAs 63 and 64) might be manipulating the signaling molecular cascade of PKC-α, PLD1 and SPHK1, by a mechanism very similar to ES-62, to inhibit mast cell activation.

These data now need to be expanded by for example confocal co-localisation studies to elucidate the trafficking pathways of the SMAs and their movement inside the mast cell. A key experiment that should be undertaken at the outset would be to determine if the SMAs have ES-62's requirement for TLR4 and if so, whether interaction results in subsequent internalization (Figure 4.1).

4.4 Categorising of SMAs into inhibitory and stimulatory molecules

On investigating the effects of SMAs on translocation and expression of PKC- α , PLD1 and SPHK1, an overall picture started to emerge about the effects of these SMAs based on their structures.

Based on the above experiments, it could be seen that the molecules could be divided depending upon their stimulatory effects and inhibitory effects (Table 4.2). On observing the structure of the stimulatory molecules, a common pattern was observed, as with the inhibitory SMAs. It was noticed that compounds 63 and 64, that induced inhibitory effects were very similar in structure. Both compounds were sulphones and had the sulphone group attached through a methylene group to the benzene ring. Furthermore, SMA 64 was the closest in structure to the choline molecule. On the other hand, in the case of the stimulatory compounds such as SMA 25, 33 and 35, the methylene groups were attached through the nitrogen atom to the benzene ring. Another significant fact that emerged was that although there was a wide range in the molecular weight (MW) of the compounds, it did not seem to affect their modulatory function. This can be seen from the molecular weights of SMAs 63 (MW 306.2) and 64 (MW 368.3) considered to be inhibitory and SMAs 3 (MW 260.3), 25 (MW 347.3), 33 (MW 302.4) and 35 (MW 260.3) considered as stimulatory in nature. Further experiments need to be done to determine whether molecular weight influenced uptake of the SMAs. In addition, a related key

experiment would be to see whether internalisation is necessary for activity (Figure 4.1). However, the common factor noted with the structure of stimulatory SMAs 25, 33 and 35 was the presence of a morpholine or pyrrolidine moiety. SMA 65 that was somewhat stimulatory in character has a dimethylamine moiety in its structure. SMA 39 was again different when compared with other SMAs, as it could not be classified into definite stimulatory and inhibitory categories of molecules. It had only induced an inhibitory effect in signaling experiments where the quantitative analysis showed a decrease in total immunofluorescence when compared with the BSA control. SMA 39 had a sulphonamide group attached to the benzene ring directly through the nitrogen atom, which was unlike other inhibitory SMAs where a sulphonamide group was attached indirectly through the methylene group to the benzene ring. SMA 3, which expressed stimulatory properties more consistently than the other molecules, was dissimilar in structure to the other stimulatory compounds. This compound has two variations: first; a sulphonamide group attached through the sulphur atom to the methylene group which in turn is attached to the benzene ring; and the second variation is that this molecule belongs to the dimethylamine category (Table 3.1.2).

4.4.1 Therapeutic implications of the use of SMAs as immuno-modulatory drugs

Due to the various ethical and medical problems generated by the use of live worms, the molecules generated from the helminths offer a forward alternative approach as treatment for allergic (and autoimmune) diseases. However, due to inherent immunogenicity and problems associated with acquisition or production of these molecules, SMAs offer an attractive alternative. Some of these reagents show immense potential by inhibiting degranulation, calcium mobilisation and signaling events, which can be taken further for testing. SMAs generated on the basis of helminth products seem more palliative than actual worm ingestion, while the current

medications such as corticosteroids have significant side effects such as oral thrush, osteoporosis, weight gain, diabetes, hypertension, vulnerability to infection, cataracts and glaucoma and thinning of skin.

Encouraging results were shown by SMAs 63 and 64 as reflected in the degranulation assays and calcium mobilisation studies, where a notable decrease was induced by these molecules. The above results were later confirmed in the signaling experiments where SMAs 63 and 64 not only induced down-regulation of expression of PKC- α in the sensitised samples, but also led to a global degradation and possibly a decrease in the translocation of PKC- α in the cross-linked samples as well. These molecules also reduced the % of cells expressing PLD1 and SPHK1. As we know that cross-linking of Fc ϵ RI leads to the sequential activation of PKC- α , PLD1 and SPHK1 which further leads to increases in calcium mobilisation and degranulation, reduction and inhibition of the expression of the signaling molecules would be expected to cause a decrease in both calcium mobilisation and degranulation.

To take these molecules further with respect to investigating therapeutic potential, degranulation and calcium mobilisation assays on human derived mast cells should be performed. Such a study would offer interesting insight into the effects of SMAs, as the previous study showing effects of ES-62 in human mast cells perhaps revealed a more consistent and potent inhibition by ES-62 on human mast cells [155]. Also, it would be the next logical step to translate the studies from the animal system to the human system. Analysis of the generation of various cytokines in response to SMAs in the above experiments should also be attempted. The effects of SMAs on various other isoforms of PKC, PLD and SPHK, need to be further explored. As shown formerly, ES-62 modulated BCR signaling through the down regulation of PKC isoforms α , β , ζ , δ and ι/λ and up-regulation of PKC- γ and PKC- ϵ in murine splenic B cells and human mast cells [135, 141, 155]. Therefore, it would be prudent

to further dissect the mechanism employed by the SMAs to regulate immune responses in mast cells. The data obtained also need to be corroborated by further confocal co-localisation studies in animal models, which would give a 3-dimensional view of the location of the signaling molecules and their interaction with the SMAs, giving more information about the mechanism of action of the SMAs.

The basic principle of confocal microscopy is its use of a pinhole spatial filter that eliminates out of focus light or glares, in specimens whose thickness exceeds the immediate plane of focus [265]. It further offers the advantage of the ability to control field depth thus helping in collecting serial optical sections from a thick specimen. It also eliminates and reduces the background noise that interferes with the image clarity and leads to image degradation. Co-localisation studies, as the name suggests, refers to the spatial overlap between the two or more fluorescent specimens that lie in a very close proximity or identical spatial positions. Hence, confocal co-localisation studies would aid in the demonstration of the relationship between signaling molecules and their communication with the SMAs. It would be interesting to correlate interaction of SMAs with the degradation of PKC, PLD and SPHK as suggested by their decreased expression in my experiments. By labelling the SMAs and the signaling molecules with multiple fluorophores, the emitted immunofluorescence could be analysed in relation to their position in the mast cells. The interaction of FcεRI with the multivalent antigen, the specific position of the signaling molecules and SMAs in the plasma membrane and inside the mast cells could be analysed both before and after sensitisation and cross-linking of the mast cells. This could further elucidate the pathways of the SMAs and their movement inside the cell to induce immunomodulatory action as seen in the experiments where all the SMAs seemed to decrease nuclear translocation of PKC-α. These experiments

could be taken further in an *in vivo* system which would help to verify the *in vitro* results.

4.4.2 Future prospects

Further studies need to be done to explore the use of SMAs in allergic diseases by first converting these studies to an *in vivo* system such as the OVA airway hypersensitivity model especially in the case of SMA 63 and 64, which show clear anti-allergic activity. Also, although the SMAS do not show toxic effects *in vitro*, they need to be tested for toxic effects and any toxicity-related symptoms in animal models. Similarly, pharmacological evaluation comprising of *in vitro* and *in vivo* testing especially in animal models of asthma and allergy to check the rate of excretion of SMAs from animals needs to be undertaken. Repeated dosage studies would need to be done to check any adverse effects related to multiple dosages such as drug resistance, hypersensitivity, and systemic toxicity in these animal models. Going further, as some molecules could be genetically toxic; studies to evaluate any likelihood of carcinogenic and mutagenic effects of the SMAs would need to be carried out in future. Prior to clinical trials – the ultimate aim of this work, any teratogenic effects of the SMAs need to be ruled out by *in vivo* studies in pregnant animal models. Only, after clearing all of these stages, could SMAs be employed in clinical trials.

Table 4.1

Table summarising the effects of SMAs. NS= Not selected, C= sensitised control, XL = sensitised and cross-linked, I/P= Ionomycin/PMA. The symbols ↔, ↓ and ↑ represent no change, decrease and increase, respectively.

SMA	%Calcium compared to control	% Degranulation reduction from Control			Cytokine		PKC	Signaling PLD	SPHK
		C	XL	I/P	IL-6	TNF			
1	306	↔	↔	↔	↔	↓	NS	NS	NS
3	73	↔	↔	↔	↑	↑	↓	↓	↓
4	160	↔	↔	↔	↔	↔	NS	NS	NS
6	183.5	↔	↔	↔	↔	↔	NS	NS	NS
9	84	↔	↔	↔	↔	↔	NS	NS	NS
25	69.7	↔	↔	↔	↔	↔	↔	↓	↔
27	232.5	↔	↔	↔	↑	↔	NS	NS	NS
28	81.7	↔	↔	↔	↑	↔	NS	NS	NS
33	136	↔	↔	↔	↔	↔	↓	↓	↓
35	129.7	↔	↔	↔	↑	↔	↓	↓	↓
39	86.7	↔	↔	↔	↑	↑	↓	↓	↓
52	93	↔	↔	↔	↑	↔	NS	NS	NS
63	75	41	48	33	↓	↓	↓	↓	↓
64	74	50	57	101	↓	↓	↓	↓	↓
65	132.5	41	45	46	↔	↔	↓	↓	↓

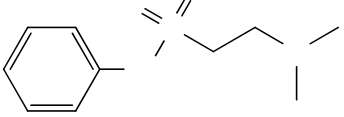
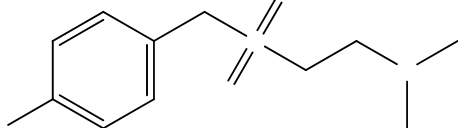
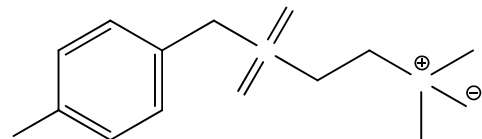
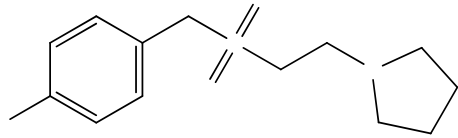
Table 4.1

Table 4.2 a and b

Table representing the final structure of molecules based on their

a) inhibitory or b) stimulatory character

a) Inhibitory Molecules

SMA	Structure	Formula
39		$C_{10}H_{16}N_2O_2S$ 228.3
63		$C_{11}H_{16}BrNO_2S$ 306.2
64		$C_{12}H_{19}INO_2S$ 368.3
65		$C_{14}H_{21}NO_2S$ 267.4

N

O

S

O

Br

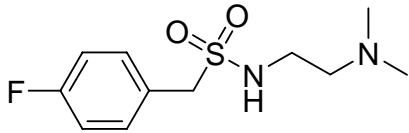
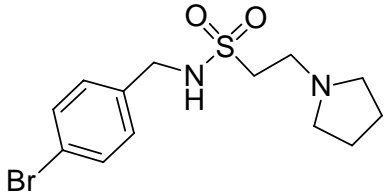
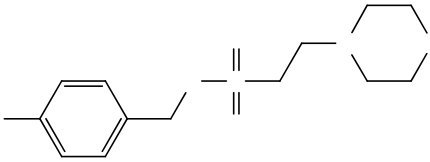
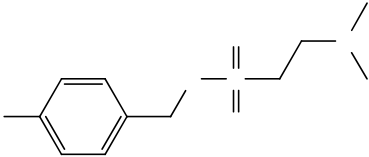
O

S

252 O

Me

b) Stimulatory Molecules

SMA	Structure	Formula
3		C ₁₁ H ₁₇ FN ₂ O ₂ S 260.3
25		C ₁₃ H ₁₉ BrN ₂ O ₂ S 347.3
33		C ₁₃ H ₁₉ FN ₂ O ₃ S 302.4
35		C ₁₁ H ₁₇ FN ₂ O ₂ S 260.3

F

HN

O

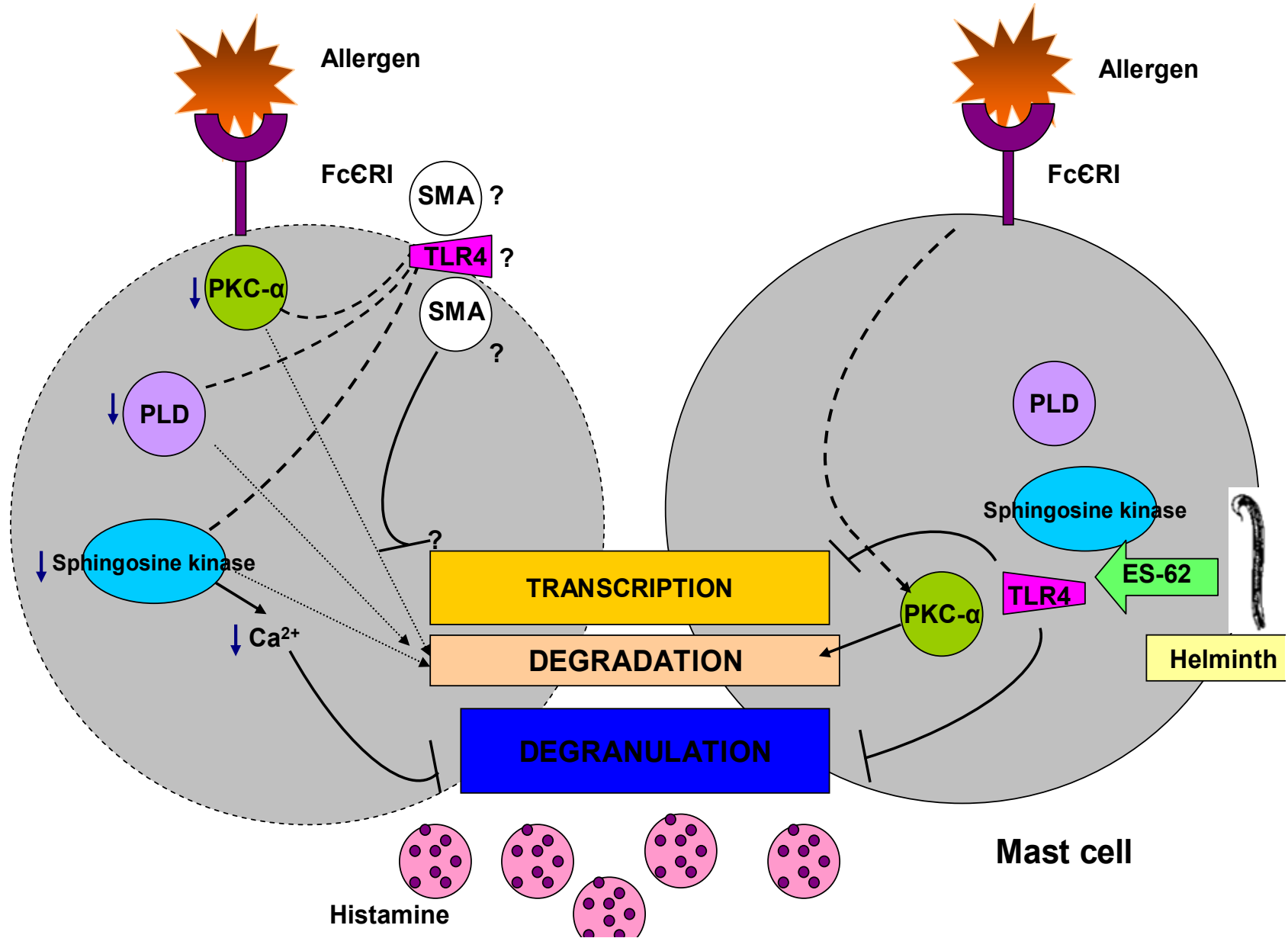
S

O

Figure 4.1

Suggested mechanism of action of SMAs as compared with ES-62. Key experiments need to be designed to determine the mode of action of the SMAs. Firstly, whether internalisation of the SMAs is necessary for its inhibitory and immunomodulatory action? Secondly, whether TLR4 is required similar to ES-62 to induce reduction in degranulation and Ca^{2+} mobilisation?

Mechanism of action of SMAs as compared with ES-62



References:

1. WHO/NHLBI workshop report. 1995. Global strategy for asthma management and prevention. National Institute of Health, National Heart, Lung and Blood Institute, Bethesda, MD. Publication No. 95-3659.
2. Cookson WO, Sharp PA, Faux JA, Hopkin JM, 'Linkage between immunoglobulin E responses underlying asthma and rhinitis and chromosome 11q.' *Lancet* 1989, 8650, 1292-5.
3. Skadhauge LR, Christensen K, Kyvik KO, Sigsgaard T, 'Genetic and environmental influence on asthma: a population-based study of 11,688 Danish twin pairs.' *Eur Respir J.* 1999, 13(1), 8-14.
4. Rémen T, Coevoet V, Acouetey DS, Guéant JL, Guéant-Rodriguez RM, Paris C, Zmirou-Navier D, 'Early incidence of occupational asthma among young bakers, pastry-makers and hairdressers: design of a retrospective cohort study.' *BMC Public Health* 2010, 10, 206.
5. Szczeklik A, Sanak M, Nizankowska-Mogilnicka E, Kiełbasa B 'Aspirin intolerance and the cyclooxygenase-leukotriene pathways.' *Curr Opin Pulm Med.* 2004, 10, 51-6.
6. Hoyle GW, Graham RM, Finkelstein JB, Nguyen KP, Gozal D, Friedman M, 'Hyperinnervation of the airways in transgenic mice overexpressing nerve growth factor.' *Am J Respir Cell Mol Biol.* 1998, 18, 149-57.
7. Kaminska M, Foley S, Maghni K, Storness-Bliss C, Coxson H, Ghezzi H, Lemièrre C, Olivenstein R, Ernst P, Hamid Q, Martin J, 'Airway remodelling in subjects with severe asthma with or without chronic persistent airflow obstruction.' *J Allergy Clin Immunol* 2009, 124, 45-51

8. Liu S, Shudou M, Maeyama K, 'Early activation of mucosal mast cells during the primary immune response in a rodent model of neonatal asthma.' *Immunol Cell Biol.* 2010, 1-7.
9. Munitz A, Bachelet I, Levi-Schaffer F, 'Reversal of airway inflammation and remodeling in asthma by a bispecific antibody fragment linking CCR3 to CD300a.' *J Allergy Clin Immunol* 2006, 118, 1082-1089.
10. Poston RN, Chanez P, Lacoste JY, Litchfield T, Lee TH., Bousquet J, 'Immunohistochemical characterization of the cellular infiltration in asthmatic bronchi.' *Am Rev Respir Dis.* 1992, 45, 918-21.
11. Bradley BL, Azzawi M, Jacobson M, Assoufi B, Collins JV, Irani AM, Schwartz LB, Durham SR, Jeffery PK, Kay AB, 'Eosinophils, T- lymphocytes, mast cells, neutrophils, and macrophages in bronchial biopsy specimens from atopic subjects with asthma: comparison with biopsy specimens from atopic subjects without asthma and normal control subjects and relationship to bronchial hyperresponsiveness.' *J Allergy Clin Immunol.* 1991, 88, 661-74.
12. McDonald DM, 'Angiogenesis and remodeling of airway vasculature in chronic inflammation.' *Am J Respir Crit Care Med* 2001, 64, S39-45.
13. Bentley AM., Menz G, Storz C, Robinson DS, Bradley B, Jeffery PK., Durham SR, Kay AB, 'Identification of T lymphocytes, macrophages, and activated eosinophils in the bronchial mucosa in intrinsic asthma. Relationship to symptoms and bronchial responsiveness.' *Am Rev Respir Dis.* 1992, 146, 500-6.

14. Tang H, Pang S, Wang M, Xiao X, Rong Y, Wang H, Zang YQ, 'TLR4 activation is required for IL-17-induced multiple tissue inflammation and wasting in mice.' *J Immunol.*2010, 185, 2563-9.
15. Létuvé S, Lajoie-Kadoch S, Audusseau S, Rothenberg ME, Fiset PO, Ludwig MS, Hamid Q, 'IL-17E upregulates the expression of proinflammatory cytokines in lung fibroblasts.' *J Allergy Clin Immunol.* 2006, 117, 590-6.
16. Zhao Y, Yang J, Gao YD, Guo W, 'Th17 immunity in patients with allergic asthma.' *Int Arch Allergy Immunol.*2010, 151, 297-307.
17. Molet S, Hamid Q, Davoine F, Nutku E, Taha R, Pagé N, Olivenstein R, Elias J, Chakir J, 'IL-17 is increased in asthmatic airways and induces human bronchial fibroblasts to produce cytokines.' *J Allergy Clin Immunol.* 2001, 108, 430-8.
18. Chabaud M, Fossiez F, Taupin JL, Miossec P, 'Enhancing effect of IL-17 on IL-1-induced IL-6 and leukemia inhibitory factor production by rheumatoid arthritis synoviocytes and its regulation by Th2 cytokines.' *J Immunol.* 1998, 161, 409-14.
19. Lajoie-Kadoch S, Joubert P, Letuve S, Halayko AJ, Martin JG, Soussi-Gounni A, Hamid Q, 'TNF-alpha and IFN-gamma inversely modulate expression of the IL-17E receptor in airway smooth muscle cells.' *Am J Physiol Lung Cell Mol Physiol* 2006, 290, L1238-1246.
20. Molet S, Hamid Q, Davoine F, Nutku E, Taha R, Page N, Olivenstein R, Elias J, Chakir J, 'IL-17 is increased in asthmatic airways and induces human bronchial fibroblasts to produce cytokines.' *J Allergy Clin Immunol* 2001, 108,430-438.

21. Schnyder-Candrian S, Togbe D, Couillin I, Mercier I, Brombacher F, Quesniaux V, Fossiez F, Ryffel B, Schnyder B, 'Interleukin-17 is a negative regulator of established allergic asthma..' *J Exp Med.*2006, 203, 2715-25.
22. Schnyder B, Lima C, Schnyder-Candrian S, 'Interleukin-22 is a negative regulator of the allergic response.' *Cytokine.* 2010, 50, 220-7.
23. Humbert M, Duraham SR, Ying S, Kimmitt P, 'IL-4 and IL-5 mRNA and protein in bronchial biopsies from patients with atopic and non-atopic asthma: evidence against "intrinsic" asthma being a distinct immunopathologic entity.' *Am J.Respir.Crit.Care.Med.*1996, 154, 1497-1504.
24. Bischoff SC, 'Role of mast cells in allergic and non-allergic immune responses: comparison of human and murine data. *Nat Rev Immunol.* 2007, 7, 93-104.
25. MacGlashan DW Jr, Bochner BS, Adelman DC, Jardieu PM, Togias A, McKenzie-White J, Sterbinsky SA, Hamilton RG, Lichtenstein LM, 'Down-regulation of Fc(epsilon)RI expression on human basophils during in vivo treatment of atopic patients with anti-IgE antibody.' *J Immunol* 1997 158, 1438-1445.
26. Galli SJ, Tsai M, Piliponsky AM, 'The Development of allergic inflammation.' *Nature reviews* 2008, 454, 445-454.
27. Cohen L E X, Tarsi J, Ramkumar T, Horiuchi TK, Cochran R, DeMartino S, Schechtman KB, Hussain I, Holtzman MJ, Castro M; and the NHLBI Severe Asthma Research Program (SARP), 'Epithelial cell proliferation contributes to airway remodeling in severe asthma.' *Am J Respir Crit Care Med.* 2007, 176, 138-45.

28. Laitinen LA, Heino M, Laitinen A, Kava T, Haahtela T, 'Damage of the airway epithelium and bronchial reactivity in patients with asthma.' *Am. Rev. Resp. Dis.* 1985, 131, 599-606.
29. Montefort S, Djukanović R, Holgate ST, Roche WR, 'Ciliated cell damage in the bronchial epithelium of asthmatics and non-asthmatics.' *Clin Exp Allergy.* 1993, 23, 185-9.
30. Dunnill MS, Massarella GR, Anderson JA, 'A comparison of the quantitative anatomy of the bronchi in normal subjects, in status asthmaticus, In chronic bronchitis, and in emphysema.' *Thorax.* 1969, 24, 176-9.
31. Cutz.E, Levison H, Cooper DM, 'Ultrastructure of airways in children with asthma.' *Histopathology* 1978, 2, 407-421.
32. Awadh N, Müller NL, Park CS, Abboud RT, FitzGerald JM, 'Airway wall thickness in patients with near fatal asthma and control groups: assessment with high resolution computed tomographic scanning.' *Thorax.* 1998, 53, 248-53.
33. Bonini S, Lambiase A, Bonini S, Angelucci F, Magrini L, Manni L, Aloe L, 'Circulating nerve growth factor levels are increased in humans with allergic diseases and asthma.' *Proc Natl Acad Sci U S A.* 1996, 93, 10955-60.
34. Bonini S, Lambiase A, Bonini S, Angelucci F, Magrini L, Manni L, Aloe L, 'Circulating nerve growth factor levels are increased in humans with allergic diseases and asthma.' *Proc Natl Acad Sci U S A.* 1996, 93, 10955-60.
35. Jeffery PK, Wardlaw AJ, Nelson FC, Collins JV, Kay AB, 'Bronchial biopsies in asthma. An ultrastructural, quantitative study and correlation with hyperreactivity.' *Am Rev Respir Dis.* 1989, 140, 1745-53.

36. Ohashi Y, Motojima S, Fukuda T, Makino S, 'Airway hyperresponsiveness, increased intracellular spaces of bronchial epithelium, and increased infiltration of eosinophils and lymphocytes in bronchial mucosa in asthma..' *Am Rev Respir Dis.* 1992, 145, 1469-76.
37. Barnes PJ, 'New Directions in allergic diseases: mechanism based anti-inflammatory therapies.' *J.Allergy and Clin. Imuno.* 2000, 106, 5-16
38. Cecil Textbook of Medicine, Goldman Bennet, 2nd edition.
39. O'Byrne PM, Parameswaran K, 'Pharmacological management of mild or moderate persistent asthma.' *Lancet.* 2006, 368,794-803
40. Kelley H, William A, 'Asthma" in *Pharmacotherapy: A Pathophysiologic Approach*, McGraw-Hill Medical Publishing, Division, New York, 1999, 430-459.
41. Guidelines for the diagnosis and management of asthma. National Asthma Education and Prevention: Expert Panel Report 2. National Institute of Health, Publication No. 97-4051, Bethesda, MD, 1997.
42. Sin DD, Man J, Sharpe H, Gan WQ, Man SF, 'Pharmacological management to reduce exacerbations in adults with asthma: A systemic review and meta-analysis.' *JAMA* 2004, 292, 367-376.
43. Bousquet J, Wenzel S, Holgate S, 'Predicting response to Omalizumab, an Anti-IgE antibody in patients with allergic asthma.' *Chest* 2004, 125, 1378-1386.
44. Cox L,Platts-Mills TA, Finegold I, Schwartz LB,Simons FE, Wallace DV, American Academy of Allergy, Asthma & Immunology,American College of Allergy, Asthma and Immunology American Academy of Allergy, Asthma & Immunology/American College of Allergy, Asthma and Immunology Joint Task Force, 'Report on omalizumab-associated anaphylaxis.' *J Allergy Clin Immunol.*2007, 120, 1373-7.

45. Strachan DP, 'Hay fever, hygiene, and household size.' *BMJ* 1989, 299, 1259-1260.
46. van den Biggelaar AH, Rodrigues LC, van Ree R, van der Zee JS, Hoeksma-Kruize YC, Souverijn JH, Missinou MA, Borrmann S, Kremsner PG, Yazdanbakhsh M, 'Long-term treatment of intestinal helminths increases mite skin-test reactivity in Gabonese schoolchildren.' *Lancet*, 1997, 350, 85-90.
47. Cooper PJ, Chico ME, Rodrigues LC, Ordonez M, Strachan D, Griffin GE, Nutman TB, 'Reduced risk of atopy among school-age children infected with geohelminth parasites in a rural area of the tropics.' *J. Allergy Clin. Immunol.* 2003, 111, 995-1000.
48. Rodrigues LC, Newcombe PJ, Cunha SS, Alcantara-Neves NM, Genser B, Cruz AA, Simoes SM, Fiaccone R, Amorim L, Cooper PJ, Barreto ML, 'Early infection with *Trichuris trichiura* and allergen skin test reactivity in later childhood.' *Clin Exp Allergy.* 2008, 38, 1769-1777.
49. Dagoye D, Bekele Z, Woldemichael K, Nida H, Yimam M, Hall A, Venn AJ, Britton JR, Hubbard R, Lewis SA, 'Wheezing, allergy, and parasite infection in children in urban and rural Ethiopia.' *Am J Respir Crit Care Med.* 2003, 67, 1369-73.
50. Medeiros M Jr, Figueiredo JP, Almeida MC, Matos MA, Araújo MI, Cruz AA, Atta AM, Rego MA, de Jesus AR, Taketomi EA, Carvalho EM, 'Schistosoma mansoni infection is associated with a reduced course of asthma.' *J Allergy Clin Immunol.* 2003, 111, 947-51.
51. Wang CC, Nolan TJ, Schad GA, and Abraham D, 'Infection of mice with the helminth *Strongyloides stercoralis* suppresses pulmonary allergic responses to ovalbumin.' *Clinical and Experimental Allergy*, 2001, 31, 495-503.

52. Kitagaki K, Businga TR, Racila D, Elliott DE, Weinstock JV, Kline JN, 'Intestinal helminths protect in a murine model of asthma.' *J Immunol.* 2006, 177, 1628-35.
53. Bashir ME, Andersen P, Fuss IJ, Shi HN, Nagler-Anderson C, 'An enteric helminth infection protects against an allergic response to dietary antigen.' *J Immunol.* 2002, 169, 3284-92.
54. Wohlleben G, Trujillo C, Müller J, Ritze Y, Grunewald S, Tatsch U, Erb KJ, 'Helminth infection modulates the development of allergen-induced airway inflammation.' *Int Immunol.* 2004, 16, 585-96.
55. Itami DM, Oshiro TM, Araujo CA, Perini A, Martins MA, Macedo MS, Macedo-Soares M, 'Modulation of murine experimental asthma by *Ascaris suum* components.' *Clin Exp Allergy.* 2005, 35, 873-9.
56. Oshiro TM, Macedo MS, Macedo-Soares MF, 'Anti-inflammatory activity of PAS-1, a protein component of *Ascaris suum*.' *Inflamm res* 2005, 54, 17–21.
57. Dubucquoi S, Desreumaux P, Janin A, Klein O, Goldman M, Tavernier J, 'Interleukin 5 synthesis by eosinophils: association with granules and immunoglobulin-dependent secretion.' *J Exp Med* 1994, 179, 703-708.
58. Sher A, Coffman RL, Hieny S, Scott P, Cheever AW, 'Interleukin 5 is required for the blood and tissue eosinophilia but not granuloma formation induced by infection with *Schistosoma mansoni*. *Proc Natl Acad Sci U S A.* 1990, 87, 61-5.
59. Collins PD, Marleau S, Griffiths-Johnson DA, Jose PJ, Williams TJ, 'Cooperation between interleukin-5 and the chemokine eotaxin to induce eosinophil accumulation in vivo.' *J Exp Med* 1995, 182, 1169– 74.

60. Kameyoshi Y, Dörschner A, Mallet AI, Christophers E, Schröder JM, 'Cytokine RANTES released by thrombin-stimulated platelets is a potent attractant for human eosinophils.' *J Exp Med.* 1992, 176, 587-92.
61. Gonzalo JA, Lloyd CM, Wen D, Albar JP, Wells TN, Proudfoot A, Martinez-A C, Dorf M, Bjerke T, Coyle AJ, Gutierrez-Ramos JC, 'The coordinated action of CC chemokines in the lung orchestrates allergic inflammation and airway hyperresponsiveness.' *J Exp Med.* 1998, 188, 157-67.
62. Araújo CA, Perini A, Martins MA, Macedo MS, Macedo-Soares MF, 'PAS-1, a protein from *Ascaris suum*, modulates allergic inflammation via IL-10 and IFN-gamma, but not IL-12.' *Cytokine.* 2008, 44, 335-41.
63. Wilson MS, Taylor MD, Balic A, Finney CA, Lamb JR, Maizels RM, 'Suppression of allergic airway inflammation by helminth-induced regulatory T cells.' *J Exp Med.* 2005, 202, 1199-212.
64. Wilson MS, Taylor MD, O'Gorman MT, Balic A, Barr TA, Filbey K, Anderton SM, Maizels RM, 'Helminth-induced CD19⁺CD23^{hi} B cells modulate experimental allergic and autoimmune inflammation.' *Eur J Immunol.* 2010, 40, 1682-96.
65. Hartmann S, Schnoeller C, Dahten A, Avagyan A, Rausch S, Lendner M, Bocian C, Pillai S, Loddenkemper C, Lucius R, Worm M, Hamelmann E, 'Gastrointestinal nematode infection interferes with experimental allergic airway inflammation but not atopic dermatitis.' *Clin Exp Allergy.* 2009, 39, 1585-1596.
66. Shea-Donohue T, Sullivan C, Finkelman FD, Madden KB, Morris SC, Goldhill J, Piñeiro-Carrero V, Urban JF Jr, 'The role of IL-4 in *Heligmosomoides polygyrus*-

- induced alterations in murine intestinal epithelial cell function.' J Immunol. 2001, 167, 2234-9.
67. Svetić A, Madden KB, Zhou XD, Lu P, Katona IM, Finkelman FD, Urban JF Jr, Gause WC, 'A primary intestinal helminthic infection rapidly induces a gut-associated elevation of Th2-associated cytokines and IL-3 J Immunol. 1993, 150, 3434-41.
68. Grencis RK, Hültner L, Else KJ, 'Host protective immunity to *Trichinella spiralis* in mice: activation of Th cell subsets and lymphokine secretion in mice expressing different response phenotypes. Immunology 1991, 74, 329-332.
69. Ihle JN, Keller J, Oroszlan S, Henderson LE, Copeland TD, Fitch F, Prystowsky MB, Goldwasser E, Schrader JW, Palaszynski E, Dy M, Lebel B, 'Biologic properties of homogeneous interleukin 3. I. Demonstration of WEHI-3 growth factor activity, mast cell growth factor activity, p cell-stimulating factor activity, colony-stimulating factor activity, and histamine-producing cell-stimulating factor activity.' J Immunol. 1983, 131, 282-7.
70. Knight PA, Wright SH, Lawrence CE, Paterson YY, Miller HR, 'Delayed expulsion of the nematode *Trichinella spiralis* in mice lacking the mucosal mast cell-specific granule chymase, mouse mast cell protease-1.' J Exp Med. 2000, 192, 1849-56
71. Gurish MF, Bryce PJ, Tao H, Kisselgof AB, Thornton EM, Miller HR, Friend DS, Oettgen HC 'IgE enhances parasite clearance and regulates mast cell responses in mice infected with *Trichinella spiralis*. J Immunol. 2004, 172, 1139-45.
72. Subramanian S, Stolk WA, Ramaiah KD, Plaisier AP, Krishnamoorthy K, Van Oortmarssen GJ, Dominic Amalraj D, Habbema JD, Das PK, 'The dynamics of

- Wuchereria bancrofti infection: a model-based analysis of longitudinal data from Pondicherry, India.' *Parasitology*.2004, 128, 467-82
73. Harnett W, Iain B, Harnett MM, 'ES-62, a filarial nematode derived immunomodulatory with anti-inflammatory potential.' *Immun Lett*, 2004, 94, 27-33.
74. Yagi H, Nomura T, Nakamura K, Yamazaki S, Kitawaki T, Hori S, Maeda M, Onodera M, Uchiyama T, Fujii S, Sakaguchi S, 'Crucial role of FOXP3 in the development and function of human CD25+CD4+ regulatory T cells.' *Int Immunol*.2004, 16, 1643-56.
75. Groux H, O'Garra A, Bigler M, Rouleau M, Antonenko S, de Vries JE, Roncarolo MG, 'A CD4+ T-cell subset inhibits antigen-specific T-cell responses and prevents colitis.' *Nature*. 1997, 389, 737-42.
76. Huehn J, Siegmund K, Lehmann JCU, Siewert C, Haubold U, Feuerer M, Debes GF, Lauber J, Frey O, Przybylski GK, 'Developmental stage, phenotype, and migration distinguish naive- and effector/memory-like CD4+ regulatory T cells.' *J. Exp. Med*. 2004, 199, 303–313.
77. Han HS, Jun HS, Utsugi T, Yoon JW, 'A new type of CD4+ suppressor T cell completely prevents spontaneous autoimmune diabetes and recurrent diabetes in syngeneic islet-transplanted NOD mice.' *J Autoimmun*. 1996, 9, 331-9.
78. McSorley HJ, Harcus YM, Murray J, Taylor MD, Maizels RM, 'Expansion of Foxp3+ regulatory T cells in mice infected with the filarial parasite *Brugia malayi*.' *J Immunol* 2008, 181, 6456-66.
79. Liu Q, Sundar K, Mishra PK, Mousavi G, Liu Z, Gaydo A, Alem F, Lagunoff D, Bleich D, Gause WC, 'Helminth infection can reduce insulinitis and type 1 diabetes through CD25- and IL-10-independent mechanisms.' *Infect Immun*. 2009, 77, 5347-58.

80. Mitre E, Chien D, Nutman TB, 'CD4 (+) (and Not CD25 (+)) T Cells Are the Predominant Interleukin-10-Producing Cells in the Circulation of Filaria-Infected Patients.' *J Infect Dis.* 2008, 197, 94-101.
81. Doetze A, Satoguina J, Burchard G, Rau T, Löliger C, Fleischer B, Hoerauf A, 'Antigen-specific cellular hyporesponsiveness in a chronic human helminth infection is mediated by T(h)3/T(r)1-type cytokines IL-10 and transforming growth factor-beta but not by a T(h)1 to T(h)2 shift.' *Int Immunol.* 2000, 12, 623-30.
82. Wammes LJ, Hamid F, Wiria AE, de Gier B, Sartono E, Maizels RM, Luty AJ, Fillié Y, Brice GT, Supali T, Smits HH, Yazdanbakhsh M, 'Regulatory T cells in human geohelminth infection suppress immune responses to BCG and *Plasmodium falciparum*.' *Eur J Immunol.* 2010, 40, 437-442.
83. Stein M, Keshav S, Harris N, Gordon S, 'Interleukin 4 potently enhances murine macrophage mannose receptor activity: a marker of alternative immunologic macrophage activation. *J Exp Med.* 1992, 176, 287-92.
84. Allen JE, MacDonald AS, 'Profound suppression of cellular proliferation mediated by the secretions of nematodes.' *Parasite Immunol* 1998, 20, 241-247.
85. Taylor MJ, Cross HF, Bilo K., 'Inflammatory responses induced by the filarial nematode *Brugia malayi* are mediated by lipopolysaccharide-like activity from endosymbiotic wolbachia bacteria.' *J Exp Med* 2000, 191, 429-1436.
86. Semnani RT, Law M, Kubofcik J, Nutman TB, 'Filaria-induced immune evasion: suppression by the infective stage of *Brugia malayi* at the earliest host-parasite interface. *J. Immunol.* 2004, 172, 6229–6238.

87. MacDonald AS, Maizels RM, Lawrence RA, Dransfield I, Allen JE, 'Requirement for in vivo production of IL-4, but not IL-10, in the induction of proliferative suppression by filarial parasites.' *J. Immunol.*1998, 160, 4124–4132.
88. Loke P, MacDonald AS, Allen JE, 'Antigen presenting cells recruited by *Brugia malayi* induce Th2 differentiation of naive CD4⁺ T cells.' *Eur. J. Immunol.*2000, 30, 1127–1135.
89. Loke P, Nair MG, Parkinson J, Guiliano D, Blaxter M, Allen JE, 'IL-4 dependent alternatively-activated macrophages have a distinctive in vivo gene expression phenotype.' *BMC Immunol.*2002, 3, 7.
90. Nair MG, Gallagher IJ, Taylor MD, Loke P, Coulson PS, Wilson RA, Maizels RM, Allen JE, ' Chitinase and Fizz family members are a generalized feature of nematode infection with selective upregulation of Ym1 and Fizz1 by antigen-presenting cells.' *Infect Immun* 2005, 73, 385–394.
91. Taylor MD, Harris A, Nair MG, Maizels RM, Allen JE, 'F4/80 Alternatively Activated Macrophages control CD4⁺ T Cell Hyporesponsiveness at Sites Peripheral to Filarial Infection.' *The Journal of Immunology*, 2006, 176, 6918–6927.
92. Lin HH, Faunce DE, Stacey M, Terajewicz A, Nakamura T, Zhang- Hoover J, Kerley M, Mucenski ML, Gordon S, Stein-treilein J, 'The macrophage F4/80 receptor is required for the induction of antigen-specific efferent regulatory T cells in peripheral tolerance.' *J. Exp. Med.*2005, 201, 1615–1625.
93. Volkmann L, Bain O, Saefte M, Specht S, Fischer K, Brombacher F,Matthaei KI, Hoerauf A, 'Murine filariasis: interleukin 4 and interleukin 5 lead to containment of different worm developmental stages.' *Med. Microbiol.Immunol.* 2003, 192, 23–31.

94. Le Goff L, Lamb TJ, Graham AL, Harnus Y, Allen JE, 'IL-4 is required to prevent filarial nematode development in resistant but not susceptible strains of mice.' *Int. J. Parasitol.* 2002, 32, 1277–1284.
95. Anthony RM, Urban JF Jr, Alem F, Hamed HA, Rozo CT, Boucher JL, Van Rooijen N, Gause WC, 'Memory T(H)2 cells induce alternatively activated macrophages to mediate protection against nematode parasites.' *Nat Med.* 2006, 12, 955-60.
96. Reece JJ, Siracusa MC, Scott AL, 'Innate immune responses to lung-stage helminth infection induce alternatively activated alveolar macrophages.' *Infect Immun.* 2006, 74, 4970-81
97. Hunter MM, Wang A, Parhar KS, Johnston MJ, Van Rooijen N, Beck PL, McKay DM, 'In vitro-derived alternatively activated macrophages reduce colonic inflammation in mice.' *Gastroenterology.* 2010, 138, 1395-405.
98. Linsley PS, Greene JL, Tan P, Bradshaw J, Ledbetter JA, Anasetti C, Damle NK, 'Coexpression and functional cooperation of CTLA-4 and CD28 on activated T lymphocytes'. *J. Exp. Med.* 1992, 176, 1595.
99. Kuhns MS, Epshteyn V, Sobel RA, Allison JP, 'Cytotoxic T lymphocyte antigen-4 (CTLA-4) regulates the size, reactivity, and function of a primed pool of CD4⁺ T cells.' *Proc. Natl. Acad. Sci. USA.* 2000, 97, 12711.
100. Tivol EA, Borriello F, Schweitzer AN, Lynch WP, Bluestone JA, Sharpe AH, 'Loss of CTLA-4 leads to massive lymphoproliferation and fatal multiorgan tissue destruction, revealing a critical negative regulatory role of CTLA-4.' *Immunity.* 1995, 3, 541.
101. Takahashi T, Tagami T, Yamazaki S, Uede T, Shimizu J, Sakaguchi N, Mak TW, Sakaguchi S, 'Immunologic self-tolerance maintained by CD25⁺CD4⁺ regulatory T

- cells constitutively expressing cytotoxic T lymphocyte-associated antigen 4.' *J. Exp. Med.* 2000, 192, 303.
102. Steinbrink K, Graulich E, Kubsch S, Knop J, Enk AH, 'CD4⁺ and CD8⁺ anergic T cells induced by interleukin-10-treated human dendritic cells display antigen-specific suppressor activity. *Blood*, 2002, 99, 2468.
 103. Steel C, 'Long term effect of pre-natal exposure to maternal microfilaremia on immune responsiveness to filarial parasite antigens.' *Lancet*, 1994, 343, 890-893.
 104. Harding FA, McArthur JG, Gross JA, Raulet DA, Allison, JP, 'CD28-mediated signaling costimulates murine T cells and prevents induction of anergy in T cell clones.' *Nature* 1992, 356: 607–609.
 105. Jenkins MK, 'The ups and downs of costimulation.' *Immunity*. 1994, 1, 443-446.
 106. Linsley ES, Ledbetter JA, 'The role of the CD28 receptor during T cell responses to antigen.' *Annu. Rev. Immunot*, 1993, 11, 191-212.
 107. Reiser H, Freeman GJ, Razi-Wolf Z, Gimmi CD, Benacerraf B, Nadler NM, 'Murine B7 antigen provides a costimulatory signal for activation of murine T lymphocytes via the T cell receptor/CD3 complex.' *Proc Natl. Acad. Sci. USA*. 1992, 89, 271-275.
 108. Linsley PS, Wallace PM, Johnson J, Gibson M, Ledbetter J, Singh C, Tepper M, 'Immunosuppression in vivo by a soluble form of the CTLA-4 T cell activation molecule.' *Science* 1992, 257, 792–795.
 109. Gimmi CD, Freeman GJ, Gribben JG, Sugita K, Freedman AS, Morimoto C, Nadler LM, 'B-cell surface antigen B7 provides a costimulatory signal that induces T cells to proliferate and secret interleukin 2.' *Proc. Natl. Acad. Sci. USA*. 1991, 88, 6575-6579.

110. Alegre ML, Shiels H, Thompson CB, Gajewski TF, 'Expression and function of CTLA-4 in Th1 and Th2 cells.' *J. Immunol.* 1998, 161, 3347.
111. Walunas TL, Bluestone JA, 'CTLA-4 regulates tolerance induction and T cell differentiation in vivo.' *J. Immunol.* 1998, 160, 3855.
112. Steel C, Nutman TB, 'CTLA-4 in Filarial Infections: Implications for a Role in Diminished T Cell Reactivity.' *J Immunol.* 2003, 70, 1930-8.
113. Taylor MD, LeGoff L, Harris A, Malone E, Allen JE, Maizels RM, 'Removal of regulatory T-cell activity reverses hyporesponsiveness and leads to filarial parasite clearance in vivo.' *J Immun* 2005, 174, 4924-4933.
114. Gillan V, Devaney E, 'Regulatory T cells modulate Th2 responses induced by *Brugia pahangi* third-stage larvae.' *Infect Immun.* 2005, 73, 4034-42.
115. Babu S, Bhat SQ, Pavan Kumar N, Lipira AB, Kumar S, Karthik C, Kumaraswami V, Nutman TB, 'Filarial lymphedema is characterized by antigen-specific Th1 and th17 proinflammatory responses and a lack of regulatory T cells.' *PLoS Negl Trop Dis.* 2009, 3, e420.
116. Harnett W, Harnett MM, Byron O, 'Structural and Functional aspects of ES-62 – A secreted immunomodulatory phosphorylcholine containing Filarial nematode Glycoprotein' 2003, *Current protein and peptide science.*
117. Houston KM, Wilson EH, Eyres L, Brombacher F, Harnett MM, Alexander J, Harnett W, 'Presence of phosphorylcholine on a filarial nematode protein influences immunoglobulin G subclass response to the molecule by IL-10 dependant mechanism' *Infect. Immunology*, 68, 2000, 5466-5468.

118. Rodger FD, 'Onchocerciasis in Zaire: A new approach to the problem of river-blindness' Pergamon Press 1977, 2-5.
119. Ackerman Claire J, Harnett MM, Harnett W, Kelly SM, Svergun DI, Byron O, '19 a solution structure of the filarial nematode immunomodulatory protein ES-62' Biophysical Journal, 84, 2003, 489-500.
120. Haslam SM, Houston KM, Harnett W, Reason AJ, Morris HR, Dell A, 'Structural Studies of N-Glycans of filarial parasites' The Journal of Biological Chemist 1999, 274, 20953-20960.
121. Stepek G, Houston KM, Goodridge HS, Devaney E, Harnett W, 'Stage-specific and species-specific differences in the production of the mRNA and protein for the filarial nematode secreted product, ES-62.' Parasitology. 2004, 128, 91-8.
122. Haslam SM, Khoo KH, Houston KM, Harnett W, Morris HR, Dell A, 'Characterisation of the Phosphorylcholine containing N-linked Oligosaccharides in the excretory secretory 62 kDA glycoprotein of *A. viteae*' Molecular and Biochemical Parasitology 1997, 85, 53-66.
123. Houston KM, Cushley W, Harnett W, 'Studies on the site and mechanism of attachment of phosphorylcholine to a filarial nematode secreted glycoprotein'. J Biol Chem. 1997 272, 1527-33.
124. Takeda K, Kaisho T, Akira S, 'Toll-like receptors.' Annu. Rev. Immunol.2003, 21, 335.
125. Goodridge HS, Marshall FA, Else KJ, Houston KM, Egan C, Al-Riyami L, Liew F-Y, Harnett W, Harnett MM, 'Immunomodulation via Novel Use of TLR4 by the Filarial Nematode Phosphorylcholine-Containing Secreted Product, ES-62.' The Journal of Immunology, 2005, 174, 284-293.

126. Harnett W, Houston KM, Tate R, Garate T, Apfel H, Adam R, Haslam SM, Panico M, Paxton T, Dell A, Morris H, Brzeski H, 'Molecular cloning and demonstration of an aminopeptidase activity in a filarial nematode glycoprotein.' *Mol Biochem Parasitol.* 1999, 104, 11- 23.
127. Snapper CM, Paul WE, 'Interferon-gamma and B cell stimulatory factor-1 reciprocally regulate Ig isotype production.' *Science* 1987, 239, 944–947.
128. Palanivel VC, Posey AM, Horauf W, Solbach WF, Piessens, Harn DA, 'B-cell outgrowth and ligand-specific production of IL-10 correlate with Th2 dominance in certain parasitic diseases. *Exp. Parasitol.* 1996, 84, 168–17
129. Harnett W, Harnett MM, 'Inhibition of murine B cell proliferation and down-regulation of protein kinase C levels by a phosphorylcholine-containing filarial excretory-secretory product.' *J. Immunol.* 1993, 151, 4829-37.
130. Wilson EH, Katz E, Goodridge HS, Harnett MM, Harnett W, 'In vivo activation of murine peritoneal B1 cells by the filarial nematode phosphorylcholine-containing glycoprotein ES-62.' *Parasite Immunol.* 2003, 25, 463-6.
131. Lal RB, Paranjape RS, Briles DE, Nutman TB, Ottesen EA, 'Circulating parasite antigen (s) in lymphatic filariasis: use of monoclonal antibodies to phosphocholine for immunodiagnosis.' *J Immunol* 1987, 138, 3454–60.
132. Harnett MM, Deehan MR, Williams DM, Harnett W, 'Induction of signalling anergy via the T-cell receptor in cultured Jurkat T cells by pre-exposure to a filarial nematode secreted product.' *Parasite Immunol.* 1998, 20, 551-63.

133. Wilson EH, Deehan MR, Katz E, Brown KS, Houston KM, O'Grady J, Harnett MM, Harnett W, 'Hyporesponsiveness of murine B lymphocytes exposed to the filarial nematode secreted product ES-62 in vivo.' *Immunology* 2003,109, 238–45.
134. Deehan MR, Harnett W, Harnett MM, 'A filarial nematode-secreted phosphorylcholine-containing glycoprotein uncouples the B cell antigen receptor from extracellular signal-regulated kinase-mitogen-activated protein kinase by promoting the surface Ig-mediated recruitment of Src homology 2 domain-containing tyrosine phosphatase-1 and Pac-1 mitogen-activated kinase-phosphatase.' *J Immunol.* 2001, 166, 7462-8.
135. Deehan MR, Harnett MM, Harnett W, 'A filarial nematode secreted product differentially modulates expression and activation of protein kinase C isoforms in B lymphocytes.' *J Immunol* 1997, 159, 6105–11.
136. Deehan MR, Frame MJ, Parkhouse RM, Seatter SD, Reid SD, Harnett MM, Harnett W, 'A phosphorylcholine-containing filarial nematode-secreted product disrupts B lymphocyte activation by targeting key proliferative signaling pathways.' *J. Immunol.* 1998, 160, 2692.
137. Harnett W, Goodridge HS, Harnett MM, 'Subversion of immune cell signal transduction pathways by the secreted filarial nematode product, ES-62.' *Parasitology.* 2005, 130 Suppl S63-8.
138. Rissoan MC, Soumelis V, Kadowaki N, Grouard G, Briere F, Malefyt R, Liu Y-J, 'Reciprocal control of T helper cell and dendritic cell differentiation.' *Science* 1999, 283, 1183.
139. Marshall FA, Grierson AM, Garside P, Harnett W, Harnett MM, 'ES-62, an immunomodulator secreted by filarial nematodes, suppresses clonal expansion and

- modifies effector function of heterologous antigen-specific T cells in vivo.' *J Immunol.* 2005, 175, 5817-26.
140. Marshall FA, Grierson AM, Garside P, Harnett W, Harnett MM, 'ES-62, an immunomodulator secreted by filarial nematodes, suppresses clonal expansion and modifies effector function of heterologous antigen-specific T cells in vivo.' *J Immunol.* 2005, 175, 5817-26.
 141. Marshall FA, Watson KA, Garside P, Harnett MM, Harnett W, 'Effect of activated antigen specific B cells on ES-62 mediated modulation of effector function of heterologous antigen specific T cells in vivo.' *Immunology.* 2008, 123, 411-25.
 142. Goodridge H.S., Wilson EH, Harnett W, Campbell CC, Harnett MM, Liew FY, 'Modulation of macrophage cytokine production by ES-62, a secreted product of the filarial nematode *Acanthocheilonema viteae*.' *J Immunol.* 2001, 167, 940-5.
 143. Whelan M, Harnett MM, Houston KM, Patel V, Harnett W, Rigley KP, 'A filarial nematode-secreted product signals dendritic cells to acquire a phenotype that drives development of Th2 cells.' *J Immunol.* 2000, 164, 6453-60.
 144. Goodridge HS, McGuinness S, Houston KM, Egan CA, Al-Riyami L, Alcocer MJ, Harnett MM, Harnett W, 'Phosphorylcholine mimics the effects of ES-62 on macrophages and dendritic cells.' *Parasite Immunol.* 2007, 29, 127-37.
 145. Goodridge HS, Marshall FA, Wilson EH, Houston KM, Liew FY, Harnett MM, Harnett W, 'In vivo exposure of murine dendritic cell and macrophage bone marrow progenitors to the phosphorylcholine-containing filarial nematode glycoprotein ES-62 polarizes their differentiation to an anti-inflammatory phenotype.' *Immunology.* 2004, 113, 491-8.

146. Sartono E, Kruize YC, Partono F, Kurniawan A, Maizels RM, Yazdanbakhsh M, 'Specific T cell unresponsiveness in human filariasis: diversity in underlying mechanisms.' *Parasite Immunol.* 1995, 17, 587-94.
147. Metcalfe DD, Boyce JA, 'Mast Cell biology in evolution' *Journal of clinical Immunology.* 2006, 117, 1227-1229.
148. Metzger H, 'The receptor with high affinity for IgE.' *Immunol Rev.* 1992, 125, 37-48.
149. Vonakis BM, Chen H, Haleem-Smith H, Metzger H, 'The unique domain as the site on Lyn kinase for its constitutive association with the high affinity receptor for IgE.' *J Biol Chem.* 1997, 272, 24072-80.
150. Pribluda VS, Pribluda C, Metzger H, 'Transphosphorylation as the mechanism by which the high-affinity receptor for IgE is phosphorylated upon aggregation.' *Proc Natl Acad Sci U S A.* 1994, 91, 11246-50.
151. Jouvin MH, Adamczewski M, Numerof R, Letourneur O, Vallé A, Kinet JP, 'Differential control of the tyrosine kinases Lyn and Syk by the two signaling chains of the high affinity immunoglobulin E receptor.' *J Biol Chem.* 1994, 269, 5918-25.
152. Kihara H, Siraganian RP, 'Src homology 2 domains of Syk and Lyn bind to tyrosine-phosphorylated subunits of the high affinity IgE receptor.' *J Biol Chem.* 1994, 269, 22427-32.
153. Dolmetsch RE, Lewis RS, Goodnow CC, Healy JI, 'Differential activation of transcription factors induced by Ca²⁺ response amplitude and duration.' *Nature.* 1997, 386, 855-8.
154. Beaven MA, Metzger H, 'Signal transduction by Fc receptors: the Fc epsilon RI.' case. *Immunol Today.* 1993, 14, 222-6.

155. Melendez AJ, Harnett MM, Pushparaj PN, Wong WSF, Tay HK, 'Inhibition of FcepsilonRI-mediated mast cell responses by ES-62, a product of parasitic filarial nematodes.' *Nature Medicine*, 2007, 13, 1375-1381.
156. Melendez AJ, Khaw AK, 'Dichotomy of Ca²⁺ signals triggered by different phospholipid pathways in antigen stimulation of human mast cells.' *J Biol Chem*, 2002, 277, 17255-62.
157. Melendez AJ, Harnett MM, Allen JM, 'Crosstalk between ARF6 and protein kinase Calpha in Fc (gamma) RI-mediated activation of phospholipase D1.' *Curr Biol*. 2001, 11, 869-74.
158. Abdel-Raheem IT, Hide I, Yanase Y, Shigemoto-Mogami Y, Sakai N, Shirai Y, Saito N, Hamada FM, El-Mahdy NA, Elsisy Ael-D, Sokar SS, Nakata Y, 'Protein kinase C-alpha mediates TNF release process in RBL-2H3 mast cells.' *Br J Pharmacol*. 2005, 145, 415-23.
159. Li G, Lucas JJ, Gelfand EW, 'Protein kinase C alpha, betaI, and betaII isozymes regulate cytokine production in mast cells through MEKK2/ERK5-dependent and -independent pathways.' *Cell Immunol*. 2005, 238, 10-8.
160. Powner DJ, Hodgkin MN, Wakelam MJ, 'Antigen-stimulated activation of phospholipase D1b by Rac1, ARF6, and PKCalpha in RBL-2H3 cells.' *Mol Biol Cell*. 2002, 13, 1252-62.
161. Leontieva OV, Black JD, 'Identification of two distinct pathways of protein kinase Calpha down-regulation in intestinal epithelial cells. *J Biol Chem*. 2004, 279, 5788-801.

162. Bryce PJ, Miller ML, Miyajima I, Tsai M, Galli SJ, Oettgen HC, 'Immune sensitization in the skin is enhanced by antigen-independent effects of IgE.' *Immunity*. 2004, 20, 381-92
163. Nigo YI, Yamashita M, Hirahara K, Shinnakasu R, Inami M, Kimura M, Hasegawa A, Kohno Y, Nakayama T, 'Regulation of allergic airway inflammation through Toll-like receptor 4-mediated modification of mast cell function.' *Proc Natl Acad Sci U S A*. 2006, 103, 2286-91.
164. Bradding P, Walls AF, Holgate ST, 'The role of the mast cell in the pathophysiology of asthma.' *J Allergy Clin Immunol*. 2006, 117, 1277-84.
165. Hamelmann E, Schwarze J, Takeda K, Oshiba A, Larsen GL, Irvin CG, Gelfand EW, 'Noninvasive measurement of airway responsiveness in allergic mice using barometric plethysmography.' *Am J Respir Crit Care Med*. 1997, 156, 766-75.
166. Pearce EJ. 'Worms tame mast cells.' *Nat Med*. 2007, 13, 1288-9.
167. Allen JE, MacDonald AS, 'Profound suppression of cellular proliferation mediated by the secretions of nematodes'. *Parasite Immunol*. 1998, 20, 241-7.
168. Péry P, Luffau G, Charley J, Petit A, Rouze P, Bernard S, 'Cytidine-5'-diphosphocholine conjugates. I.--Synthesis and fixation to phosphorylcholine-binding proteins.' *Ann Immunol (Paris)*. 1979, 130C, 517-29.
169. Eccleston E, Leonard BJ, Lowe JS, Welford HJ, 'Basophilic leukaemia in the albino rat and a demonstration of the basopoietin.' *Nat New Biol*. 1973, 244, 73-6.
170. Barsumian EL, Isersky C, Petrino MG, Siraganian RP, 'IgE-induced histamine release from rat basophilic leukemia cell lines: isolation of releasing and nonreleasing clones.' *Eur J Immunol*. 1981, 11, 317-23.

171. Gilfillan AM, Kado-Fong H, Wiggan GA, Hakimi J, Kent U, Kochan JP, 'Conservation of signal transduction mechanisms via the human Fc epsilon RI alpha after transfection into a rat mast cell line, RBL-2H3.' *J Immunol.* 1992, 149, 2445-51.
172. Birukova AA, Fu P, Chatchavalvanich S, Burdette D, Oskolkova O, Bochkov VN, Birukov KG, 'Polar head groups are important for barrier-protective effects of oxidized phospholipids on pulmonary endothelium.' *Am J Physiol Lung Cell Mol Physiol.* 2007, 292, L924-35.
173. Nonas S, Miller I, Kawkitinarong K, Chatchavalvanich S, Gorshkova I, Bochkov VN, Leitinger N, Natarajan V, Garcia JG, Birukov KG, 'Oxidized phospholipids reduce vascular leak and inflammation in rat model of acute lung injury.' *Am J Respir Crit Care Med.* 2006, 173, 1130-8.
174. Zeisel SH, 'Choline an essential nutrient for humans.' *FASEB* 1991, 5, 2093-2098.
175. Sakaida I, Kubota M, Kayano K, Takenaka K, Mori K, Okita K, 'Prevention of fibrosis reduces enzyme-altered lesions in the rat liver.' *Carcinogenesis.* 1994, 15, 2201-6.
176. Kawaratani H, Tsujimoto T, Kitazawa T, Kitade M, Yoshiji H, Uemura M, Fukui H, 'Innate immune reactivity of the liver in rats fed a choline-deficient L-amino-acid-defined diet.' *World J Gastroenterol.* 2008, 14, 6655-61.
177. Detopoulou P, Panagiotakos DB, Antonopoulou S, Pitsavos C, Stefanadis C, 'Dietary choline and betaine intakes in relation to concentrations of inflammatory markers in healthy adults: the ATTICA study.' *Am J Clin Nutr.* 2008, 87, 424-30.
178. Harnett W, Meghji M, Worms MJ, Parkhouse RM, 'Quantitative and qualitative changes in production of excretions/secretions by *Litomosoides carinii* during development in the jird (*Meriones unguiculatus*).' *Parasitology.* 1986, 93, 317-31.

179. Hintz M, Schares G, Taubert A, Geyer R, Zahner H, Stirm S, Conraths FJ, 'Juvenile female *Litomosoides sigmodontis* produce an excretory/secretory antigen (Juv-p120) highly modified with dimethylaminoethanol.' *Parasitology*. 1998, 117, 265-71.
180. Houston KM, Babayan SA, Allen JE, Harnett W, 'Does *Litomosoides sigmodontis* synthesize dimethylethanolamine from choline?' *Parasitology*. 2008, 135, 55-61.
181. Budavari S. *The Merck Index*, 13th ed. Merck and Co., Inc., Whitehouse Station, NJ 2001.
182. URL: www.drugbank.ca/drugs/DB01075
183. Raphael GD, Angello JT, Wu MM, Druce HM, 'Efficacy of diphenhydramine vs desloratadine and placebo in patients with moderate-to-severe seasonal allergic rhinitis.' *Ann Allergy Asthma Immunol*. 2006, 96, 606-14.
184. Ciardiello F, Caputo R, Bianco R, Damiano V, Pomatico G, De Placido S, Bianco AR, Tortora G, 'Antitumor effect and potentiation of cytotoxic drugs activity in human cancer cells by ZD-1839 (Iressa), an epidermal growth factor receptor-selective tyrosine kinase inhibitor.' *Clin Cancer Res*. 2000, 6, 2053-63.
185. URL: www.drugbank.ca/drugs/DB00317
186. Imming P, Sinning C, Meyer A, 'Drugs, their targets and the nature and number of drug targets.' *Nat Rev Drug Discov*. 2006, 5, 821-34
187. URL: www.drugbank.ca/drugs/DB00387
188. Abusamhadneh E, Abbott MB, Dvoretzky A, Finley N, Sasi S, Rosevear PR, 'Interaction of bepridil with the cardiac troponin C/troponin I complex.' *FEBS Lett*. 2001, 506, 51-4.
189. Kleerekoper Q, Liu W, Choi D, Putkey JA, 'Identification of binding sites for bepridil and trifluoperazine on cardiac troponin C.' *J Biol Chem*. 1998, 273, 8153-60.

190. Pribluda VS, Pribluda C, Metzger H, 'Transphosphorylation as the mechanism by which the high-affinity receptor for IgE is phosphorylated upon aggregation.' *Proc Natl Acad Sci U S A.* 1994, 91, 11246-50.
191. Beaven MA, Moore JP, Smith GA, Hesketh TR, Metcalfe JC, 'The calcium signal and phosphatidylinositol breakdown in 2H3 cells.' *J Biol Chem.* 1984, 259, 7137-42.
192. White KN, Metzger H, 'Translocation of protein kinase C in rat basophilic leukemic cells induced by phorbol ester or by aggregation of IgE receptors.' *J Immunol.* 1988, 141, 942-7.
193. Kihara H, Siraganian RP, 'Src homology 2 domains of Syk and Lyn bind to tyrosine-phosphorylated subunits of the high affinity IgE receptor.' *J Biol Chem.* 1994, 269, 22427-32.
194. Huber M, Helgason CD, Damen JE, Liu L, Humphries RK, Krystal G, 'The src homology 2-containing inositol phosphatase (SHIP) is the gatekeeper of mast cell degranulation.' *Proc Natl Acad Sci U S A.* 1998, 95, 11330-5.
195. Parravicini V, Gadina M, Kovarova M, Odom S, Gonzalez-Espinosa C, Furumoto Y, Saitoh S, Samelson LE, O'Shea JJ, Rivera J, 'Fyn kinase initiates complementary signals required for IgE-dependent mast cell degranulation.' *Nat Immunol.* 2002, 8, 741-8.
196. Barker SA, Caldwell KK, Hall A, Martinez AM, Pfeiffer JR, Oliver JM, Wilson BS, 'Wortmannin blocks lipid and protein kinase activities associated with PI 3-kinase and inhibits a subset of responses induced by Fc epsilon R1 cross-linking.' *Mol Biol Cell.* 1995, 6, 1145-58.

197. Lo TN, Saul W, Beaven MA, 'The actions of Ca²⁺ ionophores on rat basophilic (2H3) cells are dependent on cellular ATP and hydrolysis of inositol phospholipids. A comparison with antigen stimulation.' *J Biol Chem.* 1987, 262, 4141-5.
198. Di Virgilio F, Gomperts BD, 'Cytosol Mg²⁺ modulates Ca²⁺ ionophore induced secretion from rabbit neutrophils.' *FEBS Lett.* 1983, 163, 315-8.
199. Hanson DA, Ziegler SF, 'Regulation of ionomycin-mediated granule release from rat basophil leukemia cells.' *Mol Immunol.* 2002, 38, 1329-35.
200. Sagi-Eisenberg R, Pecht I, 'Protein kinase C, a coupling element between stimulus and secretion of basophils.' *Immunol Lett.* 1984, 8, 237-41.
201. Willheim M, Agis H, Sperr WR, Köller M, Bankl HC, Kiener H, Fritsch G, Füreder W, Spittler A, Graninger W, Scheiner O, Gadner H, Lechner K, Boltz-Nitulescu G, Valent P, 'Purification of human basophils and mast cells by multistep separation technique and mAb to CDw17 and CD117/c-kit.' *J Immunol Methods.* 1995, 182, 115-29.
202. Montagna W, Eisen AZ, Goldman AS, 'Tinctorial behaviour of mast cells.' *Quarterly Journal of microscopical science* 1954, 95, 1-4.
203. Razin E, Mencia-Huerta JM, Stevens RL, Lewis RA, Liu FT, Corey E, Austen KF, 'IgE-mediated release of leukotriene C₄, chondroitin sulfate E proteoglycan, beta-hexosaminidase, and histamine from cultured bone marrow-derived mouse mast cells.' *J Exp Med.* 1983, 157, 189-201.
204. Malbec O, Roget K, Schiffer C, Iannascoli B, Dumas AR, Arock M, Daëron M, 'Peritoneal cell-derived mast cells: an in vitro model of mature serosal-type mouse mast cells.' *J Immunol.* 2007, 178, 6465-75.

205. Dolmetsch RE, Lewis RS, Goodnow CC, Healy JI, 'Differential activation of transcription factors induced by Ca²⁺ response amplitude and duration.' *Nature* 1997, 386, 855-8.
206. Kinet JP, Metzger H, Hakimi J, Kochan J, 'A cDNA presumptively coding for the alpha subunit of the receptor with high affinity for immunoglobulin E.' *Biochemistry* 1987, 26, 4605-10.
207. Dahl C, Hoffmann HJ, Saito H, Schiotz PO, 'Human mast cells express receptors for IL-3, IL-5 and GM-CSF; a partial map of receptors on human mast cells cultured in vitro.' *Allergy* 2004, 59, 1087-1096.
208. Lin P, Fung SJ, Li S, Chen T, Repetto B, Huang KS, Gilfillan AM, 'Temporal regulation of the IgE-dependent 1,2-diacylglycerol production by tyrosine kinase activation in a rat (RBL-2H3) mast-cell line.' *Biochem J.* 1994, 299, 109-14.
209. Wilson BS, Pfeiffer JR, Smith AJ, Oliver JM, Oberdorf JA, Wojcikiewicz RJ, 'Calcium-dependent clustering of inositol 1,4,5-trisphosphate receptors.' *Mol Biol Cell.* 1998, 9, 1465-78.
210. Harnett MM, Kean DE, Boitelle A, McGuinness S, Thalhamer T, Steiger CN, Egan C, Al-Riyami L, Alcocer MJ, Houston KM, Gracie JA, McInnes IB, Harnett W, 'The phosphorycholine moiety of the filarial nematode immunomodulator ES-62 is responsible for its anti-inflammatory action in arthritis' *Ann Rheum Dis.* 2008, 67, 518-23.
211. Pène J, Rousset F, Brière F, Chrétien I, Bonnefoy JY, Spits H, Yokota T, Arai N, Arai K, Banchereau J, 'IgE production by normal human lymphocytes is induced by interleukin 4

- and suppressed by interferons gamma and alpha and prostaglandin E2.' Proc Natl Acad Sci U S A. 1988, 85, 6880-4.
212. Minty A, Chalon P, Derocq JM, Dumont X, Guillemot JC, Kaghad M, Labit C, Leplatois P, Liauzun P, Miloux B, 'Interleukin-13 is a new human lymphokine regulating inflammatory and immune responses.' Nature. 1993, 362, 248-50.
213. Gebhardt T, Sellge G, Lorentz A, Raab R, Manns MP, Bischoff SC, 'Cultured human intestinal mast cells express functional IL-3 receptors and respond to IL-3 by enhancing growth and IgE receptor-dependent mediator release.' Euro Jour of Immuno, 32, 2308-2316
214. Kurimoto Y, de Weck AL, Dahinden CA, 'The effect of interleukin 3 upon IgE-dependent and IgE-independent basophil degranulation and leukotriene generation' Euro Jour Immun 1991, 21, 361-368
215. Stassen M, Müller C, Arnold M, Hültner L, Klein-Hessling S, Neudörfl C, Reineke T, Serfling E, Schmitt E, 'IL-9 and IL-13 production by activated mast cells is strongly enhanced in the presence of lipopolysaccharide: NF-kappa B is decisively involved in the expression of IL-9.' J Immunol. 2001, 166, 4391-8.
216. Jones TG, Hallgren J, Humbles A, Burwell T, Finkelman FD, Alcaide P, Austen KF, Gurish MF, 'Antigen-induced increases in pulmonary mast cell progenitor numbers depend on IL-9 and CD1d-restricted NKT cells. J Immunol. 2009, 183, 5251-60.
217. McLane MP, Haczku A, van de Rijn M, Weiss C, Ferrante V, MacDonald D, Renauld JC, Nicolaides NC, Holroyd KJ, Levitt RC, 'Interleukin-9 promotes allergen-induced eosinophilic inflammation and airway hyperresponsiveness in transgenic mice.' Am J Respir Cell Mol Biol. 1998, 19, 713-20.

218. Lorentz A, Schwengberg S, Mierke C, Manns MP, Bischoff SC, 'Human intestinal mast cells produce IL-5 in vitro upon IgE receptor cross-linking and in vivo in the course of intestinal inflammatory disease.' *Eur J Immunol.* 1999, 29, 1496-503.
219. Okayama Y, Petit-Frère C, Kassel O, Semper A, Quint D, Tunon-de-Lara MJ, Bradding P, Holgate ST, Church MK, 'IgE-dependent expression of mRNA for IL-4 and IL-5 in human lung mast cells.' *J Immunol.* 1995, 155, 1796-808.
220. Okayama Y, Kobayashi H, Ashman LK, Dobashi K, Nakazawa T, Holgate ST, Church MK, Mori M, 'Human lung mast cells are enriched in the capacity to produce granulocyte-macrophage colony-stimulating factor in response to IgE-dependent stimulation.' *Eur J Immunol.* 1998, 28, 708-15.
221. Lorentz A, Schwengberg S, Sellge G, Manns MP, Bischoff SC, 'Human intestinal mast cells are capable of producing different cytokine profiles: role of IgE receptor cross-linking and IL-4.' *J Immunol.* 2000, 164, 43-8.
222. Gordon JR, Galli SJ, 'Mast cells as a source of both preformed and immunologically inducible TNF-alpha/cachectin.' *Nature.* 1990, 346, 274-6.
223. Nakae S, Ho LH, Yu M, Monteforte R, Iikura M, Suto H, Galli SJ, 'Mast cell-derived TNF contributes to airway hyperreactivity, inflammation, and TH2 cytokine production in an asthma model in mice. *J Allergy Clin Immunol.* 2007, 120, 48-55.
224. Coward WR, Okayama Y, Sagara H, Wilson SJ, Holgate ST, Church MK, 'NF- κ B and TNF- α : A Positive Autocrine Loop in Human Lung Mast Cells?' *J. Immunol.* 2002, 169, 5287 - 5293.

225. Peters AT, Tancowny B, Suh L, Agashe M, Harris K, Conley D, Kern R, Grammer L, Schleimer R, 'Evidence for Elevated IL-6 and its Signaling Components in Chronic Rhinosinusitis with Nasal Polyps.' *J. Allergy Clin Immunol*, 2007, 119, S144-S145.
226. Dawicki W, Jawdat DW, Xu N, Marshall JS, 'Mast cells, histamine, and IL-6 regulate the selective influx of dendritic cell subsets into an inflamed lymph node.' *J Immunol*. 2010, 184, 2116-23.
227. Grierson AM, Mitchell P, Adams CL, Mowat AM, Brewer JM, Harnett MM, Garside P, 'Direct quantitation of T cell signaling by laser scanning cytometry'. *J Immunol Methods*. 2005, 301, 140-53.
228. Shearman MS, Berry N, Oda T, Ase K, Kikkawa U, Nishizuka Y, 'Isolation of protein kinase C subspecies from a preparation of human T lymphocytes.' *FEBS Lett*. 1988, 234, 387-91.
229. Ono Y, Fujii T, Ogita K, Kikkawa U, Igarashi K, Nishizuka Y, 'Identification of three additional members of rat protein kinase C family: delta-, epsilon- and zeta-subspecies.' *FEBS Lett*. 1987, 226, 125-8.
230. Nakanishi H, Exton JH, 'Purification and characterization of the zeta isoform of protein kinase C from bovine kidney.' *J Biol Chem*. 1992, 267, 16347-54.
231. Diaz-Meco MT, Municio MM, Sanchez P, Lozano J, Moscat J, 'Lambda-interacting protein, a novel protein that specifically interacts with the zinc finger domain of the atypical protein kinase C isotype lambda/iota and stimulates its kinase activity in vitro and in vivo.' *Mol Cell Biol*. 1996, 16, 105-14.
232. Ozawa K, Szallasi Z, Kazanietz MG, Blumberg PM, Mischak H, Mushinski JF, Beaven MA, 'Ca (2+)-dependent and Ca(2+)-independent isozymes of protein kinase C mediate

- exocytosis in antigen-stimulated rat basophilic RBL-2H3 cells. Reconstitution of secretory responses with Ca²⁺ and purified isozymes in washed permeabilized cells.' *J Biol Chem.* 1993, 268, 1749-56.
233. White JR, Pluznik DH, Ishizaka K, Ishizaka T, 'Antigen-induced increase in protein kinase C activity in plasma membrane of mast cells.' *Proc Natl Acad Sci U S A.* 1985 82, 8193-7.
234. Jolly PS, Bektas M, Olivera A, Gonzalez-Espinosa C, Proia RL, Rivera J, Milstien S, Spiegel S, 'Transactivation of sphingosine-1-phosphate receptors by FcepsilonRI triggering is required for normal mast cell degranulation and chemotaxis.' *J Exp Med.* 2004, 199, 959-70.
235. Pushparaj PN, Manikandan J, Tay HK, H'ng SC, Kumar SD, Pfeilschifter J, Huwiler A, Melendez AJ, 'Sphingosine kinase 1 is pivotal for Fc epsilon RI-mediated mast cell signaling and functional responses in vitro and in vivo.' *J Immunol.* 2009, 183, 221-7.
236. Melendez AJ, Harnett MM, Allen JM, 'Differentiation-dependent switch in protein kinase C isoenzyme activation by Fc gamma RI, the human high-affinity receptor for immunoglobulin G.' *Immunology.* 1999, 96, 457-64.
237. Evans DJ, Lindsay MA, Webb BL, Kankaanranta H, Giembycz MA, O'Connor BJ, Barnes PJ, 'Expression and activation of protein kinase C-zeta in eosinophils after allergen challenge.' *Am J Physiol.* 1999, 277, L233-9.
238. Kuo JF, Shoji M, Girard PR, Mazzei GJ, Turner RS, Su H, 'Phospholipid/calcium-dependent protein kinase (protein kinase C) system: a major site of bioregulation.' *Adv Enzyme Regul.* 1986, 25, 387-400.

239. Brown FD, Thompson N, Saqid KM, Clark JM, Powner D, Thompson NT, Solari R, Wakelam MJO, 'Phospholipase D1 localises to secretory granules and lysosomes and is plasma-membrane translocated on cellular stimulation.' *Curr. Biol.* 1998, 8, 835.
240. Choi WS, Kim YM, Combs C, Frohman MA, Beaven MA, 'Phospholipase D1 and 2 regulate different phases of exocytosis in mast cells.' *J. Immunol.* 2002, 168, 5682.
241. O'Lunaigh N, Pardo R, Fensome A, Allen-Baume V, Jones D, Holt MR, Cockcroft S, 'Continual production of phosphatidic acid by phospholipase D is essential for antigen-stimulated membrane ruffling in cultured mast cells.' *Mol. Biol. Cell.* 2002, 13, 3730.
242. Summers RW, Elliot DE, Qadir K, Urban JF Jr, Thompson R, Weinstock JV, '*Trichuris suis* seems to be safe and possibly effective in the treatment of inflammatory bowel disease.' *Am J Gastroenterol* 2003, 98, 2034–2041.
243. Summers RW, Elliott DE, Urban JF Jr, Thompson R, Weinstock JV, '*Trichuris suis* therapy in Crohn's disease.' *Gut.* 2005, 54, 87-90.
244. Croese J, O'neil J, Masson J, Cooke S, Melrose W, Pritchard D, Speare R, 'A proof of concept study establishing *Necator americanus* in Crohn's patients and reservoir donors.' *Gut.* 2006, 55, 136-7.
245. Mortimer K, Brown A, Feary J, Jagger C, Lewis S, Antoniak M, Pritchard D, Britton J, 'Dose-ranging study for trials of therapeutic infection with *Necator americanus* in humans.' *Am J Trop Med Hyg.* 2006, 75, 914-20.
246. Schnoeller C, Rausch S, Pillai S, Avagyan A, Wittig BM, Loddenkemper C, Hamann A, Hamelmann E, Lucius R, Hartmann S, 'A helminth immunomodulator reduces allergic and inflammatory responses by induction of IL-10-producing macrophages.' *J Immunol.* 2008, 180, 4265-72.

247. Imai S, Fujita K, 'Molecules of parasites as immunomodulatory drugs.' *Curr Top Med Chem.* 2004, 4, 539-52.
248. Imai S, Tezuka H, Furuhashi Y, Muto R, Fujita K, 'A factor of inducing IgE from a filarial parasite is an agonist of human CD40.' *J Biol Chem.* 2001, 276, 46118-24.
249. Kawabe T, Naka T, Yoshida K, Tanaka T, Fujiwara H, Suematsu S, Yoshida N, Kishimoto T, Kikutani H, 'The immune responses in CD40-deficient mice: impaired immunoglobulin class switching and germinal center formation.' *Immunity.* 1994, 1, 167-78.
250. Tezuka H, Imai S, Muto R, Furuhashi Y, Fujita K, 'Recombinant *Dirofilaria immitis* polyprotein that stimulates murine B cells to produce nonspecific polyclonal immunoglobulin E antibody.' *Infect Immun.* 2002, 70, 1235-44.
251. Smith P, Fallon RE, Mangan NE, Walsh CM, Saraiva M, Sayers JR, McKenzie AN, Alcami A, Fallon PG, 'Schistosoma mansoni secretes a chemokine binding protein with antiinflammatory activity.' *J Exp Med.* 2005, 202, 1319-25.
252. McInnes IB, Leung BP, Harnett M, Gracie JA, Liew FY, Harnett W, 'A novel therapeutic approach targeting articular inflammation using the filarial nematode-derived phosphorylcholine-containing glycoprotein ES-62. *J Immunol* 2003, 171, 2127– 2133.
253. Razin E, Ihle JN, Seldin D, Mencia-Huerta JM, Katz HR, LeBlanc PA, Hein A, Caulfield JP, Austen KF, Stevens RL, 'Interleukin 3: A differentiation and growth factor for the mouse mast cell that contains chondroitin sulfate E proteoglycan.' *J Immunol.* 1984, 132, 1479-86.

254. Schrader JW, Lewis SJ, Clark-Lewis I, Culvenor JG, 'The persisting (P) cell: histamine content, regulation by a T cell-derived factor, origin from a bone marrow precursor, and relationship to mast cells.' *Proc Natl Acad Sci U S A*. 1981, 78, 323-7.
255. Valent P, Besemer J, Sillaber C, Butterfield JH, Eher R, Majdic O, Kishi K, Kleptko W, Eckersberger F, Lechner K, 'Failure to detect IL-3-binding sites on human mast cells.' *J. Immunol.* 1990, 145, 3432–3437.
256. Gebhardt T, Sellge G, Lorentz A, Raab R, Mann MP, Bischoff SC, ' Cultured human intestinal mast cells express functional IL-3 receptors and respond to IL-3 by enhancing growth and IgE receptor-dependent mediator release.' *Eur. J. Immunol.* 2002, 32, 2308–2316.
257. Kurimoto Y, De Weck, AL, Dahinden CA, 'The effect of interleukin 3 upon IgE-dependent and IgE independent basophil degranulation and leukotriene generation.' *Eur. J. Immunol.* 1991, 21, 361–368.
258. Schechter NM, Pereira PJB, Strobl S, 'Mast Cells and Basophils (eds Marone, G., Lichtenstein, L.M. Galli, S.J.) 275–290 (Academic Press, San Diego, 2000).
259. Hallgren, J, Pejler G, 'Biology of mast cell tryptase. An inflammatory mediator.' *FEBS J.* 2006, 273, 1871–1895.
260. Misiak-Tłoczek A, Brzezińska-bbłaszczyk E, 'IL-6, but not IL-4, stimulates chemokinesis and TNF stimulates chemotaxis of tissue mast cells: involvement of both mitogen-activated protein kinases and phosphatidylinositol 3-kinase signalling pathways.' *APMIS*, 2009, 117, 558-567.
261. Mohr FC, Fewtrell C, 'Depolarization of rat basophilic leukemia cells inhibits calcium uptake and exocytosis.' *J Cell Biol.* 1987, 104, 783-92.

262. Nishizuka Y, 'Intracellular signaling by hydrolysis of phospholipids and activation of protein kinase C.' *Science*. 1992, 258, 607-14.
263. Maeyama K, Hohman RJ, Metzger H, Beaven MA, 'Quantitative relationships between aggregation of IgE receptors, generation of intracellular signals, and histamine secretion in rat basophilic leukemia (2H3) cells. Enhanced responses with heavy water.' *J Biol Chem*. 1986, 261, 2583-92.
264. Nakajima T, Inagaki N, Tanaka H, Tanaka A, Yoshikawa M, Tamari M, Hasegawa K, Matsumoto K, Tachimoto H, Ebisawa M, Tsujimoto G, Matsuda H, Nagai H, Saito H, 'Marked increase in CC chemokine gene expression in both human and mouse mast cell transcriptomes following Fcε receptor I cross-linking: an interspecies comparison.' *Blood* 2002, 100, 3861–3868.
265. Claxton NS, Fellers TJ, Davidson MW, ' Laser scanning confocal microscopy', URL: www.olympusconfocal.com/theory/LSCMIntro.pdf